

# Selected Topics in Statistical Field Theory

Kay Jörg Wiese

Laboratoire de physique, Département de physique de l'ENS, École normale supérieure,  
UPMC Univ. Paris 06, CNRS, PSL Research University, 75005 Paris, France  
<http://www.phys.ens.fr/~wiese/masterENS/>

January 30, 2020 – masterENS.tex – version 5944

These notes are provided for students of the master class *Selected Topics in Statistical Field Theory*, taught by the author in spring 2018 and 2019. Not for circulation.

## Contents

<b>0</b>	<b>What statistical field theory can do: An example</b>	<b>4</b>	2.7	Evaluation of the MOPE-coefficients . . .	27
			2.8	Strategy of renormalization . . . . .	30
			2.9	Renormalization at 1-loop order . . . . .	31
			2.10	$\phi^4$ -theory at other values of $n$ . . . . .	34
<b>Part 1:</b>	<b>General Methods in Statistical Field theory</b>	<b>5</b>	<b>3</b>	<b>Dynamics</b>	<b>35</b>
<b>1</b>	<b>Key tools in field theory</b>	<b>5</b>	3.1	Markov chains, Langevin equation . . . . .	35
1.1	$\phi^4$ field theory . . . . .	5	3.2	Itô calculus . . . . .	36
1.2	Gauss-integrals and Wick's theorem . . . . .	6	3.3	From Langevin to Fokker-Planck . . . . .	36
1.3	Perturbative calculations and the Renormalization Group . . . . .	6	3.4	MSR formalism . . . . .	38
1.4	Euklidean versus relativistic field theory: Wick rotation . . . . .	11	3.5	Gaussian theory with spatial degrees of freedom . . . . .	40
1.5	Large $N$ . . . . .	11	3.6	Fluctuation-dissipation theorem . . . . .	41
1.6	Large-order behavior of perturbation theory: A toy integral . . . . .	11	3.7	Dynamics respecting Boltzmann weights . . . . .	41
1.7	Large-order behavior of field theory, instantons . . . . .	13	3.8	Dynamics of $\phi^4$ -theory: Model A . . . . .	41
1.8	Padé resummation . . . . .	15	3.9	Models B, C, D, . . . . , J . . . . .	43
1.9	Padé-Borel resummation . . . . .	15	3.10	Tunneling over a barrier: Basic equations . . . . .	43
1.10	Meijer-G resummation . . . . .	16	3.11	The Gel'fand Yaglom method . . . . .	45
1.11	Resummation in "real life": $\phi^4$ -theory . . . . .	16	3.12	Propagator for harmonic potential, and normalization of path integral . . . . .	46
1.12	Renormalons in renormalizable theories, and their absence in super-renormalizable ones . . . . .	16	3.13	Tunneling over a barrier: Results . . . . .	47
<b>2</b>	<b>Self-avoiding polymers and membranes</b>	<b>17</b>	3.14	Tunneling over a barrier: Results from the non-equilibrium steady state . . . . .	48
2.1	Self-avoiding polymers and their mapping onto $\phi^4$ theory . . . . .	17	<b>Part 2:</b>	<b>Disordered Elastic Manifolds, Avalanches</b>	<b>51</b>
2.2	Self-avoiding manifolds . . . . .	20	<b>4</b>	<b>Phenomenology</b>	<b>51</b>
2.3	Flory estimate . . . . .	23	4.1	Introduction . . . . .	51
2.4	Locality of divergences . . . . .	23	4.2	Physical realizations, model and observables . . . . .	51
2.5	More about perturbation theory . . . . .	25	4.3	Flory estimates and bounds . . . . .	54
2.6	Multilocal operator product expansion (MOPE) . . . . .	26	4.4	Replica trick and basic perturbation theory . . . . .	55
			4.5	Dimensional reduction . . . . .	57
			4.6	The Larkin-length, and the role of temperature . . . . .	57

<b>5</b>	<b>The field-theoretic treatment</b>	<b>58</b>	8.6	An effective stochastic field theory of the reaction process . . . . .	103
5.1	Derivation of the functional RG equations	58	<b>9</b>	<b>A phenomenological derivation of the stochastic field theory for the Manna model</b>	<b>104</b>
5.2	Solution of the FRG equations, and cusp	61	9.1	Basic Definitions . . . . .	104
5.3	Fixed points of the FRG equation . . . . .	62	9.2	MF solution . . . . .	106
5.4	The cusp and shocks: A toy model . . . . .	64	9.3	The complete effective equations of motion for the Manna model . . . . .	107
5.5	The cusp in the field-theory . . . . .	66	9.4	Excursion: Mapping to disordered elastic manifolds . . . . .	108
5.6	Beyond 1 loop . . . . .	67	<b>10</b>	<b>A good example to connect to elementary particle physics?</b>	<b>109</b>
<b>6</b>	<b>Dynamics, and the Depinning transition</b>	<b>70</b>	<b>11</b>	<b>Burgers, KPZ, and Cole-Hopf</b>	<b>109</b>
6.1	Phenomenology . . . . .	70	11.1	Non-linear surface growth: KPZ equation	109
6.2	Field theory of the depinning transition . . . . .	71	11.2	Burgers equation . . . . .	110
6.3	Loop expansion . . . . .	72	11.3	Cole-Hopf transformation . . . . .	110
6.4	Depinning beyond leading order . . . . .	75	11.4	Decaying KPZ, and shocks . . . . .	112
6.5	Connection with extreme-value statistics	77	11.5	All-order $\beta$ -function for KPZ . . . . .	113
<b>7</b>	<b>Avalanches</b>	<b>80</b>	11.6	Failure of the all-order $\beta$ -function for KPZ, and relation to FRG . . . . .	115
7.1	Observables and scaling relations . . . . .	80	11.7	Quenched KPZ . . . . .	115
7.2	Phenomenology . . . . .	82	11.8	The Carroro-Duchon equations . . . . .	115
7.3	ABBM model . . . . .	82	<b>12</b>	<b>Passive advection and multiscaling</b>	<b>115</b>
7.4	End of an avalanche, and an efficient simulation algorithm . . . . .	83	<b>13</b>	<b>Non-equilibrium</b>	<b>115</b>
7.5	The Brownian Force Model (BFM) . . . . .	84	<b>Appendices</b>		<b>116</b>
7.6	Short-ranged rough disorder . . . . .	84	<b>A</b>	<b>Higher-loop calculations</b>	<b>116</b>
7.7	Field theory . . . . .	85	A.1	Basics . . . . .	116
7.8	FRG and scaling . . . . .	85	A.2	1 loop in momentum space . . . . .	116
7.9	Instanton equation . . . . .	86	A.3	1 loop in position space . . . . .	116
7.10	Avalanche-size distribution . . . . .	86	A.4	2 loops . . . . .	117
7.11	Velocity distribution . . . . .	87	A.5	Nested divergences, and geometrical factors . . . . .	118
7.12	Duration distribution . . . . .	87	A.6	The diagram correcting friction in model A	119
7.13	The temporal shape of an avalanche . . . . .	88	A.7	3 loops: an example . . . . .	119
7.14	Local avalanche-size distribution . . . . .	89	<b>B</b>	<b>Supersymmetry techniques</b>	<b>120</b>
7.15	The spatial shape of avalanches . . . . .	90	B.1	Basic rules for manipulating Grassmann variables . . . . .	120
7.16	Some theorems . . . . .	91	B.2	Disorder averages with bosons and fermions . . . . .	121
7.17	Loop corrections . . . . .	92	B.3	Recovering the renormalization of the disorder . . . . .	123
7.18	Simulation results and experiments . . . . .	95	B.4	Supersymmetry and dimensional reduction	124
7.19	Avalanches with retardation . . . . .	97	B.5	CDWs and their mapping onto $\phi^4$ -theory	126
7.20	Power-law correlated random forces, relation to fractional Brownian motion . . . . .	97			
<b>Part 3: Discrete Stochastic Processes</b>		<b>98</b>			
<b>8</b>	<b>Coherent-state path integral, reaction diffusion systems, etc.</b>	<b>98</b>			
8.1	Modeling discrete stochastic processes . . . . .	98			
8.2	The coherent-state path integral, imaginary noise and its interpretation . . . . .	98			
8.3	Stochastic noise as a consequence of the discreteness of the states . . . . .	100			
8.4	Example: The reaction-annihilation process . . . . .	101			
8.5	Diffusion . . . . .	101			

<b>C</b>	<b>The coherent-state path integral (CSPI)</b>	<b>127</b>			
C.1	Quantization rules . . . . .	127			
C.2	Master equation and Hamiltonian formalism . . . . .	127			
C.3	Combinatorics . . . . .	129			
C.4	Observables . . . . .	129			
C.5	Coherent states . . . . .	129			
C.6	Many sites . . . . .	131			
C.7	Coarse-graining . . . . .	131			
C.8	Diffusion . . . . .	132			
C.9	Resolution of unity . . . . .	132			
C.10	Evolution operator in the coherent-state formalism, and action . . . . .	133			
C.11	The shift $\phi_t^* \rightarrow \phi_t^* + 1$ . . . . .	134			
C.12	Graphical interpretation of the coherent-state path-integral, first-passage probabilities, and renormalization . . . . .	135			
C.13	The initial condition . . . . .	135			
C.14	The propagator . . . . .	136			
C.15	The interactions . . . . .	136			
C.16	Perturbation theory in the CSPI . . . . .	137			
C.17	Interpretation of the “strange” quartic vertex in terms of a first-passage problem . . . . .	137			
C.18	Stochastic equation of motion for the coherent-state path integral . . . . .	139			
C.19	Equation of motion for diffusion in the CSPI . . . . .	140			
C.20	Equation of motion for reaction diffusion in the CSPI . . . . .	141			
C.21	Dual formulation: Equation of motion for $\phi_t^*$ . . . . .	141			
C.22	Testing stochastic equations of motion derived from the CSPI . . . . .	143			
	C.23 Formal derivation of the evolution of expectation values in the coherent-state path-integral . . . . .	144			
<b>D</b>	<b>Non-trivial fixed points of the Renormalization Group</b>	<b>145</b>			
<b>E</b>	<b>Quantum Mechanics: Feynman path-integral and Keldysh formalism</b>	<b>147</b>			
E.1	Real-time path-integral . . . . .	147			
E.2	Imaginary time path-integral: The partition function . . . . .	148			
E.3	The action for more general Hamiltonians and commutation-relations . . . . .	148			
E.4	The Keldysh-formalism . . . . .	149			
E.5	A change in variables and the classical limit (MSR-action) . . . . .	150			
E.6	Boundary-conditions and the Feynman-Vernon-influence function . . . . .	151			
E.7	FDT (quantum version) . . . . .	152			
E.8	The Matsubara-relation . . . . .	154			
E.9	Free theory . . . . .	155			
<b>F</b>	<b>Tools for self-avoiding membranes</b>	<b>156</b>			
F.1	Equation of motion and redundant operators . . . . .	156			
F.2	Analytic continuation of the measure . . . . .	158			
F.3	IR-regulator, conformal mapping, extraction of the residue, and its universality . . . . .	159			
F.4	Factorization for $D = 1$ . . . . .	162			
F.5	Exercises for Self-Avoiding Manifolds with solutions . . . . .	162			
<b>G</b>	<b>Non-analytic expectation values</b>	<b>167</b>			
<b>H</b>	<b>Notations</b>	<b>168</b>			

## Recommended Literature and Tools

- please install Mathematica on your laptop.

### General Books on Field Theory

[1] D.J. Amit, Field Theory, the Renormalization Group, and Critical Phenomena, World Scientific, Singapore, 2nd edition, 1984: A classic introduction with all the necessary tools for the real world.

[2] Jean Zinn-Justin, Quantum Field Theory and Critical Phenomena, Oxford University Press, Oxford, 1989: The “Bible of Field Theory”. Encyclopedic, but a little bit difficult to read. Good for reference.

- [3] Jean Zinn-Justin, Phase Transitions and Renormalization Group, Oxford University Press, Oxford, 2007. A more pedagogic version of [2]. (didn't read myself)
- [4] John Cardy, Scaling and Renormalization in Statistical Physics, Cambridge University Press, 1996. A marvel of clarity with non-standard applications by a true master of the subject.
- [5] Mehran Kardar, Statistical Physics of Fields, Cambridge University Press, 2007. While not read myself, I know Mehran as a very pedagogical lecturer.
- [6] Edouard Brézin, Introduction to Statistical Field Theory, Cambridge University Press, 2010. A pedagogic introduction by one of the grand masters.

## Disordered Systems

\*\*\*add references\*\*\*

## Stochastic Equations

- [7] K.J. Wiese, Coherent-state path integral versus coarse-grained effective stochastic equation of motion: From reaction diffusion to stochastic sandpiles, Phys. Rev. E 93 (2016) 042117, arXiv:1501.06514.
  - \*\*\*add more references\*\*\*

## 0 What statistical field theory can do: An example

As an appetizer of what we will establish in these lectures, consider Fig. 0.1: We start with a *charge density wave* (CDW), resulting from an instability of certain semiconductor devices to spontaneously create regions with a higher and lower charge density  $\rho(x)$  [7]. Supposing overall charge neutrality, the latter can be written as

$$\rho(x) = \rho_0 \cos(\phi(x)) , \quad \phi(x) = k_{\text{CDW}}x + \delta\phi(x) . \quad (0.1)$$

The function  $\delta\phi(x)$  allows for fluctuations in the phase. The latter appear when adding impurities to the system. We will see later that in order to treat this situation, a modified version of the renormalization group is necessary, termed functional RG (see section 5). Using supersymmetry techniques, the ensuing field theory can be mapped to a theory of two complex bosons, and one complex fermion (section B.5). It is equivalent to a theory with  $-1$  complex bosons, or equivalently  $-2$  real bosons. Perturbatively, the latter can then be mapped onto *loop-erased random walks* (LERWS)[8]: These are random walks (with traces drawn in red on Fig. 0.1) from which any loop is erased as soon as it is formed. The remaining object (in blue), is the LERW. On the other hand, there is an old conjecture by Narayan and Middleton [9], that charge-density waves can be mapped onto the *Abelian sandpile model*. The latter is a cellular automaton mimicking sandpiles. The rule is to *topple*  $2d$  ( $d$  is the dimension of the system) grains to their  $2d$  neighbors as long as this is possible. The name “Abelian” indicates that the state resulting from these successive topplings does not depend on their order. Finally, this ASM can be mapped onto *uniform spanning trees* [10]: these are tree diagrams connecting each vertex of a given lattice to at least one of its neighbors, s.t. the resulting graph is a connected tree, i.e. cannot be separated into two parts without cutting a link. On the other hand, it does not contain any loop, thus cutting any link the graph will contain two connected components. Choosing randomly two points on this graph, these points are connected by a single path (one may not use a link twice). This path has the same statistics as a loop-erased random walk.

In our lecture we wish to provide the reader with the necessary tools to explore the magic world of statistical physics in general, and statistical field theory in particular, by himself.

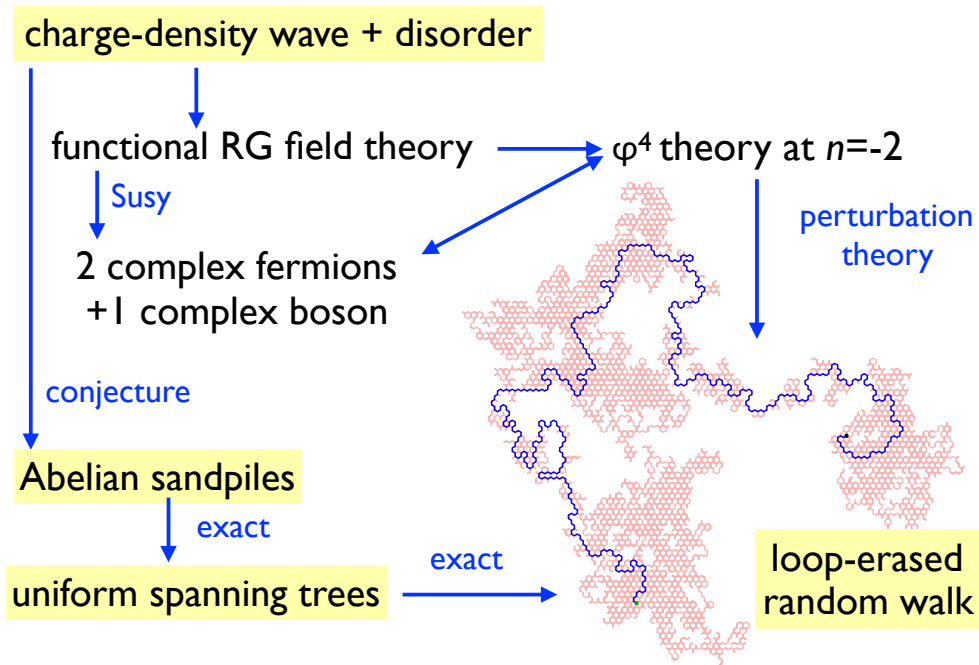


Figure 0.1: An example of the rich relations encountered in statistical field theory, as explained in the main text.

## PART 1: General Methods in Statistical Field theory

### 1 Key tools in field theory

#### 1.1 $\phi^4$ field theory

We remind our good old friend, the scalar  $\phi^4$  theory. Its (Euklidean) *action* (or energy) is

$$\mathcal{H}[\phi] = \int_x \frac{1}{2} [\nabla\phi(x)]^2 + \frac{m^2}{2} \phi(x)^2 + g\phi(x)^4 . \quad (1.1)$$

It is the field theoretic representation of the Ising model, and, as field theory distills out the universal properties of a system, of all its related models (liquid-vapor transition, etc.).

Expectation values of an observable  $\mathcal{O}[\phi]$ , which depends itself on  $\phi$ , can be defined via a path integral

$$\langle \mathcal{O} \rangle = \frac{\langle \mathcal{O} \rangle_{\mathcal{H}}}{\mathcal{Z}_{\mathcal{H}}} , \quad \langle \mathcal{O} \rangle_{\mathcal{H}} := \int \mathcal{D}[\phi] \mathcal{O}[\phi] e^{-\mathcal{H}[\phi]} , \quad \mathcal{Z}_{\mathcal{H}} := \langle 1 \rangle_{\mathcal{H}} . \quad (1.2)$$

For notational simplicity, we suppressed the dependence on temperature  $T$  in the Boltzmann factor  $e^{-\mathcal{H}[\phi]/T}$ . We will put it back when necessary; it can also be restituted by a rescaling of the field  $\phi$ ,  $m$  and  $g$ . The normalization is taken into account by dividing by the partition function, here written as expectation value of 1. The integration measure is

$$\int \mathcal{D}[\phi] := \prod_x d\phi(x) , \quad (1.3)$$

where the points  $x$  are chosen on a grid with mesh-size  $a$ .

In general, such a path integral is difficult to calculate, except if the action is quadratic. A theory with a quadratic action is termed a *free theory*

$$\mathcal{H}_0[\phi] = \int_x \frac{1}{2} [\nabla\phi(x)]^2 + \frac{m^2}{2} \phi(x)^2 \equiv \int_k \frac{1}{2} \tilde{\phi}(k) \tilde{\phi}(-k) (k^2 + m^2) . \quad (1.4)_{\text{free-theory}}$$

To arrive at the last equality, we have performed a Fourier transform, denoting by  $\tilde{\phi}(k)$  the fields in the Fourier basis. Our conventions are

$$\int_x := \int d^d x, \quad \int_k := \int \frac{d^d k}{(2\pi)^d} \quad (1.5)$$

## 1.2 Gauss-integrals and Wick's theorem

We remind that if  $\mathcal{A}$  is a symmetric  $n \times n$ -dimensional invertible matrix, and  $\vec{X}$  an  $n$ -dimensional vector, then

$$\mathcal{Z}[\vec{J}] := \int \prod_{i=1}^n \frac{dX_i}{\sqrt{2\pi}} e^{\vec{J}\vec{X} - \frac{1}{2}\vec{X}\mathcal{A}\vec{X}} = \det(\mathcal{A})^{-\frac{1}{2}} e^{\frac{1}{2}\vec{J}\mathcal{A}^{-1}\vec{J}} \quad (1.6) \text{Wick-theorem}$$

The exponential factor is obtained by completing the square, and the determinant by passing to an orthonormal eigenbasis of  $\mathcal{A}$ . In analogy to the preceding section, we can call *action* the quadratic form  $\mathcal{H} := \frac{1}{2}\vec{X}\mathcal{A}\vec{X}$ . This defines expectation values w.r.t. to this action, or as probabilists would say, the probability measure  $\mathcal{P}[\vec{S}] \sim e^{-\mathcal{H}}$ .

In particular, if we wish to calculate the expectation value of  $m$  powers of the field, we can produce such a field  $X_i$  by deriving w.r.t. the conjugate field  $J_i$ , and finally setting  $\vec{J} \rightarrow \vec{0}$ ,

$$\begin{aligned} \langle X_{i_1} \dots X_{i_m} \rangle &= \frac{1}{\mathcal{Z}[\vec{J}]} \frac{d}{dJ_{i_1}} \dots \frac{d}{dJ_{i_m}} \mathcal{Z}[\vec{J}] \Big|_{\vec{J}=\vec{0}} = \frac{d}{dJ_{i_1}} \dots \frac{d}{dJ_{i_m}} e^{\frac{1}{2}\vec{J}\mathcal{A}^{-1}\vec{J}} \Big|_{\vec{J}=\vec{0}} \\ &= e^{\frac{1}{2}\vec{\partial}_X \mathcal{A}^{-1} \vec{\partial}_X} X_{i_1} \dots X_{i_m}. \end{aligned} \quad (1.7)$$

The last expression on the first line tells us that the result is a sum over the product of all pairs of indices on the l.h.s. The last line is proven by remarking that the combinatorial factors are the same as in the preceding expression. For concreteness, let us give two examples,

$$\langle X_1 X_2 \rangle = (\mathcal{A}^{-1})_{12} \quad (1.8)$$

$$\langle X_1 X_2 X_3 X_4 \rangle = (\mathcal{A}^{-1})_{12} (\mathcal{A}^{-1})_{34} + (\mathcal{A}^{-1})_{13} (\mathcal{A}^{-1})_{24} + (\mathcal{A}^{-1})_{14} (\mathcal{A}^{-1})_{23}^{-1}. \quad (1.9)$$

Using the quadratic form (1.4), we deduce that

$$\langle \tilde{\phi}(k) \tilde{\phi}(k') \rangle_0 = (2\pi)^d \delta^d(k+k') \frac{1}{k^2 + m^2} \quad (1.10) \text{m:cor1bis}$$

In position space at  $m = 0$  this becomes

$$C(x-y) := \langle \phi(x) \phi(y) \rangle_0 = \mathcal{C}_1 |x-y|^{2-d}, \quad \mathcal{C}_1 = \frac{1}{S_d(d-2)}, \quad S_d = \frac{2\pi^{d/2}}{\Gamma(d/2)}. \quad (1.11) \text{m:cor2}$$

## 1.3 Perturbative calculations and the Renormalization Group

This topic has (or should have) been treated at lengths in any basic field-theory class. Here we rederive the main results, focusing on some conceptual points.

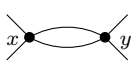
One starts with perturbation theory in the coupling constant. To this aim consider the path integral of any observable

$$\langle \mathcal{O} \rangle_{\mathcal{H}} = \int \mathcal{D}[\phi] \mathcal{O}[\phi] e^{-\mathcal{H}[\phi]} = \int \mathcal{D}[\phi] \mathcal{O}[\phi] e^{-\mathcal{H}_0[\phi] - g \int_x \phi^4(x)} \equiv \left\langle \mathcal{O}[\phi] e^{-g \int_x \phi^4(x)} \right\rangle_0. \quad (1.12)$$

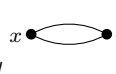
The index  $_0$  indicates expectation values w.r.t. to the free theory  $\mathcal{H}_0$ . Expanding in  $g$ , we obtain

$$\left\langle \mathcal{O}[\phi] e^{-g \int_x \phi^4(x)} \right\rangle_0 = \langle \mathcal{O}[\phi] \rangle_0 - g \left\langle \mathcal{O}[\phi] \int_x \phi^4(x) \right\rangle_0 + \frac{g^2}{2!} \left\langle \mathcal{O}[\phi] \left[ \int_x \phi^4(x) \right]^2 \right\rangle_0 + \dots \quad (1.13)$$

Considering the operator  $\mathcal{O}$  as a spectator (mathematically it is a *test-function*), we would like to “absorb” the third term into the second one with an *effective* coupling constant  $g_{\text{eff}}$ . To this aim we have to solve the problem of what is generated upon Wick-contraction from two  $\phi^4$  interactions, and what “looks again” like a  $\phi^4$ -interaction. This is

$$\left[ \int_x \phi^4(x) \right] \times \left[ \int_y \phi^4(y) \right] \longrightarrow \frac{4^2 3^2}{2} \int_{x,y} \phi^2(x) \phi^2(y) C^2(x-y) \equiv 72 \int_{x,y} \text{diagram} \quad (1.14)$$


The *effective* coupling thus becomes

$$g_{\text{eff}} = g - \frac{g^2}{2!} \times 72 \times \int_{x,y} \text{diagram} + \mathcal{O}(g^3) \quad (1.15)$$


We now have to evaluate the integral. This is easy if we choose to sit at the *critical point*  $m = 0$ . Then with  $r := |z|$

$$\begin{aligned} \int_{x-y} \text{diagram} &= \int d^d z \Theta(a < |z| < L) C(z)^2 = S_d \times \mathcal{C}_1^2 \int_a^L \frac{dr}{r} r^d \times r^{2(2-d)} \\ &= \frac{1}{S_d (d-2)^2} \frac{1}{4-d} (L^{4-d} - a^{4-d}) \simeq \left[ \frac{1}{8\pi^2} \frac{1}{\epsilon} + \mathcal{O}(\epsilon^0) \right] (L^\epsilon - a^\epsilon) \end{aligned} \quad (1.16)$$

We introduced the parameter

$$\epsilon := 4 - d. \quad (1.17)$$

In general we are interested in dimensions smaller than 4, thus dimensions for which  $\epsilon$  is positive. The parameter  $\epsilon$  is indeed the key to everything which follows, as it will serve as an expansion parameter, allowing us to construct a systematic expansion in it, which we already anticipated by retaining only the leading term in the  $\epsilon$  expansion. How does a small  $\epsilon$  help? The first important observation is that in general  $C(x-y)^2$  is non-local, thus replacing

$$\int_{x,y} \phi^2(x) \phi^2(y) C^2(x-y) \rightarrow \int_x \phi(x)^4 \int_z C(z)^2 \quad (1.18)$$

is a rather crude approximation. However, for  $\epsilon \rightarrow 0$  this approximation becomes exact, since for any smooth test function  $f(z)$  (which for simplicity of presentation we choose to depend only on  $r = |z|$ )

$$\int_z C(z)^2 f(z) \rightarrow S_d \times \mathcal{C}_1^2 \int_a^L \frac{dr}{r} r^\epsilon f(r) \simeq \frac{f(0)}{8\pi^2} \frac{1}{\epsilon} (L^\epsilon - a^\epsilon) + \mathcal{O}(\epsilon^0). \quad (1.19)$$

Mathematicians would say that

$$\frac{\epsilon}{S_d} |z|^{\epsilon-1} \simeq \delta^d(z) + \mathcal{O}(\epsilon). \quad (1.20)$$

It is exactly this type of divergences which one has to take care of when renormalizing a theory. Renormalizability means that the divergences only lead to local counter-terms. Another way to look at the integral (1.19) is to realize that for  $\epsilon \approx 0$  each scale, i.e. each piece of the integral from  $\ell$  to say  $2\ell$  contributes the same amount, and that for  $a \approx 0$  there are many scales between a small  $\ell$ , and the much smaller  $a$ . These many small scales dominate the integral, and make it local, i.e. allow us to replace  $f(z)$  by  $f(0)$ . Yet another way to state the same is to write  $f(r) = f(0) + r f'(0) + \dots$ , and insert this into the integral (1.19): due to the additional factor of  $r$ , the integral is no longer divergent at small  $r$ .

Finally, let us mention that there are stronger short-distance divergences. They usually lead to a (non-universal) shift of some parameters, as the critical temperature.



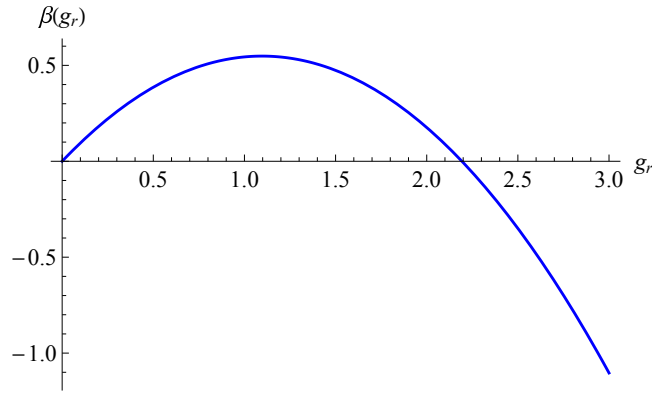


Figure 1.1: The 1-loop  $\beta$ -function (1.22).

**Exercise 1: Shift in  $T_c = m^2$ :** Show that the critical temperature  $T_c$  is corrected in 1-loop order by a term proportional to  $g(L^{2-d} - a^{2-d})$ ; it vanishes in the IR ( $L \rightarrow \infty$ ) but contains a non-universal UV scale  $a$ , say a lattice cutoff.

Let us now go one step further, and analyze what happens when we change the size of the system, or the microscopic cutoff  $a$ . As we are currently sitting at  $m = 0$ , where all correlation functions are power-laws, this does not make any difference. Our guiding idea, as proposed by Wilson in the 70's [11], is to find a limiting theory for  $L \rightarrow \infty$ . In order that the effective coupling  $g_{\text{eff}}$  does not depend on  $L$ , it is suggestive to make it first dimensionless. To this aim we define the dimensionless *renormalized* coupling constant

$$g_r := L^\epsilon g_{\text{eff}} = L^\epsilon g - \frac{9(gL^\epsilon)^2}{2\pi^2\epsilon} + \mathcal{O}(g^2). \quad (1.21)$$

The renormalization group asks: How does the renormalized  $g_r$  change under a change of  $L$ . This answer is obtained by putting together our above equations:

$$\begin{aligned} \beta(g_r) = \partial_L g_r &:= L \frac{\partial}{\partial L} g_r = L \frac{\partial}{\partial L} L^\epsilon g_{\text{eff}} = L \frac{\partial}{\partial L} \left[ L^\epsilon g - \frac{9(gL^\epsilon)^2}{2\pi^2\epsilon} + \dots \right] \equiv \epsilon g \frac{\partial}{\partial g} \left[ L^\epsilon g - \frac{9(gL^\epsilon)^2}{2\pi^2\epsilon} + \dots \right] \\ &= \epsilon \left[ L^\epsilon g - 2 \frac{9(gL^\epsilon)^2}{2\pi^2\epsilon} + \dots \right] = \epsilon g_r - \frac{9g_r^2}{2\pi^2} + \mathcal{O}(g_r^3) \end{aligned} \quad (1.22)$$

This function, plotted on figure 1.1, has the following properties:

- (i) a *Gaussian* (non-interacting) fixed point with  $\beta(0) = 0$ .
- (i) a non-trivial fixed point with  $\beta(g^*) = 0$  for

$$g^* = \frac{2\pi^2}{9}\epsilon. \quad (1.23) \text{gstar}$$

- (ii) for  $0 < g_r < g^*$  the function is positive, thus  $g_r$  increases.
- (ii) for  $g_r > g^*$  the function is negative, thus  $g_r$  decreases.

The fixed point with  $g_r = 0$  is unstable, i.e. a small value of  $g_r$  grows. On the other hand, the fixed point at  $g^*$  is attractive from both sides. Thus it governs the physics at large scales. We also call it the *IR* fixed point. Last, but no least, it is important to note that the non-trivial fixed point  $g^*$  is of order  $\epsilon$ . Thus it is accessible perturbatively (in a perturbation expansion in  $\epsilon$ ). This is crucial, as it makes this  $\epsilon$  expansion such a powerful tool. What we cannot really show here is that properties of the theory calculated at this

End  
Class 1  
(2019)  
(2020)



fixed point are universal, i.e. do not depend on microscopic details of the theory. A *hint* comes from the observation that for  $\epsilon > 0$ , the limit of  $a \rightarrow 0$  could be taken in the above calculations from the very beginning. This does not work in the critical dimension  $d = 4$ , in which the diagram (1.14) becomes  $\sim \ln(L/a)$ , thus depends on both the UV (small distance) and IR (large distance) cutoffs.

A related question, or concern, one may have is that the expression (1.16) does not diverge in the limit of  $\epsilon \rightarrow 0$ : Indeed

$$\lim_{\epsilon \rightarrow 0} \frac{1}{\epsilon} (L^\epsilon - a^\epsilon) = \ln \left( \frac{L}{a} \right), \quad (1.24)$$

and this is finite. So where is the divergence? Scale invariance appears in the *thermodynamic limit*, i.e. when  $L/a \rightarrow \infty$ , making the r.h.s. diverge. Physically, an infinite number of degrees of freedom work together *collectively*. Technically, this is reflected in the RG program, as the convergence to the fixed point given by the  $\beta$ -function (1.22) is only for  $L/a \rightarrow \infty$ . The microscopic cutoff  $a$  appears here as the starting point of the *RG* flow.

The value of the fixed point  $g^*$  is not the most interesting information contained in the  $\beta$ -function, as it depends on the chosen normalizations. A quantity which is universal is the correction-to-scaling exponent  $\omega$ ,

$$\omega(g_r) := -\beta'(g_r). \quad (1.25) \text{p1-1}$$

For the two fixed points above we find

$$\omega(0) = -\epsilon, \quad \omega(g^*) = \epsilon. \quad (1.26)$$

## Exercise 2: Correction-to-scaling exponent

Show that if a physical observable  $\mathcal{O}$  depends analytically on  $g$ , then for large  $L$  it behaves as

$$\mathcal{O} = \mathcal{O}_{L=\infty} + \text{const } L^{-\omega(g^*)} \quad (1.27) \text{p3-1}$$

### Solution

Assuming (1.27), we will show (1.25). To this aim we calculate

$$L \frac{d}{dL} \ln(\mathcal{O} - \mathcal{O}_{L=\infty}) := L \frac{d}{dL} \ln(\mathcal{O}(g_r) - \mathcal{O}(g^*)) \simeq L \frac{d}{dL} \ln(\mathcal{O}'(g^*)(g_r - g^*)) = \frac{\beta(g_r) - \beta(g^*)}{g_r - g^*} \simeq \beta'(g^*). \quad (1.28)$$

We used that  $\beta(g^*) = 0$ .

Let us now turn to the correction to the 2-point function, i.e. the anomalous exponent  $\eta$ , defined by

$$\langle \phi(x)\phi(y) \rangle \sim |x - y|^{2-d-\eta}. \quad (1.29)$$

To calculate this expectation in perturbation theory, we need to construct a diagram with two uncontracted  $\phi$  fields; this is equivalent to retaining in an OPE all terms which contain two powers of  $\phi$ .

End  
Class 1  
(2018)

## Exercise 3: Why is $\eta$ not corrected at order $g$ ?

From two  $\phi^4$  interactions one generates

$$\left[ \int_x \phi^4(x) \right] \times \left[ \int_y \phi^4(y) \right] \longrightarrow 96 \phi(x)\phi(y) \int_{x-y} C^3(x-y) = 96 \text{ } \begin{array}{c} \text{---} \text{---} \\ \text{---} \text{---} \\ \text{---} \text{---} \end{array} \text{ } . \quad (1.30) \text{p8}$$

We have

$$\phi(x)\phi(y) = \phi(x)^2 + \dots + \phi(x)\frac{1}{2}[(x-y)\nabla]^2\phi(x) \simeq \phi(x)^2 - \frac{1}{2}[(x-y)\nabla\phi(x)]^2 + \dots \quad (1.31)$$

The elasticity thus becomes corrected,

$$\frac{1}{2}[\nabla\phi(x)]^2 \rightarrow \frac{1}{2}[\nabla\phi(x)]^2 \left[ 1 + \frac{g^2 96}{2! d} C_1^3 S_d \int_a^L \frac{dr}{r} r^{3(2-d)+d+2} + \dots \right] \quad (1.32)$$

Evaluating the integral, and inserting for  $g$  its fixed-point value (1.23), we obtain

$$\frac{g^2 96}{2! d} C_1^3 S_d \int_a^L \frac{dr}{r} r^{3(2-d)+d+2} \simeq 12g^2 C_1^3 S_d \frac{1}{2\epsilon} (L^{2\epsilon} - a^{2\epsilon}) = \frac{\epsilon^2}{54} \frac{1}{2\epsilon} (L^{2\epsilon} - a^{2\epsilon}) . \quad (1.33)$$

The correlation function becomes corrected by the inverse of the square bracket in Eq. (1.32), namely

$$\langle \phi(0)\phi(L) \rangle = \frac{\langle \phi(0)\phi(L) \rangle_0}{1 + \frac{\epsilon^2}{54} \frac{1}{2\epsilon} (L^{2\epsilon} - a^{2\epsilon})} + \dots = L^{2-d} \left[ 1 - \frac{\epsilon^2}{54} \ln(L/a) + \dots \right] \simeq L^{2-d-\eta} . \quad (1.34)$$

Note that we have chosen to evaluate it at scale  $L$ , e.g. the system size. From this, we read off the exponent  $\eta$  as

$$\eta = \frac{\epsilon^2}{54} + \mathcal{O}(\epsilon^3) . \quad (1.35)$$

In standard textbooks this correction is obtained in momentum space, necessitating the evaluation of a 2-loop integral, where the number of loops stands for the independent  $k$  integrals in momentum space.

#### Exercise 4: Loop order

Show that evaluating a quantity at order  $g^n$  in perturbation theory leads to  $n$  space integrals, or equivalently  $n$  momentum integrals (loops). (Note: The correction to  $g$  in Eq. (1.13) is order  $g$ , not  $g^2$ ). Show that if the theory is renormalizable, these corrections are of order  $\epsilon^n$ .

#### Remark: Operator-Product expansion and normal-ordering

What we have done above in Eqs. (1.14) and (1.30)–(1.31) is called an *operator product expansion*. What we have put under the rug is that the  $\phi^4(x)$  in one interaction could also be Wick-contracted with itself. This problem can be taken care of by *normal-ordering*, indicated by dots. “:”. We define the normal order of an operator  $\mathcal{O}$  as

$$:\mathcal{O}: = \mathcal{O} - \text{all tadpole-like diagrams constructed from } \mathcal{O} . \quad (1.36)$$

In other words: By normal-ordering an operator, we subtract all self-contractions. Let us give some examples

$$\begin{aligned} :\phi^2(x): &= \phi^2(x) - C(0) \mathbb{1} , \\ :\phi(x)^4: &= \phi(x)^4 - 6C(0) :\phi^2(x): - 3C^2(0) \mathbb{1} . \end{aligned} \quad (1.37)$$

Normal ordering is a powerful tool to organize the perturbation expansion. Let us show this by reminding our previous calculation. We studied the short-distance behavior of two operators  $:\phi(x)^4:$  and  $:\phi^4(y):$  in an OPE. To this aim we first normal-order the product of the two interactions:

$$\begin{aligned} :\phi(x)^4: :\phi^4(y): &= :\phi(x)^4\phi^4(y): \\ &+ 16 :\phi^3(x)\phi^3(y): C(x-y) \\ &+ 72 :\phi^2(x)\phi^2(y): C^2(x-y) \\ &+ 96 :\phi(x)\phi(y): C^3(x-y) \\ &+ 24 \mathbb{1} C^4(x-y) . \end{aligned} \quad (1.38)$$

It is now essential that the normal-ordered product of two operators is free of divergences when these operators are approached; the divergences are contained in the powers of  $C(x - y)$ . E.g. at leading order, the first term in Eq. (1.38) becomes

$$:\phi(x)^4\phi^4(y): = :\phi^8(z): + \dots, \quad (1.39)$$

where  $z = \frac{x+y}{2}$ . Expanding all terms on the r.h.s. around the middle-point  $z$  gives us a systematic procedure to analyze the divergencies of the theory, and its renormalization.

### Exercise 5: Advantage of a normal-ordered theory

Show that using a normal-ordered theory, the critical temperature is not shifted at order  $g$ .

### Exercise 6: Evaluate $\eta$ from the correlation function $\langle\phi(z_1)\phi(z_2)\rangle$ .

Evaluate the correlation function  $\langle\phi(z_1)\phi(z_2)\rangle$  at scale  $|z_1 - z_2| = \ell \ll L$ . Show that two additional propagators appear between points  $x$  and  $z_1$  as well as  $y$  and  $z_2$  (plus a similar term with  $x$  and  $y$  exchanged). Show that these additional propagators ensure that the integral over  $x - y$  is cut off at scale  $\ell$ . Rederive  $\eta$ .

### Exercise 7: $\eta$ in standard diagrammatics

Recalculate  $\eta$  to 2-loop order, using standard momentum RG.

## 1.4 Euklidian versus relativistic field theory: Wick rotation

### Exercise 8: $\phi^4$ theory for a $n$ -component vector

Consider  $\mathcal{H}[\vec{\phi}] = \int_x \frac{1}{2}[\nabla\vec{\phi}(x)]^2 + \frac{m^2}{2}\vec{\phi}(x)^2 + g[\vec{\phi}(x)^2]^2$ . Derive the  $\beta$ -function and  $\eta$ . What happens for  $n = -2$ ?

### Exercise 9: An arbitrary interaction

Show that if one replaces in Eq. (1.1)  $\phi^4$  by an arbitrary analytic function  $\mathcal{V}(\phi)$ , then the 1-loop diagram (1.14) is replaced by  $\frac{1}{2} \int_{x,y} V''(\phi(x))V''(\phi(y))C(x - y)^2$ . It has some curious fixed points [12].

## 1.5 Large $N$

### Exercise 10: Simplification for large $N$

Show that at large  $N$  all diagrams renormalizing the coupling constant are a geometric sum, constructed from the 1-loop diagram. What is  $\eta$  at leading order in  $1/N$ ?

## 1.6 Large-order behavior of perturbation theory: A toy integral

Consider

$$\mathcal{I}(g) := \int_{-\infty}^{\infty} \frac{dx}{\sqrt{2\pi}} e^{-x^2/2 - gx^4}. \quad (1.40)$$

Where is the integral defined? Derive its series expansion in  $g$ . Is this series convergent? How can it be resummed? Give the expansion for large  $g$ .

## Solution

$\mathcal{I}(g)$  has a branch-cut singularity on the negative real axis for all  $g < 0$ , since the integral is not defined there. This implies that no convergent series expansion can exist. Indeed,

$$\mathcal{I}(g) = \sum_{n=0}^{\infty} a_n (-g)^n, \quad a_n = \frac{(4n)!}{2^{2n} (2n)! n!} \quad (1.41) \text{ofg}$$

Using Stirling's formula  $n! \simeq \sqrt{2\pi n} \left(\frac{n}{e}\right)^n$ , one obtains

$$a_n = \frac{(4n)!}{(2n)! n! 2^{2n}} \simeq \frac{2^{4n}}{\sqrt{2\pi n}} \times n!. \quad (1.42)$$

Thus this series is *divergent*. In field theory, we usually do not know the coefficients  $a_n$ , but we can obtain their large- $n$  asymptotics from a saddle-point analysis. To this aim write

$$a_n = \frac{2}{n!} \int_0^{\infty} \frac{dx}{\sqrt{2\pi}} (x^4)^n e^{-x^2/2} = \frac{2}{n!} \int_0^{\infty} \frac{dx}{\sqrt{2\pi}} e^{-x^2/2 + 4n \ln x} = \frac{2\sqrt{n}}{n!} \int_0^{\infty} \frac{dx}{\sqrt{2\pi}} e^{-n[x^2/2 - 4 \ln x] + 2n \ln(n)} \quad (1.43) \text{48-1}$$

The saddle point is obtained for  $\partial_x[x^2/2 - 4 \ln(x)] = 0$ , i.e. for  $x_{\text{saddle}} = 2$ . Inserting this, we find  $\partial_x^2[x^2/2 - 4 \ln(x)]|_{x=x_{\text{saddle}}} = 1/\sqrt{2}$ , thus

$$a_n \simeq \sqrt{2} \times 16^n \left(\frac{n}{e}\right)^{2n} \simeq \frac{2^{4n}}{\sqrt{2\pi n}} \times n!, \quad (1.44)$$

in agreement with Eq. (1.43).

For large  $n$ , and  $g < g_c = \frac{e}{16n}$ , the series *seemingly* converges up to order  $n$ , whereas it diverges for larger  $n$ . So what can be done? A convergent series can be obtained by using the so-called Borel transform, defined as

$$\mathcal{I}_B(t) := \sum_{n=0}^{\infty} \frac{a_n (-t)^n}{n!}. \quad (1.45) \text{-Borel-trans}$$

It indeed converges, with convergence radius of  $1/16$ . It has a branch-cut singularity at  $t = -1/16$ . If we succeed to continue  $\mathcal{I}_B(t)$  for all  $t > 0$ , then  $\mathcal{I}(g)$  can be reconstructed from  $\mathcal{I}_B(t)$  by (prove it!)

$$\mathcal{I}(g) = \int_0^{\infty} dt e^{-t} \mathcal{I}_B(tg). \quad (1.46) \text{inverse-Borel}$$

In order to continue  $\mathcal{I}_B(t)$  to the positive real axis, we map the complex plane with the branch cut starting at  $g_{bc} = -1/16$  onto the inside of the unit-circle,

$$z = \frac{\sqrt{1 - t/g_{bc}} - 1}{\sqrt{1 - t/g_{bc}} + 1} \iff t = \frac{-4g_{bc} z}{(z - 1)^2}. \quad (1.47) \text{gbc}$$

We are thus led to construct a series in  $z$ ,

$$f(z) := \sum_{n=0}^{\infty} c_n z^n = \sum_{n=0}^{\infty} \frac{a_n (-t(z))^n}{n!} = \mathcal{I}_B(t(z)),$$

by expanding both sides in  $z$ . This series is expected to converge in  $z$  for  $|z| < 1$ , a fact we can check for our example (but which is difficult to prove in general),

$$f(z) = 1 - \frac{3z}{4} + \frac{9z^2}{64} - \frac{51z^3}{256} + \frac{1353z^4}{16384} - \frac{7347z^5}{65536} + \frac{61617z^6}{1048576} + \mathcal{O}(z^7).$$

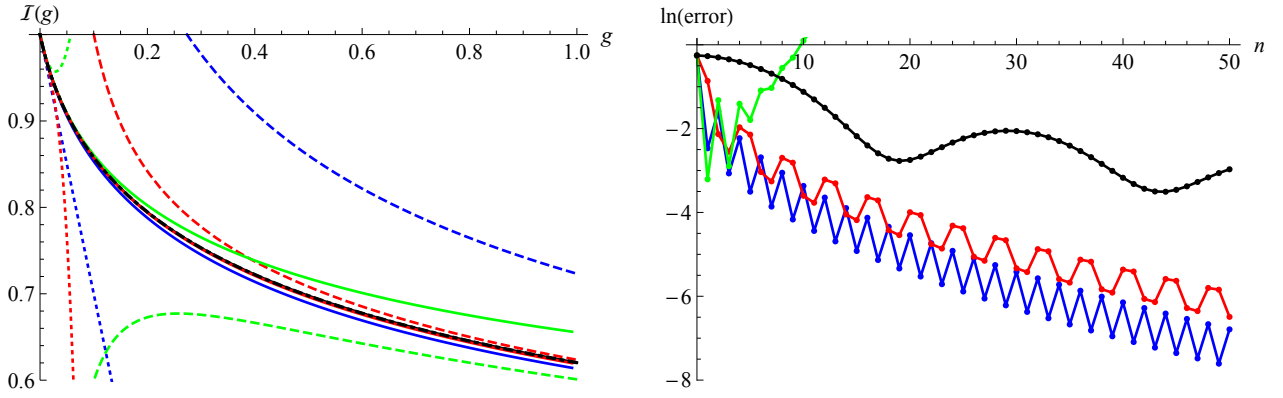


Figure 1.2: Left: The function  $\mathcal{I}(g)$  (black, thick, dot-dashed) and its diverse approximations: Dotted for the series expansion at order 1 (blue), 2 (green), and 3 (red). Solid for the resummed series at the same order. Dashed for the large- $g$  expansion (same color code). Right: Deviation of the resummed series (1.48) from the exact result (1.49) for  $g = 10$  as a function of  $n$ . In blue for  $g_{bc} = -1/16$ , in red  $g_{bc} = -1/32$ , in black  $g_{bc} = -1/1000$ . Resummation with  $g_{bc} = -1/15$  (green) does not work. (The result is even complex.) Taking a too small value of  $g_{bc}$  makes the series slowly convergent, but convergent nevertheless.

(Check this!) We finally obtain

$$\mathcal{I}(g) = \int_0^\infty dt e^{-t} \mathcal{I}_B(tg) = \frac{1}{g} \int_0^\infty dt e^{-t/g} \mathcal{I}_B(t) = \frac{1}{g} \int_0^1 dz t'(z) e^{-t(z)/g} f(z). \quad (1.48)$$

An asymptotic expansion for large  $g$  can be obtained by setting  $gx^4 \rightarrow y$ , which yields

$$\mathcal{I}(g) := \frac{1}{2\sqrt{2\pi} \sqrt[4]{g}} \int_0^\infty dy \frac{e^{-\frac{\sqrt{y}}{2\sqrt{g}} - y}}{y^{3/4}} = \frac{1}{2\sqrt{2\pi} \sqrt[4]{g}} \left[ \Gamma\left(\frac{1}{4}\right) - \frac{2}{3} \frac{\Gamma\left(\frac{7}{4}\right)}{\sqrt{g}} + \frac{\Gamma\left(\frac{5}{4}\right)}{8g} + \mathcal{O}(g^{-5/4}) \right]$$

Finally, the exact solutions for  $\mathcal{I}(g)$  and  $\mathcal{I}_B(t)$  are special functions, namely the Bessel- $K$  function for  $\mathcal{I}(g)$ , and the elliptic  $K$  function for  $\mathcal{I}_B(t)$ ,

$$\mathcal{I}(g) = \frac{e^{\frac{1}{32g}} K_{\frac{1}{4}}^{\text{Bessel}}\left(\frac{1}{32g}\right)}{4\sqrt{\pi g}}, \quad \mathcal{I}_B(t) = \frac{2K^{\text{elliptic}}\left(\frac{1}{2} - \frac{1}{2\sqrt{16t+1}}\right)}{\pi \sqrt[4]{16t+1}} \quad (1.49)_{\text{ofg-exact}}$$

On figure 1.2 one can see that the direct series expansion fails miserably already for  $g = 0.1$ . Resummation works well, at order 3 even at  $g = 1$ . For large  $g$  the asymptotic expansion becomes quite good. (Our plot is not fair, as it emphasizes the range of small  $g$ .)

## 1.7 Large-order behavior of field theory, instantons

Let us now generalize the large-order analysis of perturbation theory from the simple integral (1.40) to the partition function of  $\phi^4$  theory given in Eq. (1.2):

$$\mathcal{Z}(g) := \frac{1}{\mathcal{Z}(0)} \int \mathcal{D}[\phi] e^{-\int_x \frac{1}{2} [\nabla\phi(x)]^2 + \frac{m^2}{2} \phi(x)^2 + g\phi(x)^4} = \sum_{n=1}^{\infty} a_n \frac{(-g)^n}{n!}, \quad a_0 = 1. \quad (1.50)_{\text{phi4action}}$$

$$\begin{aligned} a_n &= \frac{1}{\mathcal{Z}(0)} \int \mathcal{D}[\phi] e^{-\int_x \frac{1}{2} [\nabla\phi(x)]^2 + \frac{m^2}{2} \phi(x)^2} \left[ \int_x \phi(x)^4 \right]^n \\ &= \frac{1}{\mathcal{Z}(0)} \int \mathcal{D}[\phi] e^{-\int_x \left\{ \frac{1}{2} [\nabla\phi(x)]^2 + \frac{m^2}{2} \phi(x)^2 \right\} + n \ln(\int_x \phi(x)^4)} \end{aligned} \quad (1.51)$$

The idea is again to find a saddle point at  $n$  large. To this aim, change variables  $\phi(x) \rightarrow \sqrt{n} \phi(x)$ . We obtain

$$a_n = \frac{\int \mathcal{D}[\phi] e^{-n \left\{ \int_x \frac{1}{2} [\nabla \phi(x)]^2 + \frac{m^2}{2} \phi(x)^2 - \ln \left( \int_x \phi(x)^4 \right) \right\} + 2n \ln(n)}}{\int \mathcal{D}[\phi] e^{-n \int_x \frac{1}{2} [\nabla \phi(x)]^2 + \frac{m^2}{2} \phi(x)^2}} \simeq n^{2n} e^{-n \mathcal{H}_{\text{sp}}[\phi_{\text{sp}}]} \quad (1.52)$$

$$\mathcal{H}_{\text{sp}}[\phi] = \int_x \frac{1}{2} [\nabla \phi(x)]^2 + \frac{m^2}{2} \phi(x)^2 - \ln \left( \int_x \phi(x)^4 \right) \quad (1.53)$$

The saddle-point equation reads

$$0 = \frac{\delta}{\delta \phi(x)} \mathcal{H}_{\text{sp}}[\phi] \Big|_{\phi=\phi_{\text{sp}}} = -\nabla^2 \phi(x) + m^2 \phi(x) - 4g_c \phi^3(x) \Big|_{\phi=\phi_{\text{sp}}} \quad (1.54) \text{SP-eq}$$

$$\frac{1}{g_c} = \int_x \phi(x)^4 \Big|_{\phi=\phi_{\text{sp}}} \quad (1.55) \text{45-1}$$

The shorthand  $g_c$  in the last equation reminds of the coupling constant in the original model. While  $g_c$  is positive, the coupling constant is  $-g_c$ , as it appears with an additional minus sign in Eq. (1.54). The corresponding saddle-point solution, also called instanton, can be interpreted as the classical solution of the equations of motion separating a collapsing from an expanding state, after adding time (we will discuss this later).

Having found the saddle-point solution  $\phi_{\text{sp}}(x)$ , one inserts the latter into Eq. (1.53) to obtain the large- $n$  behavior of  $a_n$  from Eq. (1.52). If there exist several solutions, the one with the smallest action  $\mathcal{H}_{\text{sp}}$  will dominate. Let us also mention that Eq. (1.54) is the classical equation of motion for the field  $\phi$ , and is commonly referred to as an *instanton* equation. Had we performed a Wick-rotation before, we would have found a traveling wave solution, commonly referred to as *soliton*. (Some authors use these terms interchangeably.)

In general, the instanton (saddle-point) equation (1.52) is difficult to solve in closed form. Since our main tool is the  $\epsilon$  expansion, and we are interested in the critical point  $m = 0$ , let us consider the particular case  $d = 4$  and  $m = 0$ , for which a simple analytical solution exists: Our experience from quantum mechanics tells us that the lowest-energy eigenfunctions are spherically symmetric, and have no knots. The Laplacian in radial coordinates  $r = |x|$  is

$$\nabla^2 f(r = |x|) = r^{1-d} \partial_r r^{d-1} \partial_r f(r)$$

A solution of Eq. (1.54) is given by

$$\phi_{\text{sp}}(r) = \frac{a}{\frac{g_c a^2}{2} + r^2}, \quad (1.56)$$

where the parameter  $a$  can be chosen freely. Solving Eq. (1.55), we find (independent of  $a$ )

$$g_c = \frac{2}{3} \pi^2 \quad (1.57)$$

To obtain the action  $\mathcal{H}_{\text{sp}}[\phi]$ , we have to work out the missing integral ... or be clever and lazy. Since in a more complicated setting a brute-force calculation is difficult, let us show a useful trick: Multiplying Eq. (1.54) by  $\phi(x)$ , and integrating over space yields

$$\int_x -\phi(x) \nabla^2 \phi(x) + m^2 \phi(x)^2 - 4g_c \phi^4(x) \Big|_{\phi=\phi_{\text{sp}}} = 0. \quad (1.58)$$

Integrating the first term by parts, and using the definition (1.55) for  $g_c$  yields

$$\int_x \frac{1}{2} [\nabla \phi_{\text{sp}}(x)]^2 + \frac{m^2}{2} \phi_{\text{sp}}^2(x) = 2. \quad (1.59)$$

Thus, finally

$$a_n \simeq \left(\frac{n}{e}\right)^{2n} \frac{1}{g_c^n} \simeq \frac{(n!)^2}{2\pi n} \frac{1}{g_c^n} \quad (1.60)$$

(Note how the 2 from Eq. (1.59) nicely combines with the  $n^{2n}$  in Eq. (1.52).) If again we do a Borel-transform, we realize that the radius of convergence is  $g_c$ ; thus the branch-cut starts at  $g_c$ , i.e. we can hope to again use the conformal mapping (1.47) with  $g_{\text{bc}} = g_c$ .

End  
Class 2  
(2020)

## 1.8 Padé resummation

Suppose we know a series up to order  $N$ ,

$$s(t) = \sum_{n=0}^N b_n (-t)^n + \mathcal{O}(x^{N+1}) \quad (1.61)$$

Then for all  $k_1, k_2 \in \mathbb{N}$ , with  $k_1 + k_2 = N$ , there exist coefficients  $c_n$  and  $d_n$ , s.t.

$$s_{k_2}^{k_1}(t) := \frac{\sum_{n=0}^{k_1} c_n t^n}{1 + \sum_{n=1}^{k_2} d_n t^n} = s(x) + \mathcal{O}(x^{k+1}) \quad (1.62)$$

This is the so-called *Padé resummation* of order  $(k_1, k_2)$ , and (1.62) the *Padé approximant*. In practice, the diagonal Padé approximants with  $k_1 \approx k_2$  often work best.

### Exercise 11: Padé approximants for a geometric series

Write down a geometric series as  $(1 - ax)/(1 - bx)$ , and evaluate the Padé approximants. How many series coefficients do you need to recover the full series?

## 1.9 Padé-Borel resummation

Consider again the sum (1.41), and its Borel-transform (1.45). Suppose we know the  $N$  first coefficients, i.e.

$$\mathcal{I}_B^N(t) := \sum_{n=0}^N b_n (-t)^n, \quad b_n = \frac{(4n)!}{2^{2n} (2n)! (n!)^2}. \quad (1.63)$$

Then there are  $N$  distinct Padé approximants of the form (1.62), with  $k_1$  zeroes (from the numerator) and  $k_2$  poles (zeros of the denominator). On figure 1.3 we show their location in the complex plane. For  $k_1 = k_2$  they all lie on the negative real axes. Having a pole on the positive real axes is bad; in practice it is best to have them as far away as possible. Finally, the Borel transform  $\mathcal{I}_B(t)$  in general neither blows up, nor vanishes quickly. (This is easily checked for the example.) Then it is clear that the best approximation for large  $t$  is given by a Padé approximant for which numerator and denominator *almost* cancel for large  $t > 0$ , thus  $k_1 \leq k_2$ , and  $k_1 \approx k_2$ . This choice best approximates the analytic structure of  $\mathcal{I}_B(t)$  for  $t > 0$  (right of figure 1.3), and thus yields the best resummation under the inverse Borel-transform (1.46).

Finally note that the precision achieved is much less than that using the conformal transform (1.47).



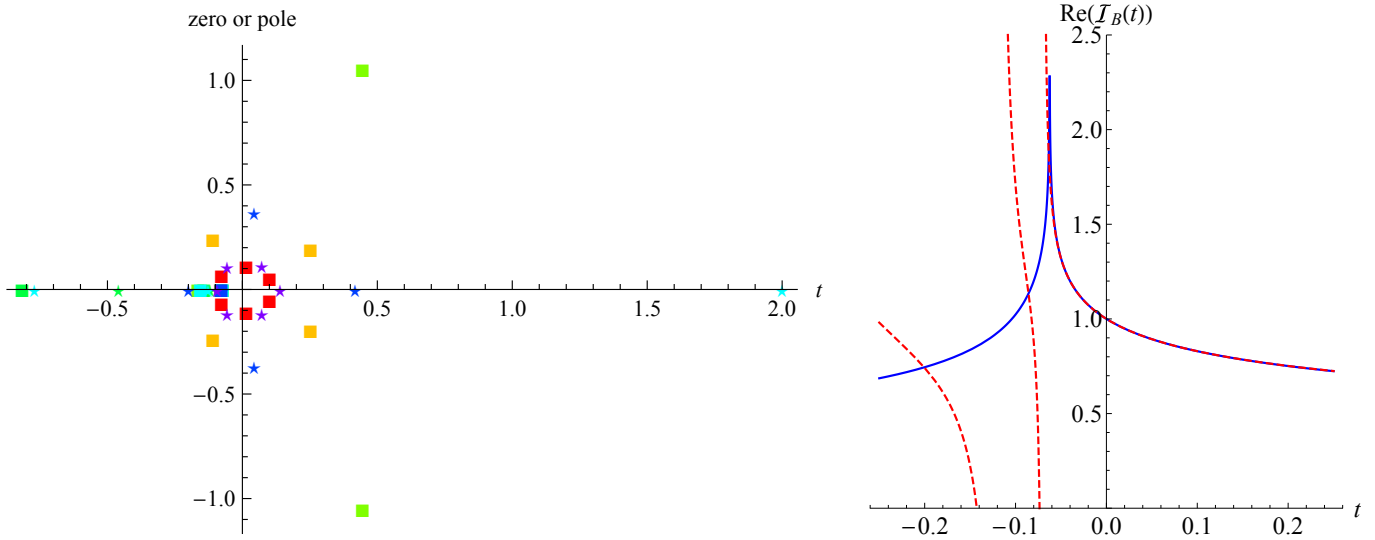


Figure 1.3: Left: Zeros (squares) and poles (stars) of the Padé-approximants (1.62) for the sum (1.63) at order  $N = 6$ . Colors are from red ( $k_1 = N$ ) over orange, yellow, green and cyan to blue ( $k_1 = 0$ ). For  $k_1 = k_2 = 3$  the three zeros and poles are on the negative real axes, yielding the best approximation. Right: Borel-transform  $\mathcal{I}_B(t)$  (in blue), and the (3,3)-Padé approximant. Note the singularity at  $t = -1/16$ , and spurious poles and zeros for smaller  $t$ .

## 1.10 Meijer-G resummation

## 1.11 Resummation in “real life”: $\phi^4$ -theory

## 1.12 Renormalons in renormalizable theories, and their absence in super-renormalizable ones

### Exercise 12: Strong-coupling expansion for $\phi^4$ -theory

Study the  $\phi^4$ -theory (1.50) on a lattice with lattice constant  $a$ . Rescale  $\phi$  s.t. for  $g \rightarrow \infty$  the pathintegral becomes up to a normalization ( $i$  indexes the lattice points, and  $\langle i, j \rangle$  indicates nearest neighbors)

$$\mathcal{Z}(g) = \prod_i \left[ \frac{2}{\Gamma(\frac{1}{4})} \int_{-\infty}^{\infty} d\varphi_i \right] e^{-\mathcal{H}[\varphi]}, \quad \mathcal{H}[\varphi] = \sum_{\langle i, j \rangle} \frac{a^{d/2-2}}{2\sqrt{g}} (\varphi_i - \varphi_j)^2 + \sum_i \frac{m^2 a^{d/2}}{2\sqrt{g}} \varphi_i^2 + \sum_i \varphi_i^4$$

Show that  $\lim_{g \rightarrow \infty} \mathcal{Z}(g) = 1$ . Construct an expansion in  $1/\sqrt{g}$ . This expansion has two vertices (which?). For which choice of  $m^2$  only one vertex remains? Study the latter expansion. It resembles the high-temperature expansion of the Ising model, except that  $\sigma_i^n \rightarrow \frac{1}{2} \sum_{\sigma_i} \sigma_i^n = \delta_{n, \text{even}}$  is replaced by

$$\varphi_i^n \rightarrow \frac{2}{\Gamma(\frac{1}{4})} \int_{-\infty}^{\infty} d\varphi_i \varphi_i^n e^{-\varphi_i^4} = \frac{\Gamma(\frac{n+1}{4})}{\Gamma(\frac{1}{4})} \delta_{n, \text{even}} .$$

This is known as the high-temperature expansion of the soft-spin version of the Ising model. Its convergence can be improved by using as measure  $e^{b\varphi^2 - \varphi^4}$ , with  $b \approx 1.14$ , instead of  $b = 0$  [13].

## 2 Self-avoiding polymers and membranes

### 2.1 Self-avoiding polymers and their mapping onto $\phi^4$ theory

The action for a self-avoiding polymer is usually written as

$$\mathcal{H}[r] = \int_0^\ell dt \frac{1}{4} [\partial_t r(t)]^2 + \frac{b}{4} \int_0^\ell dt \int_0^\ell du \delta^d(r(t) - r(u)). \quad (2.1)$$

We claim that it can be mapped onto the  $n \rightarrow 0$  limit of  $\phi^4$ -theory. To this aim consider the discretized version of the Edwards-model

$$G(r, r_0, L) = \prod_{s=1}^L \int \frac{d^d r_s}{(4\pi\lambda)^{d/2}} \exp\left(-\sum_{t=0}^{L-1} \frac{(r_t - r_{t+1})^2}{4\lambda} - \frac{b\lambda^2}{4} \sum_{t=0}^L \sum_{u=0}^L \delta^d(r_t - r_u)\right), \quad (2.2)$$

where the first and last monomer are fixed by  $r(0) = r_0, r(L) = r$ .  $L$  is the number of monomers,  $\lambda$  their length, and the integration measure is normalized such that  $\int \frac{d^d r_s}{(4\pi\lambda)^{d/2}} \exp(-r^2/4\lambda) = 1$ . With this normalization and setting  $b = 0$ ,  $G$  is the probability conserving diffusion propagator at time  $t = \lambda L$ .

The self-avoidance interaction can be disentangled through an auxiliary field  $\Psi(r)$ . This is sometimes referred to as *Hubbard-Stratonovich transformation*. To do so, we introduce

$$\rho(r) := \lambda \sum_{t=0}^L \delta^d(r - r_t). \quad (2.3)$$

Thus

$$\lambda^2 \sum_{t=0}^L \sum_{u=0}^L \delta^d(r_t - r_u) = \int d^d r \rho^2(r) \quad (2.4)$$

The interaction term can thus be written as

$$\begin{aligned} \exp\left(-\frac{b\lambda^2}{4} \sum_{t=0}^L \sum_{u=0}^L \delta^d(r_t - r_u)\right) &= \exp\left(-\frac{b}{4} \int d^d r \rho^2(r)\right) \\ &= \int \mathcal{D}[\Psi] \exp\left(-\int d^d r i\psi(r)\rho(r) + \frac{\Psi(r)^2}{b}\right), \end{aligned} \quad (2.5)$$

where a suitable normalization factor is absorbed into the integration measure  $\mathcal{D}[\Psi]$ . This yields

$$G(r, r_0, L) = \int \mathcal{D}[\Psi] \prod_{s=1}^L \frac{d^d r_s}{(4\pi\lambda)^{d/2}} \exp\left(-\sum_{t=0}^{L-1} \frac{(r_t - r_{t+1})^2}{4\lambda} + \sum_{t=0}^L i\lambda\Psi(r_t)\right) \exp\left(-\int d^d r \frac{\Psi(r)^2}{b}\right). \quad (2.6)$$

One then sees, that the first part, namely the partition function of the polymer in the potential  $\Psi(r)$

$$G(r, r_0, L; \Psi) := \prod_{s=1}^L \int \frac{d^d r_s}{(4\pi\lambda)^{d/2}} \exp\left(-\sum_{t=0}^{L-1} \frac{(r_t - r_{t+1})^2}{4\lambda} + \sum_{t=0}^L i\lambda\Psi(r_t)\right) \quad (2.7)$$

satisfies the equation

$$G(r, r_0, L + 1; \Psi) = \int \frac{d^d r'}{(4\pi\lambda)^{d/2}} e^{-(r'-r)^2/4\lambda} e^{i\lambda\Psi(r)} G(r', r_0, L; \Psi). \quad (2.8)$$

In the limit of a continuous chain,  $\lambda$  becomes small and the r.h.s. can be expanded in  $\lambda$ , with the result

$$G(r, r_0, L + 1; \Psi) = (1 + i\lambda\Psi(r) + \lambda\Delta_r + \mathcal{O}(\lambda^2)) G(r, r_0, L; \Psi) . \quad (2.9)$$

This can also be written as ( $\ell := \lambda L$ )

$$\frac{\partial}{\partial \ell} G(r, r_0, \ell; \Psi) = (i\Psi(r) + \Delta_r) G(r, r_0, \ell; \Psi) . \quad (2.10)$$

Using a notation inspired from quantum mechanics, the solution to this equation is

$$G(r, r_0, \ell; \Psi) = \langle r | e^{-\ell(-i\Psi(r) - \Delta_r)} | r_0 \rangle . \quad (2.11)$$

The usual method, to solve this equation in quantum mechanics, consists in going from the “time-dependent” Schrödinger-equation to the “time-independent” one. In statistical mechanics one equivalently writes down the Laplace-transform

$$\bar{G}(r, r_0, m^2; \Psi) := \int_0^\infty d\ell e^{-\ell m^2} G(r, r_0, \ell; \Psi) , \quad (2.12) \text{:LaplaceTra}$$

which gives

$$\bar{G}(r, r_0, m^2; \Psi) = \left\langle r \left| \frac{1}{m^2 - i\Psi(r) - \Delta_r} \right| r_0 \right\rangle . \quad (2.13) \text{:Green}$$

This is up to a factor of  $Z^{-n}$  the correlation-function of a  $n$ -component scalar field theory,

$$\bar{G}(r, r_0, m^2; \Psi) = Z^{-n} \int \mathcal{D}[\phi] \phi_1(r) \phi_1(r_0) e^{-\frac{1}{2} \int_r \vec{\phi}(r) [m^2 - i\Psi(r) - \Delta_r] \vec{\phi}(r)} , \quad (2.14)$$

where  $Z$  is the partition function of the 1-component version,

$$Z = \int \mathcal{D}[\phi] e^{-\frac{1}{2} \int_r \phi(r) (m^2 - i\Psi(r) - \Delta_r) \phi(r)} . \quad (2.15)$$

Formally, the factor of  $Z^{-n}$  is easily eliminated by setting  $n = 0$ . Combining Eqs. (2.6), (2.12), (2.13) and the latter statement, one obtains that the Laplace-transformed polymer correlation-function

$$\bar{G}(r, r_0, m^2) := \int_0^\infty dt e^{-\ell m^2} G(r, r_0, \ell) , \quad (2.16)$$

where  $G(r, r_0, \ell)$  is the continuum version of  $G(r, r_0, L)$ , equals

$$\bar{G}(r, r_0, m^2) = \lim_{n \rightarrow 0} \int \mathcal{D}[\Psi] \mathcal{D}[\phi] \phi_1(r) \phi_1(r_0) e^{-\frac{1}{2} \int_r \vec{\phi}(r) [m^2 - i\Psi(r) - \Delta_r] \vec{\phi}(r)} e^{-\int_r \Psi(r)^2 / b} . \quad (2.17)$$

The path-integral over  $\Psi$  can still be performed to obtain the final result

$$\bar{G}(r, r_0, m^2) = \lim_{n \rightarrow 0} \int \mathcal{D}[\phi] \phi_1(r) \phi_1(r_0) e^{-\mathcal{H}_{\phi^4}[\phi]} \quad (2.18) \text{polymer-phi}$$

$$\mathcal{H}_{\phi^4}[\phi] = \int d^d r \left( \frac{m^2}{2} \vec{\phi}^2(r) + \frac{1}{2} \left[ \nabla \vec{\phi}(r) \right]^2 + \frac{b}{16} \left[ \vec{\phi}^2(r) \right]^2 \right) .$$

This is the path-integral representation of a correlation function in the  $n$ -component  $\phi^4$ -model, after taking the limit of  $n \rightarrow 0$ . This remarkable result, first discovered by De Gennes [14], allows for two seemingly unrelated methods to calculate the same physical quantities.

The derivation given above allows for some straightforward generalizations. Consider as in Eq. (2.2)

$$G(r, r_0, L) = \prod_{s=1}^L \int \frac{d^d r_s}{(4\pi\lambda)^{d/2}} \exp(-\mathcal{H}_{\text{polymer}}^{\text{gen}}[r]) , \quad (2.19)$$

with

$$\mathcal{H}_{\text{polymer}}^{\text{gen}}[r] = \sum_{t=0}^{L-1} \frac{(r_t - r_{t+1})^2}{4\lambda} + \int d^d r' \mathcal{F}[\rho(r')] . \quad (2.20)$$

$\rho(r')$  is the polymer-density

$$\rho(r') = \lambda \sum_{t=0}^L \delta^d(r_t - r') , \quad (2.21)$$

and  $\mathcal{F}[\rho(r')]$  any functional of  $\rho(r')$ . Then, following the same lines as above

$$\begin{aligned} \bar{G}(r, r_0, t) &= \lim_{n \rightarrow 0} \int \mathcal{D}[\phi] \phi_1(r) \phi_1(r_0) e^{-\mathcal{H}_{\mathcal{F}}[\phi]} \\ \mathcal{H}_{\mathcal{F}}[\phi] &= \int d^d r \left( \frac{t}{2} \vec{\phi}^2(r) + \frac{1}{2} [\nabla \vec{\phi}(r)]^2 + \mathcal{F} \left[ \frac{1}{2} \vec{\phi}^2(r) \right] \right) . \end{aligned} \quad (2.22)$$

The key result (in continuous notation) is

$$\rho(r) := \int dx \delta^d(r(x) - r) \longleftrightarrow \frac{1}{2} \vec{\phi}^2(r) . \quad (2.23)$$

Other operators one can consider are

$$\int dx \int dy \delta^d(r(x) - r(y)) \longleftrightarrow \int d^d r \left[ \frac{1}{2} \vec{\phi}^2(r) \right]^2 \quad (2.24)$$

$$\int dx \int dy \int dz \delta^d(r(x) - r(y)) \delta^d(r(x) - r(z)) \longleftrightarrow \int d^d r \left[ \frac{1}{2} \vec{\phi}^2(r) \right]^3 \quad (2.25)$$

$$\int dx \int dy (-\Delta_r) \delta^d(r(x) - r(y)) \longleftrightarrow \int d^d r \left[ \frac{1}{2} \vec{\phi}^2(r) \right] (-\Delta_r) \left[ \frac{1}{2} \vec{\phi}^2(r) \right] \quad (2.26)$$

Let us give some elementary examples: First of all, the diffusion propagator for a polymer of length  $\ell$  is

$$G_0(r, r_0, \ell) = \frac{1}{(4\pi\ell)^{d/2}} e^{-\frac{(r-r_0)^2}{4\ell}} = \int \frac{d^d k}{(2\pi)^d} e^{ik(r-r_0) - k^2 \ell} \quad (2.27)$$

The latter representation of the diffusion propagator in terms of a Fourier integral is often convenient, as we will see shortly. It can also be derived as the expectation in the polymer theory, with  $r_0 \equiv r(0)$ ,

$$\begin{aligned} G_0(r, r_0, \ell) &= \langle \delta^d(r(\ell) - r) \rangle_0 = \int \frac{d^d k}{(2\pi)^d} \langle e^{ik[r-r(\ell)]} \rangle_0 = \int \frac{d^d k}{(2\pi)^d} e^{ik(r-r_0)} \langle e^{ik[r_0-r(\ell)]} \rangle_0 \\ &= \int \frac{d^d k}{(2\pi)^d} e^{ik(r-r_0)} e^{-k^2 \frac{1}{2d} \langle [r(\ell) - r_0]^2 \rangle_0} = \int \frac{d^d k}{(2\pi)^d} e^{ik(r-r_0)} e^{-k^2 \ell} \end{aligned} \quad (2.28)$$

Its Laplace-transform is

$$\int_0^\infty d\ell G_0(r, r_0, \ell) e^{-\ell m^2} = \int \frac{d^d k}{(2\pi)^d} \frac{e^{ik(r-r_0)}}{k^2 + m^2} . \quad (2.29)$$

Thus in (spatial) Fourier-space the free propagators are  $e^{-k^2\ell}$  and  $1/(k^2 + m^2)$ , respectively. We thus confirmed the mapping (2.18) at  $b = 0$ .

As a check of the above abstract derivation, let us give the order- $b$  correction to the propagator: First of all, in the polymer-language, this reads, with  $0 < x < y < \ell$ ,

$$\begin{aligned}
\text{Diagram} &= \iint_{0 < x < y < \ell} \langle \delta^d(r(\ell) - r) \delta^d(r(x) - r(y)) \rangle_0 \\
&= \iint_{0 < x < y < \ell} \int \frac{d^d k}{(2\pi)^d} \int \frac{d^d p}{(2\pi)^d} e^{ik(r-r_0)} \langle e^{ik[r(0)-r(\ell)] + ip[r(x)-r(y)]} \rangle_0 \\
&= \iint_{0 < x < y < \ell} \int \frac{d^d k}{(2\pi)^d} \int \frac{d^d p}{(2\pi)^d} e^{ik(r-r_0)} e^{-k^2(\ell-y+x) - (k+p)^2(y-x)} \quad (2.30)
\end{aligned}$$

Its Laplace transform is,

$$\begin{aligned}
\int_0^\infty d\ell e^{-m^2\ell} \text{Diagram} &= \int_0^\infty d\ell e^{-m^2\ell} \iint_{0 < x < y < \ell} \int \frac{d^d k}{(2\pi)^d} \int \frac{d^d p}{(2\pi)^d} e^{ik(r-r_0)} e^{-k^2(\ell-y+x) - (k+p)^2(y-x)} \\
&= \int_0^\infty d\ell_1 \int_0^\infty d\ell_2 \int_0^\infty d\ell_3 e^{-m^2(\ell_1+\ell_2+\ell_3)} \int \frac{d^d k}{(2\pi)^d} \int \frac{d^d p}{(2\pi)^d} e^{ik(r-r_0)} e^{-k^2(\ell_1+\ell_3) - (k+p)^2\ell_2} \quad (2.31)
\end{aligned}$$

In the last line we changed variables to the distances  $\ell_1 = x$ ,  $\ell_2 = y - x$ , and  $\ell_3 = \ell - y$ . Doing the  $\ell$ -integrals, we arrive at

$$\int_0^\infty d\ell e^{-m^2\ell} \text{Diagram} = \int \frac{d^d k}{(2\pi)^d} \int \frac{d^d p}{(2\pi)^d} e^{ik(r-r_0)} \frac{1}{(k^2 + m^2)^2} \frac{1}{p^2 + m^2} \quad (2.32)$$

(We shifted the momentum  $p$  in the last expression.) This is the same expression as the Fourier-transformed 2-point function in  $\phi^4$ -theory. In the latter theory, there is a second diagram at the same order in  $b$ , normally drawn as

$$\text{Diagram} \quad (2.33)$$

It has the same momentum integral as Eq. (2.32), but contains an additional factor of  $n$ , thus vanishes at  $n = 0$ .

### Exercise 13: Combinatorial factors of self-avoiding polymers versus $\phi^4$ theory

Show that in both theories the diagram (2.32) comes with a factor of  $-b/2$ .

## 2.2 Self-avoiding manifolds

We start from the continuous model for a  $D$ -dimensional flexible polymerized membrane introduced in [15, 16]. This model is a simple extension of the well known Edwards' model for continuous chains. The

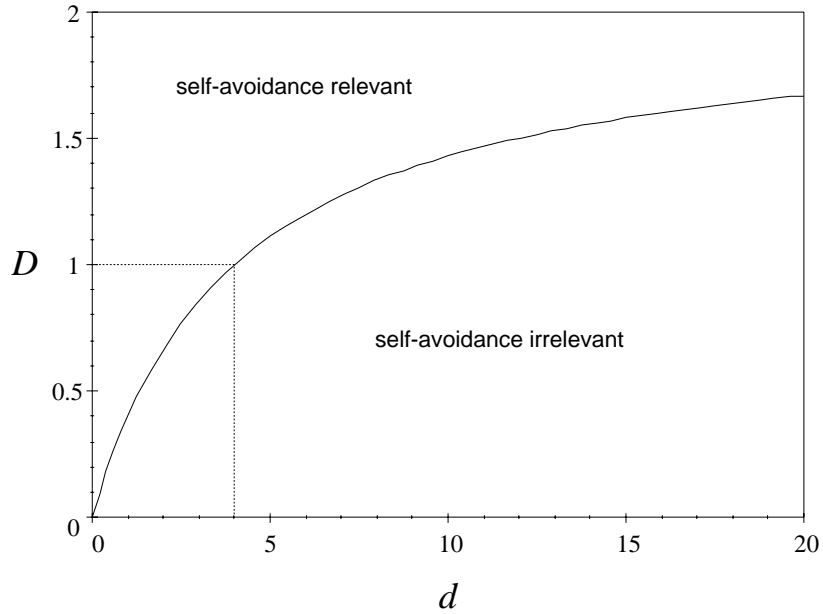


Figure 2.1: The critical curve  $\epsilon(D, d) = 0$ . The dashed line corresponds to the standard polymer perturbation theory, critical in  $d = 4$ .

membrane fluctuates in  $d$ -dimensional space. Points in the membrane are labeled by coordinates  $x \in \mathbb{R}^D$  and the configuration of the membrane in physical space is described by the field  $r : x \in \mathbb{R}^D \rightarrow r(x) \in \mathbb{R}^d$ , i.e. from now on we note  $r$  instead of  $\vec{r}$ . At high temperatures the free energy for a configuration is given by the (properly rescaled) Hamiltonian

$$\mathcal{H}[r] = \frac{Z}{2-D} \int_x \frac{1}{2} (\nabla r(x))^2 + b Z_b \mu^\epsilon \iint_{x,y} \tilde{\delta}^d(r(x) - r(y)) . \quad (2.34)$$

The so-called renormalization-factors  $Z$  and  $Z_b$  have the form  $Z = 1 + O(b)$  and  $Z_b = 1 + O(b)$ ; they will be explained later. The reader may safely set both to 1 for the moment. The integral  $\int_x$  runs over  $D$ -dimensional space and  $\nabla$  is the usual gradient operator. The normalizations are

$$\int_x := \frac{1}{S_D} \int d^D x , \quad S_D = 2 \frac{\pi^{D/2}}{\Gamma(D/2)} \quad (2.35)$$

and

$$\tilde{\delta}^d(r(x) - r(y)) = (4\pi)^{d/2} \delta^d(r(x) - r(y)) . \quad (2.36)$$

The latter term is normally used in Fourier-representation

$$\tilde{\delta}^d(r(x) - r(y)) = \int_p e^{ip[r(x)-r(y)]} , \quad (2.37)$$

where the normalization of  $\int_p$  is given by

$$\int_p = \pi^{-d/2} \int d^d p \quad (2.38)$$

to have

$$\int_p e^{-p^2 a} = a^{-d/2} . \quad (2.39)$$

All normalizations are chosen in order to simplify the calculations, but are unimportant for the general understanding.  $\mu$  is an internal momentum scale, such that  $\mu x$  is dimensionless. It is introduced to render the coupling  $b$  dimensionless. The first term in the Hamiltonian is a Gaussian elastic energy which is known to describe the free “phantom” surface. The interaction term corresponds (for  $b > 0$ ) to a weak repulsive interaction upon contact. The expectation values of physical observables are obtained by performing the average over all field-configurations  $r(x)$  with the Boltzmann weight  $e^{-\mathcal{H}[r]}$ . This average can not be calculated exactly, but one can expand about the configurations of a phantom, i.e. non-interacting surface.

Such a perturbation theory is constructed by performing the series expansion in powers of the coupling constant  $b$ . This expansion suffers from ultraviolet (UV) divergences which have to be removed by renormalization and which are treated by dimensional regularization, i.e. analytical continuation in  $D$  and  $d$ . A physical UV-cutoff could be introduced instead, but would render the calculations more complicated. Long-range infrared (IR) divergences also appear. They can be eliminated by using a finite membrane, or by studying translationally invariant observables, whose perturbative expansion is also IR-finite in the thermodynamic limit (infinite membrane). Such observables are “neutral” products of vertex operators

$$\mathcal{O} = \prod_{a=1}^N e^{ik_a r(x_a)}, \quad \sum_{a=1}^N k_a = 0. \quad (2.40)$$

An example is given at the end of subsection 2.5.

Let us now analyze the theory by power-counting. We use internal units  $\mu \sim 1/x$ , and note  $[x]_x = 1$ , and  $[\mu]_x = -[\mu]_\mu = -1$ . The dimension of the field and of the coupling-constant are:

$$\nu := [r]_x = \frac{2-D}{2}, \quad \epsilon := [b\mu^\epsilon]_\mu = 2D - \nu d. \quad (2.41)$$

In the sense of Wilson [11] the interaction is relevant for  $\epsilon > 0$ , see figure 2.1. Perturbation theory is then expected to be UV-finite except for subtractions associated to relevant operators. We shall come back to this point later.

For clarity, we represent graphically the different interaction terms which have to be considered. The local operators are

$$1 = \mathbf{1} \quad (2.42)$$

$$\frac{1}{2}(\nabla r(x))^2 = \text{✦} . \quad (2.43)$$

The bi-local operator, the dipole, is

$$\tilde{\delta}^d(r(x) - r(y)) = \bullet \text{---} \bullet . \quad (2.44)$$

The expectation-value of an observable is

$$\langle \mathcal{O}[r] \rangle_b = \frac{\int \mathcal{D}[r] \mathcal{O}[r] e^{-\mathcal{H}[r]}}{\int \mathcal{D}[r] e^{-\mathcal{H}[r]}} . \quad (2.45)$$

Perturbatively, all expectation-values are taken with respect to the free theory:

$$\langle \mathcal{O}[r] \rangle_0 = \frac{\int \mathcal{D}[r] \mathcal{O}[r] e^{-\frac{1}{2-D} \int_x \frac{1}{2}(\nabla r(x))^2}}{\int \mathcal{D}[r] e^{-\frac{1}{2-D} \int_x \frac{1}{2}(\nabla r(x))^2}} . \quad (2.46)$$



A typical term in the expansion of (2.45) is

$$(-bZ_b\mu^\epsilon)^n \iint \dots \iint \langle \mathcal{O} \bullet \text{---} \bullet \dots \bullet \text{---} \bullet \rangle_0^c, \quad (2.47)$$

where the integral runs over the positions of all dipole-endpoints.

## 2.3 Flory estimate

Before going on to the *real* theory, let us give a rough estimate for the radius of gyration. The latter is defined as

$$R_g^2 = \frac{1}{L^{2D}} \int_{x,y} [r(x) - r(y)]^2. \quad (2.48)$$

Flory suggests that it can be estimated by balancing the two terms in Eq. (2.34). Replacing  $r$  by  $R_g$ , this yields

$$L^{D-2} R_g^2 \sim L^{2D} R_g^{-d}. \quad (2.49)$$

Solving for  $R_g$  yields

$$R_g \sim L^\nu, \quad \nu = \nu_{\text{Flory}} := \frac{D+2}{d+2}. \quad (2.50)$$

For self-avoiding polymers ( $D=1$ ) in  $d=2, 3$  and  $d=4-\epsilon$  this yields

$$\nu_{\text{Flory}}(d=2) = \frac{3}{4}, \quad \nu_{\text{Flory}}(d=3) = \frac{3}{5}, \quad \nu_{\text{Flory}}(d=4-\epsilon) = \frac{1}{2} + \frac{\epsilon}{12} + \frac{\epsilon^2}{72} + \mathcal{O}(\epsilon^3). \quad (2.51)$$

While the value in  $d=2$  is exact, in  $d=3$  the [best](#) known value is  $\nu = 0.59\dots$  [\[1\]](#). Also, the coefficient of order  $\epsilon$  is not  $1/12$ , but  $1/16$ , see Eq. (2.122). So while a good approximation, the Flory estimate is systematically wrong.

## 2.4 Locality of divergences

In this section, we show that all divergences are short distance divergences. Note that even for massless theories and in the absence of IR-divergences, this is not trivial. Divergences could as well appear, when some of the distances involved become equal, or multiple of each other. A simple counter-example is the integral of  $\left||a| - |b|\right|^{-\nu d}$ , where  $a$  and  $b$  are two of the distances involved.

That divergences only occur at short distances (i.e. when at least one of the distances involved tends to 0), is a consequence of Schoenbergs theorem [\[17\]](#). Here, we present an proof, based on the equivalence with electrostatics.

We first state that with our choice of normalizations, the free correlation function  $C(x_1, x_2)$

$$\begin{aligned} C(x_1, x_2) &:= \frac{1}{d} \left\langle \frac{1}{2} [r(x_1) - r(x_2)]^2 \right\rangle_0 = |x_1 - x_2|^{2-D} \\ &\equiv (2-D) S_D \int \frac{d^D p}{(2\pi)^D} \frac{1}{p^2} (1 - e^{ip(x_1-x_2)}) \end{aligned} \quad (2.52)$$

is the Coulomb potential in  $D$  dimensions. Furthermore, the interaction part of the Hamiltonian  $\mathcal{H}$  is reminiscent of a dipole, and can be written as

$$\begin{aligned} \mathcal{H}_{\text{int}} &= bZ_b\mu^\epsilon \int_{x_1} \int_{x_2} \tilde{\delta}^d(r(x_1) - r(x_2)) \\ &= bZ_b\mu^\epsilon \int_{x_1} \int_{x_2} \int_k e^{ik[r(x_1)-r(x_2)]}, \end{aligned} \quad (2.53)$$

where  $k$  may be seen as a  $d$ -component (vector-) charge.

The next step is to analyze the divergences appearing in the perturbative calculation of expectation values of observables. To simplify the calculations, we focus on the normalized partition function

$$\frac{\mathcal{Z}}{\mathcal{Z}_0} = \frac{1}{\mathcal{Z}_0} \sum_{\text{all configurations}} e^{-\mathcal{H}} = \langle e^{-\mathcal{H}_{\text{int}}} \rangle_0 . \quad (2.54)$$

To exhibit the similarity to Coulomb systems, consider the second order term

$$\begin{aligned} \frac{1}{2} \langle \mathcal{H}_{\text{int}}^2 \rangle_0 &= \frac{(bZ_b\mu^\epsilon)^2}{2} \int \int \int \int \int \int \langle e^{ik[r(x_1)-r(x_2)]} e^{ip[r(y_1)-r(y_2)]} \rangle_0 \\ &= \frac{(bZ_b\mu^\epsilon)^2}{2} \int \int \int \int \int \int e^{-E_c} \\ E_c &= k^2 C(x_1 - x_2) + p^2 C(y_1 - y_2) \\ &\quad + kp [C(x_1 - y_2) + C(x_2 - y_1) - C(x_1 - y_1) - C(x_2 - y_2)] , \end{aligned} \quad (2.55)$$

where  $E_c$  is the Coulomb-energy of a configuration of dipoles with charges  $\pm k$ , and  $\pm p$ , respectively. More generally, for any number of dipoles (and even for any Gaussian measure) we have

$$\langle e^{i \sum_i k_i r(x_i)} \rangle_0 = e^{-E_c} , \quad E_c = \frac{1}{2} \sum_{i,j} \langle k_i r(x_i) k_j r(x_j) \rangle_0 . \quad (2.56)$$

Since  $\sum_i k_i = 0$ , the latter can be rewritten with the help of the usual correlation function  $C(x - y) = \frac{1}{2d} \langle [r(x) - r(y)]^2 \rangle_0$  as

$$E_c = -\frac{1}{4d} \sum_{i,j} k_i k_j \langle [r(x_i) - r(x_j)]^2 \rangle_0 . \quad (2.57)$$

As for any configuration of dipoles, specified by their coordinates and charges, the total charge is zero, the Coulomb-energy is bounded from below, i.e.

$$E_c \geq 0 . \quad (2.58)$$

Formally, this is proven by the following line of equalities (remember that  $D < 2$ )

$$\begin{aligned} E_c &= \frac{1}{2} \sum_{i,j} \langle k_i r(x_i) k_j r(x_j) \rangle_0 \\ &= \frac{(2-D)S_D}{2} \int \frac{d^D p}{(2\pi)^D} \sum_{i,j} k_i k_j \frac{1}{p^2} e^{ip(x_i - x_j)} \\ &= \frac{(2-D)S_D}{2} \int \frac{d^D p}{(2\pi)^D} \frac{1}{p^2} \left| \sum_i k_i e^{ipx_i} \right|^2 \geq 0 . \end{aligned} \quad (2.59)$$

The last inequality is again due to the global charge neutrality, which ensures convergence of the integral for small  $p$ . Hence,  $E_c$  vanishes, if and only if the charge density vanishes everywhere. This implies that

$$e^{-E_c} \leq 1 , \quad (2.60)$$

and the equality is obtained for vanishing charge density. Noting  $E_c = \sum_{i,j} k_i k_j Q_{ij}$ , Eq. (2.59) even states that as long as  $x_i \neq x_j$  for all  $i \neq j$ ,  $Q_{ij}$  is a non-degenerate form on the space of  $k_i$  with  $\sum_i k_i = 0$ . This

implies that integrating  $e^{-E_c}$  as in Eq. (2.55) over all  $k_i$  with  $\sum_i k_i = 0$  gives a finite result, as long as not some of the  $x_i$  coalesce. Consequently, divergences in the integration over  $x_i$  can only appear when at least some of the distances vanish, as stated above.

This does of course not rule out IR-divergences. We will see later that they are absent in translationally invariant observables. An explicit example is given at the end of the next section; for a proof see [18].

## 2.5 More about perturbation theory

Let us apply the above observation to evaluating the integrals in Eq. (2.55); this will give an intuitive idea of the kind of counter-terms needed to cancel the UV-divergences, as will be made formal later. The basic idea is to look for classes of configurations which are similar. The integral over the parameter which indexes such configurations is the product of a divergent factor, and a “representative” operator. For the case of two dipoles, one with charge  $k$  and the other with charge  $p - k$ , and approaching its endpoints (as indicated by the dashed lines below), one only sees a single dipole with charge  $p$  from far away, i.e.

$$\begin{array}{c} k \quad \text{---} \quad -k \\ \text{---} \quad \text{---} \\ p-k \quad \text{---} \quad -p+k \end{array} \approx p \text{---} \text{---} -p \times e^{-k^2(|s|^{2-D} + |t|^{2-D})}. \quad (2.61)$$

The second factor on the r.h.s. contains the dominant part of the Coulomb energy  $E_c = k^2(|s|^{2-D} + |t|^{2-D})$  of the interaction between the two dipoles;  $s$  and  $t$  are the distances between the contracted (approached) ends. The integral over  $k$  is now factorized, and we obtain

$$\int_k e^{-k^2(|s|^{2-D} + |t|^{2-D})} = (|s|^{2-D} + |t|^{2-D})^{-d/2}. \quad (2.62)$$

Finally integrating over  $p$  in Eq. (2.61) gives back the  $\delta$ -interaction  $\text{---} \text{---}$  multiplied with  $(\text{---} \text{---} | \text{---} \text{---})$ , where we define the coefficient as

$$(\text{---} \text{---} | \text{---} \text{---}) = (|s|^{2-D} + |t|^{2-D})^{-d/2}. \quad (2.63)$$

The notation, which will be explained later, reminds of a scalar product or projection of a singular configuration of two dipoles onto a single dipole. Eq. (2.63) contains the dominant UV-divergence upon approaching the endpoints; this will be made formal later.

As an example of an expectation value, use in Eq. (2.40) the observable  $\mathcal{O} = e^{ik[r(s) - r(t)]}$ , which is the generating function for the moments of  $[r(s) - r(t)]$ ; the series up to first order in  $b$  reads (remind  $Z_b = 1 + O(b)$ )

$$\begin{aligned} \langle \mathcal{O} \rangle_b &= e^{-k^2 C(s-t)} \times \\ &\left\{ 1 + b\mu^\epsilon \iint_{x,y} \left[ 1 - \exp\left( \frac{1}{4} k^2 \frac{[C(s-x) + C(t-y) - C(s-y) - C(t-x)]^2}{C(x-y)} \right) \right] C(x-y)^{-d/2} \right. \\ &\quad \left. + O(b^2) \right\}. \end{aligned} \quad (2.64)$$

Note that the integral over  $x$  and  $y$  is IR-convergent, but UV-divergent at  $\epsilon \leq 0$ : There is a singularity for  $|x - y| \rightarrow 0$ . This is a general feature of such expectation values. The purpose of the rest of this section is to introduce the basic tools to handle these divergences. On the example of Eq. (2.64), this is verified in exercise F.5, see page 166.

## 2.6 Multilocal operator product expansion (MOPE)

In section 2.4, we showed that for self-avoiding membranes divergences only occur at short distances. The situation is thus similar to local field-theories for which we discussed in the last section how the techniques of operator product expansion can be used to analyze the divergences. Our aim is now, to generalize these techniques to the multilocal case [19, 18]. Intuitively, in the context of multilocal theories – by which we mean that the interaction depends on more than one point – we also expect multilocal operators to appear in such an operator product expansion, which therefore will be called “multi-local operator product expansion” (MOPE). Its precise definition is the aim of this section, whereas we shall calculate some examples in the following one.

We start our analysis by recalling the general form of a (local) operator product expansion of two scaling-operators  $\Phi_\alpha(z + \lambda x)$  and  $\Phi_B(z + \lambda y)$  in a massless theory in the limit of  $\lambda \rightarrow 0$ :

$$\Phi_\alpha(z + \lambda x)\Phi_B(z + \lambda y) = \sum_i C_i(z, \lambda x, \lambda y) \Phi_i(z), \quad (2.65)\text{m:OPE}$$

where  $C_i(z, \lambda x, \lambda y)$  are homogeneous functions of  $\lambda$

$$C_i(z, \lambda x, \lambda y) = \lambda^{[\Phi_\alpha]_x + [\Phi_B]_x - [\Phi_i]_x} C_i(z, x, y). \quad (2.66)\text{m:OPE-coef}$$

Here  $[\Phi]_x$  is the canonical dimension of the operator  $\Phi$  in space-units such that  $[x]_x = 1$ , as obtained by naive power-counting. If the theory is translationally invariant,  $C_i(z, x, y)$  is also independent of  $z$ , and we will suppose that this is the case, if not stated otherwise<sup>1</sup>. Also recall that this relation is to be understood as an operator identity, i.e. it holds inserted into *any* expectation value, as long as none of the other operators sits at the point  $z$ , to which the contraction is performed.

An example for the multilocal theory is

$$= \sum_i C_i(\dots) \dots \quad (2.67)\text{m:contraction}$$

Let us explain the formula. We consider  $n$  dipoles (here  $n = 5$ ) and we separate the  $2n$  end-points into  $m$  subsets (here  $m = 3$ ) delimited by the dashed lines. The MOPE describes how the product of these  $n$  dipoles behaves when the points inside each of the  $m$  subsets are contracted towards a single point  $z_j$ . The result is a sum over *multilocal* operators  $\Phi_i(z_1, \dots, z_m)$ , depending on the  $m$  points  $z_1, \dots, z_m$ , of the form

$$\sum_i C_i(x_1 - z_1, \dots) \Phi_i(z_1, z_2, \dots, z_m), \quad (2.68)\text{m:etheMope}$$

where the MOPE-coefficients  $C_i(x_1 - z_1, \dots)$  depend only on the distances  $x_l - z_j$  *inside each subset*. This expansion is again valid as an operator-identity, i.e. inserted into any expectation value and in the limit of small distances between contracted points. Again, no other operator should appear at the points  $z_1, \dots, z_m$ , towards which the operators are contracted. As the Hamiltonian (2.34) does not contain a mass-scale, the MOPE-coefficients are as in Eq. (2.66) homogeneous functions of the relative positions between

<sup>1</sup>Translation invariance is e.g. broken when regarding systems with boundaries or initial time problems, see [20] for a review. It is also broken when the underlying metric is not constant, see [18, 21].

the contracted points, with the degree of homogeneity given by simple dimensional analysis. In the case considered here, where  $n$  dipoles are contracted to an operator  $\Phi_i$ , this degree is simply  $-n\nu d - [\Phi_i]_x$ . This means that

$$C_i(\lambda(x_1 - z_1), \dots) = \lambda^{-n\frac{2-D}{2}d - [\Phi_i]_x} C_i(x_1 - z_1, \dots), \quad (2.69)$$

where  $[\Phi_i]_x$  is the canonical dimension of the operator  $\Phi_i$  and  $-d(2-D)/2$  is simply the canonical dimension of the dipole.

In order to evaluate the associated singularity, one finally has to integrate over all relative distances inside each subset. This gives an additional scale factor with degree  $D(2n - m)$ . A singular configuration, such as in Eq. (2.67), will be UV-divergent if this degree of divergence

$$D(2n - m) - n\frac{2-D}{2}d - [\Phi_i]_x, \quad (2.70)$$

is negative. It is superficially divergent if the degree is zero and convergent otherwise. The idea of renormalization, formalized in section 2.9 and proven to work in [22], is to remove exactly these superficially divergent contributions recursively.

## 2.7 Evaluation of the MOPE-coefficients

The MOPE therefore gives a convenient and powerful tool to calculate the dominant and all subdominant contributions from singular configurations. In this section, we explain how to calculate the MOPE-coefficients on some explicit examples. These examples will turn out to be the necessary diagrams at 1-loop order.

In the following we shall use the notion of normal-ordering introduced at the end of section 1.3. The first thing, which we use, is that

$$:e^{ikr(x)}: = e^{ikr(x)}. \quad (2.71)\text{m:NO}$$

Explicitly, tadpole-like contributions which are powers of

$$\int d^D p \frac{1}{p^2} \quad (2.72)$$

are omitted. This is done via a finite part prescription (analytic continuation, dimensional regularization), valid for infinite membranes, for which the normal-order prescription is defined. Let us stress that this is a pure technical trick, which is not really necessary. However, adopting this notation, the derivation of the MOPE-coefficients is much simplified, and we will henceforth stick to this convention. The suspicious reader may always check that the same results are obtained without this procedure. This is clear from the uniqueness of the finite-part prescription.

The key-formula for all further manipulations is

$$:e^{ikr(x)}::e^{ipr(y)}: = e^{kpC(x-y)} :e^{ikr(x)}e^{ipr(y)}: . \quad (2.73)\text{m:key}$$

This can be proven as follows: Consider the (free) expectation value of any observable  $\mathcal{O}$  times the operators of Eq. (2.73). Then the the left- and right-hand sides of the above equation read

$$\begin{aligned} \mathcal{L} &= \langle \mathcal{O} :e^{ikr(x)}::e^{ipr(y)}: \rangle_0 \\ \mathcal{R} &= e^{kpC(x-y)} \langle \mathcal{O} :e^{ikr(x)}e^{ipr(y)}: \rangle_0 . \end{aligned}$$

First of all, for  $\mathcal{O} = 1$ , the desired equality of  $\mathcal{L} = \mathcal{R}$  holds, because

$$\langle :e^{ikr(x)}e^{ipr(y)}: \rangle_0 = 1 \quad \text{and} \quad \langle :e^{ikr(x)}::e^{ipr(y)}: \rangle_0 = e^{kpC(x-y)} .$$

Now consider a non-trivial observable  $\mathcal{O}$ , and contract all its fields  $r$  with  $e^{ikr(x)}$  or  $e^{ipr(y)}$ , before contracting any of the fields  $r(x)$  with  $r(y)$ . The result is a product of correlation-functions between the points in  $\mathcal{O}$  and  $x$  or  $y$ , and these are equivalent for both  $\mathcal{L}$  and  $\mathcal{R}$ . However, contracting an arbitrary number of times  $e^{ikr(x)}$ , leaves the exponential  $e^{ikr(x)}$  invariant. Completing the contractions for  $\mathcal{L}$  therefore yields a factor of  $e^{kpC(x-y)}$ , and the latter one also appears in  $\mathcal{R}$ . Thus, the equality of  $\mathcal{L}$  and  $\mathcal{R}$  holds for all  $\mathcal{O}$  and this proves Eq. (2.73).

Now proceed to the first explicit example, the contraction of a single dipole with endpoints  $x$  and  $y$ .

$$\text{Diagram: A circle with two dots labeled } x \text{ and } y \text{ inside.} = \int_k :e^{ikr(x)}::e^{-ikr(y)}: . \quad (2.74)$$

This configuration may have divergences when  $x$  and  $y$  come close together. Let us stress that in contrast to  $\phi^4$ -theory, these divergences are not obtained as a finite sum of products of correlators: Since  $C(x-y) = |x-y|^{2-D}$ , the latter is always well-behaved at  $x=y$ . The singularity only appears when summing an infinite series of diagrams as we will do now. To this purpose, we first normal-order the two exponentials using Eq. (2.73)

$$\int_k :e^{ik[r(x)-r(y)]}: e^{-k^2|x-y|^{2\nu}} . \quad (2.75)$$

Note that the operators  $e^{ikr(x)}$  and  $e^{-ikr(y)}$  are free of divergences upon approaching each other, since no more contractions can be made. The divergence is captured in the factor  $e^{-k^2|x-y|^{2\nu}}$ . Therefore, we can expand the exponential  $:e^{ik[r(x)-r(y)]}: for small  $x-y$  and consequently in powers of  $[r(x)-r(y)]$ . This expansion is$

$$\int_k \left\{ \mathbf{1} + ik[r(x)-r(y)] - \frac{1}{2}(k[r(x)-r(y)])^2 + \dots \right\} :e^{-k^2|x-y|^{2\nu}}: . \quad (2.76)$$

We truncated the expansion after the third term. It will turn out later that this is sufficient, since subsequent terms in the expansion are proportional to irrelevant operators for which the integral over the MOPE-coefficient is UV-convergent.

Due to the symmetry of the integration over  $k$  the term linear in  $k$  vanishes. Also due to symmetry, the next term can be simplified with the result

$$\int_k \left[ \mathbf{1} - \frac{k^2}{2d} : [r(x)-r(y)]^2 : + \dots \right] e^{-k^2|x-y|^{2\nu}} . \quad (2.77)$$

Finally, the integration over  $k$  can be performed. Recall that normalizations were chosen such that  $\int_k e^{-sk^2} = s^{-d/2}$  to obtain

$$|x-y|^{-\nu d} \mathbf{1} - \frac{1}{4} : (x-y)\nabla r \left( \frac{x+y}{2} \right) :^2 : |x-y|^{-\nu(d+2)} + \dots . \quad (2.78)$$

The second operator has a tensorial structure, which has to be taken into account in order to construct the subtraction operator. Using the short-hand notation  $\alpha \dashv \beta = \frac{1}{2}(\partial_\alpha r)(\partial_\beta r)$ , we can write this symbolically as

$$\text{Diagram: A circle with two dots labeled } \alpha \text{ and } \beta \text{ inside.} = \left( \text{Diagram: A circle with two dots and a vertical line segment labeled } \mathbf{1} \text{ to its right.} \right) \mathbf{1} + \left( \text{Diagram: A circle with two dots and a vertical line segment labeled } \alpha \dashv \beta \text{ to its right.} \right) \alpha \dashv \beta + \dots , \quad (2.79)$$

with the MOPE-coefficients (reminding Feynman's bra-ket notation)

$$\left( \text{Diagram: A circle with two dots and a vertical line segment labeled } \mathbf{1} \text{ to its right.} \right) = |x-y|^{-\nu d} \quad (2.80)$$

$$\left( \text{Diagram: A circle with two dots and a vertical line segment labeled } \alpha \dashv \beta \text{ to its right.} \right) = -\frac{1}{2} (x-y)_\alpha (x-y)_\beta |x-y|^{-\nu(d+2)} . \quad (2.81)$$

As long as the angular average is taken (and this will be the case when integrating the MOPE-coefficient to obtain the divergence), we can replace in Eq. (2.79)  $\alpha \dashv \beta$  by  $\dashv := \frac{1}{2}(\nabla r)^2$  and Eq. (2.81) by

$$\left( \text{Diagram: a circle with two dots inside and a vertical line with a dot on top} \right) = -\frac{1}{2D} |x - y|^{D-\nu d}. \quad (2.82)$$

Next consider a real multi-local example of an operator-product expansion, namely the contraction of two dipoles towards a single dipole:

$$\begin{array}{c} x+u/2 \\ \bullet \\ x-u/2 \end{array} \begin{array}{c} \bullet \\ \bullet \end{array} \begin{array}{c} y+v/2 \\ \bullet \\ y-v/2 \end{array} = \int_k e^{ik[r(x+u/2)-r(y+v/2)]} \int_p e^{ip[r(x-u/2)-r(y-v/2)]}. \quad (2.83)$$

This has to be analyzed for small  $u$  and  $v$ , in order to control the divergences in the latter distances. As above, we normal-order operators which are approached, yielding

$$e^{ikr(x+u/2)} e^{ipr(x-u/2)} = :e^{ikr(x+u/2)} : :e^{ipr(x-u/2)} : = :e^{ikr(x+u/2)} e^{ipr(x-u/2)} : e^{kpC(u)}. \quad (2.84)$$

A similar formula holds when approaching  $e^{-ikr(y+v/2)}$  and  $e^{-ipr(y-v/2)}$

$$e^{-ikr(y+v/2)} e^{-ipr(y-v/2)} = :e^{-ikr(y+v/2)} : :e^{-ipr(y-v/2)} : = :e^{-ikr(y+v/2)} e^{-ipr(y-v/2)} : e^{kpC(v)}. \quad (2.85)$$

Eq. (2.83) then becomes

$$\int_k \int_p :e^{ikr(x+u/2)+ipr(x-u/2)} : :e^{-ikr(y+v/2)-ipr(y-v/2)} : e^{kp[C(u)+C(v)]}. \quad (2.86)$$

In order to keep things as simple as possible, let us first extract the leading contribution before analyzing subleading corrections. This leading contribution is obtained when expanding the exponential operators (here exemplified for the second one) as

$$:e^{-ikr(y+v/2)} e^{-ipr(y-v/2)} : = :e^{-i(k+p)r(y)} (1 + O(\nabla r)) : \quad (2.87)$$

and dropping terms of order  $\nabla r$ . This simplifies Eq. (2.86) to

$$\int_k \int_p :e^{i(k+p)r(x)} : :e^{-i(k+p)r(y)} : e^{kp[C(u)+C(v)]}. \quad (2.88)$$

In the next step, first  $k$  and second  $p$  are shifted

$$k \longrightarrow k - p, \quad \text{then} \quad p \longrightarrow p + \frac{k}{2}. \quad (2.89)$$

The result is, dropping the normal-ordering according to Eq. (2.71)

$$\int_k e^{ik[r(x)-r(y)]} \int_p e^{(\frac{1}{4}k^2 - p^2)[C(u)+C(v)]}. \quad (2.90)$$

The factor of  $\int_k e^{ik[r(x)-r(y)]}$  is again a  $\delta$ -distribution, and the leading term of the short distance expansion of Eq. (2.90). Derivatives of the  $\delta$ -distribution appear when expanding  $e^{(\frac{1}{4}k^2 - p^2)[C(u)+C(v)]}$  in  $k^2$ ; these are less relevant and only the first sub-leading term will be displayed for illustration:

$$\begin{aligned} & \int_k e^{ik[r(x)-r(y)]} \int_p e^{-p^2[C(u)+C(v)]} \left( 1 + \frac{k^2}{4} [C(u) + C(v)] + \dots \right) \\ & = \left( \text{Diagram: two dipoles connected by a line} \right) + \left( \text{Diagram: two dipoles connected by a line with a dot} \right) + \dots, \end{aligned} \quad (2.91)$$



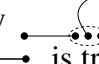
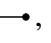
where in analogy to Eqs. (2.79) and (2.81)

$$\begin{aligned} \left( \begin{array}{c} \text{---} \\ \text{---} \end{array} \right) &= [C(u) + C(v)]^{-d/2}, \\ \left( \begin{array}{c} \text{---} \\ \text{---} \end{array} \right) &= \frac{1}{4} [C(u) + C(v)]^{1-d/2} \end{aligned} \quad (2.92)$$

and

$$\text{---} = \tilde{\delta}^d(r(x) - r(y)), \quad \text{---} = (-\Delta_r) \tilde{\delta}^d(r(x) - r(y)). \quad (2.93)$$

Let us already mention that the leading contribution proportional to the  $\delta$ -distribution will renormalize the coupling-constant, and that the next-to-leading term is irrelevant and can be neglected. The same holds true for the additional term proportional to  $(\nabla r)$  which was dropped in Eq. (2.87).

There is one more possible divergent contribution at the 1-loop level, namely . We now show that the leading term of its expansion, which is expected to be proportional to , is trivial. To this aim consider



$$\begin{aligned} \text{---} \begin{array}{c} \text{---} \\ \text{---} \end{array} &= \int_{k,p} :e^{ikr(u)}: :e^{-ikr(x)}: :e^{ipr(y)}: :e^{-ipr(z)}: \\ &= \int_{k,p} :e^{ikr(u)}: :e^{-ikr(x)}: e^{ipr(y)} e^{-ipr(z)} : e^{-p^2 C(y-z)} e^{kp[C(x-z)-C(x-y)]} . \end{aligned} \quad (2.94)$$

We want to study the contraction of  $x$ ,  $y$ , and  $z$ , and look for all contributions which are proportional to

$$\text{---} = \int_k :e^{ikr(u)}: :e^{-ikr((x+y+z)/3)}: . \quad (2.95)$$

The key-observation is that in Eq. (2.94) the leading term is obtained by approximating  $e^{kp[C(x-z)-C(x-y)]} \approx 1$ . All subsequent terms yield factors of  $k$ , which after integration over  $k$  give derivatives of the  $\tilde{\delta}^d$ -distribution. The result is that

$$\left( \begin{array}{c} \text{---} \\ \text{---} \end{array} \right) - \left( \begin{array}{c} \text{---} \\ \mathbf{1} \end{array} \right) = 0. \quad (2.96) \text{m:no div}$$

This means that divergences of  are already taken into account by a proper treatment of the divergences in , analyzed in Eq. (2.79).

## 2.8 Strategy of renormalization

In the last two sections, we discussed how divergences occur, how their general structure is obtained by the MOPE, and how the MOPE-coefficients are calculated. In the next step, the theory shall be renormalized. The basic idea is to identify the divergences through the MOPE, and then to introduce counter-terms which subtract these divergences. These counter-terms are nothing else than integrals over the MOPE-coefficients, properly regularized, i.e. cut off.

In order to properly understand this point, let us recall the two main strategies employed in renormalization: The first one subtracts divergences in correlation-functions or equivalently vertex-functions. This amounts to adding counter-terms to the Hamiltonian which can be interpreted as a change of the parameters in this Hamiltonian. Calculating observables with this modified Hamiltonian leads to finite physical expectation values, but it is not evident that the integrals appearing in these calculations are convergent.

The other procedure is inspired by ideas employed in a formal proof of renormalizability, or more precisely when applying the  $\mathbf{R}$ -operation to the perturbation expansion, as will be discussed in the next section ???. It consists in adding to the Hamiltonian counter-terms which are *integrals*, such that each *integrand* which appears in the perturbative expansion becomes an integrable function, and *as a consequence* the integrals and thus the perturbation expansion are finite. Of course, to finally obtain the critical exponents, the integral counter-terms have to be reduced to numbers. However, we really want to think of them as integrals in the intermediate steps. The reason is the following: It is extremely difficult to calculate observables. However, this is not really necessary as long as one is only interested in renormalization. The above-mentioned procedure is then sufficient to ensure finiteness of any observable as long as there is no additional divergence when the dipole is contracted towards this observable. The latter situation would require a new counter-term, which is a proper renormalization of the observable itself. The procedure of considering whole integrals as counter-terms is in the heart of our renormalization procedure, and the reader should bear this idea in mind throughout this review.

## 2.9 Renormalization at 1-loop order

Let us continue on the concrete example of the 1-loop divergences, from which are obtained the scaling exponents to first order in the dimensional regularization parameter  $\epsilon$ . Explicitly, the model shall be renormalized through two renormalization group factors  $Z$  (renormalizing the field  $r$ ) and  $Z_b$  (renormalizing the coupling  $b$ ). Recalling Eq. (2.34), this is

$$\mathcal{H}[r] = \frac{Z}{2-D} \int_x \frac{1}{2} (\nabla r(x))^2 + b Z_b \mu^\epsilon \int_x \int_y \tilde{\delta}^d(r(x) - r(y)), \quad (2.97)$$

where  $r$  and  $b$  are the renormalized field and renormalized dimensionless coupling constant, and  $\mu = L^{-1}$  is the renormalization momentum scale.

Let us start to eliminate the divergences in the case, where the end-points  $(x, y)$  of a single dipole are contracted towards a point (taken here to be the center-of-mass  $z = (x + y)/2$ ). The MOPE is

$$\left( \text{dipole} \right)_{x, y} = \left( \text{dipole} \left| \mathbf{1} \right. \right)_{x, y} \mathbf{1} + \left( \text{dipole} \left| \alpha \dagger \beta \right. \right)_{x, y} \alpha \dagger \beta + \dots$$

The MOPE-coefficients were obtained in the last section as

$$\left( \text{dipole} \left| \mathbf{1} \right. \right)_{x, y} = |x - y|^{-\nu d}, \quad (2.98)$$

$$\left( \text{dipole} \left| \alpha \dagger \beta \right. \right)_{x, y} = -\frac{1}{2} (x - y)_\alpha (x - y)_\beta |x - y|^{-\nu(d+2)}. \quad (2.99)$$

We now have to distinguish between counter-terms for relevant operators and those for marginal operators. The former can be defined by analytic continuation, while the latter require a subtraction scale. Indeed, the divergence proportional to  $\mathbf{1}$  is given by the integral

$$\int_{\Lambda^{-1} < |x-y| < L} \left( \text{dipole} \left| \mathbf{1} \right. \right)_{x, y} = \int_{\Lambda^{-1}}^L \frac{dx}{x} x^{D-\nu d} = \frac{1}{D-\epsilon} (\Lambda^{D-\epsilon} - L^{\epsilon-D}), \quad (2.100)$$

where  $\Lambda$  is a high-momentum UV-regulator and  $L$  a large distance regulator. For  $\epsilon \approx 0$  this is UV-divergent but IR-convergent. The simplest way to subtract this divergence is therefore to replace the dipole operator by

$$x \text{---} y \longrightarrow x \text{---} y - x \text{---} \dots \text{---} y, \quad (2.101)$$

where  $\langle \text{diagram} \rangle_{x,y} = |x-y|^{-\nu d}$ . This amounts to adding to the bare Hamiltonian (2.34) the UV-divergent counter-term

$$\Delta\mathcal{H}_1 = -bZ_b\mu^\epsilon \int_x \int_y |x-y|^{-\nu d}, \quad (2.102) \text{m: CT for } +$$

which is a pure number and thus does not change the expectation-value of any physical observable.

We next consider marginal operators: In the MOPE of Eq. (2.98), the integral over the relative distance of  $\int_{x-y} \left( \text{diagram} \Big|_{\alpha \dagger \beta} \right)_{\alpha \dagger \beta}$  is logarithmically divergent at  $\epsilon = 0$ . In order to find the appropriate counter-term, we use dimensional regularization, i.e. set  $\epsilon > 0$ . An IR-cutoff  $L$ , or equivalently a subtraction momentum scale  $\mu = L^{-1}$ , has to be introduced in order to define the subtraction operation. *As a general rule, let us integrate over all distances appearing in the MOPE-coefficient, bounded by the subtraction scale  $L = \mu^{-1}$ .* Defining

$$\left\langle \text{diagram} \Big|_{\alpha \dagger \beta} \right\rangle_L := \int_{|x-y| < L} \left( \text{diagram} \Big|_{\alpha \dagger \beta} \right) \quad (2.103) \text{m: CT for } +$$

we need the following counter-term in the Hamiltonian

$$\Delta\mathcal{H}_+ = -b\mu^\epsilon \left\langle \text{diagram} \Big|_{\alpha \dagger \beta} \right\rangle_L \int_x \alpha \dagger \beta_x, \quad (2.104) \text{m: CT for } +$$

subtracting explicitly the divergence in the integrals, as discussed in the last section. The reader is invited to verify this explicitly in exercise F.5 (see page 166) on the example of the expectation value of  $\mathcal{O} = e^{ik[r(s)-r(t)]}$ , as given in Eq. (2.64).

Since the angular integration in Eq. (2.103) reduces  $\alpha \dagger \beta$  to  $\dagger$ , we can replace Eq. (2.104) by the equivalent expression

$$\Delta\mathcal{H}_+ = -b\mu^\epsilon \left\langle \text{diagram} \Big|_{\dagger} \right\rangle_L \int_x \dagger_x, \quad (2.105)$$

for which the numerical value of the diagram is calculated as

$$\left\langle \text{diagram} \Big|_{\dagger} \right\rangle_L = \int_{|x-y| < L} \left( \text{diagram} \Big|_{\dagger} \right) = -\frac{1}{2D} \int_0^L \frac{dx}{x} x^{2D-\nu d} = -\frac{1}{2D} \frac{L^\epsilon}{\epsilon}. \quad (2.106) \text{m:MOPEL}$$

We can now subtract this term in a minimal subtraction scheme (MS). The internal dimension of the membrane  $D$  is kept fixed and (2.106) is expanded as a Laurent series in  $\epsilon$ , which here starts at  $\epsilon^{-1}$ . Denoting by  $\langle \text{diagram} \Big|_{\dagger} \rangle_{\epsilon^p}$  the term of order  $\epsilon^p$  of the Laurent expansion of  $\langle \text{diagram} \Big|_{\dagger} \rangle_L$  for  $L = 1$ , the residue of the pole in Eq. (2.106) is found to be

$$\left\langle \text{diagram} \Big|_{\dagger} \right\rangle_{\epsilon^{-1}} = -\frac{1}{2D} \frac{1}{\epsilon}. \quad (2.107) \text{m:i} \rightarrow \text{j} \text{ ep}$$

We shall also frequently employ the notation for the residue

$$\left\langle \text{diagram} \Big|_{\dagger} \right\rangle_\epsilon = -\frac{1}{2D}. \quad (2.108) \text{m:i} \rightarrow \text{j} \text{ ep}$$

It is this pole that is subtracted in the MS-scheme by adding to the Hamiltonian a counter-term

$$\Delta\mathcal{H}_+ = -b \left\langle \text{diagram} \Big|_{\dagger} \right\rangle_{\epsilon^{-1}} \int_x \dagger_x. \quad (2.109) \text{m:CT number}$$

Note that by going from Eq. (2.104) to Eq. (2.109), we have reduced the integral counter-term to a number. We recall our initial remark that if one wants to check that this counter-term renders the theory finite, one should think of it as its defining integral (2.104), and verify that in the resulting perturbation theory, the first-order divergence is absent.

Similarly, the divergence arising from the contraction of two dipoles to a single dipole is subtracted by a counter-term

$$\Delta\mathcal{H}_{\text{c.t.}} = b^2\mu^{2\epsilon} \left\langle \left( \text{diagram} \right) \Big| \text{diagram} \right\rangle_L \int_x \int_y x \text{---} y, \quad (2.110)$$

with

$$\left\langle \left( \text{diagram} \right) \Big| \text{diagram} \right\rangle_L = \int_{|x|<L} \int_{|y|<L} \left( \text{diagram} \Big| \text{diagram} \right). \quad (2.111)$$

Reducing this integral counter-term to a number, we subtract the residue of the single pole of

$$\left\langle \left( \text{diagram} \right) \Big| \text{diagram} \right\rangle_L = \int_{|x|<L} \int_{|y|<L} \left( \text{diagram} \Big| \text{diagram} \right) = \int_{|x|<L} \int_{|y|<L} (|x|^{2\nu} + |y|^{2\nu})^{-d/2}. \quad (2.112)$$

Note that the regulator  $L$  cuts off both integrations. One can now either utilize some simple algebra or show by the methods of conformal mapping [22] that the residue is obtained by fixing one distance to equal 1 and by freely integrating over the remaining one

$$\left\langle \left( \text{diagram} \right) \Big| \text{diagram} \right\rangle_\epsilon = \int_0^\infty \frac{dx}{x} x^D (1 + x^{2-D})^{-2D/(2-D)}. \quad (2.113)$$

(Recall that  $d/2 = 2D/(2-D) + \mathcal{O}(\epsilon)$ .) The above is easily related to Euler's B-function and reads

$$\left\langle \left( \text{diagram} \right) \Big| \text{diagram} \right\rangle_\epsilon = \frac{1}{2-D} \frac{\Gamma\left(\frac{D}{2-D}\right)^2}{\Gamma\left(\frac{2D}{2-D}\right)}. \quad (2.114)$$

As a result, the model is UV-finite at 1-loop order, if we use in the renormalized Hamiltonian (2.97) the renormalization factors  $Z$  and  $Z_b$

$$Z = 1 - (2-D) \left\langle \left( \text{diagram} \right) \Big| \text{diagram} \right\rangle_\epsilon \frac{b}{\epsilon} + \mathcal{O}(b^2) \quad (2.115)$$

$$Z_b = 1 + \left\langle \left( \text{diagram} \right) \Big| \text{diagram} \right\rangle_\epsilon \frac{b}{\epsilon} + \mathcal{O}(b^2). \quad (2.116)$$

Note that due to Eq. (2.96) no counter-term for  $\text{diagram}$  is necessary.

The renormalized field and coupling are re-expressed in terms of their bare counterparts through

$$r_0(x) = Z^{1/2} r(x), \quad b_0 = b Z_b Z^{d/2} \mu^\epsilon. \quad (2.117)$$

Finally, the renormalization group functions are obtained from the variation of the coupling constant and the field with respect to the renormalization scale  $\mu$ , keeping the bare coupling fixed. (For a derivation, see appendix A.4 of [22]). The flow of the coupling is written in terms of  $Z$  and  $Z_b$  as

$$\begin{aligned} \beta(b) &:= \mu \frac{\partial}{\partial \mu} \Big|_{b_0} b = \frac{-\epsilon b}{1 + b \frac{\partial}{\partial b} \ln Z_b + \frac{d}{2} b \frac{\partial}{\partial b} \ln Z} \\ &= -\epsilon b + \left( \left\langle \left( \text{diagram} \right) \Big| \text{diagram} \right\rangle_\epsilon - \nu d \left\langle \left( \text{diagram} \right) \Big| \text{diagram} \right\rangle_\epsilon \right) b^2 + \mathcal{O}(b^3) \\ &= -\epsilon b + \left( \frac{1}{2-D} \frac{\Gamma\left(\frac{D}{2-D}\right)^2}{\Gamma\left(\frac{2D}{2-D}\right)} + \frac{(2-D)d}{4D} \right) b^2 + \mathcal{O}(b^3). \end{aligned} \quad (2.118)$$

Similarly, the full dimension of the field (the exponent entering into the correlation function) is obtained as

$$\begin{aligned}
 \nu(b) &:= \frac{2-D}{2} - \frac{1}{2} \mu \frac{\partial}{\partial \mu} \Big|_{b_0} \ln Z = \frac{2-D}{2} - \frac{1}{2} \beta(b) \frac{\partial}{\partial b} \ln Z \\
 &= \frac{2-D}{2} \left[ 1 - b \left\langle \text{loop} \right\rangle_{\epsilon} \right] + O(b^2) \\
 &= \frac{2-D}{2} \left[ 1 + b \frac{1}{2D} \right] + O(b^2).
 \end{aligned} \tag{2.119}$$

Note that minimal subtraction is used on the level of counter-terms or equivalently  $Z$ -factors. Since  $Z$  enters as  $Z^d$  into the  $\beta$ -function, the latter also contains a factor of  $d$  in the 1-loop approximation, i.e.  $Z^d$  is not minimally renormalized. In order to calculate the leading order in  $\epsilon$ , the factor of  $d$  can be replaced by  $d_c = \frac{4D}{2-D}$ .

The  $\beta$ -function has a non-trivial fixed-point with  $\beta(b^*) = 0$ , which has positive slope and thus describes the behavior of the model at large distances:

$$b^* = \frac{\epsilon}{\frac{1}{2-D} \frac{\Gamma\left(\frac{D}{2-D}\right)^2}{\Gamma\left(\frac{2D}{2-D}\right)} + 1} + O(\epsilon^2). \tag{2.120}$$

The anomalous dimension  $\nu^* := \nu(b^*)$  becomes to first order in  $\epsilon$

$$\nu^* = \frac{2-D}{2} \left[ 1 + \frac{\epsilon}{2D} \frac{1}{\frac{1}{2-D} \frac{\Gamma\left(\frac{D}{2-D}\right)^2}{\Gamma\left(\frac{2D}{2-D}\right)} + 1} \right] + O(\epsilon^2). \tag{2.121}$$

For polymers, this result reduces to the well-known formula


$$\nu^*(D=1) = \frac{1}{2} + \frac{4-d}{16} + O((4-d)^2). \tag{2.122}$$

### Exercise 14: Non-renormalization of long-range interactions

Show that if one replaces the short-ranged  $\delta$ -interaction by a long-range interaction ( $\alpha > 0$ )

$$\bullet \times \bullet = \int_k |k|^{-\alpha} e^{ik[r(x)-r(y)]} \sim |r(x) - r(y)|^{\alpha-d} \tag{2.123}$$

the latter is not renormalized. What will the scaling dimension  $\nu$  of the field become?

Hint: Consider the MOPE , and show that it only generates short-range interactions. The solution is given in [22], section 3.9.

## 2.10 $\phi^4$ -theory at other values of $n$

$n$	model	phenomena, tools, equivalences, comments
-2	loop-erased random walk	CDW, Abelian sandpile, uniform spanning tree, SUSY
0	self-avoiding polymers	MOPE
1	Ising model	self-dual at $T_c$ in high-temperature expansion
2	XY-model	vortices, Kosterlitz Thouless transition
3	Heisenberg-model	isotropic magnets
$\infty$	spherical model	large- $n$ expansion

We have already seen self-avoiding polymers ( $n = 1$ ), and the Ising model ( $n = 1$ ). The XY-model is given by  $n = 2$ . In two dimensions, it has additional topological contributions, termed vortices, whose proliferation leads to the Kosterlitz-Thouless transition. The large- $n$  limit is also known as the spherical model. Finally,  $n = -2$  maps onto loop erased random walks, charge-density waves (CDW) pinned by disorder, Abelian sandpiles (ASM), and uniform spanning trees (UST). The mapping between CDWs and LERWs can be done via supersymmetry [8].

## 3 Dynamics

### 3.1 Markov chains, Langevin equation

We often encounter Markov chains, where the state at time  $t_N := N\tau$  is given by the product of *transition probabilities*

$$\mathcal{P}(x_N, x_{N-1}, \dots, x_1, x_0) = \prod_{i=1}^N \mathcal{P}_\tau(x_i | x_{i-1}) \quad (3.1)$$

In general, the transition probabilities are drawn from a Gaussian distribution. We wish to know the probability to be at  $x$  (the variable) given  $x'$  (prime as previous),

$$\mathcal{P}_\tau(x|x') = \frac{1}{\sqrt{4\pi\tau D(x')}} e^{-\frac{[\eta(x-x') - \tau F(x')]^2}{4\eta\tau D(x')}}. \quad (3.2) \text{Transition}$$

Note that both  $F$  and  $D$  depend on the previous position, i.e. we use Itô discretization. As a stochastic process, this reads

$$\eta(x_{i+1} - x_i) = \tau F(x_i) + \sqrt{\tau} \xi_i, \quad (3.3)$$

$$\langle \xi_i \rangle = 0, \quad \langle \xi_i \xi_j \rangle = 2\delta_{ij} \eta D(x_i) \quad (3.4)$$

Formally, the limit of  $\tau \rightarrow 0$  is the *Itô-Langevin equation*,

$$\eta \dot{x}(t) = F(x(t)) + \xi(t), \quad (3.5)$$

$$\langle \xi(t) \rangle = 0, \quad \langle \xi(t) \xi(t') \rangle = 2\eta \delta(t - t') D(x(t)). \quad (3.6)$$

The factor of  $\eta$  is the friction coefficient in Newton's equation of motion. Indeed, for the problem at hand the latter reads

$$M \partial_t \dot{x}(t) = F(x(t)) + \xi(t) - \eta \dot{x}(t). \quad (3.7)$$

On the l.h.s. is the mass  $M$  (or inertia) of the particle (not to be confounded with the mass  $m$  in field theory), times its acceleration. This defines a characteristic time scale

$$\tau_M = \frac{M}{\eta}. \quad (3.8)$$

For times  $t \gg \tau_M$ , inertia plays no role,  $M$  can be set to 0, and we arrive at Eq. (3.5).

The situation is different, when the noise is correlated on a time scale  $\tau \gg \tau_M$ . Then in the equation of motion  $F(x(t))$  changes, since  $x(t)$  changes, and it is better to discretize this limit as

$$\eta(x_{i+1} - x_i) = \tau F\left(\frac{x_i + x_{i+1}}{2}\right) + \sqrt{\tau} \xi_i. \quad (3.9)$$

This prescription is known as mid-point or Stratonovich discretization.

Let us finally rescale time,  $t \rightarrow \eta t$ , which effectively sets  $\eta \rightarrow 1$ . Note that  $\eta$  can always be restored by multiplying each time derivative with  $\eta$ .

## 3.2 Itô calculus

Consider (with  $\eta = 1$ )

$$\begin{aligned}
 g(x_{i+1}) - g(x_i) &= g(x_i + \tau F(x_i) + \sqrt{\tau}\xi_i) - g(x_i) \\
 &= g'(x_i) [\tau F(x_i) + \sqrt{\tau}\xi_i] + \frac{1}{2}g''(x_i)\tau\xi_i^2 + \mathcal{O}(\tau^{3/2}) \\
 &= g'(x_i) [\tau F(x_i) + \sqrt{\tau}\xi_i] + g''(x_i)\tau D(x_i) + \mathcal{O}(\tau^{3/2})
 \end{aligned} \tag{3.10}$$

The last relation is justified since in any time slice maximally two powers of  $\xi_i$  can appear. (If there could be 4 then one would have to use Wick's theorem to decouple them pairwise.) It is implicitly understood that the noise is independent of  $x$ , thus  $\langle g(x_i)\xi_i \rangle = 0$ , and  $\langle g(x_i)\xi_i^2 \rangle = 2g(x_i)D(x_i)dt$ .

Mathematicians like to set  $x_i \rightarrow x$ ,  $\tau \rightarrow dt$ ,  $\xi_i\sqrt{\tau} \rightarrow d\xi$ , and write the Langevin equation as

$$dx = F(x)dt + d\xi, \quad \langle d\xi \rangle = 0, \quad d\xi^2 = \langle d\xi^2 \rangle = 2D(x)dt. \tag{3.11}$$

The stochastic evolution of a function  $g(x)$  can then be written with these “differentials” as

$$\begin{aligned}
 dg(x) &= g'(x)dx + \frac{1}{2}g''(x)dx^2 + \dots \\
 &= g'(x)[F(x)dt + d\xi] + \frac{1}{2}g''(x)[F(x)dt + d\xi]^2 + \dots \\
 &= [g'(x)F(x) + g''(x)D(x)]dt + g'(x)d\xi
 \end{aligned} \tag{3.12}$$

This is known as *Itô calculus*. The rule of thumb to remember is that when expanding to first order in the time differential  $dt$ , as  $d\xi \sim \sqrt{dt}$ , one has to keep all terms up to second order in  $d\xi$ .

## 3.3 From Langevin to Fokker-Planck

**Derivation of (forward) Fokker-Planck equation using Itô's formalism:** The forward Fokker-Planck equation can be derived from Itô's formalism. Consider the expectation of a test function  $g(x)$  at time  $t$ :

$$\langle g(x_t) \rangle \equiv \int_x g(x)P(x, t). \tag{3.13}$$

Taking the expectation of the first line of Eq. (3.12) yields

$$\langle dg(x_t) \rangle = \langle g'(x_t)dx \rangle + \frac{1}{2} \langle g''(x_t)dx^2 \rangle + \dots \tag{3.14}$$

Averaging over the noise gives

$$\frac{d}{dt} \langle g(x_t) \rangle = \langle g'(x_t)F(x_t) \rangle + \langle g''(x_t)D(x_t) \rangle. \tag{3.15}$$

Expressing the expectation values with the help of Eq. (3.13) gives

$$\int_x g(x)\partial_t P(x, t) = \int_x g'(x)F(x)P(x, t) + g''(x)D(x)P(x, t). \tag{3.16}$$

Integrating by part, and using that  $g(x)$  is an arbitrary test function, we obtain the *forward Fokker-Planck equation*

$$\partial_t P(x, t) = \frac{\partial^2}{\partial x^2} [D(x)P(x, t)] - \frac{\partial}{\partial x} [F(x)P(x, t)]. \tag{3.17}$$

Our derivation is valid for any initial condition, thus the propagator  $P(x_f, t_f | x_i, t_i)$  also satisfies the forward Fokker Planck-equation as a function of  $x = x_f$ ,  $t = t_f$ .



**The backward Fokker-Planck equation:** Let us now study the behavior of  $P(x_f, t_f | x_i, t_i)$  as a function of its initial time and position. To this purpose, write down the exact equation, using the notations of Eq. (3.11),

$$P(x_f, t_f | x, t) = \langle P(x_f, t_f | x + dx, t + dt) \rangle . \quad (3.18) \text{B.18}$$

The average is over all realizations of the noise  $\eta$  during a time step  $dt$ . Expanding inside the expectation value to first order in  $dt$  and second order in  $dx$ , and then taking the expectation, we find

$$\begin{aligned} & \langle P(x_f, t_f | x + dx, t + dt) \rangle \\ &= \left\langle P(x_f, t_f | x, t) + dt \partial_t P(x_f, t_f | x, t) + dx \partial_x P(x_f, t_f | x, t) + \frac{dx^2}{2} \partial_x^2 P(x_f, t_f | x, t) \right\rangle \\ &= P(x_f, t_f | x, t) + dt \left[ \partial_t P(x_f, t_f | x, t) + F(x) \partial_x P(x_f, t_f | x, t) + D(x) \partial_x^2 P(x_f, t_f | x, t) \right] . \end{aligned} \quad (3.19)$$

Comparing to Eq. (3.18) implies that the term of order  $dt$  vanishes, thus

$$-\partial_t P(x_f, t_f | x, t) = F(x) \frac{\partial}{\partial x} P(x_f, t_f | x, t) + D(x) \frac{\partial^2}{\partial x^2} P(x_f, t_f | x, t) . \quad (3.20) \text{backwardFP}$$

This is the *backward Fokker-Planck equation*. Note that contrary to the forward equation, all derivatives act on  $P(x_f, t_f | y, t)$ , but not on  $F$  or  $D$ .

**Remark on Consistency:** The form of the backward and forward equations is constraint by an important consistency relation: Using that our process is Markovian, we can write the *Chapman-Kolmogorov equation*

$$P(x_f, t_f | x_i, t_i) = \int_x P(x_f, t_f | x, t) P(x, t | x_i, t_i) . \quad (3.21)$$

This relation must hold for all  $t$  between  $t_i$  and  $t_f$ . Taking a  $t$  derivative and using the backward Fokker-Planck equation for the first propagator  $P(x_f, t_f | x, t)$ , and the forward equation for the second  $P(x, t | x_i, t_i)$ , we find cancelation of all terms upon partial integration in  $x$ , due to the specific arrangement of the derivatives in Eqs. (3.17) and (3.20).

**Remark on Steady State:** Let us find a steady-state solution of Eq. (3.17), i.e. a solution which does not depend on time. Integrating once and dropping the time argument yields

$$\frac{\partial}{\partial x} [D(x)P(x)] = F(x)P(x) + \text{const.} \quad (3.22)$$

Let us suppose that the probability  $P(x)$  vanishes when  $x \rightarrow \infty$ . This implies that the constant vanishes. The solution is obtained as ( $x_0$  is arbitrary)

$$P(x) = \frac{\mathcal{N}}{D(x)} \exp \left( \int_{x_0}^x \frac{F(y)}{D(y)} dy \right) , \quad \mathcal{N}^{-1} = \int_{-\infty}^{\infty} dx \frac{1}{D(x)} \exp \left( \int_{x_0}^x \frac{F(y)}{D(y)} dy \right) . \quad (3.23) \text{FP-ss1}$$

The simplest case is obtained for thermal noise, i.e.  $D(x) = T$ , and when the force  $F(x)$  is derivative of a potential,  $F(x) = -V'(x)$ . Eq. (3.23) can then be written as

$$P(x) = \mathcal{N} e^{-V(x)/T} , \quad \mathcal{N}^{-1} = \int_{-\infty}^{\infty} dx e^{-V(x)/T} \quad (3.24) \text{FP-ss2}$$

This is Boltzmann's law [23].

### Exercise 15: Space-dependent noise

Suppose that  $D(X) = T|x|^\alpha$ , and  $F(x) = -x$ . Study the solution (3.23). Show that for  $\alpha \geq 1$  the particle gets localized at  $x = 0$ .

### 3.4 MSR formalism

**The path integral:** The transition probability (3.2) from  $x'$  to  $x$  was **\*\*\*there was some contradiction with (3.2); corrected the former. The equation below looks correct. Notation: Think of  $x'$  as  $x^{\text{previous}}$ ; the random variable we are interested in is  $x^{\text{***}}$**

$$\mathcal{P}_\tau(x|x')dx = \frac{dx}{\sqrt{4\pi\tau D(x')}} e^{-\frac{[x-x'-\tau F(x')]^2}{4\tau D(x')}} \quad (3.25)$$

This is ugly: our standard field-theory calculations work with polynomials in the exponential. We therefore rewrite this measure as

$$\mathcal{P}_\tau(x|x')dx = dx \int_{-i\infty}^{i\infty} \frac{d\tilde{x}}{2\pi i} e^{-\mathcal{S}_\tau[x,\tilde{x}]} \quad (3.26)$$

$$\mathcal{S}_\tau[x,\tilde{x}] = \tilde{x}(x - x' - \tau F(x')) - \tau \tilde{x}^2 D(x') \quad (3.27)$$

The term  $\mathcal{S}_\tau[x,\tilde{x}]$  is termed *action*. Reassembling all time slices, it is normally written in the limit of  $\tau \rightarrow 0$  as

$$\mathcal{P}(x|x_0)dx = \int_{x_0=x(0)}^{x(x)=x} \mathcal{D}[x] \mathcal{D}[\tilde{x}] e^{-\mathcal{S}[x,\tilde{x}]} \quad (3.28)$$

$$\mathcal{S}[x,\tilde{x}] = \int_t \tilde{x}(t) [\dot{x}(t) - F(x(t))] - \tilde{x}(t)^2 D(x(t)) \quad (3.29)$$

$$\mathcal{D}[x] \mathcal{D}[\tilde{x}] = \prod_{i=1}^N \int_{-\infty}^{\infty} dx_i \int_{-i\infty}^{i\infty} \frac{d\tilde{x}_i}{2\pi i} \quad (3.30)$$

This is known as the MSR formalism (Martin-Siggia-Rose) [24], the action also as Martin-Siggia-Rose-Janssen-DeDominicis action, in honor of their respective work [25, 26] **cite DeDominicis**.

**Changing the discretization:** Let us turn back to a single time slice, as given in Eq. (3.26). The variables  $\tilde{x}$  and  $x$  are conjugate, i.e.

$$\int \frac{dx d\tilde{x}}{2\pi i} e^{-\tilde{x}(x-x')} \tilde{x}^n f(x,\tilde{x}) = \int \frac{dx d\tilde{x}}{2\pi i} e^{-\tilde{x}(x-x')} \partial_x^n f(x,\tilde{x}), \quad (3.31)$$

$$\int \frac{dx d\tilde{x}}{2\pi i} e^{-\tilde{x}(x-x')} (x-x')^n f(x,\tilde{x}) = \int \frac{dx d\tilde{x}}{2\pi i} e^{-\tilde{x}(x-x')} \partial_{\tilde{x}}^n f(x,\tilde{x}). \quad (3.32)$$

We wish to change our discretization scheme, i.e. replace  $F(x') \rightarrow F(\bar{x})$ ,  $D(x') \rightarrow D(\bar{x})$ , where

$$\bar{x} = \alpha x + (1-\alpha)x', \quad 0 \leq \alpha \leq 1. \quad (3.33)$$

We will see later cases where this change has advantages. On the other hand, the microscopic dynamics may be such that  $F$  and  $D$  depend on  $\bar{x}$  instead of  $x'$ .

One quickly realizes that this induces a change in the physics. This is understood from the following example: Expand  $e^{\tau\tilde{x}F(\bar{x})} - 1$  to linear order in  $\tau$ ,

$$\tau \int \frac{dx d\tilde{x}}{2\pi i} e^{-\tilde{x}(x-x')} \tilde{x}F(\bar{x})f(x, \tilde{x}) = \tau \int \frac{dx d\tilde{x}}{2\pi i} e^{-\tilde{x}(x-x')} \partial_x [F(\bar{x})f(x, \tilde{x})] . \quad (3.34)$$

As the derivative also acts on  $F(\bar{x})$ , this depends on  $\alpha$ , since  $\partial_x \bar{x} = \alpha$ . Luckily, we can compensate this by an explicit  $x$  derivative: Wherever we change  $x \rightarrow \bar{x}$ , we also replace  $\tilde{x}$  by  $\tilde{x} - \partial_x$ . This yields for the action for a single time slice

$$\begin{aligned} \mathcal{S}_\tau[x, \tilde{x}] &= \tilde{x}(x - x') - \tau(\tilde{x} - \partial_x)F(\bar{x}) - \tau(\tilde{x} - \partial_x)^2 D(\bar{x}) \\ &= \alpha\tau F'(\bar{x}) - \alpha^2\tau D''(\bar{x}) + \tilde{x}[x - x' - \tau F(\bar{x}) + 2\alpha\tau D'(\bar{x})] - \tau\tilde{x}^2 D(\bar{x}) . \end{aligned} \quad (3.35)_{\text{MSR}}$$

Thus: the noise-correlator  $D(x)$  did not change, but there is an additional contribution to the force

$$F(x') \rightarrow F(\bar{x}) - 2\alpha D'(\bar{x}) . \quad (3.36)$$

The first two terms,  $\alpha F'(\bar{x}) - \alpha^2 D''(\bar{x})$  can be interpreted as a change in the integration measure. You will see this explicitly in an exercise. Let us stress that the change in the action *leaves the physics of the problem invariant*. One may arrive at  $\alpha = \frac{1}{2}$  also when the bath is evolving more slowly than the time scale set by viscosity. You will also discuss this in an exercise.

**Interpretation of the field  $\tilde{x}(t)$ :** Let us now turn to an interpretation of the two fields  $x(t)$  and  $\tilde{x}(t)$ , and modify equation (3.5) to

$$\dot{x}(t) = F(x(t)) + \xi(t) + f\delta(t - t_0) . \quad (3.37)$$

Thus at time  $t = t_0$ , we kick the system with an infinitely small force  $f$ . Then, the probability changes by

$$\begin{aligned} \partial_f \Big|_{f=0} \mathcal{P}(x|x_0) dx &= \partial_f \Big|_{f=0} \int_{x(0)=x_0}^{x(t)=x} \mathcal{D}[x] \mathcal{D}[\tilde{x}] e^{-\mathcal{S}[x, \tilde{x}]} \\ &= \int_{x_0=x(0)}^{x(t)=x} \mathcal{D}[x] \mathcal{D}[\tilde{x}] \tilde{x}(t_0) e^{-\mathcal{S}[x, \tilde{x}]} \end{aligned} \quad (3.38)$$

Multiplying with  $x(t)$  and integrating over all final configurations, we obtain

$$R(t, t_0) = \partial_f \Big|_{f=0} \langle x(t) \rangle = \langle x(t) \tilde{x}(t_0) \rangle . \quad (3.39)_{\text{response}}$$

The expectation is w.r.t the measure given by  $\mathcal{D}[x] \mathcal{D}[\tilde{x}] e^{-\mathcal{S}[x, \tilde{x}]}$ . As (3.39) is the response of the system to a change in force,  $\tilde{x}$  is called *response field*, and  $R(t, t_0)$  *response function*. *Correlation functions* are similarly obtained as

$$C(t, t') = \langle x(t)x(t') \rangle . \quad (3.40)$$

Since the probability is normalized

$$\int \mathcal{P}(x|x_0) dx = 1 \quad (3.41)$$

for all forces, one shows by taking derivatives w.r.t. forces at different times that expectations of the sole response field vanish,

$$\langle \tilde{x}(t) \rangle = \langle \tilde{x}(t) \tilde{x}(t') \rangle = \langle \tilde{x}(t) \tilde{x}(t') \tilde{x}(t'') \rangle = \dots = 0 . \quad (3.42)$$

### 3.5 Gaussian theory with spatial degrees of freedom

Let us now consider theories with spatial dependence, and let us suppose that the energy is given by

$$\mathcal{H}[u] = \int_x \frac{1}{2} [\nabla u(x)]^2 + \frac{m^2}{2} u(x)^2 . \quad (3.43)$$

This corresponds to an elastic manifold inside a confining potential of curvature  $m^2$ . The *elastic forces* acting on a piece of the manifold at position  $x$  are given by

$$F(x) = -\frac{\delta\mathcal{H}[u]}{\delta u(x)} = (\nabla^2 - m^2) u(x) . \quad (3.44)$$

Its Langevin dynamics reads

$$\partial_t u(x, t) = (\nabla^2 - m^2) u(x, t) + \xi(x, t) , \quad \langle \xi(t)\xi(t') \rangle = 2T\delta(t-t')\delta(x-x') . \quad (3.45)$$

The action in Itô discretization is

$$\mathcal{S}[u, \tilde{u}] = \int_{x,t} \tilde{u}(x, t) [\partial_t - \nabla^2 + m^2] u(x, t) - T\tilde{u}(x, t)^2 . \quad (3.46)$$

It can be diagonalized in momentum and frequency space,

$$\begin{aligned} \mathcal{S}[u, \tilde{u}] &= \int_{k,\omega} \tilde{u}(-k, -\omega) [i\omega + k^2 + m^2] u(k, \omega) - T\tilde{u}(-k, -\omega)\tilde{u}(k, \omega) \\ &= \frac{1}{2} \int_{k,\omega} \begin{pmatrix} u(-k, -\omega) \\ \tilde{u}(-k, -\omega) \end{pmatrix} \mathcal{M} \begin{pmatrix} u(k, \omega) \\ \tilde{u}(k, \omega) \end{pmatrix} \end{aligned} \quad (3.47)$$

$$\mathcal{M} = \begin{pmatrix} 0 & i\omega + k^2 + m^2 \\ -i\omega + k^2 + m^2 & 2T \end{pmatrix} \implies \mathcal{M}^{-1} = \begin{pmatrix} \frac{2T}{(i\omega+k^2+m^2)(-i\omega+k^2+m^2)} & \frac{1}{i\omega+k^2+m^2} \\ \frac{1}{-i\omega+k^2+m^2} & 0 \end{pmatrix} \quad (3.48)$$

This implies

$$R(k, \omega) := \langle u(-k, -\omega)\tilde{u}(k, \omega) \rangle = \frac{1}{i\omega + k^2 + m^2} , \quad (3.49)$$

$$C(k, \omega) := \langle u(-k, -\omega)u(k, \omega) \rangle = \frac{2T}{|i\omega + k^2 + m^2|^2} . \quad (3.50)$$

Inverse Fourier transforming  $R$  leads to

$$R(k, t) = \langle u(-k, t)\tilde{u}(k, 0) \rangle = \int_{-\infty}^{\infty} \frac{d\omega}{2\pi} \frac{e^{-i\omega t}}{i\omega + k^2 + m^2} = e^{-(k^2+m^2)t}\theta(t) . \quad (3.51)$$

We used the residue theorem. Note that

$$(\partial_t + k^2 + m^2)R(k, t) = \delta(t) . \quad (3.52)$$

Correlation functions can also be obtained,

$$\begin{aligned} C(k, t-t') &= \langle u(k, t)u(-k, t') \rangle = 2T \int_{-\infty}^{\infty} d\tau R(k, t-\tau)R(k, t'-\tau) \\ &= 2T \int_{-\infty}^{\min(t,t')} d\tau e^{-(k^2+m^2)(t+t'-2\tau)} = \frac{T}{k^2 + m^2} e^{-(k^2+m^2)|t-t'|} \end{aligned} \quad (3.53)$$

Note that for equal times, one recovers the equilibrium correlator,

$$C(k, 0) = \langle u(k, t)u(-k, t) \rangle = \frac{T}{k^2 + m^2} \quad (3.54)$$

Another important relation is **\*\*\*signs\*\*\***

$$\partial_t C(k, t - t') = T [R(k, t' - t) - R(k, t - t')] \quad (3.55) \text{pert-FDT}$$

This relation is known as fluctuation-dissipation theorem. As we will see later, it is quite more generally valid.

### 3.6 Fluctuation-dissipation theorem

Camille will write.

### 3.7 Dynamics respecting Boltzmann weights

Talk about detailed balance.

$$\partial_t \phi(x, t) = - \int_{x'} \mathbb{R}(x, x') \frac{\delta \mathcal{H}[\phi]}{\delta \phi(x', t)} + \xi(x, t) \quad (3.56)$$

$$\langle \xi(x, t) \xi(x', t') \rangle = \delta(t - t') \mathbb{R}(x, x') \quad (3.57)$$

Then

$$\partial_t P(x, t) = \frac{\partial^2}{\partial x^2} \left[ \int_{x'} \mathbb{R}(x, x') P(x', t) \right] - \frac{\partial}{\partial x} \left[ \int_{x'} \mathbb{R}(x, x') \frac{\delta \mathcal{H}[\phi]}{\delta \phi(x, t)} P(x, t) \right] \quad (3.58)$$

One gets back to steady state if  $\mathbb{R}$  commutes with  $\partial_x$

Janssen [26] writes on page 11

$$\mathcal{S}[\tilde{\phi}, \phi] = \int_t \tilde{\phi} \left[ \dot{\phi} + R(\phi) \cdot \frac{\delta \mathcal{H}[\phi]}{\delta \phi} - \frac{\delta R[\phi]}{\delta \phi} \right] - \tilde{\phi} \cdot R[\phi] \cdot \tilde{\phi} \quad (3.59)$$

### 3.8 Dynamics of $\phi^4$ -theory: Model A

The simplest possible dynamics of the  $\phi^4$  theory introduced in section 1.1 is the so-called model A [27]

$$\begin{aligned} \eta \partial_t \phi(x, t) &= - \frac{\delta \mathcal{H}[\phi]}{\delta \phi(x, t)} + \xi(x, t) \\ &= (\nabla^2 - m^2) \phi(x, t) - 4g \phi^3(x, t) + \xi(x, t) \end{aligned} \quad (3.60)$$

$$\langle \xi(x, t) \xi(x', t') \rangle = 2\eta T \delta(x - x') \delta(t - t') . \quad (3.61)$$

The field theory constructed according to Eq. (3.35) from the Hamiltonian (1.1) reads

$$\mathcal{S}[\phi, \tilde{\phi}] = \int_{x,t} \tilde{\phi}(x, t) [\eta \partial_t - \nabla^2 + m^2] \phi(x, t) - \eta T \tilde{\phi}(x, t)^2 + 4g \tilde{\phi}(x, t) \phi^3(x, t) . \quad (3.62) \text{action-mode}$$

**Renormalization of  $g$ :** In order to keep the calculations simple, we set  $T \rightarrow 1$  in the following, restoring the factors of  $T$  only when necessary. This is analogous to what we have done in the statics in section 1.1, where implicitly  $T = 1$ .

Since the action (3.62) reproduces all equilibrium observables, and since the effective coupling is a measurable observable, the effective coupling  $g$  has to be the same in both theories. It is instructive to see how this works at 1-loop order. From two interactions proportional to  $g$ , one obtains

$$\begin{aligned}
\delta g \tilde{\phi}(x, t) \phi^3(x, t) &= -72g^2 \text{diag} \left( \begin{array}{c} \bullet \text{---} \bullet \\ \text{---} \text{---} \end{array} \right) \\
&= -72g^2 \tilde{\phi}(x, t) \phi(x, t) \int_{x', t'} R(x - x', t - t') C(x - x', t - t') \phi(x', t')^2 \\
&= -72g^2 \tilde{\phi}(x, t) \phi(x, t) \int_{x', t'} \left[ -\partial_t C(x - x', t - t') \right] C(x - x', t - t') \phi(x', t')^2 \\
&= -72g^2 \tilde{\phi}(x, t) \phi(x, t) \int_{x', t'} \left[ \frac{1}{2} \partial_{t'} C(x - x', t - t')^2 \right] \phi(x', t')^2 \\
&= -36g^2 \tilde{\phi}(x, t) \phi(x, t) \left[ \int_{x'} C(x - x')^2 \phi(x', t)^2 - \int_{x', t'} C(x - x', t - t')^2 \partial_{t'} \phi(x', t')^2 \right].
\end{aligned} \tag{3.63}$$

First, going from the second to the third line Eq. (3.55) was used. In the second step was used that  $C$  depends on the difference in times. Third, integrating by part gives two terms: The first one is the 1-loop correction to the  $\phi^4$  interaction given in Eq. (1.14), with the same positioning of fields. It leads to the effective interaction (1.15). Note that in the correction  $\delta g$ , all factors of  $T$  cancel. The second term is not present in the original action. Since the associated integral is non-diverging, no counter-term is necessary.

**Renormalization of the 2-point function:** Similar to the renormalization of the coupling constant, we have

$$\begin{aligned}
288g^2 \text{diag} \left( \begin{array}{c} \bullet \text{---} \bullet \\ \text{---} \text{---} \end{array} \right) &= 288g^2 \tilde{\phi}(x, t) \int_{x', t'} R(x - x', t - t') C(x - x', t - t')^2 \phi(x', t') \\
&= 96g^2 \tilde{\phi}(x, t) \int_{x', t'} \left[ \partial_{t'} C(x - x', t - t')^3 \right] \phi(x', t') \\
&= 96g^2 \tilde{\phi}(x, t) \int_{x', t'} \left[ \int_{x'} C(x - x')^3 \phi(x', t) - \int_{x', t'} C(x - x', t - t')^3 \partial_{t'} \phi(x', t') \right].
\end{aligned} \tag{3.64}$$

While the first term appears in the statics in Eqs. (1.30) ff., the last term renormalizes the friction coefficient  $\eta$ . Transforming to momentum space and using Eq. (3.53) yields apart from a factor of  $T^3$

$$\frac{1}{2} \text{diag} \left( \begin{array}{c} \bullet \text{---} \bullet \\ \text{---} \text{---} \end{array} \right) \Big|_{T=1} = \int_{k_1, k_2} \frac{1}{k_1^2 + m^2} \frac{1}{k_2^2 + m^2} \frac{1}{(k_1 + k_2)^2 + m^2} \frac{1}{k_1^2 + k_2^2 + (k_1 + k_2)^2 + 3m^2} \tag{3.65}$$

The factor of  $1/2$  is written as the graphical notation does not make apparent the condition  $t' < t$ . The first three factors are the denominators explicitly given in Eq. (3.53), as they also appear in the static diagram. The last term comes from the additional time integral; its denominator is the sum of the other three denominators. Its value is calculated in appendix A.6, with the result (A.26), i.e.

$$\frac{1}{2} \frac{\text{diag} \left( \begin{array}{c} \bullet \text{---} \bullet \\ \text{---} \text{---} \end{array} \right)}{\left[ \text{diag} \left( \begin{array}{c} \bullet \text{---} \bullet \\ \text{---} \text{---} \end{array} \right) \right]^2} = \frac{3}{4\epsilon} \ln \left( \frac{4}{3} \right) + \mathcal{O}(\epsilon^0). \tag{3.66}$$

This leads to

$$\delta\eta = 48g^2T^2 \left[ x,t \begin{array}{c} \bullet \\ \leftarrow \text{---} \text{---} \text{---} \bullet \\ \rightarrow \text{---} \text{---} \text{---} \bullet \end{array} y,t' \right]_{T=1} . \quad (3.67) \text{Delta-eta}$$

Finally, the dynamical critical exponent  $z$  is obtained as

$$z = 2 - \eta + \frac{\epsilon^2}{9} \ln\left(\frac{4}{3}\right) + \mathcal{O}(\epsilon^3) . \quad (3.68)$$

**Corrections to the noise term:** In the dynamical action also appears the term  $\eta T \tilde{\phi}(x, t)^2$ . As  $T$  is a parameter, we expect it to have the same correction as the friction coefficient. On a diagrammatic level this is seen by calculating the corrections

$$\delta\eta T \tilde{\phi}(x, t)^2 = 48g^2T \begin{array}{c} \leftarrow \bullet \\ \leftarrow \text{---} \text{---} \text{---} \bullet \\ \rightarrow \text{---} \text{---} \text{---} \bullet \\ \rightarrow \bullet \end{array} y,t' \quad (3.69)$$

(Factors of  $T$  in the diagram are set to 1.)

$$\delta(\eta T) = 48g^2T \left[ x,t \begin{array}{c} \bullet \\ \leftarrow \text{---} \text{---} \text{---} \bullet \\ \rightarrow \text{---} \text{---} \text{---} \bullet \end{array} y,t' \right]_{T=1} \quad (3.70)$$

This is consistent with Eq. (3.67), and no correction to  $T$ .

### 3.9 Models B, C, D, ..., J

**Model B** No divergences except the static ones leads to

$$z = 4 - \eta . \quad (3.71)$$

**Model C**

**Model J**

### 3.10 Tunneling over a barrier: Basic equations

The equation of motion in the classical case is using Itô discretization

$$\partial_t u(t) = F(u(t)) + \xi(t) , \quad \langle \xi(t)\xi(t') \rangle = 2T\delta(t - t') . \quad (3.72)$$

The functional integral from time  $t_i$  to time  $t_f$  is in mid-point or Stratonovich discretization (also known as Onsager-Machlup functional)

$$\mathcal{Z} = \int_{u(t_i)=u_i}^{u(t_f)=u_f} \mathcal{D}[u] e^{-\frac{1}{4T} \int_t [\partial_t u(t) - F(u(t))]^2} e^{-\frac{1}{2} \int_t F'(u(t))} . \quad (3.73)$$

The saddle-point equation reads

$$[\partial_t u(t) - F(u(t))] F'(u(t)) + \partial_t [\partial_t u(t) - F(u(t))] - TF''(u(t)) = 0 . \quad (3.74)$$

Magically, the cross-terms vanish, and one is left with

$$F(u(t))F'(u(t)) - \partial_t^2 u(t) + TF''(u(t)) = 0 . \quad (3.75)$$

Multiplying with  $\partial_t u(t)$ , we find complete derivatives, which are integrated to

$$\partial_t \left[ \frac{1}{2} F(u(t))^2 + T F'(u(t)) \right] = \partial_t \left[ \frac{1}{2} \partial_t u(t) \right]^2. \quad (3.76)$$

The square-brackets on the left and right-hand side can be thought off as minus the potential, and plus the kinetic energy of a particle. Let us note (minus) the potential energy as (Onsager-Machlup functional)

$$\mathcal{U}(u) := \frac{F(u)^2}{2} + T F'(u) \quad (3.77)$$

Supposing that the velocity goes to zero for  $t \rightarrow t_i$  and  $t \rightarrow t_f$ , there are two solutions. The first one is the ‘‘classical’’ equation of motion

$$\partial_t^2 u_0(t) = \mathcal{U}'(u_0(t)), \quad \Leftrightarrow \quad \partial_t u_0(t) = \sqrt{2[\mathcal{U}(u_0(t)) - \mathcal{U}(u_i)]}. \quad (3.78)$$

The second solution is the non-trivial time-reversed solution, a.k.a. instanton solution

$$\partial_t^2 u_{\text{inst}}(t) = -\mathcal{U}'(u_{\text{inst}}(t)), \quad \Leftrightarrow \quad \partial_t u_{\text{inst}}(t) = -\sqrt{2[\mathcal{U}(u_{\text{inst}}(t)) - \mathcal{U}(u_i)]}. \quad (3.79)$$

We are interested in the small- $T$  regime, and when the particle starts at a local maximum or minimum, i.e.  $F(u_i) = 0$ . Then the equation of motion can be expanded as

$$\partial_t u_{\text{inst}}(t) = -F(u_{\text{inst}}(t)) - T \frac{F'(u_{\text{inst}}(t)) - F'(u_i)}{F(u_{\text{inst}}(t))} + \mathcal{O}(T^2) \quad (3.80)$$

To expand around the instanton solution we set

$$u(t) = u_{\text{inst}}(t) + x(t). \quad (3.81)$$

Rewrite the partition function (3.73) as

$$\mathcal{Z} = e^{-\frac{1}{4T} \int_t [\partial_t u(t) + F(u(t))]^2} e^{\frac{1}{T} \int_t F(u(t)) \partial_t u(t)} e^{-\frac{1}{2} \int_t F'(u(t))}. \quad (3.82)$$

Note the change in sign in the first term as compared to Eq. (3.73), which makes it (at least almost) disappear for the instanton solution (3.79). Three simplifications can be made:

(i) supposing that the force is derivative of a potential, i.e.  $F(u) = -V'(u)$ , the second term in the exponential can be rewritten as a total derivative, i.e.  $\int_t F(u(t)) \partial_t u(t) = -\int_t \partial_t V(u(t)) = -V(u_f) + V(u_i)$ . Here  $u_i = u(t_i)$  and  $u_f = u(t_f)$  are the initial and final states.

(ii) the cross-term  $\int_t \partial_t x(t) \partial_t u_{\text{inst}}(t)$  can be rewritten as

$$\int_t \partial_t x(t) \partial_t u_{\text{inst}}(t) = -\int_t x(t) \partial_t^2 u_{\text{inst}}(t) = -\int_t x(t) \mathcal{U}'(u_{\text{inst}}(t)) \quad (3.83)$$

(iii) inserting the instanton solution (3.80) into Eq. (3.82), we obtain with these simplifications

$$\mathcal{Z} = \mathcal{Z}_{\text{fluct}} \times \mathcal{Z}_{\text{Arrhenius}} \quad (3.84)$$

$$\mathcal{Z}_{\text{Arrhenius}} = \exp \left( -\frac{1}{T} [V(u^f) - V(u^i)] - \frac{T}{4} \int_t \left[ \frac{F'(u_{\text{inst}}(t)) - F'(u_i)}{F(u_{\text{inst}}(t))} \right]^2 + \mathcal{O}(T^2) \right) \quad (3.85)$$

$$\begin{aligned} \mathcal{Z}_{\text{fluct}} &= \int \mathcal{D}[x] \exp \left( -\frac{1}{2T} \int_t \frac{[\partial_t x(t)]^2}{2} + \mathcal{U}(u_{\text{inst}}(t) + x(t)) - \mathcal{U}(u_{\text{inst}}(t)) - x(t) \mathcal{U}'(u_{\text{inst}}(t)) \right) \times \\ &\quad \times \exp \left( -\frac{1}{2} \int_t F'(u_{\text{inst}}(t)) \right). \end{aligned} \quad (3.86)$$



This expression tells us the following: First of all, the probability to reach a state with a higher potential energy is proportional to the classical Arrhenius factor (3.85), with corrections at higher temperatures.

Second, corrections to this law can be calculated from Eq. (3.86). While this formula is difficult to evaluate in general, one can calculate the contribution from small fluctuations.

$$\mathcal{Z}_{\text{fluct}} \approx \mathcal{Z}_{\text{fluct}}^{\text{quad}} := \exp\left(-\frac{1}{2} \int_t F'(u_{\text{inst}}(t))\right) \int \mathcal{D}[x] \exp\left(-\frac{1}{2T} \int_t \frac{[\partial_t x(t)]^2}{2} + \mathcal{U}''(u_{\text{inst}})^2 \frac{x(t)^2}{2}\right) \quad (3.87) \text{Zfluctquad}$$

Retaining only the leading contribution for small  $T$ , we can rewrite this as

$$\mathcal{Z}_{\text{fluct}}^{\text{quad}} \simeq \exp\left(-\frac{1}{2} \int_t F'(u_{\text{inst}}(t))\right) \int \mathcal{D}[x] \exp\left(-\frac{1}{4T} \int_t [\partial_t x(t)]^2 + \frac{\partial_t^3 u_{\text{inst}}(t)}{\partial_t u_{\text{inst}}(t)} x(t)^2\right). \quad (3.88)$$

### 3.11 The Gel'fand Yaglom method

We want to compute functional determinants of the form

$$f(\alpha, m^2) := \frac{\det[-\nabla^2 + \alpha V(x) + m^2]}{\det[-\nabla^2 + m^2]} \quad (3.89)$$

with Dirichlet boundary conditions at  $x = 0$  and  $x = L$ , and finally  $\alpha = 1$ . In order for the problem to be well-defined,  $-\nabla^2 + \alpha V(x) + m^2$  has to have a discrete spectrum.

In dimension  $d = 1$ , this can efficiently be calculated using the Gel'fand Yaglom method [28]. Let us consider solutions of the ODE

$$[-\nabla^2 + \alpha V(x) + m^2]\psi_\alpha(x) = 0, \quad (3.90)$$

with the boundary conditions

$$\psi_\alpha(0) = 0, \quad \psi'_\alpha(0) = 1. \quad (3.91) \text{bc}$$

Define

$$g(\alpha, m^2) := \frac{\psi_\alpha(L)}{\psi_0(L)}. \quad (3.92) \text{B64}$$

Then the ratio of determinants is given by

$$f(\alpha, m^2) = g(\alpha, m^2). \quad (3.93)$$

**Proof:** Set  $\Lambda_\alpha := -\nabla^2 + \alpha V(x) + m^2$ . Call its eigenvalues  $\lambda_i(\alpha)$ , ordered, and non-degenerate. Consider the analytic structure of  $f(\alpha, m^2 - \lambda)$  and  $g(\alpha, m^2 - \lambda)$ , as a function of  $\lambda$ . First,  $f$  can be written as a product over the eigenvalues,

$$f(\alpha, m^2 - \lambda) = \prod_i \frac{\lambda_i(\alpha) - \lambda}{\lambda_i(0) - \lambda}. \quad (3.94) \text{B66}$$

Note that for large  $i$  the ratio  $\lambda_i(\alpha)/\lambda_i(0)$  goes to 1, thus the product should converge; that was the reason why the ratio of determinants was introduced in the first place. If we want to make the proof rigorous, we can put the system on a lattice, replacing the Laplacian by its lattice-version. Then the spectrum will be finite, and the product converges. As a consequence of Eq. (3.94),  $f(\alpha, m^2 - \lambda)$  is an analytic function of  $\lambda$ , which vanishes at  $\lambda = \lambda_i(\alpha)$ .

Now consider  $g(\alpha, m^2 - \lambda)$ . If  $\lambda$  is an eigenvalue,  $\lambda = \lambda_i(\alpha)$ , then the solution of (3.90) vanishes at  $x = L$ . Playing around with solutions of differential equations, we can convince ourselves that for  $\lambda - \lambda_i(\alpha) \rightarrow 0$ ,

$$\psi_\alpha(L) \sim \lambda - \lambda_i(\alpha). \quad (3.95)$$

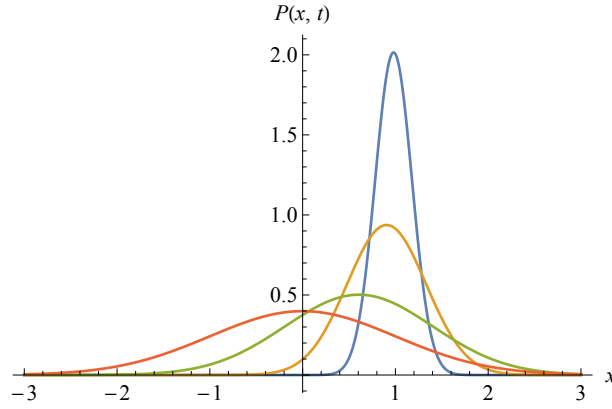


Figure 3.1: Solution (3.99) for a particle in a harmonic potential, with  $m = 1$ ,  $T = 1$ , and  $x_0 = 1$ . Times are  $t = 0.02$  (blue),  $t = 0.1$  (yellow),  $t = 0.5$  (green), and  $t = 10000$  (red).

We further expect  $g$  to be analytic in  $\lambda$ .

Thus, as a function of  $\lambda$ ,  $f$  and  $g$  have the same analytic structure, i.e. the same zeros and poles. The latter cancel in the ratio

$$r(\lambda) := \frac{f(\alpha, m^2 - \lambda)}{g(\alpha, m^2 - \lambda)}. \quad (3.96)$$

The only possibility for a zero or a pole we have to check is for  $|\lambda| \rightarrow \infty$ .

Consider now  $f$  in the limit of  $\lambda \rightarrow -\infty$ : Each factor in (3.94) will go to 1, s.t. also  $f$  goes to 1. (For the discretized version, this is evident, and does not depend on the phase of  $\lambda$ ; for the continuous version one has to work a little bit, and take the limit away from the positive real axes, where the spectrum lies.)

Now consider the differential equation (3.90) with  $m^2 \rightarrow m^2 - \lambda$ , in the same limit  $\lambda \rightarrow -\infty$ . In this case, one can convince oneself that both solutions grow exponentially, and that  $V(x)$  is a small perturbation, s.t. again  $g(\alpha, m^2 - \lambda) \rightarrow 1$ . Thus  $r(\lambda)$  is a function in the complex plane which has no poles. As a consequence,  $r(\lambda)$  is bounded. According to Liouville's theorem it is a constant. This constant can be extracted from the limit of  $\lambda \rightarrow \infty$ , which shows that  $r(\lambda) = 1$ . This concludes our proof.

A more rigorous proof can be found in [29]: The idea there is to show that  $\partial_\alpha f(\alpha, m^2) = \partial_\alpha g(\alpha, m^2)$  for all  $\alpha$ , as both can be written as Green functions at the given value of  $\alpha$ . A proof similar to ours, using Fredholm-determinant theory, can be found in section 7, appendix 1 of [30].

### 3.12 Propagator for harmonic potential, and normalization of path integral

Consider  $d = 1$ , and  $F(u) = -\partial_u V(u)$ , with

$$V(u) = \frac{m^2}{2} u^2. \quad (3.97)$$

Then the Fokker-Planck equation becomes

$$\partial_t P(u, t) = T \frac{\partial^2}{\partial u^2} P(u, t) + m^2 \frac{\partial}{\partial u} [u P(u, t)]. \quad (3.98)$$

Making an ansatz  $P(u, t) = \exp(-a(t)u^2 + c(t)u)/b(t)$ , we find a unique normalized solution localized at  $u_0$  at  $t = 0$ :

$$P(u, t|u_0) = \frac{m \exp\left(\frac{m^2(-(u^2+u_0^2) \coth(m^2 t) + 2u_0 u \operatorname{csch}(m^2 t) + 2tT - u^2 + u_0^2)}{4T}\right)}{2\sqrt{\pi T \sinh(m^2 t)}} \quad (3.99) \text{Pharmonic}$$

For  $u = u_0 = 0$ , we obtain

$$P(0, t|0) = \frac{m}{2\sqrt{\pi T}} \frac{e^{-\frac{m^2 t}{2}}}{\sqrt{\sinh(m^2 t)}} \quad (3.100)_{\text{B72}}$$

For large times, this converges against

$$\lim_{t \rightarrow \infty} P(u, t|u_0) = \frac{m}{\sqrt{2\pi T}} e^{-\frac{m^2 u^2}{2T}}. \quad (3.101)$$

The propagator  $P(0, t|0)$  can also be written as path-integral of the harmonic oscillator; from (3.73) we obtain

$$P(u, t|u_0) = \int_{u(0)=u_0}^{u(t)=u} \mathcal{D}[u] e^{-\frac{1}{4T} \int_0^t d\tau u'(\tau)^2 + m^4 u(\tau)^2} \times e^{-\frac{m^2(u^2 - u_0^2)}{4T}} \times e^{-\frac{m^2 t}{2}} \quad (3.102)$$

Note that the latter factor comes from  $e^{-\frac{1}{2} \int_t F'(u(t))} \equiv e^{-\frac{m^2 t}{2}}$ . Let us specify to  $u = u_0 = 0$ ,

$$P(0, t|0) = \int_{u(0)=0}^{u(t)=0} \mathcal{D}[u] e^{-\frac{1}{4T} \int_0^t d\tau u'(\tau)^2 + m^4 u(\tau)^2} \times e^{-\frac{m^2 t}{2}} =: \mathcal{N} \det\left(\frac{-\partial_\tau^2 + m^4}{4T}\right)^{-1/2} \times e^{-\frac{m^2 t}{2}} \quad (3.103)_{\text{B75}}$$

Yaglom-Gelfand tells us that

$$\frac{\det\left(\frac{-\partial_t^2 + m^4}{4T}\right)}{\psi_{m^4}(t)} = \text{independent of } m \quad (3.104)$$

where

$$\psi_{m^4}(0) = 1, \quad \psi'_{m^4}(0) = 1, \quad (-\partial_t^2 + m^4)\psi_{m^4}(t) = 0 \implies \psi_{m^4}(t) = \frac{\sinh(m^2 t)}{m^2}. \quad (3.105)$$

Define

$$4\pi T \mathcal{N}^2 := \frac{\det\left(\frac{-\partial_\tau^2 + m^4}{4T}\right)}{\psi_{m^4}(t)}. \quad (3.106)_{\text{GY-norm}}$$

Then Eq. (3.103) reproduces Eq. (3.100). Let us note the generally valid formulae

$$\begin{aligned} \int_{u(0)=0}^{u(t)=0} \mathcal{D}[u] e^{-\frac{1}{2T} \int_0^t d\tau \frac{u'(\tau)^2}{2} + \mathcal{F}(\tau) \frac{u(\tau)^2}{2}} &= \mathcal{N} \det\left(\frac{-\partial_\tau^2 + \mathcal{F}(\tau)}{4T}\right)^{-1/2} \\ &= \frac{m}{\sqrt{4\pi T \sinh(m^2 t)}} \det\left(\frac{-\partial_\tau^2 + m^4}{-\partial_\tau^2 + \mathcal{F}(\tau)}\right)^{1/2} = \frac{1}{\sqrt{4\pi T \psi_{\mathcal{F}}(t)}}, \end{aligned} \quad (3.107)$$

where

$$\psi_{\mathcal{F}}(0) = 0, \quad \psi'_{\mathcal{F}}(0) = 1, \quad (-\partial_\tau^2 + \mathcal{F}(\tau)) \psi_{\mathcal{F}}(\tau) = 0. \quad (3.108)_{\text{Gelfand-Yag}}$$

### 3.13 Tunneling over a barrier: Results

**\*\*\*this needs rethinking\*\*\*** In Eq. (3.82), we had written that  $\mathcal{Z} = \mathcal{Z}_{\text{Arrhenius}} \times \mathcal{Z}_{\text{fluct}}$ , where the leading low- $T$  behavior for the Arrhenius factor was

$$\mathcal{Z}_{\text{Arrhenius}} = \exp\left(-\frac{1}{T} [V(u^f) - V(u^i)] + \mathcal{O}(T^0)\right) \quad (3.109)_{\text{P11-bis}}$$

Using Eqs. (3.87), and (3.107)

$$\mathcal{Z}_{\text{fluct}}^{\text{quad}} \simeq \exp\left(-\frac{1}{2} \int_t F'(u_{\text{inst}}(t))\right) \frac{m}{\sqrt{4\pi T \sinh(m^2(t_f - t_i))}} \det\left(\frac{-\partial_t^2 + m^4}{-\partial_t^2 + \mathcal{U}''(u_{\text{inst}}(t))}\right)^{1/2} \quad (3.110)$$

Let us now exploit this formula. This is done in three steps:

- (i) if we choose  $m^4 = \mathcal{U}''(u_{\text{inst}}(t))|_{t=t_i}$ , then the operator inside the determinant will be 1 for small times, and since the particle spends most of its time close to the beginning and end, to a good approximation up to half the total time. Noting that  $F(u_i) = 0$

$$\mathcal{U}''(u_{\text{inst}}(t))|_{t=t_i} = F'(u_i)^2 + \mathcal{O}(T) \quad (3.111)$$

and our choice implies  $m = \sqrt{|F'(u_i)|} = \sqrt{|V''(u_i)|}$ .

- (ii) since  $t_f - t_i$  is large,  $\sinh(m^2(t_f - t_i))$  can be replaced by  $1/2$ .

- (iii) redoing the argument for the end of the classical trajectory will give a similar factor of  $m \rightarrow V''(u_f)$ .

Thus, we expect

$$\mathcal{Z}_{\text{fluct}}^{\text{quad}} \simeq \frac{\sqrt{|V''(u_i)V''(u_f)|}}{\sqrt{\pi T}} \quad (3.112)$$

\*\*\*we can argue whether we are entitled to have a second factor of  $\sqrt{\pi T}$ . Is there an asymmetry, because we do not allow the particle to oscillate to the left?

Remark: If we replace the quadratic potential by a linearized one, then the Gelfand-Yaglom solution will simply be linear in time,  $\psi(t) = t$ . The needed time in question is given by

$$\partial_t u_{\text{inst}}(t) = -F(u_{\text{inst}}(t)) = \frac{V(u_f) - V(u_i)}{u_f - u_i} \quad (3.113)$$

This implies

$$t_f - t_i = \frac{(u_f - u_i)^2}{V(u_f) - V(u_i)} \quad (3.114)$$

Using  $\psi(t) = t$ , the last formula in Eq. (3.107) yields

$$\mathcal{Z}_{\text{fluct}}^{\text{quad}} \simeq \frac{1}{\sqrt{4\pi T}} \sqrt{\frac{V(u_f) - V(u_i)}{(u_f - u_i)^2}} \quad (3.115)$$

### 3.14 Tunneling over a barrier: Results from the non-equilibrium steady state

(Section written by Camille Aron)

**Physical setup.** Let us consider a classical particle of coordinate  $x(t)$  undergoing overdamped dynamics at temperature  $T$  in a static potential  $V(x)$  such as the one represented in Fig. 3.2. The particle is initially located in a local minimum at  $x = 0$ . The closest local maximum is located at  $x = x_b$ .

**Goal.** Solve Kramers' problem, *i.e.* compute the typical time for the particle to escape the local minimum  $x = 0$  and pass the barrier at  $x = x_b$ .

**Roadmap.** Place an absorbing wall at  $x = x_b$  and consider periodic boundary conditions. Compute the non-equilibrium steady-state (NESS) probability distribution  $P_{\text{NESS}}(x)$ , the probability current  $J_{\text{NESS}}$ , and deduce the typical escape time  $\tau_{0 \rightarrow b} := 1/J_{\text{NESS}}$ .

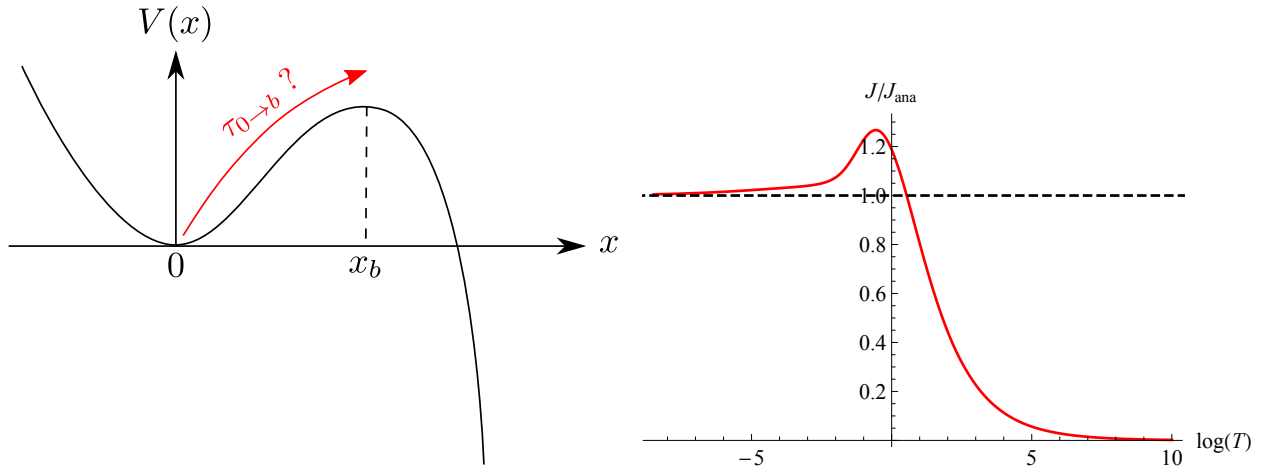


Figure 3.2: Left: Kramers' problem, i.e. what is the typical time it takes for thermal fluctuations to help a particle pass the potential barrier? Right: The exact result (3.121) compared to the approximate formula (3.125), where we used  $V(x) = x^2(1 + 2x^2 - 2x^3)$ .

**Formalism.** The corresponding Langevin equation reads

$$\eta \partial_t x(t) = -V'(x) + \xi(t), \quad (3.116)$$

with  $\langle \xi(t)\xi(t') \rangle = 2\eta T \delta(t - t')$ , where  $T$  is measured in units of  $k_B$ . We set  $\eta = 1$  by reparameterizing time accordingly. The associated Fokker-Planck equation reads

$$\partial_t P(x, t) + \partial_x J(x, t) = 0, \quad (3.117)$$

with the probability current

$$J(x, t) = -[V'(x)P(x, t) + T\partial_x P(x, t)]. \quad (3.118)$$

**Solution.** By putting an absorbing boundary at  $x = x_b$ , and by considering periodic boundary conditions, we create a situation where the particle is automatically reinjected at  $x = -\infty$  each time it manages to reach  $x = x_b$ . This non-equilibrium situation has a non-vanishing particle current, which is expected to reach a steady-state value,  $J_{\text{NESS}} > 0$ , and which can be used to deduce the typical escape time *via* the relation  $\tau_{0 \rightarrow b} := 1/J_{\text{NESS}}$ .

In the NESS, the probability current is constant; thus  $\partial_t J_{\text{NESS}} = 0$ , and  $P_{\text{NESS}}(x)$  satisfies

$$J_{\text{NESS}} = -[V'(x)P_{\text{NESS}}(x) + T\partial_x P_{\text{NESS}}(x)]. \quad (3.119)$$

The generic solution of the above first-order differential equation above reads

$$P_{\text{NESS}}(x) = \alpha e^{-V(x)/T} + \frac{J_{\text{NESS}}}{T} e^{-V(x)/T} \int_x^{x_b} dy e^{V(y)/T}, \quad (3.120)$$

where  $\alpha$  and  $J_{\text{NESS}}$  are two constants that can be determined by the absorbing boundary condition,  $P_{\text{NESS}}(x = x_b) = 0$ , and the normalization condition,  $\int_{-\infty}^{x_b} dx P_{\text{NESS}}(x) = 1$ . The former condition yields  $\alpha = 0$ , while the latter yields the result

$$\tau_{0 \rightarrow b} = J_{\text{NESS}}^{-1} = \frac{1}{T} \int_{-\infty}^{x_b} dx e^{-V(x)/T} \int_x^{x_b} dy e^{V(y)/T}. \quad (3.121) \quad \color{blue}{271}$$

When the temperature  $T$  is smaller than the typical variations of  $V(x)$ , and  $V(x)$  varies quadratically around its maxima and minima, we can make the following two saddle-point approximations,

$$V(x) \simeq V(0) + \frac{1}{2}V''(0)x^2, \quad (3.122)$$

$$V(y) \simeq V(x_b) + \frac{1}{2}V''(x_b)(y - x_b)^2. \quad (3.123)$$

Thus the escape time is given by two nested Gaussian integrals

$$\tau_{0 \rightarrow b} \simeq e^{\frac{V(x_b) - V(0)}{T}} \frac{1}{T} \int_{-\infty}^{x_b \rightarrow \infty} dx e^{-\frac{1}{2T}V''(0)x^2} \int_{x \rightarrow -\infty}^{x_b} dy e^{+\frac{1}{2T}V''(x_b)(y - x_b)^2}, \quad (3.124)$$

that can be decoupled and simplified by extending the boundaries of integration as indicated. Finally, we obtain an explicit formula for Kramers' escape time,

$$\tau_{0 \rightarrow b} = \frac{\pi \eta}{\sqrt{|V''(0)V''(x_b)|}} e^{\frac{V(x_b) - V(0)}{T}}. \quad (3.125) \text{278}$$

### Comments:

- The result was computed for low temperatures,  $T \ll V(x_b) - V(0)$ .
- The Arrhenius exponential factor,  $e^{\frac{V(x_b) - V(0)}{T}}$ , does not involve the details of the potential, but only the relative height of the energy barrier to be passed.
- $V''(0)$  and  $V''(x_b)$  correspond to the frequencies of the harmonic potential around the local minimum  $x = 0$  and the local maximum  $x = x_b$ . They set the timescale of the escape time.
- Reflect on the symmetric role played by  $V''(0)$  and  $V''(x_b)$  in the final formula. Why is that so?
- Write down the first principle of thermodynamics in the steady-state regime. Identify the work and the heat in that problem.
- Show that if the potential grows linearly between 0 and  $x_b$ , and one puts a reflecting boundary at  $x = 0$ , then

$$\tau_{0 \rightarrow b} = \left( \frac{T x_b}{\delta V} \right)^2 \left[ e^{\frac{\delta V}{T}} - 1 - \frac{\delta V}{T} \right], \quad \delta V = V(x_b) - V(0). \quad (3.126)$$

# PART 2: Disordered Systems

## 4 Phenomenology

### 4.1 Introduction

Statistical mechanics is by now a rather mature branch of physics. For pure systems like a ferromagnet, it allows one to calculate so precise details as the behavior of the specific heat on approaching the Curie-point. We know that it diverges as a function of the distance in temperature to the Curie-temperature, we know that this divergence has the form of a power-law, we can calculate the exponent, and we can do this with at least 3 digits of accuracy. Best of all, these findings are in excellent agreement with the most precise simulations, and experiments. This is a true success story of statistical mechanics. On the other hand, in nature no system is really pure, i.e. without at least some disorder (“dirt”). As experiments (and theory) seem to suggest, a little bit of disorder does not change much. Otherwise experiments on the specific heat of Helium would not so extraordinarily well confirm theoretical predictions. But what happens for strong disorder? By this we mean that disorder dominates over entropy, so effectively our system is at zero temperature. Then already the question: “What is the ground-state?” is no longer simple. This goes hand in hand with the appearance of so-called metastable states. States, which in energy are very close to the ground-state, but which in configuration-space may be far apart. Any relaxational dynamics will take an enormous time to find the correct ground-state, and may fail altogether, as can be seen in computer-simulations as well as in experiments. This means that our way of thinking, taught in the treatment of pure systems, has to be adapted to account for disorder. We will see that in contrast to pure systems, whose universal large-scale properties can be described by very few parameters, disordered systems demand the knowledge of the whole disorder-correlation function (in contrast to its first few moments). We show how universality nevertheless emerges.

Experimental realizations of strongly disordered systems are glasses, or more specifically spin-glasses, vortex-glasses, electron-glasses and structural glasses (not treated here). Furthermore random-field magnets, and last not least elastic systems in disorder.

What is our current understanding of disordered systems? There are a few exact solutions, there are phenomenological methods (like the droplet-model), and there is the mean-field approximation, involving a method called replica-symmetry breaking (RSB). This method correctly predicts the properties of infinitely connected systems, as e.g. the SK-model (Sherrington Kirkpatrick model). The most notable feature is the presence of an extensive number of ground states arranged in a hierarchic way.

Magnetic domain walls in presence of disorder, contact lines wetting a disordered substrate, or fracture in brittle heterogenous systems have a quite different phenomenology, with notably a single ground state. Increasing an external applied field yields to jumps in the center-of-mass of the system (the total magnetization in a magnet), also termed shock or avalanche. The sequence of avalanches is deterministic given a specific disorder. However, we are more interested in typical behavior, i.e. an average over disorder. The latter average can often be obtained by watching the system for an extended time (self-averaging).

### 4.2 Physical realizations, model and observables

Before developing the theory to treat elastic systems in a disordered environment, let us give some physical realizations. The simplest one is an Ising magnet. Imposing boundary conditions with all spins up at the upper and all spins down at the lower boundary (see figure 1), at low temperatures, a domain wall separates a region with spin up from a region with spin down. In a pure system at temperature  $T = 0$ , this domain

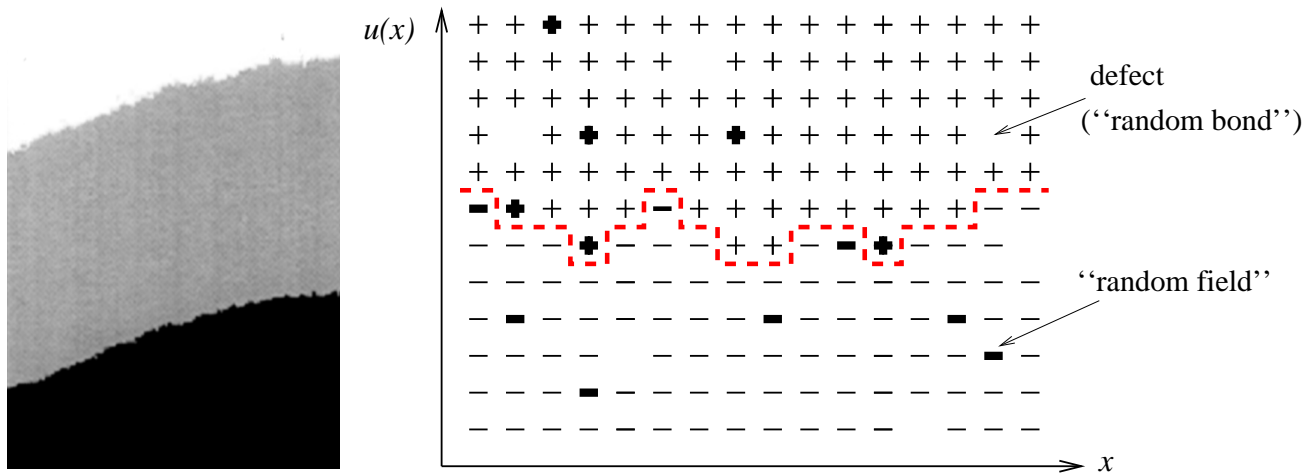


Figure 4.1: An Ising magnet at low temperatures forms a domain wall described by a function  $u(x)$  (right). An experiment on a thin Cobalt film (left) [31]; with kind permission of the authors.

wall is completely flat. Disorder can deform the domain wall, making it eventually rough again. Figure 1 shows, how the domain wall is described by a displacement field  $u(x)$ . Two types of disorder are common:

- random bond disorder (RB), where the bonds between neighboring sites are random. On a coarse-grained level this also represents missing spins. Here the correlations of the random potential are short-ranged.
- random field (RF), i.e. coupling of the spins to an external random magnetic field. This disorder is “long-ranged”, as the random potential is the sum over all random fields below the domain wall. Taking a derivative of the potential, one obtains the random forces, which are short-ranged.

Another example is the contact line of a liquid (water, isobutanol, or liquid helium), wetting a rough substrate, see figure 4.2. (The elasticity is “long-ranged”, see Eq. (4.13)). A realization with a 2-parameter

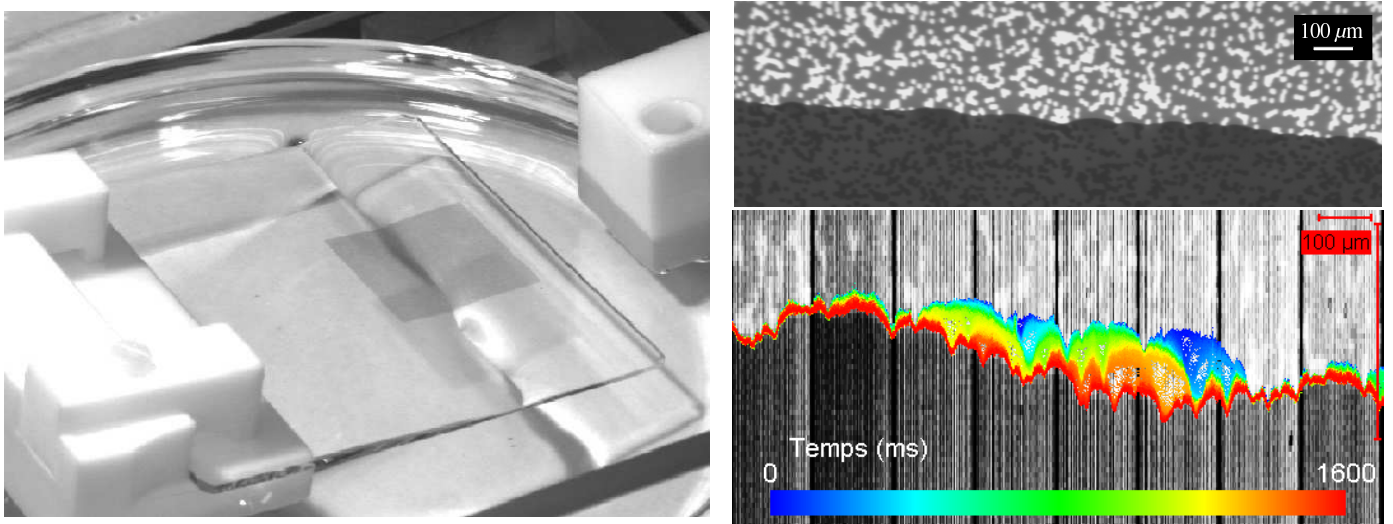


Figure 4.2: A contact line for the wetting of a disordered substrate by Glycerine [32]. Experimental setup (left). The disorder consists of randomly deposited islands of Chromium, appearing as bright spots (top right). Temporal evolution of the retreating contact-line (bottom right). Note the different scales parallel and perpendicular to the contact-line. Pictures courtesy of S. Moulinet, with kind permission.



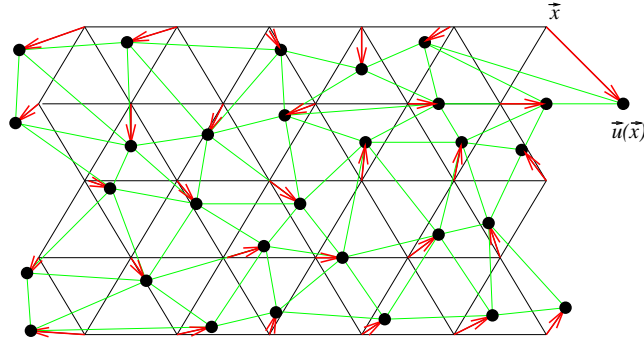


Figure 4.3: Cartoon of an elastic lattice (e.g. vortex lattice) deformed by disorder. This is described by a vector \*\*\*

displacement field  $\vec{u}(\vec{x})$  is the deformation of a vortex lattice: the position of each vortex is deformed from  $\vec{x}$  to  $\vec{x} + \vec{u}(\vec{x})$ . A 3-dimensional example are charge density waves, more difficult to represent graphically.

All these models have in common that they are described by a displacement field

$$x \in \mathbb{R}^d \longrightarrow \vec{u}(x) \in \mathbb{R}^N . \quad (4.1)$$

For simplicity, we set  $N = 1$  in the following. After some initial coarse-graining, the energy  $\mathcal{H} = \mathcal{H}_{\text{el}} + \mathcal{H}_{\text{conf}} + \mathcal{H}_{\text{DO}}$  consists out of three parts: the elastic energy

$$\mathcal{H}_{\text{el}}[u] = \int d^d x \frac{1}{2} [\nabla u(x)]^2 , \quad (4.2)$$

the confining potential

$$\mathcal{H}_{\text{conf}}[u] = \int_x \frac{m^2}{2} \int_x [u(x) - w]^2 , \quad (4.3)$$

and the disorder

$$\mathcal{H}_{\text{DO}}[u] = \int d^d x V(x, u(x)) . \quad (4.4)$$

In order to proceed, we need to specify the correlations of disorder. Suppose that fluctuations  $u$  in the transversal direction scale as

$$\overline{[u(x) - u(y)]^2} \sim |x - y|^{2\zeta} \quad (4.5)$$

with a roughness-exponent  $\zeta < 1$ . Starting from a disorder correlator

$$\overline{V(x, u)V(x', u')} = f(x - x')R(u - u') \quad (4.6)$$

and performing one step in the RG-procedure, one has to rescale more in the  $x$ -direction than in the  $u$ -direction. This will eventually reduce  $f(x - x')$  to a  $\delta$ -distribution, whereas the structure of  $R(u - u')$  remains visible. We therefore choose as our starting model

$$\overline{V(x, u)V(x', u')} := R(u - u')\delta^d(x - x') . \quad (4.7)$$

There are a couple of useful observables. We already mentioned the roughness-exponent  $\zeta$ . The second is the renormalized (effective) disorder  $R(u)$ .

Noting  $F(x, u) := -\partial_u V(x, u)$ , the corresponding force-force correlator can be written as

$$\overline{\langle F(x, u)F(x', u') \rangle} = \Delta(u - u')\delta^d(x - x') . \quad (4.8)$$

On the other hand,  $\overline{\langle F(x, u)F(x', u') \rangle} = \partial_u \partial_{u'} \overline{V(x, u)V(x', u')} = -R''(u - u')\delta^d(x - x')$ , identifying

$$\Delta(u) = -R''(u) . \quad (4.9)$$

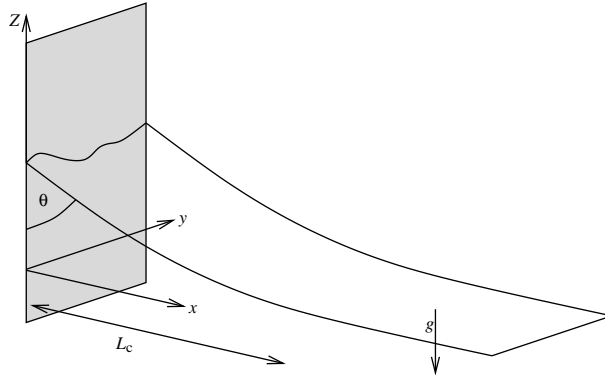


Figure 4.4: The coordinate system for a vertical wall, and contact angle  $\theta = 90^\circ$ . The air/liquid interface becomes flat for large  $x$ . The height  $h(x, y)$  is along the  $z$ -direction.

### Exercise 16: Elasticity of fluid contact line.

Suppose that one has a liquid with height  $h(x, y)$ , defined in the half-space  $x \geq 0$ . Further suppose that its elastic energy is given by

$$\mathcal{H}_{\text{el}}[h] = \int_y \int_{x>0} \frac{\gamma}{2} [\nabla h(x, y)]^2 \quad (4.10)$$

What is the effective elastic energy as a function of the height  $u(y) := h(0, y)$  on the boundary  $x = 0$ ?

### Solution

The minimum energy is attained when

$$0 \stackrel{!}{=} \frac{\delta \mathcal{H}_{\text{el}}[h]}{\delta h(x, y)} = -\gamma \nabla^2 h(x, y). \quad (4.11)$$

This is achieved by the ansatz

$$h(x, y) = \int \frac{dk}{2\pi} \tilde{u}(k) e^{iky - |k|x}. \quad (4.12)$$

At  $x = 0$  this is the standard Fourier transform of the height  $u(y)$  on the boundary  $x = 0$ . Integrating by parts, the elastic energy becomes

$$\begin{aligned} \mathcal{H}_{\text{el}}[h] &= \int_y \int_{x>0} \frac{\gamma}{2} [\nabla h(x, y)]^2 = \frac{\gamma}{2} \left[ \int_y \int_{x>0} \nabla \left( h(x, y) \nabla h(x, y) \right) - h(x, y) \nabla^2 h(x, y) \right] \\ &= -\frac{\gamma}{2} \int_y h(x, y) \partial_x h(x, y) \Big|_{x=0} = \frac{\gamma}{2} \int \frac{dk}{2\pi} |k| \tilde{u}(k) \tilde{u}(-k) \end{aligned} \quad (4.13)$$

## 4.3 Flory estimates and bounds

Four types of disorder have to be distinguished, resulting in different universality classes:

- (i) Random-Bond disorder (RB): short-range correlated potential-potential correlations, i.e. short-range correlated  $R(u)$ .
- (ii) Random-Field disorder (RF): short-range correlated force-force correlator  $\Delta(u) := -R''(u)$ . As the name says, this disorder is relevant for Random-field systems, where the disorder potential is the sum over all magnetic fields in say the spin-up phase.

(iii) Generic long-range correlated disorder:  $R(u) \sim |u|^{-\gamma}$ .

(iv) Random-Periodic disorder (RP): Relevant when the disorder couples to a phase, as e.g. in charge-density waves.  $R(u) = R(u + 1)$ , supposing that  $u$  is periodic with period 1.

To get an idea how large the roughness  $\zeta$  becomes in these situations, one compares the contributions of elastic energy and disorder, and demands that they scale in the same way. This estimate has first been used by Flory for self-avoiding polymers, and is therefore called the Flory estimate, see section 2.3. Despite the fact that Flory estimates are conceptually crude, they often yield a rather good approximation. For RB this gives for an  $N$ -component field  $u$ :  $\int_x (\nabla u)^2 \sim \int_x \sqrt{V\overline{V}}$ , or  $L^{d-2}u^2 \sim L^d \sqrt{L^{-d}u^{-N}}$ , i.e.  $u \sim L^\zeta$  with

$$\zeta_{\text{Flory}}^{\text{RB}} = \frac{4-d}{4+N}. \quad (4.14)$$

For RF it is  $R''$  that is short-ranged, and we obtain

$$\zeta_{\text{Flory}}^{\text{RF}} = \frac{4-d}{2+N}. \quad (4.15)$$

For LR

$$\zeta_{\text{Flory}}^{\text{LR}} = \frac{4-d}{4+\gamma}. \quad (4.16)$$

For RP, the amplitude of  $u$  is fixed, and thus  $\zeta_{\text{RP}} = 0$ .

## 4.4 Replica trick and basic perturbation theory

In disordered systems, the particular configuration one sees strongly depends on the disorder, and therefore general statements about such a configuration are not possible. What one searches for are averages, of the form

$$\overline{\mathcal{O}[u]} := \frac{\langle \mathcal{O}[u] e^{-\mathcal{H}[u]/T} \rangle}{\langle e^{-\mathcal{H}[u]/T} \rangle} \xrightarrow{T \rightarrow 0} \frac{\overline{\mathcal{O}[u_{\text{gs}}] e^{-\mathcal{H}[u_{\text{gs}}]/T}}}{e^{-\mathcal{H}[u_{\text{gs}}]/T}} \equiv \overline{\mathcal{O}[u_{\text{gs}}]} \quad (4.17)$$

Note that division by the partition function  $\mathcal{Z} = \langle e^{-\mathcal{H}[u]/T} \rangle$  itself is crucial. This particularly pronounced in the limit  $T \rightarrow 0$ , where  $\mathcal{Z} \rightarrow e^{-\mathcal{H}[u_{\text{gs}}]/T}$  diverges or vanishes when  $T \rightarrow 0$ , except if by chance  $\mathcal{H}[u_{\text{gs}}] = 0$ . The denominator, i.e. an inverse power of the partition function is difficult to handle, while  $\mathcal{Z}^n$ , with  $n \in \mathbb{N}$  could be achieved by using  $n$  copies or replicas of the system. Further observe that, independent of  $n$ ,

$$\overline{\mathcal{O}[u]} = \frac{\langle \mathcal{O}[u] e^{-\mathcal{H}[u]/T} \rangle \mathcal{Z}^{n-1}}{\mathcal{Z}^n}. \quad (4.18)$$

The replica-trick consists in setting  $n = 0$ , thus eliminating the denominator.

$$\overline{\mathcal{O}[u]} = \lim_{n \rightarrow 0} \overline{\langle \mathcal{O}[u] e^{-\mathcal{H}[u]/T} \rangle \mathcal{Z}^{n-1}}. \quad (4.19)$$

Since thermal averages over distinct replicas factorize, we write their joint measure as

$$\begin{aligned} \overline{\langle \mathcal{O}[u] e^{-\mathcal{H}[u]/T} \rangle \mathcal{Z}^{n-1}} &= \overline{\left\langle \mathcal{O}[u_1] \prod_{a=1}^n e^{-\mathcal{H}[u_a]/T} \right\rangle} = \overline{\left\langle \mathcal{O}[u_1] e^{-\sum_{a=1}^n \mathcal{H}[u_a]/T} \right\rangle} \\ &= \overline{\left\langle \mathcal{O}[u_1] \exp \left( -\frac{1}{T} \int_x \sum_{a=1}^n \left[ \frac{1}{2} [\nabla u_a(x)]^2 + \frac{m^2}{2} [u_a(x) - w_a]^2 + V(x, u_a(x)) \right] \right) \right\rangle}. \end{aligned} \quad (4.20)$$

Note that in the second equality we have exchanged thermal and disorder averages. We have also allowed for different positions  $w$  of the parabola for the different copies, denoted  $w_a$ . Finally, we used that  $\mathcal{O}[u]$  does not depend on the disorder. Since  $V$  is a Gaussian variable,

$$\begin{aligned} \overline{\exp\left(-\frac{1}{T} \int_x \sum_a V(x, u_a(x))\right)} &= \exp\left(\frac{1}{2T^2} \int_x \int_y \sum_{a,b=1}^n \overline{V(x, u_a(x))V(y, u_b(y))}\right) \\ &= \exp\left(\frac{1}{2T^2} \int_x \sum_{a,b=1}^n R(u_a(x) - u_b(x))\right) \end{aligned} \quad (4.21)$$

In the last step we used the correlator (4.7).

To summarize: to evaluate the expectation of an observable, we take averages with the help of the *replica Hamiltonian* or *action*  $e^{-\mathcal{S}^{\text{rep}}[u]}$

$$\mathcal{S}^{\text{rep}}[u] := \frac{1}{T} \sum_{a=1}^n \int_x \left\{ \frac{1}{2} [\nabla u_a(x)]^2 + \frac{m^2}{2} [u_a(x) - w_a]^2 \right\} - \frac{1}{2T^2} \int_x \sum_{a,b=1}^n R(u_a(x) - u_b(x)). \quad (4.22)$$

Let us now turn to perturbation theory. The free propagator (indicated by the index “0”) is

$$\langle u_a(x) u_b(y) \rangle_0 = T \delta_{ab} C(x - y), \quad (4.23)$$

where  $C(x - y)$  is given by Eqs. (1.10) and (1.11). Let us now calculate an expectation in the full theory, namely

$$\begin{aligned} \overline{\langle [u(x) - w_1] \rangle_{w_1} \langle [u(z) - w_2] \rangle_{w_2}} &\equiv \langle [u_1(x) - w_1][u_2(z) - w_2] \rangle_{\mathcal{S}^{\text{rep}}} \\ &= - \int_y C(x - y) C(z - y) R''(w_1 - w_2) + \dots \end{aligned} \quad (4.24)$$

Let us clarify what these objects mean: Thirst,  $\langle [u(x) - w_1] \rangle$  is the thermal average of  $u(x) - w_1$ , obtained by evaluating the path integral for a fixed disorder configuration  $V$ , and at a position of the parabola given by  $w_1$ . This procedure is then repeated for  $\langle [u(z) - w_2] \rangle_{w_2}$ , and finally the average over the disorder potential  $V$  is taken. According to the calculations shown above, this can be evaluated with the help of the replica action  $\mathcal{S}^{\text{rep}}[u]$ , represented by  $\langle [u_1(x) - w_1][u_2(z) - w_2] \rangle_{\mathcal{S}^{\text{rep}}}$ . Note that the latter is already averaged over disorder. The result is the leading order in perturbation theory. Finally, let us integrate this expression over  $x$  and  $z$ , and multiply by  $m^4/L^d$ . This leads to

$$\frac{m^4}{L^d} \int_{x,z} \overline{\langle [u(x) - w_1] \rangle_{w_1} \langle [u(z) - w_2] \rangle_{w_2}} = -R''(w_1 - w_2) + \dots \quad (4.25)$$

The combination  $m^2[u(x) - w_1]$  is the force acting on point  $x$  (a density), its integral over  $x$  the total force acting on the interface. Force correlations are short ranged, leading to the factor of  $L^d$ . Note that the term (4.23) is absent.

### Exercise 17: Corrections to Eq. (4.24).

Construct perturbative corrections to Eq. (4.25). Show that they cancel in the limit of  $T \rightarrow 0$ , if one supposes that  $R(w)$  is an analytic function. Further show that  $\langle uuuu \rangle^c = 0$ .

## 4.5 Dimensional reduction

What was shown in exercise 17 is that (we set  $w_1 = w_2 = 0$ ) at  $T = 0$  (which eliminates the thermal expectations since only the ground state survives)

$$\overline{\tilde{u}(k)\tilde{u}(-k)} = -\frac{R''(0)}{(k^2 + m^2)^2}. \quad (4.26)$$

Fourier-transforming back to space yields (with some geometrical amplitude  $\mathcal{A}$ )

$$\overline{u(x)u(y)} = -R''(0) \mathcal{A} |x - y|^{4-d}. \quad (4.27)$$

This looks very much like the thermal expectation (4.23), except that the dimension of space has been shifted by 2. Further, both theories are seemingly Gaussian, i.e. higher cumulants vanish.

We have just given a simple version of a beautiful and rather mind-boggling theorem relating disordered systems to pure systems (i.e. without disorder). The latter applies to a large class of systems, even when non-linearities are present in the absence of disorder. It is called dimensional reduction and reads as follows[33]:

**Theorem:** *A  $d$ -dimensional disordered system at zero temperature is equivalent to all orders in perturbation theory to a pure system in  $d - 2$  dimensions at finite temperature. Moreover, the temperature is (up to a constant) nothing but the variance of the disorder distribution.*

We give in appendix B a proof of this theorem using a supersymmetric field theory. The equivalence is a little more complicated than stated here, since the supersymmetric theory knows also about different replicas.

However, evidence from experiments, simulations, and analytic solutions show that the above theorem is actually *wrong*. A simple counter-example is the 3-dimensional random-field Ising model at zero temperature; according to the theorem it should be equivalent to the pure 1-dimensional Ising-model at finite temperature. On the other hand, it has been shown rigorously, that the former has an ordered phase, whereas we have all solved the latter and we know that there is no such phase at finite temperature. So what went wrong? Let us stress that there are no missing diagrams or any such thing, but that the problem is more fundamental: As we will see later, the proof makes assumptions, which are not satisfied. Nevertheless, the above theorem remains important since it has a devastating consequence for all perturbative calculations in the disorder: However clever a procedure we invent, as long as we do a perturbative expansion, expanding the disorder in its moments, all our efforts are futile: dimensional reduction tells us that we get a trivial and unphysical result. Before we try to understand why this is so and how to overcome it, let us give one more example. Dimensional reduction allowed us in Eq. (4.27) to calculate the roughness-exponent  $\zeta$  defined in equation (4.5), as

$$\zeta_{\text{DR}} = \frac{4 - d}{2}. \quad (4.28)$$

There is again a well-studied counter example: The directed polymer in dimension  $d = 1$  with a roughness exponent of

$$\zeta_{d=1}^{\text{RB}} = \frac{2}{3}. \quad (4.29)$$

## 4.6 The Larkin-length, and the role of temperature

To understand the failure of dimensional reduction, let us turn to an interesting argument given by Larkin [34]. He considers a piece of an elastic manifold of size  $L$ . If the disorder has correlation length  $r$ , and characteristic potential energy  $\bar{\mathcal{E}}$ , this piece will typically see a potential energy of strength

$$E_{\text{DO}} = \bar{\mathcal{E}} \left( \frac{L}{r} \right)^{\frac{d}{2}}. \quad (4.30)$$

On the other hand, there is an elastic energy, which scales like

$$E_{\text{el}} = c L^{d-2}. \quad (4.31)$$

These energies are balanced at the *Larkin-length*  $L = L_c$  with

$$L_c = \left( \frac{c^2}{\bar{\mathcal{E}}^2} r^d \right)^{\frac{1}{4-d}}. \quad (4.32)$$

More important than this value is the observation that in all physically interesting dimensions  $d < 4$ , and at scales  $L > L_c$ , the disorder energy (4.30) wins, and the membrane is pinned by disorder; whereas on small scales the elastic energy dominates. Since the disorder has a lot of minima which are far apart in configurational space but close in energy (metastability), the manifold can be in either of these minimas, and the ground-state is no longer unique. However exactly this is assumed in e.g. the proof of dimensional reduction.

Another important question is, what the role of temperature is. In (4.5), we had supposed that  $u$  scales with the systems size,  $u \sim L^\zeta$ . From the first term in (4.22) we conclude that

$$T \sim a^\theta, \quad \theta = d - 2 + 2\zeta, \quad (4.33)$$

where  $a$  is a length scale, as e.g. a microscopic cutoff. The thermodynamic limit is obtained by taking  $L \rightarrow \infty$ , or equivalently  $a \rightarrow 0$ . Temperature is thus irrelevant when  $\theta > 0$ , which is the case for  $d > 2$ , and when  $\zeta > 0$  even below. The RG fixed point we will be looking for later is at zero temperature.

From the second term in (4.22) we conclude that the (microscopic) disorder scales as

$$R \sim a^{d-4+4\zeta}. \quad (4.34)$$

This is another way to see that  $d = 4$  is the upper critical dimension.

## 5 The field-theoretic treatment

### 5.1 Derivation of the functional RG equations

In section 4.6, we had seen that 4 is the upper critical dimension. As for standard critical phenomena [?], we now construct an  $\epsilon = (4 - d)$ -expansion. Taking the dimensional reduction result (4.28) in  $d = 4$  dimensions tells us that the field  $u$  is dimensionless. Thus, the width  $\sigma = -R''(0)$  of the disorder is not the only relevant coupling at small  $\epsilon$ , but any function of  $u$  has the same scaling dimension in the limit of  $\epsilon = 0$ , and might thus equivalently contribute. The natural conclusion is to follow the full function  $R(u)$  under renormalization, instead of just its second moment  $R''(0)$ . Such an RG-treatment is most easily implemented in the replica approach: The  $n$  times replicated partition function led after averaging over disorder to a path integral with weight  $e^{-S^{\text{rep}}[u]}$  with action (4.22). Perturbation theory is constructed as follows: The bare correlation function, graphically depicted as a solid line, is with momentum  $k$  flowing through and replicas  $a$  and  $b$

$$a \text{ --- } b = \frac{T \delta_{ab}}{k^2 + m^2}. \quad (5.1)$$

The disorder vertex is **\*\*\*where to put the factors of  $T$ ???**

$$\begin{array}{c} a \bullet \\ \vdots \\ b \bullet \\ \bullet \\ x \end{array} = R_0(u_a(x) - u_b(x)). \quad (5.2)$$

The rules of the game are to find all contributions which correct  $R$ , and which survive in the limit of  $T \rightarrow 0$ . At leading order, i.e. order  $R_0^2$ , counting of factors of  $T$  shows that only the terms with one or two correlators contribute. On the other hand,  $\sum_{a,b} R_0(u_a - u_b)$  has two independent sums over replicas. Thus at order  $R_0^2$  four independent sums over replicas appear, and in order to reduce them to two, one needs at least two correlators (each contributing a  $\delta_{ab}$ ). Thus, at leading order, only diagrams with two propagators survive. These are the following (noting  $C(x - y)$  the Fourier transform of  $1/(k^2 + m^2)$ ): **\*\*\* where do the derivatives comes from???**

$$\begin{array}{c} a \bullet \text{---} a \bullet \\ | \quad | \\ b \bullet \text{---} b \bullet \\ | \quad | \\ x \quad y \end{array} = \int_x R_0''(u_a(x) - u_b(x)) R_0''(u_a(y) - u_b(y)) C(x - y)^2 \quad (5.3)$$

$$\begin{array}{c} a \bullet \text{---} a \bullet \\ | \quad / \\ b \bullet \text{---} b \bullet \\ | \quad | \\ x \quad y \end{array} = - \int_x R_0''(u_a(x) - u_b(x)) R_0''(u_a(y) - u_b(y)) C(x - y)^2 . \quad (5.4)$$

In a renormalization program, we are looking for the divergences of these diagrams. These divergences are localized at  $x = y$ , which allows us to approximate  $R_0''(u_a(y) - u_b(y))$  by  $R_0''(u_a(x) - u_b(x))$ . The integral

$$I_1 := \int_{x-y} C(x - y)^2 = \int_k \frac{1}{(k^2 + m^2)^2} = \frac{m^{-\epsilon}}{\epsilon} \frac{2\Gamma(1 + \frac{\epsilon}{2})}{(4\pi)^{d/2}} \quad (5.5)$$

calculated in Eq. (5.5) is the standard 1-loop diagram from  $\phi^4$ -theory. We have chosen to regulate it in the infrared by a mass, i.e. physically by the harmonic well introduced in section 5.5. Note that the following diagram also contains two correlators (correct counting in powers of temperature), but is not a 2-replica but a 3-replica sum:

$$\begin{array}{c} a \bullet \text{---} a \bullet \\ | \quad | \\ b \bullet \text{---} c \bullet \\ | \quad | \\ x \quad y \end{array} \quad (5.6)$$

Taking into account combinatorial factors, we obtain for the effective disorder correlator  $\hat{R}(u)$

$$\hat{R}(u) = R_0(u) + \left[ \frac{1}{2} R_0''(u)^2 - R_0''(u) R_0''(0) \right] I_1 + \dots \quad (5.7)$$

We can now study its flow, by taking a derivative w.r.t.  $m$ , and replacing on the r.h.s.  $R_0$  with  $\hat{R}$ , as given by the above equation. This leads to

$$-m \frac{\partial}{\partial m} \hat{R}(u) = \left[ \frac{1}{2} \hat{R}''(u)^2 - \hat{R}''(u) \hat{R}''(0) \right] \epsilon I_1 . \quad (5.8)$$

This equation still contains the factor of  $\epsilon I_1$ , which contains both a scale  $m^{-\epsilon}$ , as a finite amplitude. There are two convenient ways out of this: We can parameterize the flow by the integral  $I_1$  itself, defining

$$\partial_t \hat{R}(u) := - \frac{\partial}{\partial I_1} \hat{R}(u) = \frac{1}{2} \hat{R}''(u)^2 - \hat{R}''(u) \hat{R}''(0) . \quad (5.9)$$

This is convenient to study the flow numerically.

To arrive at a fixed point, it is more convenient to rescale both  $\hat{R}$  and  $u$ , to make them dimensionless. The field  $u$  has dimension  $u \sim L^\zeta \sim m^{-\zeta}$ , whereas the dimension of  $\hat{R}$  can be read off from Eq. (5.3), namely  $\hat{R}(u) \sim \hat{R}''(u)^2 m^{-\epsilon}$ , equivalent to  $\hat{R} \sim m^{\epsilon-4\zeta}$ . The dimensionless effective disorder  $\tilde{R}$ , as function of the dimensionless field  $\mathbf{u}$  is then defined as

$$\tilde{R}(\mathbf{u}) := \epsilon I_1 m^{4\zeta} \hat{R}(u = \mathbf{u} m^{-\zeta}) . \quad (5.10)$$



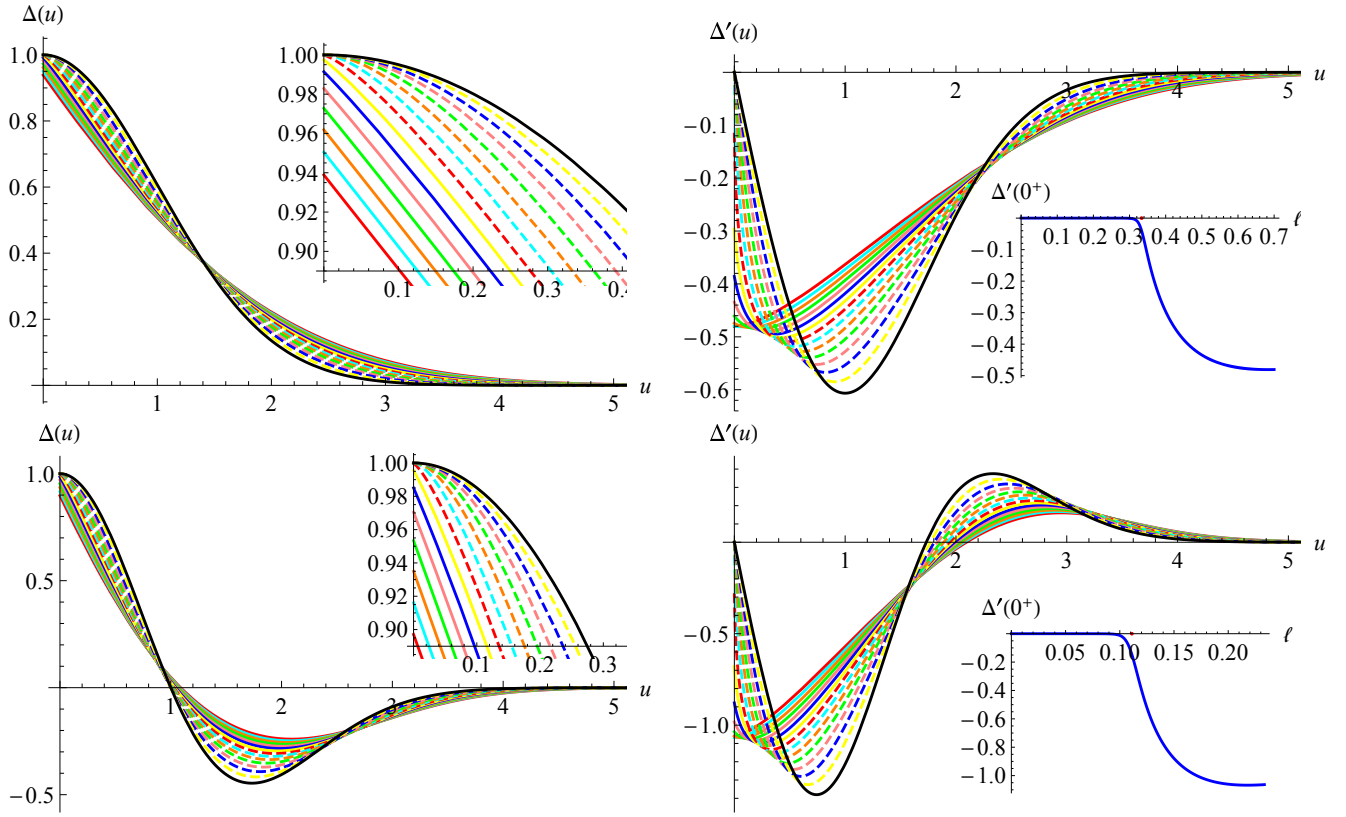


Figure 5.1: Top: Change of  $\Delta(u) := -R''(u)$  under renormalization and formation of the cusp. Left: Explicit numerical integration of Eq. (5.9), starting from  $\Delta(u) = e^{-u^2/2}$  (in solid black, top curve for  $u \rightarrow 0$ ). The function at scale  $\ell$  is shown in steps of  $\delta\ell = 0.05$ . The cusp appears for  $\ell = 1/3$  (red dot). Bottom: ibid for RB disorder, starting from  $R(u) = e^{-u^2/2}$ ; the cusp appears for  $\ell = 1/9$ .

Inserting into Eq. (5.9), we arrive at

$$\partial_\ell \tilde{R}(\mathbf{u}) := -m \frac{\partial}{\partial m} \tilde{R}(\mathbf{u}) = (\epsilon - 4\zeta) \tilde{R}(\mathbf{u}) + \zeta \mathbf{u} \tilde{R}'(\mathbf{u}) + \frac{1}{2} \tilde{R}''(\mathbf{u})^2 - \tilde{R}''(\mathbf{u}) \tilde{R}''(0). \quad (5.11) \text{RG1loop}$$

We will in general set  $\mathbf{u} \rightarrow u$  in the above equation, to simplify notations, and suppress the tilde as long as this does not lead to confusion.

Note that the field does not get renormalized due to the exact statistical tilt symmetry  $u(x) \rightarrow u(x) + \alpha x$ : The bare action (4.22), including the mass term, changes according to  $\mathcal{H}^{\text{bare}}[u] \rightarrow \mathcal{H}^{\text{bare}}[u] + \delta\mathcal{H}[u]$ , with

$$\delta\mathcal{H}[u] = c \int d^d x \left[ \nabla u(x) \alpha + \frac{1}{2} \alpha^2 \right] + m^2 \left[ u(x) \alpha x + \frac{1}{2} \alpha^2 x^2 \right]. \quad (5.12) \text{A11}$$

To render the presentation clearer, the elastic constant  $c$  set to  $c = 1$  in equation (4.22) has been introduced. The important observation is that all fields  $u$  involved are *large-scale* variables, which are also present in the renormalized action, changing according to  $\mathcal{H}^{\text{ren}}[u] \rightarrow \mathcal{H}^{\text{ren}}[u] + \delta H[u]$ . The latter can be used to define the renormalized elastic coefficient  $c^{\text{ren}}$  and mass  $m^{\text{ren}}$ . Since  $\delta H[u]$  gives the change in energy both for the bare and the renormalized action with unchanged coefficients,  $c^{\text{ren}} \equiv c$  and  $m^{\text{ren}} \equiv m$ , so neither elasticity nor mass changes under renormalization.



## 5.2 Solution of the FRG equations, and cusp

We now analyze the FRG flow equations (5.9) and (5.11). To simplify our arguments, we first derive them twice w.r.t.  $u$ , to obtain flow equations for  $\Delta(u) \equiv -R''(u)$ . This yields

$$\text{no rescaling: } \quad \partial_\ell \hat{\Delta}(u) = -\partial_u^2 \frac{1}{2} [\hat{\Delta}(u) - \hat{\Delta}(0)]^2, \quad (5.13)$$

$$\text{with rescaling: } \quad \partial_\ell \tilde{\Delta}(u) = (\epsilon - 2\zeta) \tilde{\Delta}(u) + \zeta u \tilde{\Delta}'(u) - \partial_u^2 \frac{1}{2} [\tilde{\Delta}(u)^2 - \tilde{\Delta}(0)]^2. \quad (5.14)$$

For simplicity of notations from now on we drop the hat on  $\hat{\Delta}$  in Eq. (5.13).

For concreteness, consider Eq. (5.13), and start with an analytic function,

$$\Delta_0(u) = e^{-u^2/2}. \quad (5.15) \text{Delta-initial}$$

According to our classification, this is microscopically RF disorder. Since  $\Delta(u) - \Delta_{\text{eff}}(0)$  grows quadratically in  $u$ , the r.h.s. of Eq. (5.13) also grows  $\sim u^2$  at  $u = 0$ , and both  $\Delta(0)$  as well as  $\Delta'(0^+)$  will not flow in the beginning. This can be seen on the plots of figure 5.1.

Integrating further, a cusp forms, i.e.  $\Delta''(0) \rightarrow \infty$ , and as a consequence  $\Delta'(0^+)$  becomes non-zero. This can best be seen by taking two more derivatives of Eq. (5.13), and then taking the limit of  $u \rightarrow 0$ ,

$$\partial_\ell \Delta''(0^+) = -3\Delta''(0^+)^2 - 4\Delta'(0^+)\Delta'''(0^+). \quad (5.16)$$

Since in the beginning  $\Delta'(0^+) = 0$ , only the first term survives. Integrating this equation yields

$$\Delta_\ell''(0) = \frac{\Delta_0''(0)}{1 + 3\Delta_0''(0)\ell} = -\frac{1}{3} \frac{1}{\ell_c - \ell}, \quad \ell_c = -\frac{1}{3\Delta_0''(0)} \xrightarrow{\Delta_0''(0)=-1} \frac{1}{3}. \quad (5.17)$$

In the last equality we used the initial condition (5.15). With this,  $\Delta_\ell''(0)$  diverges at  $\ell = \frac{1}{3}$ , thus  $\Delta_\ell(u)$  acquires a cusp, i.e.  $\Delta_\ell'(0^+) \neq 0$  for all  $\ell > 1/3$ . Physically, this is the scale where multiple minima appear. In terms of the Larkin-scale  $L_c$  defined in section 4.6

$$\ell_c = \ln(L_c/a). \quad (5.18)$$

Our numerical solution shows the appearance of the cusp only approximately, see the inset in the right plot of figure 5.1. This discrepancy comes from discretization errors. It is indeed not simple to numerically integrate equation (5.13) for large times, as  $\Delta_\ell''(0)$  diverges at  $\ell = \ell_c$ , and all further derivatives at  $u = 0^+$  were extracted from numerical *extrapolations* of the obtained functions, in the limit of  $u \rightarrow 0$ . Interpreting derivatives in this sense is actually an *assumption*, to be justified, without which one cannot continue to integrate the flow equations. In this spirit, let us again look at the flow equation for  $\Delta(0)$ , now including the rescaling terms,

$$\partial_\ell \Delta(0) = (\epsilon - 2\zeta) \Delta(0) - \Delta'(0^+)^2. \quad (5.19)$$

This equation tells us that as long as  $\Delta'(0^+) = 0$ ,

$$\zeta_{\ell < \ell_c} \simeq \zeta_{\text{DR}} = \frac{\epsilon}{2} = \frac{4-d}{2}, \quad (5.20)$$

the dimensional-reduction result. Beyond that scale, we have (as long as we are at least close to a fixed point)

$$\zeta_{\ell > \ell_c} = \frac{\epsilon}{2} - \frac{\Delta'(0^+)^2}{\Delta(0)} < \frac{\epsilon}{2}. \quad (5.21) \text{zeta-bound}$$

Let us repeat our analysis for RB disorder, starting from a microscopic disorder

$$R_0(u) = e^{-u^2/2} \quad \iff \quad \Delta(u) = e^{-u^2/2}(1 - u^2). \quad (5.22)$$

This is shown on the bottom of figure 5.1. Phenomenologically, the scenario is rather similar, with a critical scale  $\ell_c = 1/9$  instead of  $1/3$ .

### 5.3 Fixed points of the FRG equation

We had seen in the last section that integrating the flow-equation explicitly is rather cumbersome; moreover, an estimation of the critical exponent  $\zeta$  will be rather imprecise. For this purpose, it is better to directly search for a solution of the fixed-point equation (5.14), i.e.  $\partial_\ell \tilde{\Delta}(u) = 0$ . This yields

$$0 = (\epsilon - 2\zeta)\tilde{\Delta}(u) + \zeta u \tilde{\Delta}'(u) - \partial_u^2 \frac{1}{2} \left[ \tilde{\Delta}(u)^2 - \tilde{\Delta}(0) \right]^2 . \quad (5.23)_{\text{RF-FP}}$$

We start with situations where  $u$  is unbounded, as for the position of an interface. An important observation is that then the fixed point is not unique; indeed, if  $\tilde{\Delta}(u)$  is solution of Eq. (5.23), so is

$$\tilde{\Delta}_\kappa(u) := \kappa^{-2} \tilde{\Delta}(\kappa u) . \quad (5.24)_{\text{marginal-m}}$$

There is one solution we can find analytically: To this purpose integrate Eq. (5.23) from 0 to  $\infty$ , assuming that  $\tilde{\Delta}(u)$  has a cusp at  $u = 0$ , but no stronger singularity:

$$0 = \int_0^\infty (\epsilon - 2\zeta)\tilde{\Delta}(u) + \zeta u \tilde{\Delta}'(u) du - \partial_u^2 \frac{1}{2} \left[ \tilde{\Delta}(u)^2 - \tilde{\Delta}(0) \right]^2 du . \quad (5.25)$$

Integrating the second term by part, and using that the last term is a total derivative which vanishes both at 0 and at  $\infty$  yields

$$0 = (\epsilon - 3\zeta) \int_0^\infty \tilde{\Delta}(u) du . \quad (5.26)_{\text{B57}}$$

This equation has two solutions: either the integral vanishes, which is the case e.g. for RB disorder, or

$$\zeta_{\text{RF}} = \frac{\epsilon}{3} . \quad (5.27)_{\text{zeta-RF-1lo}}$$

Let us remark that this remains valid for all orders in  $\epsilon$ , as long as  $\Delta(u)$  is the second derivative of  $R(u)$ , s.t. the additional terms at 2- and higher-loop order are all total derivatives, as is the last term in Eq. (5.23).

Let us pursue our analysis with the latter solution; inserting Eq. (5.27) into Eq. (5.23), and setting for convenience  $\tilde{\Delta}(u) = \frac{\epsilon}{3} y(u)$  yields

$$\partial_u \left[ u y(u) - \frac{1}{2} \partial_u \left( y(u) - y(0) \right)^2 \right] = 0 . \quad (5.28)$$

This implies that the expression in the square bracket is a constant, fixed to 0 by considering either the limit of  $u \rightarrow 0$  or  $u \rightarrow \infty$ . Simplifying yields

$$u y(u) + [y(0) - y(u)] y'(u) = 0 . \quad (5.29)$$

Dividing by  $y(u)$  and integrating once again yields

$$\frac{u^2}{2} - y(u) + y(0) \log(y(u)) = \text{const.} \quad (5.30)$$

Let us now use Eq. (5.24) to set  $y(0) \rightarrow 1$ . This fixes the constant to  $-1$ . Dropping the argument of  $y$ , we obtain

$$y - \ln(y) = 1 + \frac{u^2}{2} . \quad (5.31)_{\text{RF-FP-y}}$$

This is plotted on figure 5.2.

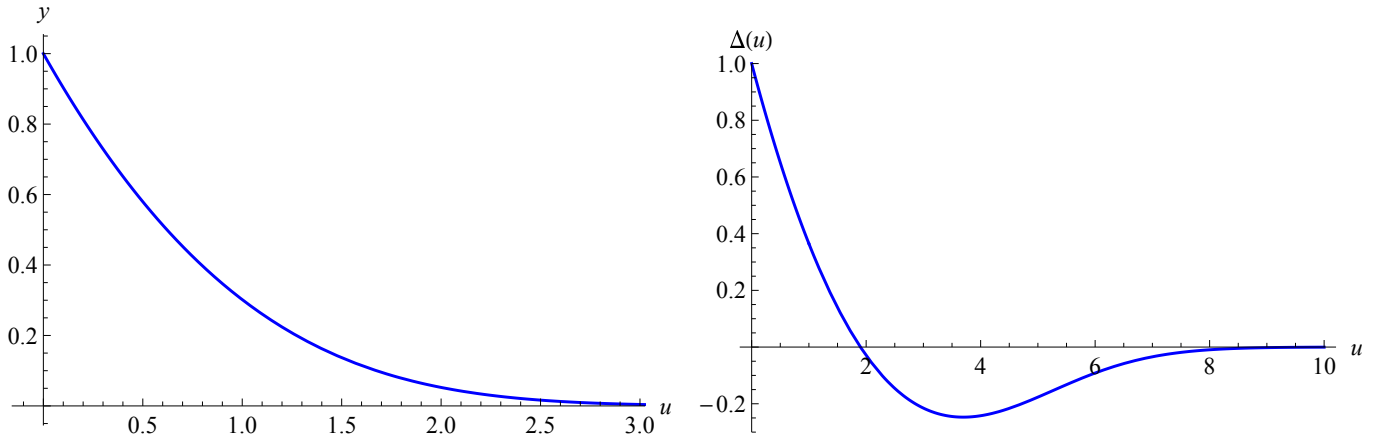


Figure 5.2: Left: The RF fixed point (5.31). Right: The RB fixed point.

The other option for a fixed point is to have the integral in Eq. (5.26) vanish. A numerical analysis of the fixed-point equation (5.23) proceeds as follows: Choose  $\tilde{\Delta}(0) = 1$ ; choose  $\zeta$ ; solve the differential equation (5.23) for  $\tilde{\Delta}''(u)$ . Integrate the latter from  $u = 0$  to  $u = \infty$ . In practice, to avoid numerical problems for  $u \approx 0$ , one first solves the differential equation in a Taylor-expansion around 0; as the latter does not converge for large  $u$  one then solves, with the information from the Taylor series evaluated at  $u = 0.1$ , the differential equation numerically up to  $u_\infty \approx 30$ . One then reports, as a function of  $\zeta$  the value of  $\tilde{\Delta}(u_\infty)$ . As in quantum mechanics, one finds that there are several discretized values of  $\zeta$  with  $\tilde{\Delta}(u_\infty) = 0$ . The largest value of  $\zeta$  is the one given in Eq. (5.27), where  $\tilde{\Delta}(u)$  has no zero crossing. The next smaller value of  $\zeta$  is

$$\zeta_{\text{RB}} = 0.208298\epsilon . \tag{5.32} \text{zeta-RB}$$

The corresponding function is plotted on figure 5.2 (right). It has one zero-crossing. Consistent with Eq. (5.26), it integrates to zero. This is the random-bond fixed point. It is surprisingly close, but distinctly different, from the Flory estimate (4.14),  $\zeta = \epsilon/5$ . The next solution, at

$$\zeta_{\text{3crit}} = 0.14366\epsilon \tag{5.33}$$

has two zero-crossings, and corresponds to a tricritical point. We do not know of any physical application.

If  $\zeta$  is not one of these special values, then the solution of the fixed-point Eq. (5.23) decays algebraically: Suppose that  $\Delta(u) \sim u^\alpha$ . Then the first two terms of Eq. (5.23) are dominant over the last one, as long as  $\alpha < 2$ . Solving Eq. (5.23) in this limit one finds

$$\Delta_\zeta(u) \sim u^{2-\frac{\epsilon}{\zeta}} \quad \text{for } u \rightarrow \infty . \tag{5.34} \text{zeta-LR}$$

An important application are the ABBM and BFM models to be discussed later in sections 7.3, 7.5, for which  $\zeta = \epsilon$ ; then  $\Delta(0) - \Delta(u) = \sigma|u|$  are the correlations of a random walk. In this case  $\Delta(0)$  is formally infinite, s.t. the bound (5.21) does not apply. Generically, however, the bound (5.21) applies, implying that the exponent in Eq. (5.34) is negative, and  $\Delta_\zeta(u)$  decays algebraically. This is what we mostly see in numerical solutions of the fixed-point Eq. (5.23).

In the considerations above, we had supposed that  $u$  can take any real value. There are also important applications where the disorder is periodic, or  $u$  is a phase between 0 and  $2\pi$ . This is the case for CDWs introduced above. To be consistent with the standard conventions employed in the literature [9, 35, 36, 37, 38, 39], we take the period of the disorder to be 1. One checks that the following ansatz is a fixed point of

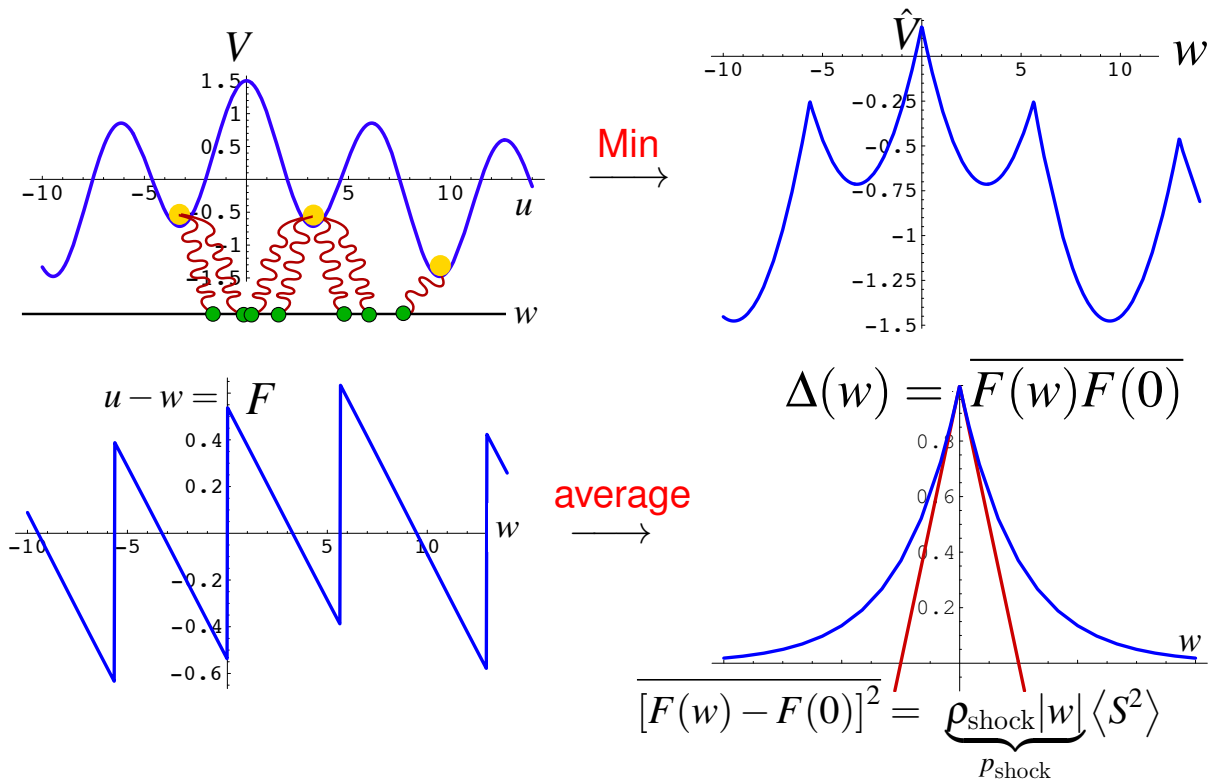


Figure 5.3: Generation of the cusp, as explained in the main text.

the FRG equation (5.23)

$$\zeta_{\text{RP}} = 0, \quad \Delta_{\text{RP}}(u) = \frac{g}{12} - \frac{g}{2}u(1-u), \quad 0 \leq u \leq 1. \quad (5.35)_{\text{RP-fixed-point}}$$

This ansatz is unique, due to the following three constraints: (i)  $\zeta = 0$ , as the period is fixed and cannot change under renormalization. (ii)  $\Delta(u) = \Delta(-u) = \Delta(1-u)$  due to the symmetry  $u \rightarrow -u$ , and periodicity. Thus  $\Delta(u)$  is a polynomial in  $u(1-u)$ . (iii) a polynomial of degree 2 in  $u$  closes under RG. (iv) the integral  $\int_0^1 du \Delta(u) = 0$ , since  $\Delta(u) = -R''(u)$ , and  $R(u)$  itself is periodic. The fixed point has

$$g = \frac{\epsilon}{3} + \dots \quad (5.36)$$

Let us finally test the method on the directed polymer in  $d = 1$ , which has roughness  $\zeta_{d=1}^{\text{RB}} = \frac{2}{3}$ . Our result (5.32) yields  $\zeta(d = 1) = 0.624894 + \mathcal{O}(\epsilon^2)$ . This is quite good, knowing that  $\epsilon = 3$  is rather large. This value gets improved at 2-loop order, with  $\zeta(d = 1) = 0.686616 + \mathcal{O}(\epsilon^3)$ . It seems we capture the physics correctly. But what does this strange cusp mean?

## 5.4 The cusp and shocks: A toy model

Let us give a simple argument of why a cusp is a physical necessity, and not an artifact. The argument is quite old and appeared probably first in the treatment of correlation-functions by shocks in Burgers turbulence. It became popular in [40]. Suppose, we want to solve the problem for a single degree of freedom which sees both disorder and a parabolic trap centered at  $w$ , which we can view as a spring attached to the point  $w$ . This is graphically represented on figure 5.3 (upper left), with the quenched disorder having roughly a sinusoidal shape. For this disorder realization, the minimum of the potential as a

function of  $w$  is

$$\hat{V}(w) := \min_u \left[ V(u) + \frac{m^2}{2}(u - w)^2 \right] \quad (5.37)$$

This is reported on figure 5.3 (upper right). Note that it has non-analytic points, which mark the transition from one minimum to another. The remaining parts are parabolic, and come almost entirely from the spring, as long as the minima of the disorder are sharp, i.e. have a high curvature as compared to the spring. This is indeed rather natural, knowing that the disorder varies on small scales, while the confining potential changes on large scales.

Taking the derivative of the potential leads to the force in figure 5.3 (lower left). It is characterized by almost linear pieces, and shocks (i.e. jumps). Let us now calculate the force-force correlator **\*\*\*should be connected\*\*\***

$$\Delta(w) := \overline{F(w')F(w' - w)}. \quad (5.38)$$

Here the average is over disorder realizations, or equivalently  $w'$ , on which it should not depend. Let us analyze its behavior at small distances,

$$\begin{aligned} \Delta(0) - \Delta(w) &= \frac{1}{2} \overline{[F(w') - F(w' - w)]^2} \\ &= \frac{1}{2} p_{\text{shock}}(w) \langle \delta F^2 \rangle + \mathcal{O}(w^2) \end{aligned} \quad (5.39)$$

As written, the leading contribution is proportional to the probability to have a shock (jump) inside the window of size  $w$ , times the expectation of the second moment of the force jump  $\delta F$ . If shocks are not dense, then the probability to have a shock is given by the density  $\rho_{\text{shock}}$  of shocks times the size  $w$  of the window, i.e.

$$p_{\text{shock}}(w) = \rho_{\text{shock}} |w|. \quad (5.40)$$

Let us now relate  $\delta F$  to the change in  $u$ ; as the spring-constant is  $m^2$ ,

$$\delta F = m^2 \delta u \equiv m^2 S. \quad (5.41)$$

Here we have introduced the *avalanche size*  $S := \delta u$ . Putting everything together yields

$$\Delta(0) - \Delta(w) = \frac{m^4}{2} \langle S^2 \rangle \rho_{\text{shock}} |w| + \mathcal{O}(w^2). \quad (5.42)$$

We can still eliminate  $\rho_{\text{shock}}$  by observing that on average the particle follows the spring, i.e.

$$w - w' = \overline{u(w) - u(w')} = \langle S \rangle \rho_{\text{shock}} (w - w'). \quad (5.43)$$

This yields

$$\rho_{\text{shock}} = \frac{1}{\langle S \rangle} \quad (5.44)$$

Expanding (5.42) in  $w$ , and retaining only the term linear in  $w$  finally yields

$$-\Delta'(0^+) = m^4 \frac{\langle S^2 \rangle}{2 \langle S \rangle}. \quad (5.45)$$

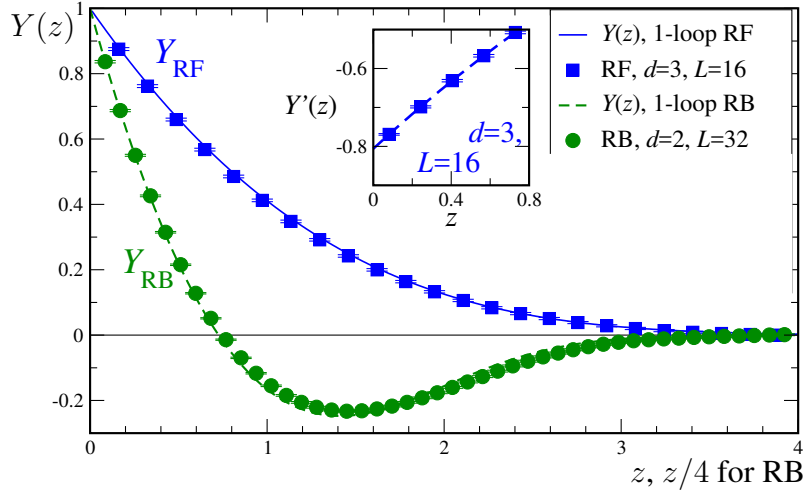


Figure 5.4: Filled symbols show numerical results for  $Y(z)$ , a normalized form of the interface displacement correlator  $-R''(u)$  [Eq. (5.52)], for  $D = 2 + 1$  random field (RF) and  $D = 3 + 1$  random bond (RB) disorders. These suggest a linear cusp. The inset plots the numerical derivative  $Y'(z)$ , with intercept  $Y'(0) \approx -0.807$  from a quadratic fit (dashed line). Open symbols plot the cross-correlator ratio  $Y_s(z) = \Delta_{12}(z)/\Delta_{11}(0)$  between two related copies of RF disorder. It does not exhibit a cusp. The points are for confining wells with width given by  $M^2 = 0.02$ . Comparisons to 1-loop FRG predictions (curves) are made with no adjustable parameters. Reprinted from [42].

## 5.5 The cusp in the field-theory

The above toy model can indeed be generalized to the field theory [41]. Consider an interface in a random potential, and add an external quadratic potential well, centered around  $w$ :

$$\mathcal{H}_{\text{tot}}^w[u] = \int_x \frac{m^2}{2} [u(x) - w]^2 + \mathcal{H}_{\text{el}}[u] + \mathcal{H}_{\text{DO}}[u]. \quad (5.46)$$

Physically, the role of the well is to forbid the interface to wander off to infinity. This avoids that observables are dominated by rare events. In each sample (i.e. disorder configuration), and given  $w$ , one finds the minimum energy configuration. This ground state energy, or effective potential, is

$$\hat{V}(w) := \min_{u(x)} \mathcal{H}_{\text{tot}}^w[u]. \quad (5.47)$$

Let us call  $u_w^{\min}(x)$  this configuration. Its center of mass position is

$$u_w := \frac{1}{L^d} \int_x u_w^{\min}(x). \quad (5.48)$$

Both  $\hat{V}(w)$  and  $u_w$  vary with  $w$  as well as from sample to sample. Let us now look at their second cumulants. For the effective potential,

$$\overline{\hat{V}(w)\hat{V}(w')^c} = L^d R(w - w') \quad (5.49)$$

defines a function  $R(w)$  which is the same function computed in the field theory, defined from the zero-momentum action. The factor of volume  $L^d$  is necessary, since the width  $\overline{u^2}$  of the interface in the well cannot grow much more than  $m^{-\zeta}$ . This means that the interface is made of roughly  $L/L_m$  pieces of internal size  $L_m \approx m$  pinned independently: Eq. (5.49) expresses the central limit theorem and  $R(w)$  measures the second cumulant of the disorder seen by any one of the independent pieces. The nice thing about (5.49) is that it can be measured. One varies  $w$  and computes (numerically) the new ground-state energy, finally averaging over many realizations.

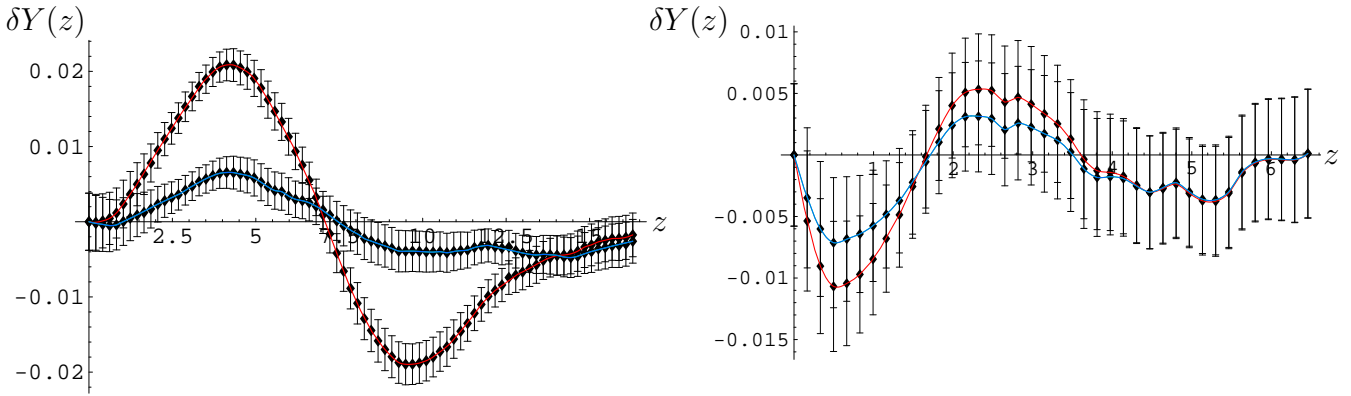


Figure 5.5: The measured  $Y(z)$  with the 1-loop (red) and 2-loop corrections (blue) subtracted. Left: RB-disorder, right: RF-disorder. One sees that the 2-loop corrections improve the precision.

In fact, what is even better to measure are the fluctuations of the center-of-mass position  $u_w$ , related to the total force acting on the interface. To see this, write the condition for the interface to be in a minimum-energy configuration,

$$0 = -\frac{\delta\mathcal{H}[u]}{\delta u(x)} = \nabla^2 u(x) - m^2[u(x) - w] + F(x, u(x)), \quad F(x, u) = -\partial_u V(x, u). \quad (5.50)$$

Integrating over space, using periodic boundary conditions, the term  $\sim \nabla^2 u(x)$  vanishes. At the minimum-energy configuration  $u_w^{\min}(x)$ , this yields

$$m^2(u_w - w) = \frac{m^2}{L^d} \int_x u_w^{\min}(x) - w = \frac{1}{L^d} \int_x F(x, u_w^{\min}(x)) =: \hat{F}(w). \quad (5.51)$$

The last equation defines the effective force  $\hat{F}(w)$ . Its second cumulant reads

$$\overline{\hat{F}(w)\hat{F}(w')^c} \equiv m^4 \overline{[w - u_w][w' - u_{w'}]^c} = L^{-d} \Delta(w - w'). \quad (5.52)$$

Taking two derivatives of Eq. (5.49), one verifies that the effective correlators for potential and force are related by  $\Delta(u) = -R''(u)$ , as in the microscopic relation (4.9).

A numerical check has been performed in [42] using a powerful exact-minimization algorithm, which finds the ground state in a time polynomial in the system size. The result of this measurement is represented in figure 5.4. It was found convenient to plot the function  $Y = \Delta(u)/\Delta(0)$  and normalize the  $u$ -axis to eliminate all non-universal scales. As a result, the plot is parameter free, thus what one compares is purely the shape. It has several remarkable features. First, it clearly shows that a linear cusp exists in all dimensions. Next it is very close to the 1-loop prediction. Even more remarkably the statistics is good enough to reliably estimate the deviations from the 2-loop predictions of [39], see figure 5.5.

Note that when we vary the position  $w$  of the center of the well, it is not a real motion. It just means to find the new ground state for each  $w$ . Literally “moving”  $w$  is another interesting possibility: It measures the universal properties of the so-called *depinning transition* [43, 44].

\*\*\*talk about effective action, and why we have  $\hat{\Delta}(w)$  from the experiment, and not  $\tilde{\Delta}(u)$ . explain the Legendre transform between the two\*\*\*

## 5.6 Beyond 1 loop

### The problem

Functional renormalization has successfully been applied to a bunch of problems at 1-loop order. From a field theory, we however demand more. Namely that it



- allows for systematic corrections beyond 1-loop order
- be renormalizable
- and thus allows to make universal predictions.

This has been a puzzle since 1986, and it was even suggested that the theory is not renormalizable due to the appearance of terms of order  $\epsilon^{\frac{3}{2}}$  [45]. Why is the next order so complicated? The reason is that it involves terms proportional to  $R'''(0)$ . A look at figure 5.1 or 5.4 explains the puzzle. Shall we use the symmetry of  $R(u)$  to conclude that  $R'''(0)$  is 0? Or shall we take the left-hand or right-hand derivatives, related by

$$R'''(0^+) := \lim_{\substack{u>0 \\ u \rightarrow 0}} R'''(u) = - \lim_{\substack{u<0 \\ u \rightarrow 0}} R'''(u) =: -R'''(0^-). \quad (5.53)$$

In the following, we will present our solution of this puzzle, obtained at 2-loop order, at large  $N$ , and in the driven dynamics.

### The flow-equation beyond 1-loop order

For the flow-equation at 2- and 3-loop order, the result is [37, 39, 46, 47, 48, 49, 50]

$$\begin{aligned} \partial_t R(u) = & (\epsilon - 4\zeta) R(u) + \zeta u R'(u) + \frac{1}{2} R''(u)^2 - R''(u) R''(0) \\ & + (\frac{1}{2} + \mathcal{C}_1 \epsilon) \left[ (R''(u) - R''(0)) R'''(u)^2 - R'''(0^+)^2 R''(u) \right] \\ & + \mathcal{C}_4 [\tilde{R}'''(u) [\tilde{R}'''(u)^2 \tilde{R}''''(u) - \tilde{R}'''(0^+)^2 \tilde{R}''''(0^+)] - \tilde{R}'''(0^+) \tilde{R}'''(u)^2 \tilde{R}''''(u)] \\ & + \mathcal{C}_3 [\tilde{R}''(u) - \tilde{R}''(0^+)]^2 \tilde{R}''''(u)^2 + \mathcal{C}_2 [\tilde{R}'''(u)^4 - 2\tilde{R}'''(u)^2 \tilde{R}'''(0^+)^2] \end{aligned} \quad (5.54)$$

$$\mathcal{C}_1 = \frac{1}{36} [9 + 4\pi^2 - 6\psi'(\frac{1}{3})] = -0.3359768096723647, \quad (5.55)$$

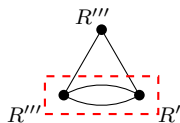
$$\mathcal{C}_2 = \frac{3}{4}\zeta(3) + \frac{\pi^2}{18} - \frac{\psi'(\frac{1}{3})}{12} = 0.6085542725335131, \quad (5.56)$$

$$\mathcal{C}_3 = \frac{\psi'(\frac{1}{3})}{6} - \frac{\pi^2}{9} = 0.5859768096723648, \quad (5.57)$$

$$\mathcal{C}_4 = 2 + \frac{\pi^2}{9} - \frac{\psi'(\frac{1}{3})}{6} = 1.4140231903276352. \quad (5.58)$$

The first line is the result at 1-loop order, already given in Eq. (5.11). The second line is new; setting there  $\epsilon = 0$  is the 2-loop result. All remaining terms (porportional to  $\mathcal{C}_1, \dots, \mathcal{C}_4$ ) are 3-loop contributions, which we put here for completeness.

Consider now the last term of the second line, which involves  $R'''(0^+)^2$  and which we call *anomalous*. The hard task is to fix the prefactor  $-1$ . We have found different prescriptions to do this: The sloop-algorithm, recursive construction, reparametrization invariance, renormalizability, potentiality and exact RG [39, 37, 50]. For lack of space, let us consider renormalizability only. The following 2-loop diagram leads to the anomalous term

$$\begin{array}{c} R''' \\ \diagup \quad \diagdown \\ \bullet \quad \bullet \\ \diagdown \quad \diagup \\ R''' \end{array} \longrightarrow \frac{1}{2} \left[ (R''(u) - R''(0)) R'''(u)^2 - R''(u) R'''(0^+)^2 \right]. \quad (5.59) \text{rebi}$$


The momentum integral, not written here but given in Eq. (A.20), contains a sub-divergence, which is indicated by the box. Renormalizability demands that its leading divergence (which is of order  $1/\epsilon^2$ ) be



$\zeta_{\text{eq}}$	one loop	two loop	three loop	Padé-(2,1)	simulation and exact
$d = 3$	0.208	0.215	0.204	0.211	$0.22 \pm 0.01$ [51]
$d = 2$	0.417	0.444	0.358	0.423	$0.41 \pm 0.01$ [51]
$d = 1$	0.625	0.687	0.396	0.636	$2/3$ [52]

Figure 5.6: Roughness exponent for random bond disorder obtained by an  $\epsilon$ -expansion in comparison with exact results and numerical simulations. In the fourth column is an estimate value using a (2,1)-Padé approximant of the 3-loop result.

canceled by a 1-loop counter-term. The latter is unique; it is obtained by replacing  $R(u)$  in the 1-loop correction  $\delta R(u) = \frac{1}{2}R''(u)^2 - R''(u)R''(0)$  by  $\delta R(u)$  itself; the last term then yields

$$\delta R''(0) := \lim_{u \rightarrow 0} \delta R''(u) = \lim_{u \rightarrow 0} R'''(u)^2 = R'''(0^+)^2. \quad (5.60)$$

This fixes the prefactor of the last (anomalous) term in Eq. (5.54).

A physical requirement is that the disorder correlations remain potential, i.e. that forces still derive from a potential. The force-force correlations being  $-R''(u)$ , this means that the flow of  $R'(0^+)$  has to be strictly 0. (The simplest way to see this is to study a periodic potential.) From Eq. (5.54) one can check that this does not remain true if one changes the prefactor of the last term in Eq. (5.54); thus fixing it.

### RP disorder

Let us give some results for cases of physical interest. First of all, for a periodic potential (RP), which is relevant for charge-density waves, the fixed-point function can be calculated analytically as (we choose period 1, the following is for  $u \in [0, 1]$ )

$$R^*(u) = - \left[ \frac{\epsilon}{72} + \frac{\epsilon^2}{108} + \epsilon^3 \frac{9 + 2\pi^2 - 3\psi'(\frac{1}{3}) - 18\zeta(3)}{1944} + \mathcal{O}(\epsilon^4) \right] u^2(1-u)^2 + \text{const.} \quad (5.61)$$

This leads to a universal amplitude for the 2-point function [37, 49].

### RF disorder

Consider now random-field disorder (short-ranged force-force correlation function). Here our argument given in Eq. (5.26) remains valid, and  $\zeta = \frac{\epsilon}{3}$  remains valid, equivalent to the Flory estimate (4.15).

### RB disorder

For random-bond disorder (short-ranged potential-potential correlation function) we have to solve Eq. (5.54) numerically, order by order in  $\epsilon$ . The result is [49]

$$\zeta_{\text{RB}} = 0.20829804\epsilon + 0.006858\epsilon^2 - 0.01075\epsilon^3 + \mathcal{O}(\epsilon^4). \quad (5.62)$$

This compares well with numerical simulations, see figure 5.6. It is also surprisingly close, but distinctly different, from the Flory estimate (4.14),  $\zeta = \epsilon/5$ .

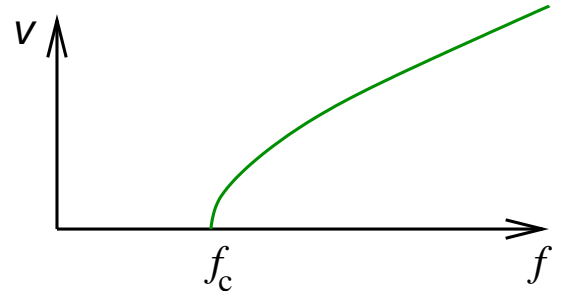


Figure 6.1: Left: Snapshot of a contact-line at depinning, courtesy E. Rolley [movie]. Right: Velocity of a pinned interface as a function of the applied force. Zero force: equilibrium.  $f = f_c$ : depinning.

## 6 Dynamics, and the Depinning transition

### 6.1 Phenomenology

Another important class of phenomena for elastic manifolds in disorder is the so-called *depinning transition*: Applying a constant force to the elastic manifold, e.g. a constant magnetic field to the ferromagnet mentioned in the introduction, the latter will move if, and only if, a certain critical threshold force  $f_c$  is surpassed, see figure 6.1. (This is fortunate, since otherwise the magnetic domain walls in the hard-disc drive onto which this article is stored would move, with the effect of deleting all information, depriving you from all reading.) At  $f = f_c$ , the so-called depinning transition, the manifold has a distinctly different roughness exponent  $\zeta$  (see Eq. (4.5)) from the equilibrium ( $f = 0$ ). The equation describing the movement of the interface is

$$\partial_t u(x, t) = (\nabla^2 - m^2)u(x, t) + F(x, u(x, t)) + f, \quad F(x, u) = -\partial_u V(x, u). \quad (6.1) \text{eq-motion-f}$$

There are two main driving protocols, depending whether one controls the applied force, or the mean driving velocity

#### Force-controlled depinning

Let us impose a driving force  $f$ , and set  $m \rightarrow 0$ . For  $f > f_c$ , the manifold then moves with velocity  $v$ . Close to the transition, new critical exponents appear:

- a velocity-force relation given by (see figure 6.1)

$$v \sim |f - f_c|^\beta \quad \text{for } f > f_c, \quad (6.2)$$

- a *dynamic* exponent  $z$  relating correlation functions in space and time

$$t \sim x^z. \quad (6.3) \text{exponent-z}$$

Thus if one has a correlation or response function  $R(x, t)$ , it will be for short times and distances be a function of  $t/x^z$  only,

$$R(x, t) \simeq R(x^z/t). \quad (6.4)$$

- a correlation length  $\xi$  set by the distance to  $f_c$

$$\xi \sim |f - f_c|^{-\nu} . \quad (6.5)$$

Remarkably, this relation holds on both sides of the transition: For  $f < f_c$ , it describes how starting from a flat or equilibrated configuration, the correlation length  $\xi$ , which can be interpreted as the avalanche extension, increases as one approaches  $f_c$ . Arriving at  $f_c$ , each segment of the interface has moved. Above  $f_c$ , the interface is always moving, and the correlation length  $\xi$  (which now decreases upon an increase in  $f$ ) gives the size of coherently moving pieces.

- The new exponents  $z$ ,  $\beta$  and  $\nu$  are not independent, but related [53]. Suppose that one is above  $f_c$ , and we witnessed an avalanche of extension  $\xi$ . Then its mean velocity scales as

$$v \sim \frac{u}{t} \sim \frac{\xi^\zeta}{\xi^z} \sim |f - f_c|^{-\nu(\zeta-z)} \quad \Longrightarrow \quad \beta = \nu(z - \zeta) . \quad (6.6) \text{beta-rel}$$

One can make the same argument below  $f_c$ , by slowly increasing  $f$  to  $f_c$ .

- Suppose that below  $f_c$  the manifold is in a pinned configuration. Increasing  $f$  will lead to an avalanche, of extension  $\xi$ , and a change of elastic force (per site)  $\sim \xi^{\zeta-2}$ . This has to be balanced by the driving force, i.e.

$$\xi^{\zeta-2} \sim |f - f_c| \quad \Longrightarrow \quad \nu = \frac{1}{2 - \zeta} . \quad (6.7) \text{nu-rel}$$

## Velocity-controlled depinning

If  $m > 0$ , then we can rewrite the equation of motion (6.1) as

$$\partial_t u(x, t) = (\nabla^2 - m^2)[u(x, t) - w] + F(x, u(x, t)) , \quad w = vt . \quad (6.8) \text{eq-motion-w}$$

The phenomenology changes:

- Here the driving force acting on the interface is fluctuating as well as the velocity, while the mean driving velocity is fixed

$$\overline{\dot{u}(x, t)} = v , \quad f = \frac{1}{L^d} \int_x \overline{F(x, u(x, t))} . \quad (6.9)$$

- The correlation length  $\xi$  is set by the confining potential,

$$\xi = \frac{1}{m} . \quad (6.10)$$

## 6.2 Field theory of the depinning transition

As we did in section 3.4, we write down a field theory for the equation of motion (6.8),

$$\mathcal{S}[u, \tilde{u}, F] = \int_{x,t} \tilde{u}(x, t) [(\partial_t - \nabla^2 + m^2)(u(x, t) - w) - F(x, u(x, t))] \quad (6.11)$$

We need to average over disorder, to obtain the disorder-averaged action  $e^{-\mathcal{S}[u, \tilde{u}]} := \overline{e^{-\mathcal{S}[u, \tilde{u}, F]}}$ , with

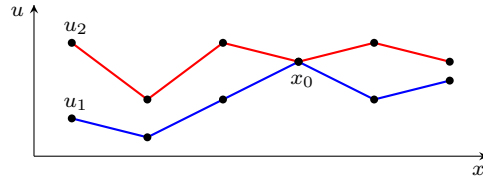
$$\mathcal{S}[u, \tilde{u}] = \int_{x,t} \tilde{u}(x, t) (\partial_t - \nabla^2 + m^2)[u(x, t) - w] - \frac{1}{2} \int_{x,t,t'} \tilde{u}(x, t) \Delta(u(x, t) - u(x, t')) \tilde{u}(x, t') . \quad (6.12) \text{dyn-action}$$

We remind the definition of the force-force correlator given in Eq. (4.8). We now state the famous [54]

**Middleton Theorem:** If  $F(x, u)$  is continuous in  $u$ , and  $\dot{u}(x, t) \geq 0$ , then  $\dot{u}(x, t') \geq 0$  for all  $t' \geq t$ . Moreover, if two configurations are ordered,  $u_2(x, t) \leq u_1(x, t)$ , then they remain ordered for all times, i.e.  $u_2(x, t'') \geq u_1(x, t')$  for all  $t'' \geq t' > t$ .

**Proof:** Consider an interface discretized in  $x$ . The trajectories  $u(x, t)$  are a function of time. Suppose that there exists  $x$  and  $t' > t$  s.t.  $\dot{u}(x, t') < 0$ . Define  $t_0$  as the first time when this happens,  $t_0 := \inf_x \inf_{t' > t} \{\dot{u}(x, t') < 0\}$ , and  $x_0$  the corresponding position  $x$ . By continuity of  $F$  in  $u$ , the velocity  $\dot{u}$  is continuous in time, and  $\dot{u}(x_0, t_0) = 0$ . This implies that the disorder force acting on  $x_0$  does not change in the next (infinitesimal) time step, and the only changes in force can come from a change in the elastic terms. Since by assumption no other point has a negative velocity, this change in force can not be negative, contradicting the assumption.

To prove the second part of the theorem, consider the following configuration at time  $t_0$ :



Here the red configuration is ahead of the blue one, except at position  $x_0$ , where they coincide. As in the first part of the proof, we wish to bring to a contradiction the hypothesis that at some time later  $u_1(x_0)$  (blue) is ahead of  $u_2(x_0)$  (red). For this reason, we have chosen  $t_0$  the infimum of times contradicting the theorem,  $t_0 := \inf_{t' > t} \{u_1(x_0, t') > u_2(x_0, t')\}$ . Consider the equation of motion Eq. (6.8) for the difference between  $u_1$  and  $u_2$ ,

$$\partial_t [u_2(x_0, t_0) - u_1(x_0, t_0)] = \nabla^2 [u_2(x_0, t_0) - u_1(x_0, t_0)] . \quad (6.13)$$

Note that the disorder force terms have canceled as well as the term of order  $m^2$ , since by assumption  $u_2(x_0, t_0) = u_1(x_0, t_0)$ . By construction, the r.h.s. is positive, leading to the desired contradiction.

### Remark: Uniqueness of perturbation theory

As in the statics, one encounters terms proportional to  $\Delta'(0^+) \equiv -R'''(0^+)$ . Here the sign-problem can uniquely be solved by observing that due to Middleton's theorem the membrane only moves forward,

$$t' > t \quad \implies \quad u(x, t') - u(x, t) \geq 0 . \quad (6.14) \text{ump-ahead}$$

Thus the argument of  $\Delta(u(x, t') - u(x, t))$  has a well-defined sign, allowing us to interpret derivatives at vanishing argument correctly. Practically this means that when evaluating diagrams containing  $\Delta(u(x, t) - u(x, t'))$ , one splits them into two pieces, one with  $t < t'$  and one with  $t > t'$ . Both pieces are well defined, even in the limit of  $t \rightarrow t'$ .

## 6.3 Loop expansion

We now consider the field theory defined by the action (6.12). Let us remember what we did in section 3: We reformulated a given model given by its Boltzmann weight with the help of a Langevin equation. This allowed us to evaluate equilibrium expectations as expectations in the dynamic field theory. This also led to identical renormalizations, e.g. for the effective coupling in  $\phi^4$  theory, see sections 3.8–3.9. We should therefore not be surprised to see the same renormalization for the disorder appearing in the driven dynamics. This is *partially* true, with significant differences appearing at 2-loop order.

Let us start by rederiving the corrections to the renormalized disorder correlator. The replica diagram in Eq. (5.3) is one of the two contributions to the effective potential-potential correlator  $R(u)$  given in Eq. (5.7). The perturbation in the dynamics is in terms of the *bare* force-force correlator  $\Delta_0(u)$ , which we note graphically as

$$\int_{x,t_1,t_2} \tilde{u}(x,t_1)\tilde{u}(x,t_2) \Delta_0(u(x,t_1) - u(x,t_2)) = \begin{array}{c} t_2 \bullet \longrightarrow \\ | \\ t_1 \bullet \longrightarrow \\ x \end{array} \quad (6.15)$$

The arrows are the response fields  $\tilde{u}(x,t_1)\tilde{u}(x,t_2)$ , sometimes represented by a wiggly line. Since the response function has a time direction, the static diagram (5.3) has two *descendants* in the dynamic formulation,

$$\begin{array}{c} \bullet \longrightarrow \bullet \\ | \qquad | \\ \bullet \longrightarrow \bullet \\ x \qquad y \end{array} \longrightarrow \begin{array}{c} \bullet \longrightarrow \bullet \longrightarrow \\ | \qquad | \\ \bullet \longrightarrow \bullet \longrightarrow \\ x \qquad y \end{array} + \begin{array}{c} \bullet \longrightarrow \bullet \longrightarrow \\ | \qquad | \\ \bullet \longleftarrow \bullet \longleftarrow \\ x \qquad y \end{array} \quad (6.16)$$

The first descendant with the corresponding times is

$$\begin{aligned} \begin{array}{c} t_2 \bullet \longrightarrow \bullet \longrightarrow t_4 \\ | \qquad | \\ t_1 \bullet \longrightarrow \bullet \longrightarrow t_3 \\ x \qquad y \end{array} &= - \int_{t_1,t_2,x} R(x-y,t_4-t_2)R(x-y,t_3-t_1) \times \\ &\quad \times \Delta_0(u(x,t_2) - u(x,t_1))\Delta_0''(u(y,t_4) - u(y,t_3))\tilde{u}(y,t_3)\tilde{u}(y,t_4) \\ &\simeq - \int_k \int_{t_1 < t_3, t_2 < t_4} e^{-(k^2+m^2)(t_4-t_2)} e^{-(k^2+m^2)(t_3-t_1)} \times \\ &\quad \times \Delta_0(u(y,t_4) - u(y,t_3))\Delta_0''(u(y,t_4) - u(y,t_3))\tilde{u}(y,t_3)\tilde{u}(y,t_4) \\ &= - \int_k \frac{1}{(k^2+m^2)^2} \Delta_0(u(y,t_4) - u(y,t_3))\Delta_0''(u(y,t_4) - u(y,t_3))\tilde{u}(y,t_3)\tilde{u}(y,t_4). \end{aligned} \quad (6.17)$$

Some remarks are in order: First, we have not explicitly written the integrations over  $t_3$ ,  $t_4$  and  $y$ . Second, the global minus sign in the first line originates from the derivatives acting once on the field at time  $t_3$ , and once at time  $t_4$ . Going to the second line, we have in the argument of  $\Delta$  replaced fields at time  $t_2$  by those at time  $t_4$ , and fields at time  $t_1$  by those at time  $t_3$ ; this is justified since the response function  $R$  decays rapidly in time. In the argument of  $\Delta$  we have also replaced  $x$  by  $y$ , as we did in the statics after arriving at Eq. (5.4). The remaining two times  $t_3$  and  $t_4$  can be taken arbitrarily far apart, thus this diagram encodes a contribution to the effective disorder.

The second descendant similarly gives

$$\begin{array}{c} t_2 \bullet \longrightarrow \bullet \longrightarrow t_4 \\ | \qquad | \\ t_1 \bullet \longleftarrow \bullet \longleftarrow t_3 \\ t_{1,x} \qquad y \end{array} \simeq - \int_k \frac{1}{(k^2+m^2)^2} \Delta_0'(u(y,t_4) - u(y,t_3))^2 \tilde{u}(y,t_3)\tilde{u}(y,t_4) \quad (6.18)$$

We used that  $\Delta_0'(u)$  is odd in  $u$ . Together, these two diagrams give with  $I_1$  defined in Eq. (5.5)

$$\begin{array}{c} \bullet \longrightarrow \bullet \longrightarrow \\ | \qquad | \\ \bullet \longrightarrow \bullet \longrightarrow \\ \bullet \longrightarrow \bullet \longrightarrow \\ | \qquad | \\ \bullet \longleftarrow \bullet \longleftarrow \\ \bullet \longleftarrow \bullet \longleftarrow \end{array} + \begin{array}{c} \bullet \longrightarrow \bullet \longrightarrow \\ | \qquad | \\ \bullet \longrightarrow \bullet \longrightarrow \\ \bullet \longleftarrow \bullet \longleftarrow \\ | \qquad | \\ \bullet \longleftarrow \bullet \longleftarrow \\ \bullet \longleftarrow \bullet \longleftarrow \end{array} \quad (6.19)$$

$$\simeq -I_1 \left[ \Delta_0(u(y,t_4) - u(y,t_3))\Delta_0''(u(y,t_4) - u(y,t_3)) + \Delta_0'(u(y,t_4) - u(y,t_3))^2 \right] \tilde{u}(y,t_3)\tilde{u}(y,t_4)$$

Taking care of the combinatorial factors, and the factors of 1/2 in the action, we read off their contribution to the effective disorder  $\hat{\Delta}(u)$ ,

$$\delta_1 \hat{\Delta}(u) = - \left[ \Delta_0(u)\Delta_0''(u) + \Delta_0'(u)^2 \right] I_1 = -\partial_u^2 \frac{1}{2} \Delta_0(u)^2 I_1 \quad (6.20)$$

This is the same contribution as given by the diagram in Eq. (5.3), noting that  $\Delta(u) = -R''(u)$ , and using the combinatorial factor 1/2 reported in Eq. (5.7).

To complete our analysis, consider the second diagram; it also has two descendants,

$$\begin{array}{c} \bullet \\ \vdots \\ \bullet \\ \vdots \\ \bullet \end{array} \begin{array}{c} \bullet \\ \vdots \\ \bullet \\ \vdots \\ \bullet \end{array} \begin{array}{c} \bullet \\ \vdots \\ \bullet \\ \vdots \\ \bullet \end{array} \begin{array}{c} \bullet \\ \vdots \\ \bullet \\ \vdots \\ \bullet \end{array} \rightarrow \begin{array}{c} \bullet \\ \vdots \\ \bullet \\ \vdots \\ \bullet \end{array} \begin{array}{c} \bullet \\ \vdots \\ \bullet \\ \vdots \\ \bullet \end{array} \begin{array}{c} \bullet \\ \vdots \\ \bullet \\ \vdots \\ \bullet \end{array} \begin{array}{c} \bullet \\ \vdots \\ \bullet \\ \vdots \\ \bullet \end{array} + \begin{array}{c} \bullet \\ \vdots \\ \bullet \\ \vdots \\ \bullet \end{array} \begin{array}{c} \bullet \\ \vdots \\ \bullet \\ \vdots \\ \bullet \end{array} \begin{array}{c} \bullet \\ \vdots \\ \bullet \\ \vdots \\ \bullet \end{array} \begin{array}{c} \bullet \\ \vdots \\ \bullet \\ \vdots \\ \bullet \end{array} \quad (6.21)$$

After time-integration this yields

$$\begin{array}{c} \bullet \\ \vdots \\ \bullet \\ \vdots \\ \bullet \end{array} \begin{array}{c} \bullet \\ \vdots \\ \bullet \\ \vdots \\ \bullet \end{array} \begin{array}{c} \bullet \\ \vdots \\ \bullet \\ \vdots \\ \bullet \end{array} \begin{array}{c} \bullet \\ \vdots \\ \bullet \\ \vdots \\ \bullet \end{array} \simeq \int_k \frac{1}{(k^2 + m^2)^2} \Delta_0(0) \Delta_0''(u(y, t_4) - u(y, t_3)) \quad (6.22)$$

$$\begin{array}{c} \bullet \\ \vdots \\ \bullet \\ \vdots \\ \bullet \end{array} \begin{array}{c} \bullet \\ \vdots \\ \bullet \\ \vdots \\ \bullet \end{array} \begin{array}{c} \bullet \\ \vdots \\ \bullet \\ \vdots \\ \bullet \end{array} \begin{array}{c} \bullet \\ \vdots \\ \bullet \\ \vdots \\ \bullet \end{array} \simeq \int_k \frac{1}{(k^2 + m^2)^2} \Delta_0'(0^+) \Delta_0''(u(y, t_4) - u(y, t_3)) \quad (6.23)$$

The last diagram is asymmetric under exchange of  $t_3$  and  $t_4$ , thus vanishes after integrating over these times. (B.t.w., inserted into a 2-loop diagram, it is this diagram which is responsible for the differences seen there.) Together, they give a second contribution to the effective disorder

$$\delta_2 \hat{\Delta}(u) = \Delta_0(0) \Delta_0''(u) I_1 = \partial_u^2 \Delta_0(0) \Delta_0(u) I_1. \quad (6.24) \quad 7.24$$

This is the same contribution as given by Eq. (5.4).

The last diagram we drew for the equilibrium was given in Eq. (5.6). Its descendant reads

$$\begin{array}{c} \bullet \\ \vdots \\ \bullet \\ \vdots \\ \bullet \end{array} \begin{array}{c} \bullet \\ \vdots \\ \bullet \\ \vdots \\ \bullet \end{array} \begin{array}{c} \bullet \\ \vdots \\ \bullet \\ \vdots \\ \bullet \end{array} \begin{array}{c} \bullet \\ \vdots \\ \bullet \\ \vdots \\ \bullet \end{array} \rightarrow \begin{array}{c} \bullet \\ \vdots \\ \bullet \\ \vdots \\ \bullet \end{array} \begin{array}{c} \bullet \\ \vdots \\ \bullet \\ \vdots \\ \bullet \end{array} \begin{array}{c} \bullet \\ \vdots \\ \bullet \\ \vdots \\ \bullet \end{array} \begin{array}{c} \bullet \\ \vdots \\ \bullet \\ \vdots \\ \bullet \end{array} \quad (6.25) \quad 7.25$$

While the static diagram on the l.h.s. does not contribute to the effective disorder since it is a 3-replica term (three independent sums over replicas), the second term (r.h.s.) does not contribute due to the acausal loop, as it does not allow for any time integration, thus vanishes.

For completeness, we write the effective disorder-force correlator at 1-loop order

$$\hat{\Delta}(u) = \Delta_0(u) - \partial_u^2 [\Delta_0(u)^2 - \Delta_0(0) \Delta_0(u)] I_1 \quad (6.26)$$

This result can also be obtained by applying  $-\partial_u^2$  to Eq. (5.7). We thus recover the same flow equation as given in Eq. (5.7),

$$\partial_\ell \tilde{\Delta}(u) = (\epsilon - 2\zeta) \tilde{\Delta}(u) + \zeta u \tilde{\Delta}'(u) - \partial_u^2 \frac{1}{2} [\tilde{\Delta}(u)^2 - \tilde{\Delta}(0)]^2. \quad (6.27)$$

While this might not be surprising on a formal level, it is indeed *very surprising* on a physical level: The effective disorder (5.7) is for the minimum energy state, while the derivation given above is for a state at depinning. We will see in the next section 6.4 that there are indeed corrections at 2-loop order which account for this difference, and which are important to reconcile the physically observed exponents with the theoretical prediction.

Before going there, let us complete our analysis with two additional contributions not present in the statics, and which we will interpret as the critical force at depinning, and a renormalization of friction, leading to a non-trivial dynamical exponent  $z$ , already introduced in Eq. (6.3).

$$\begin{array}{c} \bullet \\ \vdots \\ \bullet \\ \vdots \\ \bullet \end{array} \begin{array}{c} \bullet \\ \vdots \\ \bullet \\ \vdots \\ \bullet \end{array} \begin{array}{c} \bullet \\ \vdots \\ \bullet \\ \vdots \\ \bullet \end{array} \begin{array}{c} \bullet \\ \vdots \\ \bullet \\ \vdots \\ \bullet \end{array} = \tilde{u}(x, t_2) \int_{t_1, k} \Delta_0'(u(x, t_2) - u(x, t_1)) e^{-(t_2 - t_1)(k^2 + m^2)} \Theta(t_1 < t_2) \\ \simeq \tilde{u}(x, t_2) \int_{t_1, k} \left[ \Delta_0'(0^+) + \Delta_0''(0^+) (t_2 - t_1) \dot{u}(x, t_2) + \dots \right] e^{-(t_2 - t_1)(k^2 + m^2)} \Theta(t_1 < t_2) \\ = \tilde{u}(x, t_2) \int_k \frac{\Delta_0'(0^+)}{k^2 + m^2} + \frac{\Delta_0''(0^+)}{(k^2 + m^2)^2} \dot{u}(x, t_2) + \dots \quad (6.28)$$

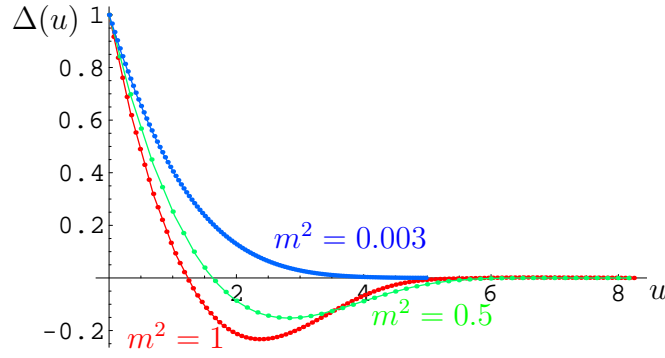


Figure 6.2: Doing RG in a simulation: Crossover from RB disorder to RF for a driven particle [42].

The first term corresponds to a constant driving force  $f$  in Eq. (6.1), and can be interpreted as the threshold force below which the manifold will not move:

$$f_c = - \int_k \frac{\Delta'_0(0^+)}{k^2 + m^2}. \quad (6.29)$$

Its value is non-universal, but gives us a pretty good idea how strong we have to drive. In the driving protocol with a parabola centered at  $w$  as given in Eq. (6.8), it gives us the size of the *hysteresis loop*,

$$m^2 \left[ \overline{u_w - w}^{\text{forward}} - \overline{u_w - w}^{\text{backward}} \right] = 2f_c. \quad (6.30)$$

Let us now turn to the second term in Eq. (6.28). Restoring the friction coefficient  $\eta$  in front of  $\partial_t u(x, t)$  in the equation of motion (6.8) yields

$$\eta_{\text{eff}} = 1 - \Delta''_0(0^+) I_1 + \dots \quad (6.31)$$

The dynamical exponent  $z$  is then obtained as

$$z = 2 - m \partial_m \ln \eta_{\text{eff}} = 2 - \tilde{\Delta}''(0^+) + \dots \quad (6.32)$$

Taking one derivative of Eq. (5.23), and evaluating it in the limit of  $u \rightarrow 0$  allows us to conclude that

$$\tilde{\Delta}''(0^+) = \frac{\epsilon - \zeta}{3}. \quad (6.33)$$

Thus

$$z = 2 - \frac{\epsilon - \zeta}{3} + \dots = \begin{cases} 2 - \frac{\epsilon}{3} + \dots & \text{RP disorder} \\ 2 - \frac{2\epsilon}{9} + \dots & \text{RF disorder} \end{cases} \quad (6.34)$$

## 6.4 Depinning beyond leading order

Renormalization at the depinning transition was first treated at 1-loop order by Natterman et al. [53], soon followed by Narayan and Fisher [55]. As we have seen, the 1-loop flow-equations are identical to those of the statics. This is surprising, since physically, the phenomena at equilibrium and at depinning are quite different. There was even a claim by [55], that the roughness exponent in the random field universality class is  $\zeta = \epsilon/3$  also at depinning. After a long debate among numerical physicists, the issue is now resolved: The roughness is significantly larger, and reads e.g. for the driven polymer  $\zeta = 1.25 \pm 0.005$  [56, 57], and

possibly exactly  $\zeta = \frac{5}{4}$  [58]; this should be contrasted to  $\zeta = 1$  in the statics, see Eq. (5.27). Clearly, a 2-loop analysis is necessary to resolve these issues. The latter was performed in [39, 38].

At the depinning transition, the 2-loop functional RG reads [39, 38] \*\*\* recheck, \*\*

$$\begin{aligned} \partial_\ell \Delta(u) = & (\epsilon - 2\zeta)\Delta(u) + \zeta u \Delta'(u) - \frac{1}{2} \partial_u^2 [\Delta(u) - \Delta(0)]^2 \\ & + \frac{1}{2} \partial_u^2 \{ [\Delta(u) - \Delta(0)] \Delta'(u)^2 + \Delta'(0^+)^2 \Delta(u) \} . \end{aligned} \quad (6.35)$$

Compared to the RG-equation (5.54) for the statics the only change is in the last sign on the second line of (6.35), given in red. This has important consequences for the physics: First of all, the roughness exponent  $\zeta$  for the random-field universality class changes from  $\zeta = \frac{\epsilon}{3}$  to

$$\zeta = \frac{\epsilon}{3} (1 + 0.143317\epsilon + \dots) . \quad (6.36) \text{zetaRFdyn}$$

The reason why the argument in the derivation of Eq. (5.27) fails is that when integrating Eq. (6.35) the last term yields a boundary term at  $u = 0$ , due to the different sign.

Second, the random-bond universality class is unstable and always renormalizes to the random-field universality class. This is physically expected: Since the membrane only moves forwards, it always experiences a new disorder configuration, and it has no way to “know” whether this disorder is derived from a potential or not. This crossover can already be seen for a toy model with a single particle, measuring the renormalized disorder correlator at a scale  $\ell = 1/m$  set by the confining potential, see figure 6.2. Generalizing the arguments of section 5.5 [43], it was confirmed numerically for a string that both RB and RF disorder flow to the RF fixed point [44], and that this fixed point is very close to the analytic solution of Eq. (6.35), see figure 6.4.

This non-potentiality is most strikingly observed in the random periodic universality class, which is the relevant one for charge density waves. The fixed point for a periodic disorder of period one reads (remember  $\Delta(u) = -R''(u)$ )

$$\Delta^*(u) = \frac{\epsilon}{36} + \frac{\epsilon^2}{108} - \left( \frac{\epsilon}{6} + \frac{\epsilon^2}{9} \right) u(1-u) \quad (6.37) \text{and-per-fp}$$

Integrating over a period, we find (suppressing in  $F(x, u)$  the dependence on the coordinate  $x$  for simplicity of notation)

$$\int_0^1 du \Delta^*(u) \equiv \int_0^1 du \overline{F(u)F(u')} = -\frac{\epsilon^2}{108} . \quad (6.38) \text{period}$$

	$d$	$\epsilon$	$\epsilon^2$	estimate	simulation
	3	0.33	0.38	$0.38 \pm 0.02$	$0.355 \pm 0.01$ [59]
$\zeta$	2	0.67	0.86	$0.82 \pm 0.1$	$0.753 \pm 0.002$ [59]
	1	1.00	1.43	$1.2 \pm 0.2$	$1.25 \pm 0.005$ [57]
	3	0.89	0.85	$0.84 \pm 0.01$	$0.84 \pm 0.02$
$\beta$	2	0.78	0.62	$0.53 \pm 0.15$	$0.64 \pm 0.02$
	1	0.67	0.31	$0.2 \pm 0.2$	$0.25 \dots 0.4$
	3	0.58	0.61	$0.62 \pm 0.01$	
$\nu$	2	0.67	0.77	$0.85 \pm 0.1$	$0.77 \pm 0.04$
	1	0.75	0.98	$1.25 \pm 0.3$	$1 \pm 0.05$

	$\epsilon$	$\epsilon^2$	estimate	simulation
$\zeta$	0.33	0.47	$0.47 \pm 0.1$	$0.39 \pm 0.002$
$\beta$	0.78	0.59	$0.6 \pm 0.2$	$0.68 \pm 0.06$
$z$	0.78	0.66	$0.7 \pm 0.1$	$0.74 \pm 0.03$
$\nu$	1.33	1.58	$2 \pm 0.4$	$1.52 \pm 0.02$

Figure 6.3: The critical exponents at the depinning transition, for short range elasticity (left) and for long range elasticity (right).



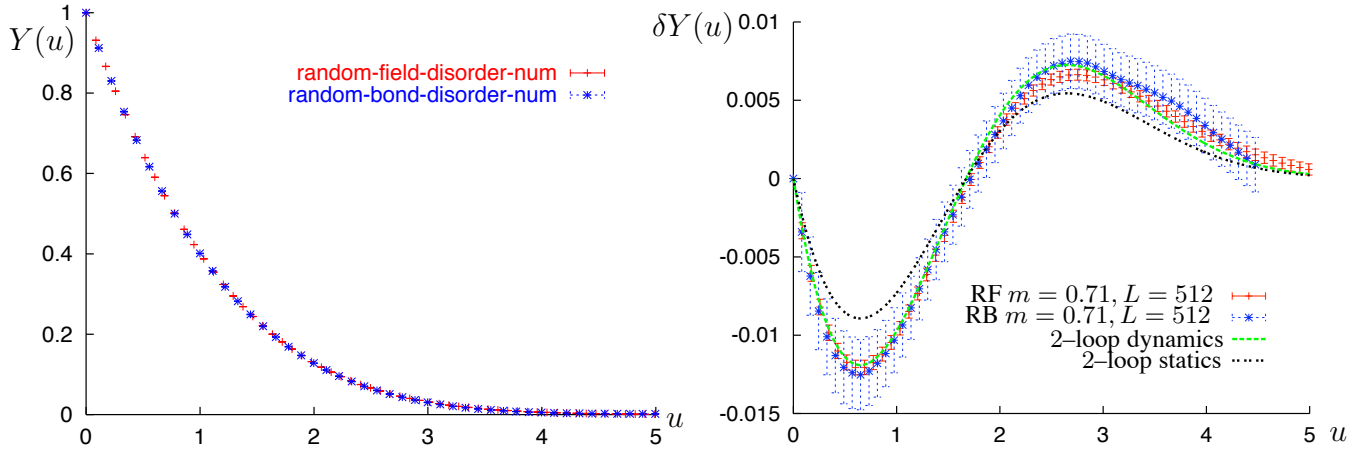


Figure 6.4: Left: The rescaled fixed point  $Y(u)$  for the force-force correlations  $\Delta(u)$ , starting both from a RB and RF initial condition. Right: Residual error  $\delta Y(u)$  for a string [44], after subtracting the 1-loop correction. The measured difference is consistent with the depinning fixed point, but not the static one.

In an equilibrium situation, this correlator would vanish, since potentiality requires  $\int_0^1 du F(u) \equiv 0$ . Here, there are non-trivial contributions at 2-loop order (order  $\epsilon^2$ ), violating this condition and rendering the problem non-potential. This same mechanism is also responsible for the violation of the conjecture  $\zeta = \frac{\epsilon}{3}$ , which could be proven on the assumption that the problem remains potential under renormalization. This breaking of potentiality under renormalization is a quite novel mechanism.

The other critical exponents mentioned above can also be calculated. The dynamical exponent  $z$  (for RF-disorder) reads [39, 38]

$$z = 2 - \frac{2}{9}\epsilon - 0.04321\epsilon^2 + \dots \quad (6.39)$$

For RP disorder, one can go further [8] **\*recheck\***

$$z = 2 - \frac{\epsilon}{3} - \frac{\epsilon^2}{9} + \left[ \frac{2\zeta(3)}{9} - \frac{1}{18} \right] \epsilon^3 - \left[ \frac{70\zeta(5)}{81} - \frac{\zeta(4)}{6} - \frac{17\zeta(3)}{162} + \frac{7}{324} \right] \epsilon^4 - \left[ \frac{541\zeta(3)^2}{162} + \frac{37\zeta(3)}{36} + \frac{29\zeta(4)}{648} + \frac{703\zeta(5)}{243} + \frac{175\zeta(6)}{162} - \frac{833\zeta(7)}{216} + \frac{17}{1944} \right] \epsilon^5 + \mathcal{O}(\epsilon^6). \quad (6.40)$$

Other exponents are related via the scaling relations (6.6) and (6.7). That the method works well even quantitatively can be inferred from table 6.3.

## 6.5 Connection with extreme-value statistics

**\*\*\*recheck section\*\*\*** For a single particle, there is a very nice geometrical construction to obtain the trajectories, as indicated in figure 6.5: For a given  $w$ , draw a line of slope  $m^2(u - w)$ . For forward driving,  $u(w)$  is the leftmost intersection with the pinning force  $F(u)$ , while for backward driving it is the rightmost such intersection. As indicated by the arrows, this is equivalent to shine light with slope  $m^2$ , either from the left for forward driving, or from the right for backward driving. Parts in the shadow are not visited, while illuminated ones are. The jumps are the avalanches of section 5.4.

Using this construction, one can obtain both the distribution of critical forces, as well as the renormalized disorder force-force correlator  $\Delta(w)$  analytically [60]. As we will see below, the distribution of threshold forces correspond to the three main classes of extreme-value statistics. Let us consistent with Eq. (5.52) define

$$\Delta(w - w') = m^4 \overline{[w - u(w)][w' - u(w')]^c}. \quad (6.41)$$

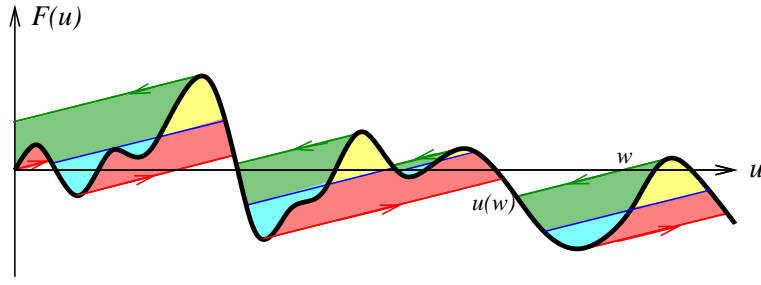


Figure 6.5: Construction of  $u(w)$  in  $d = 0$ , for the pinning force  $F(u)$  (bold black line). The two quasi-static motions driven to the right and to the left are indicated by red and green arrows, and exhibit jumps (“dynamical shocks”). The position of the shocks in the statics is shown for comparison, based on the Maxwell construction (equivalence of light blue and yellow areas, both bright in black and white). The critical force is  $1/(2m^2)$  times the area bounded by the hull of the construction.

Each class (discussed below), has its own exponent  $\zeta$ , setting a scale  $\rho_m \sim m^{-\zeta}$ . At small  $m$ , force-force correlations are universal, given by

$$\Delta(w) = m^4 \rho_m^2 \tilde{\Delta}(w/\rho_m). \quad (6.42)$$

The fixed-point function  $\tilde{\Delta}(w)$  depends on the universality class. The three classes are distinguished by the distribution of the random forces  $F$  for the *most blocking* forces.

#### Gumbel class:

$$P(F) \simeq e^{-A(-F)^\gamma} \quad \text{as} \quad F \rightarrow -\infty. \quad (6.43)$$

The threshold forces are distributed according to a *Gumbel* distribution,

$$F_c(m) = F_c^0(m) + x m^2 \rho_m, \quad P_G(x) = e^{-x} \exp(-e^{-x}). \quad (6.44)$$

The constant  $F_c^0(m)$ , the scale  $\rho_m$ , and the exponent  $\zeta$  are

$$F_c^0(m) = A^{-\frac{1}{\gamma}} (\ln m^{-2})^{\frac{1}{\gamma}}, \quad \rho_m^{-1} = \gamma A^{\frac{1}{\gamma}} m^\zeta (\ln m^{-2})^{1-\frac{1}{\gamma}}, \quad \zeta = 2. \quad (6.45)$$

The effective disorder correlator reads

$$\tilde{\Delta}_G(w) = \frac{w^2}{2} + \text{Li}_2(1 - e^w) + \frac{\pi^2}{6}. \quad (6.46)$$

#### Fréchet class:

$$P(F) \simeq A \alpha (\alpha + 1) (-F)^{-2-\alpha} \Theta(-F) \quad \text{as} \quad F \rightarrow -\infty. \quad (6.47)$$

The threshold forces are distributed according to a *Fréchet* distribution ( $\alpha > 0$ ),

$$F_c(m) = x m^2 \rho_m, \quad P_F(x) = \alpha x^{-\alpha-1} e^{-x^{-\alpha}} \Theta(x). \quad (6.48)$$

The mean pinning force  $\overline{F_c(m)}$ , the scale  $\rho_m$ , and the exponent  $\zeta$  are

$$\overline{F_c(m)} = \Gamma(1 - \frac{1}{\alpha}) m^2 \rho_m, \quad \rho_m = A^{\frac{1}{\alpha}} m^{-\zeta}, \quad \zeta = 2 + \frac{2}{\alpha}. \quad (6.49)$$

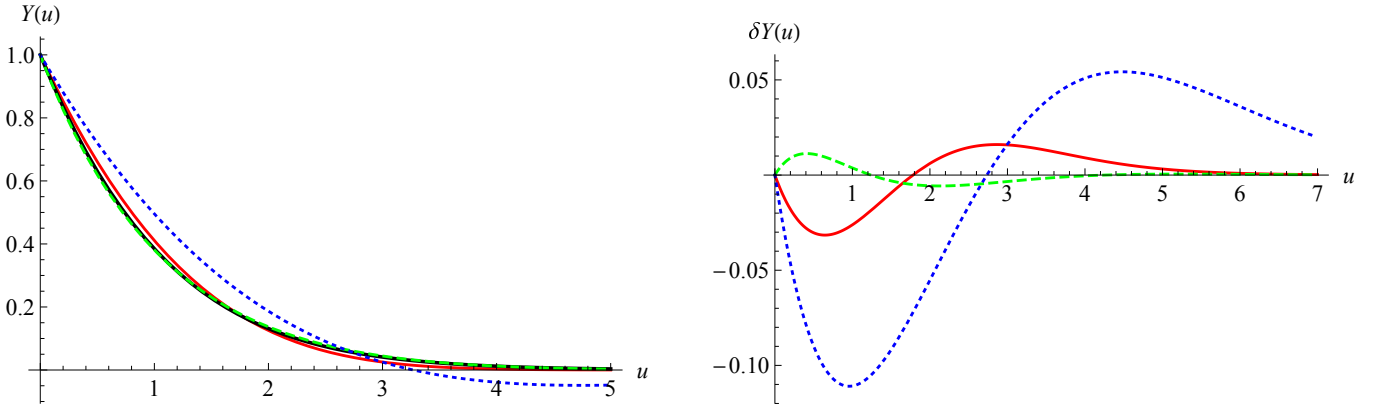


Figure 6.6: Left: The function (6.46) rescaled s.t.  $Y(0) = 1$ , and  $\int_u Y(u) = 1$  (in black). This is compared to the similarly rescaled 1-loop prediction (5.31) (in red), and the straightforward 2-loop prediction obtained from Eq. (6.35) (blue dashed). To improve convergence, we have used a Padé-(1,1) resummation (green, dashed). Right: The same functions with the black curve subtracted. We see that the 1-loop result is quite good, and that the Padé-resummed 2-loop result improves on it.

The effective disorder correlator can be written as an integral, and is ill-defined for  $\alpha < 2$ , where the second moment of the force-force fluctuations vanishes. For  $\alpha > 2$  it has a cusp at small  $w$ , and decays algebraically at large  $w$ ,

$$\begin{aligned} \tilde{\Delta}_F(w) &\simeq \Gamma\left(\frac{\alpha-2}{\alpha}\right) - \Gamma\left(1 - \frac{1}{\alpha}\right)^2 + \frac{1}{\alpha^2} \Gamma\left(-\frac{1}{\alpha}\right) w + \frac{\alpha w^2}{4\alpha + 2} + \dots \quad \text{for } w \rightarrow 0 \\ \tilde{\Delta}_F(w) &\simeq \frac{w^{2-\alpha} \alpha}{(\alpha-2)(\alpha-1)} + \dots \quad \text{for } w \rightarrow \infty \end{aligned} \quad (6.50)$$

**Weibull class:** In this class, the random forces are bounded from below, growing as a power law above the threshold, here chosen to be zero,

$$P(F) = A \alpha (\alpha - 1) F^{\alpha-2} \theta(F), \quad \alpha > 1. \quad (6.51)$$

The threshold forces are distributed according to a *Weibull* distribution

$$F_c(m) = x m^2 \rho_m, \quad P_W(x) = \alpha (-x)^{\alpha-1} e^{-(x)^\alpha} \Theta(-x). \quad (6.52)$$

The mean pinning force  $\overline{F_c(m)}$ , the scale  $\rho_m$ , and the exponent  $\zeta$  are

$$\overline{F_c(m)} = -A^{-\frac{1}{\alpha}} m^{\frac{2}{\alpha}} \Gamma\left(1 + \frac{1}{\alpha}\right), \quad \rho_m = A^{-\frac{1}{\alpha}} m^{-\zeta}, \quad \zeta = 2 - \frac{2}{\alpha}. \quad (6.53)$$

The most important class is the box distribution with minimum at 0 ( $\alpha = 2$ ). Its force-force correlator is

$$\tilde{\Delta}_W^{\alpha=2}(w) = \frac{e^{-w^2}}{4w} \left[ 2w - e^{w^2} \sqrt{\pi} (2w^2 + 1) \operatorname{erfc}(w) + \sqrt{\pi} \right] + \frac{1}{2} \sqrt{\pi} \left[ w e^{-w^2} - \Gamma\left(\frac{3}{2}, w^2\right) \right]. \quad (6.54) \text{DeltaWeibull}$$

An interesting question is whether one of the cases discussed above can be related to the  $\epsilon$  expansion. The most natural candidate is the Gumbel class with  $\gamma = 1$ , or  $\gamma = 2$ . In that case  $\zeta = 2$ , close to the 2-loop result (6.36), i.e.  $\zeta(\epsilon = 4) = 2.098$ . A comparison for the renormalized force-force correlator  $\Delta(u)$ , rescaled to a function  $Y(u)$  with  $Y(0) = 1$ , and  $\int_0^\infty dy Y(u) = 1$ , is shown on figure 6.6. The agreement, especially after proper resummation, is quite good. Note however, that the functions (6.54) and (6.46) are close, so that the  $\epsilon$  expansion cannot really discriminate between them.

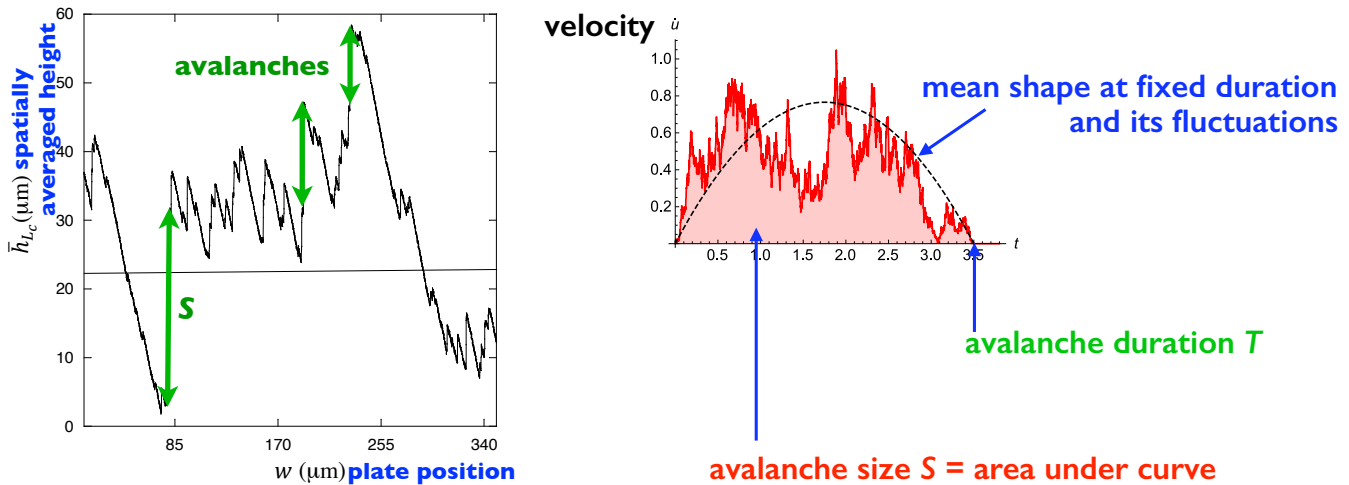


Figure 7.1: Left: The mean spatial height in the contact-line depinning experiment of Fig. 6.1. Right: Increasing the time resolution to resolve a single avalanche (jump, marked by the arrow), the velocity inside a single avalanche can be viewed as a random walk with absorbing boundary conditions at vanishing velocity. This allows to define observables as the mean avalanche shape, the size  $S$  (area under the curve), or its duration  $T$ .

## 7 Avalanches

### 7.1 Observables and scaling relations

When driving a system very slowly, long times of inactivity are followed by bursts of activity, which on these long time scales look almost instantaneous. This can be seen of Fig. 7.1. Observables of interest are avalanche size  $S$ , duration  $T$ , velocity  $\dot{u}$ , and shape  $\langle \dot{u}(t) \rangle$ , to name a few. Below, we list the main *scalar* ones, and give their scaling relations. We will get back to the shape (expectation of velocity as a function of time) below. This setting is for depinning. Some observables, as the avalanche-size distribution can also be formulated in the statics: These *static avalanches*, also termed *shocks*, are the changes in the ground-state configuration upon a change in an applied field, i.e. the position  $w$  of the confining potential. We will comment on differences between these two at the appropriate positions.

- Avalanches are the response of the system to an increase in force. They have a typical size

$$S_m := \frac{\langle S^2 \rangle}{2 \langle S \rangle} \sim \xi^{d+\zeta} \sim m^{-(d+\zeta)} . \quad (7.1)_{Sm}$$

- the avalanche-size distribution per unit force,

$$\rho_f(S) := \frac{\delta N(S)}{\delta f} \simeq S^{-\tau} f_S(S/S_m) g_S(S/S_0) , \quad S_0 \ll S_m \quad (7.2)_{hof}$$

has a large-scale cutoff  $S_m$  defined in Eq. (7.1) due to the confining potential, and a small-scale cutoff  $S_0$  due to the size of the kick or discretization effects (as in a spin system). The scaling functions are expected to have a finite limit when  $m \rightarrow 0$ , i.e.  $\lim_{x \rightarrow 0} f(x) = \text{const}$ , and  $\lim_{x \rightarrow \infty} g(x) = 1$ . An increase  $\delta f$  in the force is then given by an increase  $\delta u(x)$  in  $u$ , which integrated over space gives  $S = \int_x \delta u(x)$ . On the other hand, we can integrate Eq. (7.2) over  $S$ . Together, these relations give

$$\delta f = m^2 \int_x \delta u(x) = m^2 S = \delta f m^2 \int_0^\infty dS S \rho_f(S) \sim \delta f m^2 [S_m^{2-\tau} - \mathcal{O}(S_0^{2-\tau})] \quad (7.3)$$

	$\rho(S)$	$\rho(S_\phi)$	$\rho(T)$	$\rho(\dot{u})$	$\rho(\dot{u}_\phi)$
	$S^{-\tau}$	$S_\phi^{-\tau_\phi}$	$T^{-\alpha}$	$\dot{u}^{-a}$	$\dot{u}_\phi^{-a_\phi}$
SR elasticity	$\tau = 2 - \frac{2}{d+\zeta}$	$\tau_\phi = 2 - \frac{2}{d_\phi+\zeta}$	$\alpha = 1 + \frac{d-2+\zeta}{z}$	$a = 2 - \frac{2}{d+\zeta-z}$	$a_\phi = 2 - \frac{2}{d_\phi+\zeta-z}$
LR elasticity	$\tau = 2 - \frac{1}{d+\zeta}$	$\tau_\phi = 2 - \frac{1}{d_\phi+\zeta}$	$\alpha = 1 + \frac{d-1+\zeta}{z}$	$a = 2 - \frac{1}{d+\zeta-z}$	$a_\phi = 2 - \frac{1}{d_\phi+\zeta-z}$

Table 7.1: Scaling relations discussed in the main text for SR elasticity. LR elasticity is given for comparison.

As we will see below  $\tau < 2$ , and the last term can be dropped for  $m \rightarrow 0$ . Inserting  $S_m$  from Eq. (7.1) then yields

$$\tau = 2 - \frac{2}{d + \zeta} . \quad (7.4)_{\text{au-relation}}$$

- the distribution of avalanche sizes in a submanifold  $\phi$  of dimension  $d_\phi$ ,

$$\rho_f^\phi(S^\phi) \sim S^{-\tau_\phi} , \quad S_m^\phi \gg S^\phi \gg S_0^\phi , \quad \tau_\phi = 2 - \frac{2}{d_\phi + \zeta} . \quad (7.5)_{\text{au-phi-relat}}$$

The derivation proceeds as for Eq. (7.4).

- avalanche size and duration are related via

$$S_m \sim T_m^\gamma , \quad \gamma = \frac{d + \zeta}{z} . \quad (7.6)$$

This is obtained from the scaling relations  $S_m \sim m^{-d-\zeta}$ , and  $T_m \sim m^{-z}$ .

- the (unnormalized) duration distribution per unit force is

$$\rho_f(T) \sim T^{-\alpha} , \quad T_m \gg T \gg T_0 , \quad T_m = \frac{\langle T^3 \rangle}{\langle T^2 \rangle} . \quad (7.7)_{\text{ho-T}}$$

The exact integral relation  $\rho(S)dS = \rho(T)dT$  implies  $S_m^{1-\tau} \sim T_m^{1-\alpha}$ . Setting  $S_m \sim m^{-(d+\zeta)}$ , and  $T_m \sim m^{-z}$  yields with the help of Eq. (7.4)

$$\alpha = 1 + \frac{d + \zeta - 2}{z} . \quad (7.8)$$

- the (unnormalized) velocity distribution

$$\rho_f(\dot{u}) \sim \dot{u}^{-a} , \quad \dot{u}_m \gg \dot{u} \gg \dot{u}_0 , \quad \dot{u}_m = \frac{S_m}{\tau_m} . \quad (7.9)_{\text{ho-dotu}}$$

The exponent  $a$  is obtained from arguments similar to those used in the derivation of Eqs. (7.4) and (7.5), with the result that in the denominator the dimension of the observable in question appears. For the velocity distribution it yields

$$a = 2 - \frac{2}{d + \zeta - z} . \quad (7.10)$$

- avalanche extensions: In general, avalanches have a well-defined spatial extension  $\ell$ , allowing us to define their distribution  $P(\ell)$ . If  $\ell \ll \xi = 1/m$ , then  $\ell$ , and not  $\xi$  is the relevant scale, and  $S \sim \ell^{d+\zeta}$ . Writing  $P(S)dS = P(\ell)d\ell$  allows us to conclude [61] that for extensions between the lattice cutoff  $a$  and  $\xi = 1/m$ ,

$$P(\ell) \sim \ell^{-\kappa} , \quad a \ll \ell \ll \frac{1}{m} , \quad \kappa = d + \zeta - 1 . \quad (7.11)$$

- avalanche volume: in higher dimensions, it is difficult to define the spatial extension of an avalanche, while its volume is well-defined. Using  $P(V)dV = P(S)dS$ , and  $S = m^{-d-\zeta}$ ,  $V \sim m^{-\zeta}$ , we arrive at

$$P(\ell) \sim \ell^{-\kappa_V}, \quad a^d \ll V \ll \frac{1}{m^d}, \quad \kappa_V = 2 - \frac{2 - \zeta}{d}. \quad (7.12)$$

\*\*\*check notation with Ale paper\*\*\*

- differences between static avalanches (shocks) and avalanches at depinning: A conceptually and practically important question is whether static avalanches and avalanches at depinning are in the same universality class. As the roughness exponent  $\zeta$  differs from one class to the other, Eq. (7.4) implies that they also have a different avalanche-size exponent  $\tau$ , and thus must be different. We will see below that this difference is not visible at 1-loop order, but has to show up at 2-loop order.

## 7.2 Phenomenology

\*\*\*talk about experiments, SR versus LR. Say that ABBM is MF, and is LR.\*\*\* For magnetic avalanches, also known as *Barkhausen noise*, a good review is [62].

\*\*\*talk about ABBM  $\rightarrow$  BFM  $\rightarrow$  SR

Up to now, our modeling of depinning was based on the equation of motion (6.8) for the position of the interface. This formulation makes it difficult to extract observables involving the velocity. For this purpose it is better to take a time derivative of Eq. (6.8), to get an equation of motion for the velocity  $\dot{u}(x, t)$ ,

$$\partial_t \dot{u}(x, t) = (\nabla^2 - m^2) [\dot{u}(x, t) - \dot{w}(t)] + \partial_t F(x, u(x, t)). \quad (7.13)$$

Taking the derivative yields

$$\partial_t \dot{u}(x, t) = (\nabla^2 - m^2) [\dot{u}(x, t) - \dot{w}(t)] + \dot{u}(x, t) \partial_u F(x, u(x, t)). \quad (7.14)$$

## 7.3 ABBM model

The field theory to be constructed below gives a quantitative description of avalanches in a force field  $F(x, u)$ , with short-ranged correlations in both the  $x$  and  $u$ -directions. We start with a toy model for a single degree of freedom, and then proceed in two steps to short-range correlated forces for an interface.

The toy model in question is the ABBM model, introduced in 1990 by Alessandro, Beatrice, Bertotti and Montorsi [63, 64], see also [65, 66]. It reads, setting  $w(t) = vt$ ,

$$\partial_t \dot{u}(t) = m^2 [v - \dot{u}(t)] + \partial_t F(u(t)) \quad (7.15)$$

$$\partial_t F(u(t)) = \sqrt{\dot{u}(t)} \xi(t), \quad \langle \xi(t) \xi(t') \rangle = 2\sigma \delta(t - t') \quad (7.16)$$

The last equation implies that  $F(u)$  is a random walk, as can be seen as follows: As  $\dot{u}$  is non-negative,  $t$  is an increasing function of  $u$ , and we can change variables from  $t$  to  $u$ ,

$$\partial_u F(u) = \bar{\xi}(u), \quad \langle \bar{\xi}(u) \bar{\xi}(u') \rangle = 2\sigma \delta(u - u'). \quad (7.17)$$

Thus  $F(u)$  has the statistics of a random walk. Its correlations are

$$\Delta(0) - \Delta(u - u') \equiv \frac{1}{2} \langle [F(u) - F(u')]^2 \rangle = \sigma |u - u'|. \quad (7.18)$$

In the language introduced above, the (bare) disorder has a cusp, with amplitude  $|\Delta'(0^+)| = \sigma$ .

Let us note that the ABBM model was traditionally solved [63, 64, 65] via the associated Fokker-Planck equation (3.17)

$$\partial_t P(\dot{u}, t) = \sigma \frac{\partial^2}{\partial \dot{u}^2} [\dot{u} P(\dot{u}, t)] + m^2 \frac{\partial}{\partial \dot{u}} [(\dot{u} - v) P(\dot{u}, t)]. \quad (7.19)$$

This approach is difficult for time-dependent quantities, but efficient for observables in the steady state. As an example, consider the steady-state distribution of velocities, obtained by solving  $\partial_t P(\dot{u}, t) = 0$ . Setting  $\sigma = 1$  to simplify the expressions yields

$$P(\dot{u}) = \frac{\dot{u}^{\frac{m^2 v}{\sigma} - 1} e^{-\dot{u} \frac{m^2}{\sigma}}}{\Gamma\left(\frac{m^2 v}{\sigma}\right)} \left(\frac{m^2}{\sigma}\right)^{\frac{m^2 v}{\sigma}}. \quad (7.20)$$

Setting  $\sigma = m = 1$  yields

$$P(\dot{u}) = \frac{\dot{u}^{v-1} e^{-\dot{u}}}{\Gamma(v)}. \quad (7.21)$$

## 7.4 End of an avalanche, and an efficient simulation algorithm

It is important to remark that an avalanche stops at a given well-defined time. To see this, we solve Eqs. (7.15)-(1.59) for  $m = 0$ , given that at time  $t = 0$  the velocity is  $\dot{u}_0$ . The associated Fokker-Planck equation is

$$\partial_t P(\dot{u}, t) = \partial_{\dot{u}}^2 [\sigma \dot{u} P(\dot{u}, t)] \quad (7.22)$$

It can be solved analytically, for a given initial distribution, as

$$P(\dot{u}, 0) = \delta(\dot{u} - \dot{u}_0)$$

$$P(\dot{u}, t) = \delta(\dot{u}) \exp\left(-\frac{\dot{u}_0}{\sigma t}\right) + \frac{\exp\left(-\frac{\dot{u}_0 + \dot{u}}{\sigma t}\right) \sqrt{\frac{\dot{u}_0}{\dot{u}}}}{\sigma t} I_1\left(\frac{2\sqrt{\dot{u}_0 \dot{u}}}{\sigma t}\right). \quad (7.23)$$

( $I_1$  is the Bessel-function of the first kind.) This can be checked by inserting the solution into the differential equation (7.22). Eq. (7.23) teaches us that for an initial velocity  $\dot{u}_0$ , with a finite probability  $\exp(-\frac{\dot{u}_0}{\sigma t})$  the velocity will be zero after time  $t$ . It also means that the end of an avalanche is well defined in time, which is crucial to define the duration of an avalanche. This would not be the case for a particle in a smooth potential: Linearizing the potential yields

$$\partial_t X(t) = -\alpha X_t \quad \implies \quad X(t) = X_0 e^{-\alpha t}. \quad (7.24)$$

Eq. (7.23) can serve as an efficient simulation algorithm [67], replacing  $t$  by the time-discretization step  $\delta t$ , and alternately integrating the forcing term  $\delta \dot{u}(t) = m^2 [v - \dot{u}(t)] \delta t$  and the stochastic process according to Eq. (7.23). In practice this requires an additional trick: Observe that the solution (7.23) can be written as

$$P(\dot{u}, t) = \delta(\dot{u}) \exp\left(-\frac{\dot{u}_0}{\sigma t}\right) + \sum_{n=1}^{\infty} \frac{\left(\frac{\dot{u}_0}{\sigma t}\right)^n \exp\left(-\frac{\dot{u}_0}{\sigma t}\right)}{n!} \times \frac{1}{\sigma t} \frac{\left(\frac{\dot{u}}{\sigma t}\right)^{n-1} \exp\left(-\frac{\dot{u}}{\sigma t}\right)}{(n-1)!} = \sum_{n=0}^{\infty} p_n \frac{1}{\sigma t} P_n\left(\frac{\dot{u}}{\sigma t}\right) \quad (7.25)$$

Here,  $p_n$  is a normalized probability vector, i.e.  $\sum_{n=0}^{\infty} p_n = 1$ , and each probability  $P_n(x)$  is normalized,  $\int_0^{\infty} dx P_n(x) = 1$ . Explicitly, we have

$$p_n = \frac{\left(\frac{\dot{u}_0}{\sigma t}\right)^n \exp\left(-\frac{\dot{u}_0}{\sigma t}\right)}{n!} \quad (7.26)$$

$$P_0(x) = \delta(x) \quad (7.27)$$

$$P_n(x) = \frac{x^{n-1} \exp(-x)}{(n-1)!}, \quad n \geq 1. \quad (7.28)$$

Given  $\dot{u}_0$ , one obtains  $\dot{u}$  with probability  $P(\dot{u}, t)$  as follows:

- (i) draw an integer random number  $n$ , from the Poisson distribution  $p_n$ ; the latter has parameter  $\dot{u}_0/(\sigma t)$ .
- (ii) if  $n = 0$ , return  $\dot{u} = 0$
- (iii) else draw a positive real random number  $x$ , from the Gamma distribution with parameter  $n$ .
- (iv) return  $\dot{u} = \sigma t x$

Contrary to a naive integration of the stochastic differential equation which yields  $\partial_t F(u(t)) \delta t = \xi_t \sqrt{\delta t}$ ,  $\langle \xi_t \xi_{t'} \rangle = \delta_{tt'}$ , this algorithm is linear in  $\delta t$ .

This allows us to define the distribution of durations, given below in Eq. (7.62), and the mean temporal shape (7.68).

## 7.5 The Brownian Force Model (BFM)

The model defined in Eqs. (7.15) and (1.59) is a model for a single degree of freedom, not for an interface. A model for an interface can be defined as follows [68]

$$\partial_t \dot{u}(x, t) = \nabla^2 u(x, t) + m^2 [v - \dot{u}(x, t)] + \partial_t F(x, u(x, t)) \quad (7.29)$$

$$\partial_t F(u(x, t), x) = \sqrt{\dot{u}(x, t)} \xi(x, t), \quad \langle \xi(x, t) \xi(x', t') \rangle = 2\sigma \delta(t - t') \delta^d(x - x') \quad (7.30)$$

Since each degree of freedom sees a force which is a random walk, this model is termed the *Brownian Force Model* (BFM).

## 7.6 Short-ranged rough disorder

Both the ABBM model as its spacial generalization, the BFM model, are pathologic in the sense that the force-force correlator grows for all distances instead of saturating as expected in short-range correlated systems, and as is reflected in the FRG fixed points discussed in section 5.3. To remedy this, one can add an additional damping term in the evolution equation of the force,

$$\partial_t \dot{u}(x, t) = \nabla^2 u(x, t) + m^2 [v - \dot{u}(x, t)] + \partial_t F(x, u(x, t)) \quad (7.31)$$

$$\partial_t F(x, u(x, t)) = -\gamma \dot{u}(x, t) F(x, u(x, t)) + \sqrt{\dot{u}(x, t)} \xi(x, t) \quad (7.32)$$

$$\langle \xi(x, t) \xi(x', t') \rangle = 2\sigma \delta(t - t') \delta^d(x - x') . \quad (7.33)$$

As  $\dot{u}(x, t) \geq 0$ , this is equivalent to

$$\partial_u F(x, u) = -\gamma F(x, u) + \tilde{\xi}(x, u) \quad (7.34)$$

$$\langle \tilde{\xi}(x, u) \tilde{\xi}(x', u') \rangle = 2\sigma \delta(u - u') \delta^d(x - x') . \quad (7.35)$$

This system has the force-force correlator

$$\langle F(u, x) F(u', x') \rangle^c = \sigma \delta^d(x - x') \frac{e^{-\gamma|u-u'|}}{\gamma} . \quad (7.36) \quad 71$$



## 7.7 Field theory

Consider the equation of motion (7.13) with generic short-ranged force-force correlators. The dynamical action is obtained by multiplying the equation of motion with  $\tilde{u}(x, t)$ , and averaging over disorder,

$$\mathcal{S} = \int_{x,t} \tilde{u}(x, t) \left[ (\partial_t - \nabla^2) \dot{u}(x, t) + m^2 (\dot{u}(x, t) - \dot{w}) \right] - \frac{1}{2} \int_{x,t,t'} \tilde{u}(x, t) \tilde{u}(x, t') \partial_t \partial_{t'} \Delta(u(x, t) - u(x, t')) , \quad (7.37) \text{dyn-action2}$$

Note that the fields  $\tilde{u}(x, t)$  are different from those in the dynamical action (6.12). (The old ones are obtained from the new ones by a time derivative). Now consider

$$\begin{aligned} \partial_t \partial_{t'} \Delta(u(x, t) - u(x, t')) &= \dot{u}(x, t) \partial_{t'} \Delta'(u(x, t) - u(x, t')) \\ &= \dot{u}(x, t) \left[ \Delta'(0^+) \partial_{t'} \text{sign}(t - t') - \Delta''(0^+) \dot{u}(x, t') + \dots \right] \\ &= -2\dot{u}(x, t) \Delta'(0^+) \delta(t - t') - \Delta''(0^+) \dot{u}(x, t) \dot{u}(x, t') + \dots \end{aligned} \quad (7.38)$$

The terms dropped in this expansion are higher derivatives of  $\Delta(u)$ , and they come with higher powers of  $\dot{u}(x, t)$ , and its time-integral  $u(x, t) - u(x, t') = \int_{t'}^t d\tau \dot{u}(x, \tau)$ , reminding that  $\dot{u}(x, t)$  and not  $u(x, t)$  is the variable for which we wrote down the equation of motion.

This expression is quite remarkable: The leading term is proportional to  $\delta(t - t')$ , rendering the last term in Eq. (7.37) *local* in time. We start our analysis of the theory with this term only. We will find in agreement with theorems 2 and 3 on page 91 that it produces the results of the BFM model, and that the remaining terms in Eq. (7.38) lead to loop corrections, of order  $\epsilon = d_c - d$ .

To conclude, let us write down the action of the BFM model:

$$\mathcal{S}_{\text{BFM}}[\dot{u}, \tilde{u}] = \int_{x,t} \tilde{u}(x, t) \left[ (\partial_t - \nabla^2) \dot{u}(x, t) + m^2 (\dot{u}(x, t) - \dot{w}(x, t)) \right] + \Delta'(0^+) \tilde{u}(x, t)^2 \dot{u}(x, t) . \quad (7.39) \text{dyn-action3}$$

Corrections are obtained by adding the missing terms perturbatively. The leading order (sufficient at 1-loop order) is

$$\mathcal{S}[\dot{u}, \tilde{u}] = \mathcal{S}_{\text{BFM}}[\dot{u}, \tilde{u}] + \frac{1}{2} \int_{x,t,t'} \tilde{u}(x, t) \tilde{u}(x, t') \dot{u}(x, t) \dot{u}(x, t') \Delta''(0^+) + \dots . \quad (7.40) \text{corrections2}$$

## 7.8 FRG and scaling

The FRG equation (6.35) for the disorder has the following general structure

$$\partial_\ell \tilde{\Delta}(u) = (\epsilon - 2\zeta) \tilde{\Delta}(u) + \zeta u \tilde{\Delta}'(u) + \sum_{n=1}^{\infty} \partial_u^{2n} \left[ \tilde{\Delta}(u) - \tilde{\Delta}(0) \right]^{n+1} . \quad (7.41) \text{78}$$

The  $n$ -loop terms are highly symbolic, since the derivatives can be distributed arbitrarily on the  $n + 1$  factors, and we have dropped all prefactors. We now assume that the microscopic disorder has the form (7.18), thus  $\tilde{\Delta}(0) - \tilde{\Delta}(u)$  has only a linear term in  $u$ . This implies that the term of order  $n = 1$  may contribute a constant to Eq. (7.41), while terms with  $n \geq 2$  vanish. Thus to all orders, the roughness exponent is given by

$$\zeta_{\text{BFM}} = \epsilon = 4 - d . \quad (7.42) \text{80}$$

As a consequence, the unrescaled disorder is scale independent (does not renormalize),

$$\Delta_{\text{BFM}}(0) - \Delta_{\text{BFM}}(u) \equiv \sigma |u| . \quad (7.43)$$

Note that  $\Delta(0)$  is not well-defined.

Similarly, the dynamical exponent  $z$  has corrections proportional to  $\Delta''(0)$ , which vanishes. As a consequence,  $z = 2$ , and all exponents can be obtained analytically,

$$z_{\text{BFM}} = 2, \quad \beta_{\text{BFM}} = a_{\text{BFM}} = 1, \quad \gamma_{\text{BFM}} = \alpha_{\text{BFM}} = 2, \quad \tau_{\text{BFM}} = \frac{3}{2}, \quad \kappa_{\text{BFM}} = 3. \quad (7.44)$$

## 7.9 Instanton equation

In general we want to construct observables for the BFM such as

$$\left\langle e^{\int_{x,t} \lambda(x,t) \dot{u}(x,t)} \right\rangle = \int \mathcal{D}[\dot{u}] \mathcal{D}[\tilde{u}] e^{\int_{x,t} \lambda(x,t) \dot{u}(x,t) - \mathcal{S}_{\text{BFM}}[\dot{u}, \tilde{u}]}. \quad (7.45)$$

This includes the avalanche-size distribution with  $\lambda(x, t) = \lambda$ , the velocity distribution with  $\lambda(x, t) = \lambda \delta(t)$ , the local avalanche-size distribution with  $\lambda(x, t) = \lambda \delta(x)$ , a.s.o.

The key observation is that  $\dot{u}(x, t)$  appears linearly in the exponent, thus the path integral over  $\dot{u}$  can be done *exactly*, enforcing an *instanton equation* for  $\tilde{u}(x, t)$ ,

$$(-\partial_t - \nabla^2 + m^2) \tilde{u}_{\text{inst}}(x, t) - \sigma \tilde{u}_{\text{inst}}(x, t)^2 = \lambda(x, t). \quad (7.46)$$

Here  $\sigma \equiv -\Delta'(0^+) > 0$ , see e.g. Eqs. (7.18) and (7.36). The expectation (7.45) is obtained from

$$Z[\lambda, w] := \left\langle e^{\int_{x,t} \lambda(x,t) \dot{u}(x,t)} \right\rangle = e^{\int_{x,t} m^2 \dot{w}(x,t) \tilde{u}(x,t)} \Big|_{\tilde{u}=\tilde{u}_{\text{inst}}}. \quad (7.47)$$

Let us consider some examples.

## 7.10 Avalanche-size distribution

The simplest example is the avalanche-size distribution. Noting that  $S = \int_{x,t} \dot{u}(x, t)$ , we have to solve the instanton equation (7.46) for  $\lambda(x, t) = \lambda$ . The solution for  $\tilde{u} = \tilde{u}_{\text{inst}}$  will be constant in space and time, thus the instanton equation (7.46) reduces to

$$m^2 \tilde{u} - \sigma \tilde{u}^2 = \lambda. \quad (7.48)$$

This quadratic equation has two solutions. The relevant one vanishes at  $\lambda = 0$ ,

$$\tilde{u} = \frac{m^2 - \sqrt{m^4 - 4\lambda\sigma}}{2\sigma}. \quad (7.49)$$

We now insert this solution into Eq. (7.47). As  $\tilde{u}(x, t)$  is constant in space and time, we define

$$w := \int_{x,t} \dot{w}(x, t) > 0. \quad (7.50)$$

This yields with  $\tilde{u}$  given in Eq. (7.49)

$$\langle e^{\lambda S} \rangle = e^{m^2 w \tilde{u}}. \quad (7.51)$$

Taking the inverse Laplace transform yields

$$P_w^S(S) = m^2 w \frac{e^{-\frac{m^4(S-w)^2}{4\sigma S}}}{2\sqrt{\pi\sigma S^{3/2}}}. \quad (7.52)$$

One checks that  $P_w^S(S)$  is normalized,  $\langle 1 \rangle_w = \int_0^\infty dS P_w^S(S) = 1$ , and that the first avalanche-size moment is nothing but the total displacement of the confining parabola,  $\langle S \rangle_w = \int_0^\infty dS S P_w(S) = w$ .

$P_w(S)$  is the response of the system to a displacement  $w$ , or equivalently to a *force kick*  $\delta f = m^2 w$ . We now take the limit of an infinitesimally small displacement  $w$ , and to this purpose define

$$P^S(S) := \lim_{w \rightarrow 0} \frac{\langle S \rangle_w}{w} P_w(S) = \langle S \rangle m^2 \frac{e^{-\frac{m^4 S}{4\sigma}}}{2\sqrt{\pi\sigma} S^{3/2}} \equiv \langle S \rangle \frac{e^{-\frac{S}{4S_m}}}{2\sqrt{\pi S_m} S^{3/2}}, \quad S_m := \frac{\sigma}{m^4} \equiv \frac{\langle S^2 \rangle}{2\langle S \rangle}. \quad (7.53)$$

Since  $\langle S \rangle_w = w$ , by construction all moments which do not necessitate a small- $S$  cutoff, i.e.  $\langle S^n \rangle_w$  with  $n \geq 1$  have a well-defined small- $w$  limit, given by Eq. (7.53). What one loses when taking the limit of  $w \rightarrow 0$  is normalizability, as formally  $\langle 1 \rangle = \infty$ .

## 7.11 Velocity distribution

To simplify further considerations, we set

$$m^2 \rightarrow 1, \quad -\Delta'(0^+) \equiv \sigma \rightarrow 1. \quad (7.54)$$

To obtain the instantaneous velocity distribution, we evaluate Eqs. (7.45)-(7.47) for  $\lambda(x, t) = \lambda\delta(t)$ , setting  $\dot{w}(x, t) = v$  (uniform driving). The instanton equation to be solved is

$$-\partial_t \tilde{u}(t) + \tilde{u}(t) - \tilde{u}(t)^2 = \lambda\delta(t). \quad (7.55)$$

To impose proper boundary conditions, look at the r.h.s. of Eq. (7.47): Driving at times  $t > 0$  does not affect the velocity distribution at  $t = 0$ , thus the instanton solution  $\tilde{u}(t)$  must vanish for positive times. Eq. (7.55) with this constraint is solved by

$$\tilde{u}(t) = \frac{\lambda\Theta(-t)}{\lambda + (1 - \lambda)e^{-t}}. \quad (7.56)$$

With the above solution Eq. (7.47) reduces to

$$\left\langle e^{\lambda \int_x \dot{u}(x,0)} \right\rangle = e^{vL^d \int_t \tilde{u}(t)} = e^{-vL^d \ln(1-\lambda)} = (1 - \lambda)^{-vL^d}. \quad (7.57)$$

The inverse Laplace transform is

$$P_{v,L}^{\dot{u}}(\dot{u}) = \frac{\dot{u}^{vL^d-1} e^{-\dot{u}}}{\Gamma(vL^d)}. \quad (7.58)$$

This result is independent of the dimension  $d$ , and agrees with the ABBM-result Eq. (7.20), there derived for a single degree of freedom. We can take the limit of  $v \rightarrow 0$ , and define

$$P^{\dot{u}}(\dot{u}) := \lim_{v \rightarrow 0} \frac{P_{v,L}^{\dot{u}}(\dot{u})}{vL^d} = \frac{e^{-\dot{u}}}{\dot{u}}. \quad (7.59)$$

## 7.12 Duration distribution

The probability that the avalanche has velocity zero at time 0 after a kick of size  $w$  at time  $t = -T$ , with  $T > 0$ , can be obtained from the central result (7.47) with the instanton (7.56) as

$$P(\dot{u}(x, 0) = 0 \forall x) = \lim_{\lambda \rightarrow -\infty} \left\langle e^{\lambda \int_x \dot{u}(x,0)} \right\rangle = \lim_{\lambda \rightarrow -\infty} e^{w \tilde{u}(-T)} = \exp\left(-\frac{w}{e^T - 1}\right). \quad (7.60)$$

This is also the probability that the duration following a kick of size  $w$  is smaller than  $T$ . The distribution of durations is obtained by taking a derivative w.r.t.  $T$ ,

$$\begin{aligned} P_w^{\text{duration}}(T) &= \partial_T \exp\left(-\frac{w}{e^T - 1}\right) = w \exp\left(-\frac{w}{e^T - 1}\right) \frac{e^{-T}}{(e^{-T} - 1)^2} \\ &= w \exp\left(-\frac{w}{e^T - 1}\right) \frac{1}{[2 \sinh(T/2)]^2}. \end{aligned} \quad (7.61)$$

This distribution is normalized to unity. As at the end of section 7.10, one defines the (unnormalized) probability density in the limit of  $w \rightarrow 0$ ,

$$P^{\text{duration}}(T) := \lim_{w \rightarrow 0} \frac{P_w^{\text{duration}}(T)}{w} = \frac{1}{[2 \sinh(T/2)]^2}. \quad (7.62) \text{P-duration}$$

### 7.13 The temporal shape of an avalanche

In order to obtain the temporal shape of an avalanche, we need to solve the instanton equation

$$-\partial_t \tilde{u}(t) + \tilde{u}(t) - \tilde{u}(t)^2 = \lambda \delta(t_f - t) + \eta \delta(t - t_m), \quad (7.63) \text{v-inst-eq2}$$

where  $t_f$  is the final time (where the avalanche stops) and  $t_m$  the time at which the velocity is measured. Since we only need its first moment, we can construct  $\tilde{u}(t)$  perturbatively in  $\eta$ . To that purpose write

$$\tilde{u}(t) = \tilde{u}_0(t) + \eta \tilde{u}_1(t) + \eta^2 \tilde{u}_2(t) + \mathcal{O}(\eta^3), \quad \tilde{u}_0(t) = \frac{\Theta(t_f - t)}{1 - e^{t_f - t}}. \quad (7.64) \text{96}$$

The solution  $\tilde{u}_0(t)$  is the solution (7.56), translated to stop at  $t = t_f$ , in the limit of  $\lambda \rightarrow -\infty$ . Inserting Eq. (7.64) into Eq. (7.63) and collecting terms of order  $\eta$  yields

$$-\partial_t \tilde{u}_1(t) + \tilde{u}_1(t) - 2\tilde{u}_1(t)\tilde{u}_0(t) = \delta(t - t_m). \quad (7.65)$$

The solution is

$$\tilde{u}_1(t) = \frac{\sinh^2(\frac{t_f - t_m}{2})}{\sinh^2(\frac{t_f - t}{2})} \theta(t_m - t). \quad (7.66)$$

Performing a kick of size  $w$  at  $t = 0$ , and constraining the avalanche to stop at time  $t_f = T$ , the shape can be written as

$$\langle \dot{u}(t_m) \rangle = \partial_\eta \Big|_{\eta=0} \ln \left( \partial_{t_f} e^{w \tilde{u}(t)} \right) \Big|_{T=t_f} = 4w \frac{\sinh^2(\frac{T-t_m}{2})}{\sinh^2(\frac{T}{2})} + 4 \frac{\sinh(\frac{T-t_m}{2}) \sinh(\frac{t_m}{2})}{\sinh(\frac{T}{2})}. \quad (7.67)$$

Consider now the limit of  $w \rightarrow 0$ : For short durations  $T$ ,  $\langle \dot{u}(t_m) \rangle$  converges to a parabola,

$$\langle \dot{u}(t_m) \rangle = 2 \frac{t_m(T - t_m)}{T}. \quad (7.68) \text{-shape}$$

For long durations, it settles on a plateau at  $\langle \dot{u}(t) \rangle = 2$ , see figure 7.2.

Pursuing to the next order one finds for the connected average

$$\langle \dot{u}(t_m)^2 \rangle^c = 4w \frac{\sinh^3(\frac{T-t_m}{2}) \sinh(\frac{t_m}{2})}{\sinh^3(\frac{T}{2})} + 8 \frac{\sinh^2(\frac{T-t_m}{2}) \sinh^2(\frac{t_m}{2})}{\sinh^2(\frac{T}{2})}. \quad (7.69)$$

At  $w = 0$ , quite remarkably the ratio

$$\frac{\langle \dot{u}(t_m)^2 \rangle}{\langle \dot{u}(t_m) \rangle^2} = \frac{3}{2} \quad (7.70)$$

is time independent.

Further observables, as well as loop corrections are obtained in [69, 70], and compared to experiments in [71].

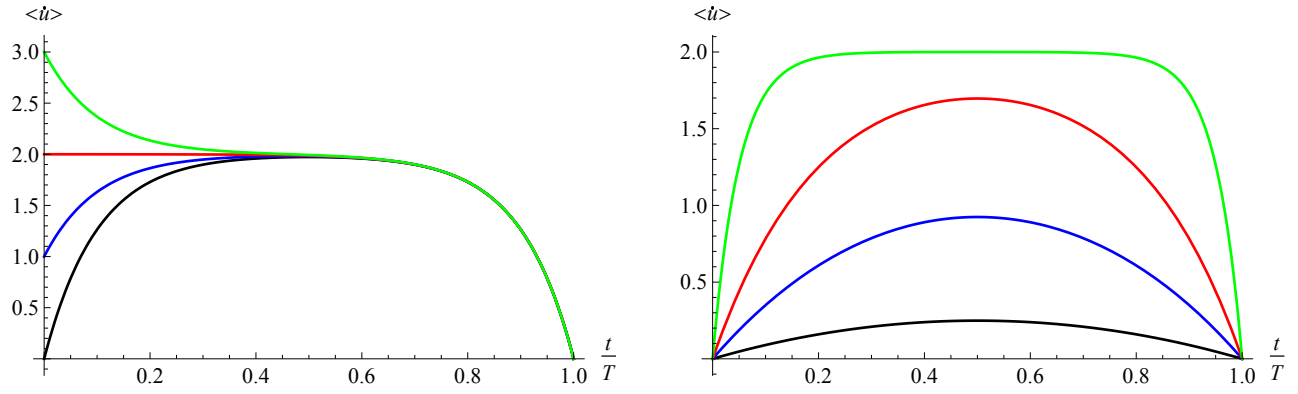


Figure 7.2: Expectation  $\langle \dot{u}(t) \rangle$ . Left:  $T = 10$ , and  $w = 0, 1, 2$ , and  $3$ . Right:  $w = 0$  (infinitesimal kick), and  $T = \frac{1}{2}, 2, 5$ , and  $20$ .

## 7.14 Local avalanche-size distribution

We now consider avalanches on a codimension-1 hyperplane, i.e. at point for a line, on a line for a 2d interface, a.s.o., by choosing

$$\lambda(x, x_{\perp}^{\vec{}}) = \lambda \delta(x). \quad (7.71)$$

As a consequence,  $x_{\perp}^{\vec{}}$  drops from the instanton equation. Setting again  $\sigma = m^2 = 1$ , one arrives at

$$\tilde{u}(x) - \tilde{u}''(x) - \tilde{u}(x)^2 = \lambda \delta(x). \quad (7.72)$$

The only solution which vanishes at infinity and satisfies the instanton equation at  $\lambda = 0$  is

$$\tilde{u}(x) = \frac{3}{1 + \cosh(x + x_0)}. \quad (7.73)$$

It can be promoted to a solution at  $\lambda \neq 0$  by setting  $\tilde{u}(-x) = \tilde{u}(x)$ . The parameter  $x_0 = x_0(\lambda)$  has to be chosen to satisfy the instanton equation at  $x = 0$ . Integrating Eq. (7.72) within a small domain around  $x = 0$  yields

$$\lambda = -2\tilde{u}'(0^+) = \frac{6 \sinh(x_0)}{[1 + \cosh(x_0)]^2}. \quad (7.74)$$

On the other hand, the generating function is

$$Z := \int_{-\infty}^{\infty} dx \tilde{u}(x) = \frac{12}{1 + e^{x_0}} \quad (7.75)$$

Solving Eq. (7.75) for  $x_0$  and inserting into Eq. (7.74) yields

$$\lambda = \frac{Z(Z - 6)(Z - 12)}{72}. \quad (7.76)$$

The inverse Laplace transform is a priori difficult to perform, as  $Z(\lambda)$  is a complicated function of  $\lambda$ . The trick is to write

$$\begin{aligned} P_w(S_0) &:= \langle e^{\lambda S_0} \rangle = \int_{-i\infty}^{i\infty} \frac{d\lambda}{2\pi i} e^{-\lambda S_0} e^{wZ(\lambda)} = \int_{-i\infty}^{i\infty} \frac{dZ}{2\pi i} \frac{d\lambda(Z)}{dZ} e^{-\lambda(Z)S_0 + wZ} \\ &= -\frac{1}{S_0} \int_{-i\infty}^{i\infty} \frac{dZ}{2\pi i} e^{wZ} \frac{d}{dZ} e^{-\lambda(Z)S_0} = \frac{w}{S_0} \int_{-i\infty}^{i\infty} \frac{dZ}{2\pi i} e^{wZ} e^{-\lambda(Z)S_0} \\ &= \frac{6e^{6w}}{\pi S_0} \int_0^{\infty} dx \cos(3x(S_0 x^2 + S_0 + 2w)) = \frac{2e^{6w} w \sqrt{S_0 + 2w}}{\pi S_0^{3/2}} K_{\frac{1}{3}} \left( \frac{2(S_0 + 2w)^{3/2}}{\sqrt{3S_0}} \right). \end{aligned} \quad (7.77)$$

Note that this can also be written in terms of the Airy function (formula (21) of Ref. [61]). In the limit of  $w \rightarrow 0$ , this reduces to

$$P(S_0) = \frac{2}{\pi S_0} K_{\frac{1}{3}} \left( \frac{2S_0}{\sqrt{3}} \right). \quad (7.78)$$

One can also give analytical expressions for the joint distribution of avalanche size  $S$  and local size  $S_0$ , as well as of size  $S$  and spatial extension  $\ell$ . The interested reader will find this in [61].

## 7.15 The spatial shape of avalanches

We noted that avalanches have a well-defined extension  $\ell$ , beyond which there is no movement. For a given avalanche, denote its advance by  $S(x)$ . Its size  $S = \int_x S(x)$ . We call avalanche extension  $\ell$  the size of the smallest ball into which we can fit the avalanche. As long as  $\ell \ll m^{-1}$ ,

$$\langle S(x) \rangle_\ell = \ell^\zeta g(x/\ell), \quad (7.79) \text{ansatz}$$

where  $g(x)$  is non-vanishing in the unit ball. Integrating over space yields  $S \sim \ell^{d+\zeta}$ , the canonical scaling relation between size and extension of avalanches, confirming the ansatz (7.79).

We now want to deduce how  $g(x)$  behaves close to the boundary. For simplicity of notations, we write our argument for the left boundary in  $d = 1$ , which we place at  $x = -\ell/2$ . Imagine the avalanche dynamics for a discretized representation of the system. The avalanche starts at some point, which in turn triggers avalanches of its neighbors, a.s.o. This leads to a shock front propagating outwards from the seed to the left and to the right. As long as the elasticity is local, the dynamics of these two shock-fronts is local: If one conditions on the position of the  $i$ -th point away from the boundary, with  $i$  being much smaller than the total extension  $\ell$  of the avalanche (in fact, we only need that the avalanche started right of this point), then we expect that the joint probability distribution for the advance of points 1 to  $i - 1$  depends on  $i$ , but is independent of the size  $\ell$ . Thus we expect that *in this discretized model* the shape  $\langle S(x - r_1) \rangle$  close to the left boundary  $r_1$  is independent of  $\ell$ . Let us now turn to avalanches of large size  $\ell$ , so that we are in the continuum limit studied in the field theory. Our argument then implies that the shape  $\langle S(x - r_1) \rangle$  measured from the left boundary  $r_1 = -\ell/2$ , is independent of  $\ell$ . In order to cancel the  $\ell$ -dependence in Eq. (7.79) this in turn implies that

$$g(x - 1/2) = \mathcal{B} \times (x - 1/2)^\zeta, \quad (7.80) \text{gofx}$$

with some amplitude  $\mathcal{B}$ . For the Brownian force model in  $d = 1$ , the roughness exponent is  $\zeta_{\text{BFM}} = 4 - d = 3$ , and one can further show that  $\mathcal{B} = \sigma/21$ .

On the left of figure 7.3, we show twenty realizations of avalanches, with mean given by the thick black line. On the right plot, we compare numerical averages with the theory sketched below. Note that the latter indeed has a cubic behavior close to the boundary, as predicted by Eq. (7.80).

We now turn to the theory: In order to get the spatial avalanche shape, one needs to construct a solution of the instanton equation (7.46), with a source

$$\lambda(x) = -\lambda_1 \delta(x - r_1) - \lambda_2 \delta(x - r_2) + \eta \delta(x - x_c), \quad \lambda_1, \lambda_2 \rightarrow \infty. \quad (7.81) \text{B0-1}$$

Looking at our central result (7.47), this choice implies that the avalanche kicked at  $x = x_0$  does not extend to  $x = r_{1,2}$ . To simplify matters further, one replaces  $m^2 w(x) \rightarrow f(x)$ , and considers the response to a kick in the force. This allows us to take the limit of  $m \rightarrow 0$ . Setting further  $\sigma = 1$ , the instanton equation to be solved is

$$\tilde{u}''(x) + \tilde{u}(x)^2 = -\lambda(x), \quad (7.82) \text{B4}$$

The source  $\eta$  generates moments of the avalanche size at  $x_c$ . While unsolvable for arbitrary  $\eta$ , Eq. (7.82) can be solved perturbatively in  $\eta$ , allowing us to construct moments of the spatial avalanche shape. This

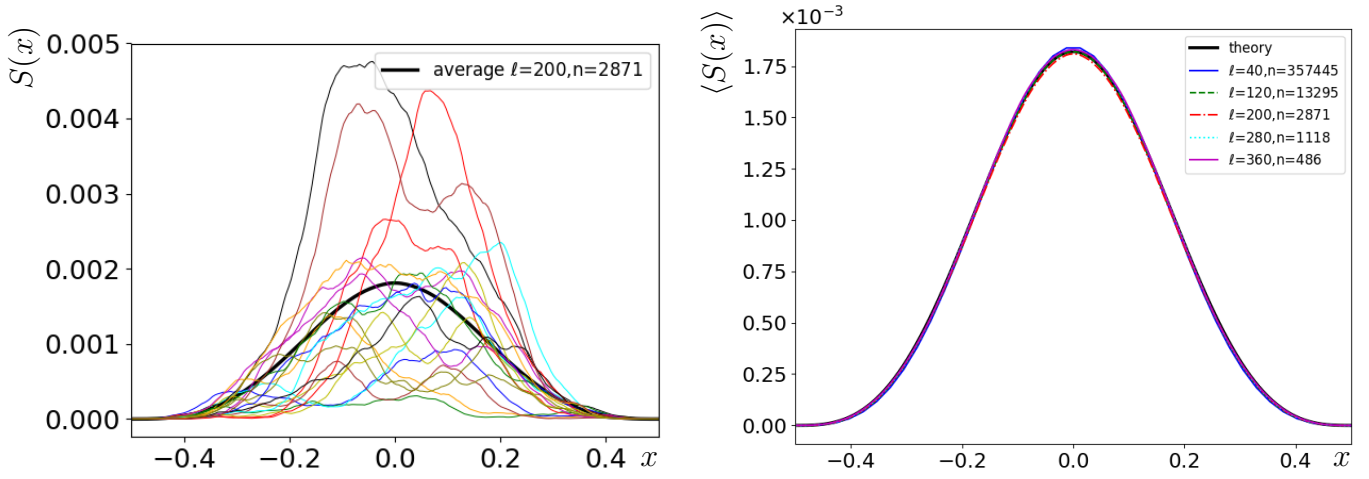


Figure 7.3: Left: 20 avalanches with extension  $\ell = 200$ , rescaled to  $\ell = 1$ .  $n = 2871$  is the number of samples used for the average. Right: The shape  $\langle S(x) \rangle \equiv \langle S(x/\ell) \rangle_\ell / \ell^3$  averaged for all avalanches with a given  $\ell$  between 40 and 360. To reduce statistical errors, we have symmetrised this function.

solution has the form

$$\tilde{u}(x) = \tilde{u}_0(x) + \eta \tilde{u}_1(x) + \eta^2 \tilde{u}_2(x) + \dots \quad (7.83)$$

$$\tilde{u}_0(x) = \frac{1}{(r_2 - r_1)^2} f\left(\frac{2x - r_1 - r_2}{2(r_2 - r_1)}\right) \quad (7.84)$$

$$f(x) = -6 \mathcal{P}\left(x + 1/2; g_2 = 0, g_3 = \frac{\Gamma\left(\frac{1}{3}\right)^{18}}{(2\pi)^6}\right). \quad (7.85)$$

Here  $\mathcal{P}$  is the Weierstrass-P function, diverging at  $x = 0$  and  $x = 1$ . The subdominant terms in  $\eta$  are obtained by realizing that if  $f(x)$  is solution of the instanton equation (7.82), so is  $\kappa^2 f(\kappa x + c)$ . The details of this calculation are cumbersome, and can be found in Ref. [72]. On the right of figure 7.3 we show  $\langle S(X) \rangle$  predicted by the theory, and its numerical test.

## 7.16 Some theorems

Inspired by the calculations done so far, one can show the following theorems [68]:

**Theorem 1:** The zero-mode  $\dot{u}(t) := \frac{1}{L^d} \int_x \dot{u}(x, t)$  of the BFM field theory (7.39) is the same random process as in the ABBM model, Eq. (7.15).

**Theorem 2:** The field theory of this process is the sum of all tree diagrams, involving  $\Delta'(0^+)$  as a vertex.

**Theorem 3:** Tree diagrams are relevant at the upper critical dimension  $d_c$ . Corrections involve loops and can be constructed in a controlled  $\epsilon$ , i.e. loop, expansion around the upper critical dimension  $d_c$ .

**Sketch of Proof:** One first constructs the generating function for a spatially constant observable, as the velocity or the size in the BFM model. As we saw, these generating functions involve instanton solutions constant in space, thus independent of the dimension. Graphically this can be understood by constructing  $\tilde{u}$  perturbatively, with vertices proportional to  $\sigma = -\Delta'(0^+)$ , and lines which are response functions, possibly



integrated over time. Since by assumption external observable vertices are at zero momentum, all response functions are at zero momentum. This proves theorems 1 and 2.

We now consider models with one of the fixed points studied above, be it RB, RF or periodic disorder, at equilibrium or at depinning. Since each vertex is proportional to  $\epsilon$ , the leading order will again be given by trees constructed from  $\Delta'(0^+)$ . The only thing which can be added are loops. Each loop will come with an additional factor of  $\epsilon$  from the additional vertex, of which the leading one is given in Eq. (7.40). As long as the ensuing momentum integrals are finite, thus do not yield a factor of  $1/\epsilon$ , these additional contributions will be of order  $\epsilon$  to the number of loops. That the momentum integrals are finite can be checked; it reflects the fact that the theory is renormalizable, i.e. that all divergences which can possibly appear have already been taken care of by the counter terms introduced earlier, see section 6.3 for depinning.

## 7.17 Loop corrections

Loop corrections are cumbersome to obtain, and prone to errors. To avoid the latter, one should check the obtained results by explicitly constructing them perturbatively in  $\Delta(u)$ , and  $\lambda$ . This is done in the relevant research literature, see Refs. [68, 73, 74]. Here we sketch the generally applicable method of Ref. [68], to which we refer for the details.

**Simplified model:** Consider the action (7.40). To the order given, we can decouple the supplementary term to the BFM model via

$$\mathcal{S}_\eta[\dot{u}, \tilde{u}] = \mathcal{S}_{\text{BFM}}[\dot{u}, \tilde{u}] + \int_{x,t} \eta(x) \tilde{u}(x,t) \dot{u}(x,t) . \quad (7.86) \text{corrections2}$$

$\eta(x)$  is an (imaginary) Gaussian disorder to be averaged over, with correlations

$$\langle \eta(x) \eta(x') \rangle_\eta = -\Delta''(0) \delta^d(x - x') . \quad (7.87) \text{etadis}$$

For each realization of  $\eta(x)$ , the theory has the same form as in the preceding sections. In particular, the total action (including the sources) is linear in the velocity field, and the only change is an additional term in the instanton equation (7.46),

$$(-\partial_t - \nabla^2 + m^2) \tilde{u}(x,t) - \sigma \tilde{u}(x,t)^2 = \lambda(x,t) + \eta(x) \tilde{u}(x,t) . \quad (7.88) \text{inst-equation}$$

Our central result (7.47) remains unchanged.

**Perturbative solution:** To simplify notations, we set  $m = 1$ , and  $\sigma = 1$ . We expand the solution of Eq. (7.88) in powers of  $\eta(x)$ , denoting by  $\tilde{u}^{(n)}(x,t)$  the term of order  $\eta^n$ ,

$$\tilde{u}(x,t) = \tilde{u}^{(0)}(x,t) + \tilde{u}^{(1)}(x,t) + \tilde{u}^{(2)}(x,t) + \dots . \quad (7.89) \text{p4}$$

The hierarchy of equations to be solved is

$$[-\partial_t - \nabla_x^2 + 1] \tilde{u}^{(0)}(x,t) = \lambda(x,t) + \tilde{u}^{(0)}(x,t)^2 , \quad (7.90)$$

$$[-\partial_t - \nabla_x^2 + 1 - 2\tilde{u}^{(0)}(x,t)] \tilde{u}^{(1)}(x,t) = \eta(x) \tilde{u}^{(0)}(x,t) , \quad (7.91)$$

$$[-\partial_t - \nabla_x^2 + 1 - 2\tilde{u}^{(0)}(x,t)] \tilde{u}^{(2)}(x,t) = \tilde{u}^{(1)}(x,t)^2 + \eta(x) \tilde{u}^{(1)}(x,t) . \quad (7.92)$$

The first line is the usual instanton equation (7.46). Let us introduce the dressed response kernel

$$[-\partial_t - \nabla_x^2 + 1 - 2\tilde{u}^{(0)}(x,t)] \mathbb{R}_{x't',xt} = \delta^d(x - x') \delta(t - t') . \quad (7.93) \text{B.21new}$$



It has the usual causal structure of a response function, and obeys a backward evolution equation. It allows us to rewrite the solution of the system of equations (7.90) to (7.92) as

$$\tilde{u}^1(x, t) = \int_{x'} \int_{t' > t} \eta(x') \tilde{u}^0(x', t') \mathbb{R}_{x't',xt} , \quad (7.94)$$

$$\tilde{u}^{(2)}(x, t) = \int_{x'} \int_{t' > t} [\tilde{u}^1(x', t')^2 + \eta(x') \tilde{u}^{(1)}(x', t')] \mathbb{R}_{x't',xt} . \quad (7.95)$$

Consider now the average (7.87) over  $\eta(x)$ . Since  $\langle \tilde{u}^{(1)}(x, t) \rangle_\eta = 0$ , the lowest-order correction is given by the average of  $\tilde{u}^2(x, t)$ ,

$$Z[\lambda] = Z_{\text{tree}}[\lambda] + \int_{xt} \langle \tilde{u}_{xt}^{(2)} \rangle_\eta + \dots . \quad (7.96)$$

Inserting Eq. (7.94) into Eq. (7.95), and performing the average over  $\eta$ , one finds

$$\begin{aligned} \langle \tilde{u}^{(2)}(x, t) \rangle_\eta &= -\Delta''(0) \int_{t < t_1 < t_2, t_3} \int_{x_1, x'} \tilde{u}^{(0)}(x', t_2) \tilde{u}^{(0)}(x', t_3) \mathbb{R}_{x't_2, x_1 t_1} \mathbb{R}_{x't_3, x_1 t_1} \mathbb{R}_{x_1 t_1, xt} \\ &\quad - \Delta''(0) \int_{t < t_1 < t_2} \int_{x'} \tilde{u}^{(0)}(x', t_2) \mathbb{R}_{x't_2, x't_1} \mathbb{R}_{x't_1, xt} . \end{aligned} \quad (7.97)$$

It admits the following graphical representation

$$\langle \tilde{u}^{(2)}(x, t) \rangle_\eta = \begin{array}{c} \text{Diagram 1: A wiggly line at the top with two vertices labeled } t_2 \text{ and } t_3 \text{ connected by a dashed line. Two double solid lines (dressed response functions) descend from } t_2 \text{ and } t_3 \text{ to a vertex } t_1. \text{ A double solid line descends from } t_1 \text{ to } t. \end{array} + \begin{array}{c} \text{Diagram 2: A wiggly line at the top with a vertex } t_2. A double solid line descends from } t_2 \text{ to } t_1. \text{ A curved double solid line (loop) connects } t_2 \text{ and } t_1. \text{ A double solid line descends from } t_1 \text{ to } t. \end{array} . \quad (7.98)$$

The symbols are as follows: (i) a wiggly line represents  $\tilde{u}^{(0)}(x, t)$ , the mean field-solution; (ii) a double solid line is a dressed response function  $\mathbb{R}$ , advancing in time following the arrow (upwards), thus times are ordered from bottom to top. We now define the combination

$$\Phi(x', x, t) := \int_{t' > t} \tilde{u}^{(0)}(x', t') \mathbb{R}_{x't',xt} , \quad (7.99)$$

in terms of which one can rewrite

$$\langle \tilde{u}^{(2)}(x, t) \rangle_\eta = \int_{t', x'} \left[ \int_y \Phi(y, x', t')^2 + \Phi(x', x', t') \right] \mathbb{R}_{x't',xt} . \quad (7.100)$$

There are in fact several additional terms: (i) a counter-term for the disorder, showing up in a change of  $\Delta'(0^+)$  to its renormalized value. (ii) a counter-term to friction. (iii) a missed boundary term, due to the replacement of  $\Delta''(u_t - u_{t'})$  which decays to zero for large times by  $\Delta''(0)$ , which does not.

**1-loop corrections to the avalanche-size distribution:** Let us construct the 1-loop corrections to the avalanche-size distribution, following the formalism developed above. For  $\lambda(x, t) = \lambda$ , the solution of the unperturbed instanton equation was given in Eq. (7.49). For  $m = \sigma = 1$ , it reads

$$Z_{\text{MF}}(\lambda) \equiv \tilde{u}^{(0)} = \frac{1}{2} \left( 1 - \sqrt{1 - 4\lambda} \right) . \quad (7.101)$$

The dressed response kernel in Fourier then becomes

$$\mathbb{R}_{k, t_2, t_1} = e^{-(k^2 + 1 - 2\tilde{u}^{(0)})(t_2 - t_1)} \theta(t_2 - t_1) , \quad (7.102)$$

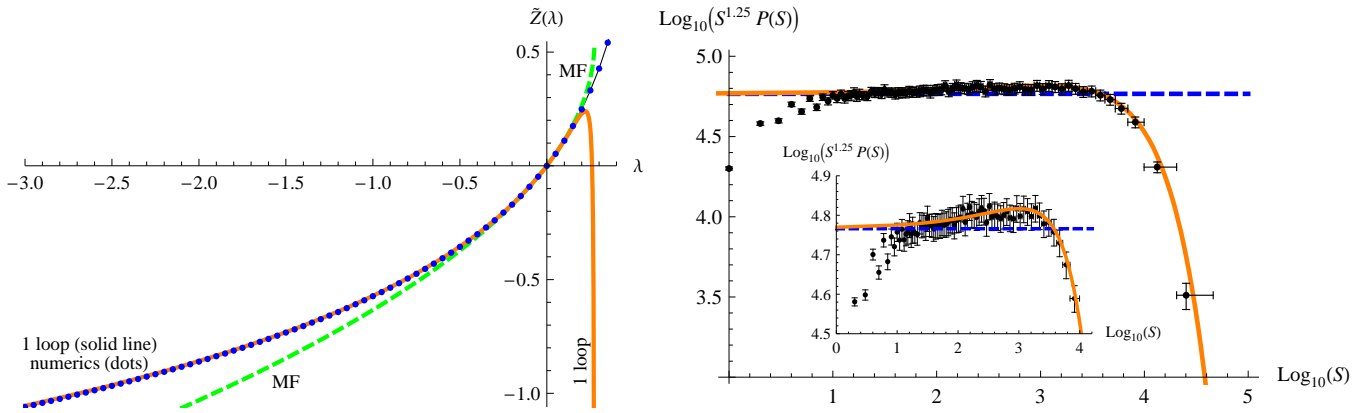


Figure 7.4: Results of Ref. [75] for RF disorder,  $d = 2$ . Left: Numerically measured  $\tilde{Z}(\lambda)$  (blue dots). MF result (7.101) (green dashed), 1-loop result (7.106) (orange solid). The latter is rather precise, almost up to the singularity at  $\lambda = 1/4$ . Right: Avalanche-size distribution  $P(S)$ , multiplied by  $S^\tau$  with  $\tau = 1.25$  from Eq. (7.4) (dots). The orange solid curve is the prediction from Eq. (7.107). The dashed line is a constant (guide to the eye). Inset: blow-up of main plot.

which is the bare response function up to the replacement  $m^2 \rightarrow m^2 - 2\tilde{u}^{(0)}(\lambda)$ . Note that the combination in the exponential simplifies,

$$k^2 + 1 - 2\tilde{u}^{(0)} = k^2 + \sqrt{1 - 4\lambda}. \quad (7.103)$$

Formula (7.99) then gives

$$\Phi(k, t_1) = \tilde{u}^{(0)} \int_{t_1 < t_2} \mathbb{R}_{k, t_2, t_1} = \frac{\tilde{u}^{(0)}}{k^2 + 1 - 2\tilde{u}^{(0)}}. \quad (7.104)$$

With the additional integral over  $\mathbb{R}$  in Eq. (7.100), the latter becomes

$$\langle \tilde{u}^{(2)} \rangle_\eta = -\frac{\tilde{\Delta}''(0^+)}{1 - 2\tilde{u}^{(0)}} \int_k \left( \frac{\tilde{u}^{(0)}}{k^2 + 1 - 2\tilde{u}^{(0)}} \right)^2 + \frac{\tilde{u}^{(0)}}{k^2 + 1 - 2\tilde{u}^{(0)}}. \quad (7.105)$$

Adding the proper counter-terms, and replacing the bare disorder by the renormalized one [68], the full generating function becomes

$$Z(\lambda) \equiv \tilde{u} = \tilde{u}^{(0)} - \frac{\tilde{\Delta}''(0^+)}{1 - 2\tilde{u}^{(0)}} \frac{1}{\epsilon I_1} \int_k \left( \frac{\tilde{u}^{(0)}}{k^2 + 1 - 2\tilde{u}^{(0)}} \right)^2 + \frac{\tilde{u}^{(0)}}{k^2 + 1 - 2\tilde{u}^{(0)}} - \frac{\tilde{u}^{(0)}}{k^2 + 1} - \frac{3(\tilde{u}^{(0)})^2}{(k^2 + 1)^2}. \quad (7.106)$$

**Avalanche-size distribution at 1-loop order:** The generating function (7.106) can be inverted analytically [73]. The result for avalanches larger than a microscopic cutoff  $S_0$  is

$$P(S) = \frac{\langle S \rangle}{2\sqrt{\pi}} S_m^{\tau-2} A S^{-\tau} \exp \left( C \sqrt{\frac{S}{S_m}} - \frac{B}{4} \left[ \frac{S}{S_m} \right]^\delta \right). \quad (7.107)$$

The coefficients are

$$A = 1 + \frac{1}{8}(2 - 3\gamma_E)\alpha, \quad B = 1 - \alpha \left( 1 + \frac{\gamma_E}{4} \right), \quad C = -\frac{\sqrt{\pi}}{2}\alpha, \quad \alpha = \frac{\zeta - \epsilon}{3}, \quad (7.108)$$

and  $\gamma_E = 0.577216$  is Euler's number. The exponent  $\tau$  is consistent with the scaling relation (7.4), while the new exponent  $\delta$  reads

$$\delta = 1 + \frac{\epsilon - \zeta}{12}. \quad (7.109)$$

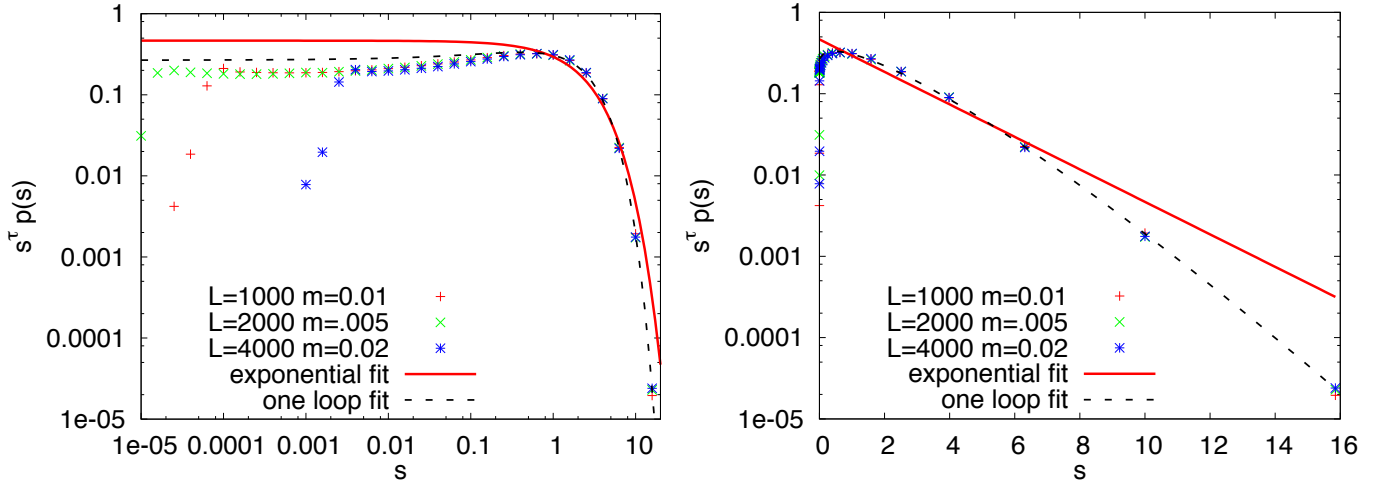


Figure 7.5: Left: Avalanche-size distribution for Random Field in  $d = 1$  at depinning. The variable  $s = S/S_m$ . Blow up of the power-law region. The red solid curve is given by the MF result Eq. (7.53), the black dashed line by Eq. (7.107), with  $A = 0.947$ ,  $B = 1.871$  and  $C = 0.606$ . Right: the same for the tail. Data from [76].

## 7.18 Simulation results and experiments

**Avalanche-size distribution:** The result for the avalanche-size distribution has been verified numerically, both for the statics [75] as for depinning [76].

For the statics (equilibrium) [75], we show plots on figure 7.4. The simulations are for a 3-dimensional RF magnet, with weak disorder s.t. only a single domain wall appears, yielding  $d = 2$ ,  $\epsilon = 2$ , and  $\zeta = 2/3$ . The generating function  $Z(\lambda)$  is verified with high precision. For the avalanche-size distribution, the agreement is good, even though there is appreciable noise due to binning, which is absent from the generating function  $Z(\lambda)$ .

At depinning avalanches are simulated for an elastic string in  $d = 1$  [76]. The results for system sizes up to  $L = 4000$  are shown on figure 7.5. The statistics is good, allowing to verify Eq. (7.107) in the tail region, with  $\delta = 7/6$ .

**The temporal avalanche shape at fixed duration  $T$ :** The temporal shape at fixed duration  $T$  is predicted by the theory [69, 70] as

$$\langle \dot{u}(t = \vartheta T) \rangle_T = 2\mathcal{N} \left[ T\vartheta(1 - \vartheta) \right]^{\gamma-1} \times \exp \left( -\frac{16\varepsilon}{9d_c} \left[ \text{Li}_2(1 - \vartheta) - \text{Li}_2\left(\frac{1 - \vartheta}{2}\right) + \frac{\vartheta \log(2\vartheta)}{\vartheta - 1} + \frac{(\vartheta + 1) \log(\vartheta + 1)}{2(1 - \vartheta)} \right] \right). \quad (7.110)$$

It is well approximated by

$$\langle \dot{u}(t = \vartheta T) \rangle_T \simeq [T\vartheta(1 - \vartheta)]^{\gamma-1} \exp(\mathcal{A}[\frac{1}{2} - \vartheta]). \quad (7.111)$$

The asymmetry  $\mathcal{A} \approx -0.336(1 - d/d_c)$  is negative for  $d$  close to  $d_c$ , skewing the avalanche towards its end, as observed in numerical simulations in  $d = 2$  and  $3$  [77]. For  $d = 1$  the asymmetry is positive in numerical simulations [78]. In experiments on magnetic avalanches (Barkhausen noise), and in fracture experiments, the asymmetry is difficult to see [78].

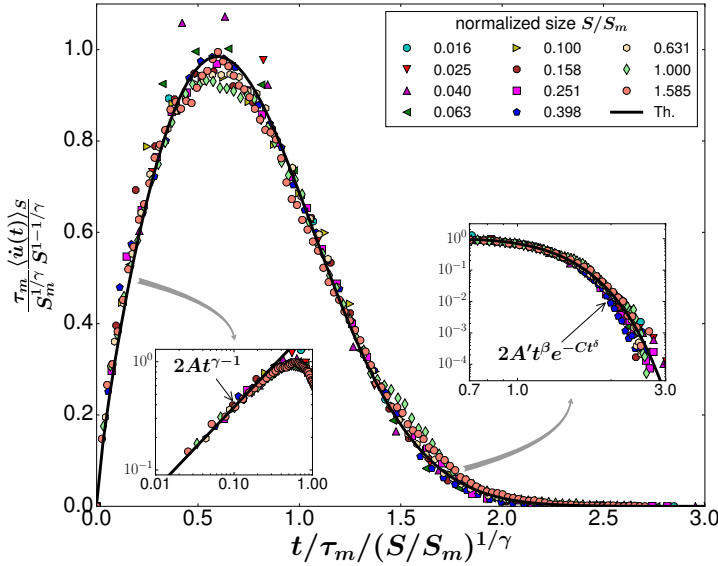


Figure 7.6: Scaling collapse of the average shape at fixed avalanche sizes  $\langle \dot{u}(t) \rangle_S$ , according to Eq. (7.112), in the FeSiB thin film. The continuous line is the prediction for the universal SR scaling function of Eq. (7.117). The insets show comparisons of the tails of the data with the predicted asymptotic behaviors of Eqs. (7.115) and (7.116), setting  $\epsilon = 2$ , with  $A = 1.094$ ,  $A' = 1.1$ ,  $\beta = 0.89$ ,  $C = 1.15$ , and  $\delta = 2.22$ . Consistent with scaling relations, the measured  $\gamma = 1.76$ .

**The temporal avalanche shape at fixed size  $S$ :** The temporal shape can also be calculated at fixed size  $S$ . Scaling suggests that

$$\langle \dot{u}(t) \rangle_S = \frac{S}{\tau_m} \left( \frac{S}{S_m} \right)^{-\frac{1}{\gamma}} f \left( \frac{t}{\tau_m} \left( \frac{S_m}{S} \right)^{\frac{1}{\gamma}} \right), \quad (7.112)_{\text{shape}S}$$

with  $\int_0^\infty dt f(t) = 1$ , where  $f(t)$  may depend on  $S/S_m$ . In mean field, the scaling function  $f(t)$  is independent of  $S/S_m$  [79], and reads

$$f_0(t) = 2te^{-t^2}, \quad \gamma = 2. \quad (7.113)$$

To one loop one obtains  $f(t) = f_0(t) - \frac{\epsilon}{9} \delta f(t)$ . Expressions for arbitrary  $S/S_m$  are lengthy. The universal small-avalanche limit reads

$$\delta f(t) = \frac{f_0(t)}{4} \left[ \pi (2t^2 + 1) \operatorname{erfi}(t) + 2\gamma_E (1 - t^2) - 4 - 2t^2 (2t^2 + 1) {}_2F_2 \left( 1, 1; \frac{3}{2}, 2; t^2 \right) - 2e^{t^2} \left( \sqrt{\pi} t \operatorname{erfc}(t) - \operatorname{Ei}(-t^2) \right) \right]. \quad (7.114)$$

It satisfies  $\int_0^\infty dt \delta f(t) = 0$ . The asymptotic behaviors are

$$f(t) \simeq_{t \rightarrow 0} 2At^{\gamma-1} \quad (7.115)_{\text{asympt}}$$

$$f(t) \simeq_{t \rightarrow \infty} 2A't^\beta e^{-Ct^\delta}, \quad \delta = 2 + \frac{\epsilon}{9}, \quad \beta = 1 - \frac{\epsilon}{18}, \quad (7.116)_{\text{asympt}2}$$

with  $A' = 1 + \frac{\epsilon}{36}(5 - 3\gamma_E - \ln 4)$  and  $C = 1 + \frac{\epsilon}{9} \ln 2$ . The amplitude  $A = 1 + \frac{\epsilon}{9}(1 - \gamma_E)$  leads to the same universal short-time behavior as in Eq. (7.110). To properly extrapolate to larger values of  $\epsilon$ , we use

$$f(t) \approx 2te^{-Ct^\delta} \mathcal{N} \exp \left( -\frac{\epsilon}{9} \left[ \frac{\delta f(t)}{f_0(t)} - t^2 \ln(2t) \right] \right), \quad (7.117)_{S\text{-shape}}$$

with the normalization  $\mathcal{N}$  chosen s.t.  $\int_0^\infty dt f(t) = 1$ . Eq. (7.117) is exact to  $\mathcal{O}(\epsilon)$  and satisfies the asymptotic expansions (7.115) and (7.116).

This result has beautifully been measured in the Barkhausen noise experiment of Ref. [71], see figure 7.6.

**The spatial avalanche shape (in  $d = 1$ ):** The spatial avalanche shape for the BFM was shown on figure 7.3. For systems with SR-correlated disorder, it was measured for two different driving protocols: tip driven (driving at a single point), and spatially homogenous driving by the parabola, the protocol used above. For tip-driven avalanches at the non-driven end, as well as for homogeneously driven avalanches, Eq. (7.80) predicts that the avalanche shape at fixed extension  $\ell$  grows close to the boundary point  $b$  as

$$\langle S(x) \rangle_\ell \sim |x - b|^\zeta. \quad (7.118)$$

For  $\zeta = 1.25$  one thus expects this curve to have a slightly positive curvature at these points, consistent with plots 3 and 5 of Ref. [80].

Let us also mention the studies of [81] for avalanches with a large aspect ratio in the BFM which are rare, and with fixed seed position [82] which are difficult to realize in an experiment.

## 7.19 Avalanches with retardation

In magnetic systems, a change in the magnetization induces an *eddy current*, which in turn can reignite an avalanche which otherwise would already have stopped [83]. The most simple model exhibiting this phenomena, and which remains analytically solvable [79] reads

$$\partial_t u(t) = F(u(t)) + m^2[w(t) - u(t)] - ah(t) \quad (7.119)$$

$$\tau \partial_t h(t) = \partial_t u(t) - h(t). \quad (7.120)$$

While many observables can be obtained analytically [79] and measured, e.g. the temporal shape given  $S$ , other ones are not well-defined, as the duration of an avalanche. Indeed, due to the eddy current  $h(t)$ , an avalanche can restart. This complicates the data-analysis in real magnets [62].

## 7.20 Power-law correlated random forces, relation to fractional Brownian motion

Suppose that the random forces are correlated as a fractional Brownian motion (fBm)

$$\Delta(0) - \Delta(u) = \sigma |u|^{2H} \quad (7.121)$$

Solving Eq. (6.35), and realizing that loop corrections are subdominant for all  $H < 2$ , we obtain similar to the derivation of Eq. (7.42)

$$\zeta = \frac{\epsilon}{2(1 - H)} \quad (7.122)$$

As a consequence of Eq. (7.4), the avalanche-size exponent is

$$\tau = 2 - \frac{2}{d + \zeta} = 2 - \frac{4(1 - H)}{4 + d(1 - 2H)} \quad (7.123)$$

Interestingly, in  $d = 0$ , i.e. for a particle, this reduces to

$$\tau|_{d=0} = 1 + H \quad (7.124)$$

This is consistent with the first-return probability derived in Refs. [84, 85]. Indeed, the probability to return to the origin of a fBm  $X_t$  with Hurst exponent  $H$  is  $P(t) = \langle \delta(X_t) \rangle \sim t^{-H}$ , equivalent to Eq. (40) of [85]. The probability to return for the first time is  $\partial_t P(t) \sim t^{-(1+H)}$ , equivalent to Eq. (7.124).

# PART 3: Discrete Stochastic Processes

## 8 Coherent-state path integral, reaction diffusion systems, etc.

### 8.1 Modeling discrete stochastic processes

Discrete stochastic processes are stochastic processes, where the elementary degrees of freedom are discrete variables. This can be the number of colloids in a suspension, the number of bacteria, fishes and their predators in the ocean, or the grains in sandpile models. There are two powerful methods to treat these systems:

- (i) the coherent-state path integral
- (ii) effective stochastic equations of motion

The first method, the coherent-state path integral is an exact method, and as such a natural starting point to study stochastic systems in a field-theoretic setting, i.e. to construct a dynamic action, as the Martin-Siggia-Rose action we saw in section 3.4. As we will see in the next section 8.2, despite the fact that it is an exact method, or maybe due to it, it has its problems. We have therefore relegated its derivation to appendix C. In appendix we cover perturbation theory in the CSPI. Appendix C.18 is devoted to the decoupling of interaction terms in the CSPI via a noise, similar to the Hubbard-Stratonovich transformation used in section 2.1, or simply Wick's theorem (1.6). This noise will in general be imaginary, leading to problems both in the interpretation, as in simulations. As a caveat to the reader we would like to mention that things sometimes get messed up in the literature: Starting with the CSPI, one sees emerging an effective stochastic equation of motion with real noise. This is, in general not possible.

Real noises appear in a different modeling of stochastic systems, via *effective stochastic equations of motion*. As we will show below, the noise here stems from the fact that one tries to approximate a *discrete* random process by a *continuous* one. Another important question we will deal with is the notion of the *Mean-Field* approximation in stochastic equations. We will give a simple and precise definition of the latter. To our astonishment, we have not found a discussion of this in the literature.

### 8.2 The coherent-state path integral, imaginary noise and its interpretation

The coherent-state path-integral derived in appendix C is constructed by using creation and annihilation operators familiar from quantum mechanics,

$$[\hat{a}, \hat{a}^\dagger] = 1, \quad |n\rangle = (\hat{a}^\dagger)^n |0\rangle. \quad (8.1) \text{commutator}$$

The formalism then uses eigenstates of these operators, which are coherent states, and which gave the name to the formalism,

$$|\phi\rangle := e^{\phi \hat{a}^\dagger} |0\rangle \quad \Rightarrow \quad \hat{a} |\phi\rangle = \phi |\phi\rangle. \quad (8.2) \text{CS2}$$

Taylor expanding  $e^{\phi \hat{a}^\dagger} |0\rangle$ , one sees that these states are Poisson distributions with  $n$ -fold occupation probability given by

$$p(n) = e^{-\phi} \frac{\phi^n}{n!}. \quad (8.3) \text{p5}$$

Note that  $\langle n \rangle = \langle n^2 \rangle^c = \phi$ , thus the parameter characterizing a coherent state is its mean and variance.

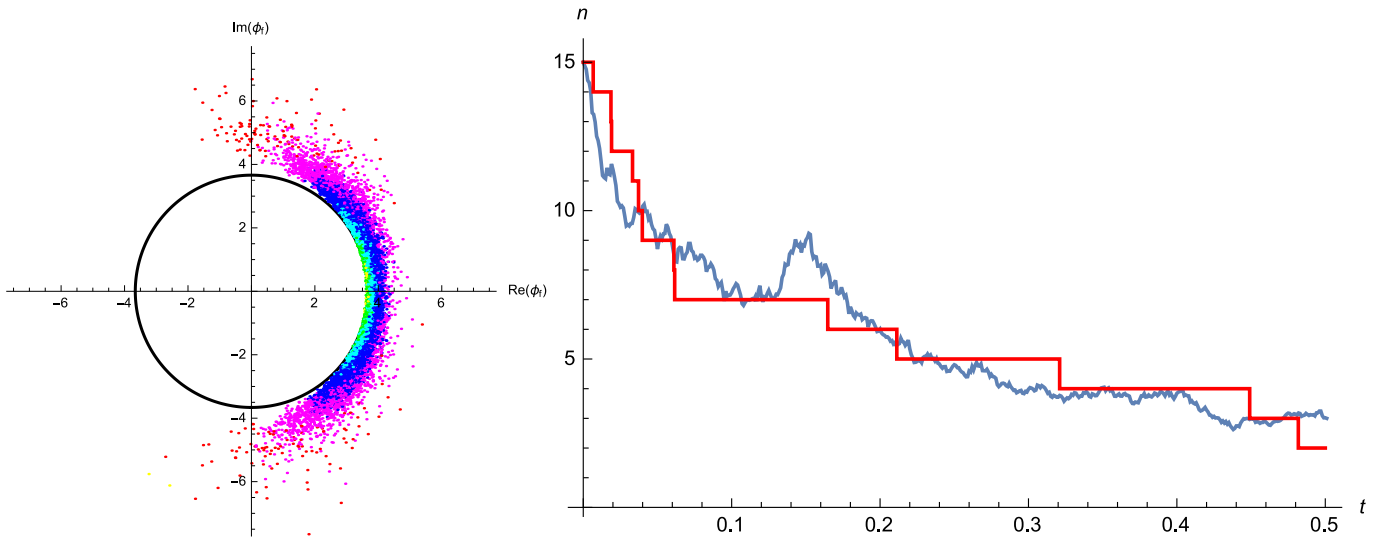


Figure 8.1: Left: Result of the integration of Eq. (7.74), with  $\nu = 1$ , total time  $t_f - t_i = 0.5$ , and initial state  $\phi_i = 15$ . The black circle has radius  $\phi_f = 3.6614$ , obtained by integrating the drift term  $\partial_t \phi_t = -\phi_t^2 + \phi_t + t/2$ . Using an algorithm which splits points which are likely to contribute more to the final result, the color codes less probable values, from yellow over green, cyan, blue, magenta to red. (Thus a red point has  $2^{-5}$  times the weight of a yellow point.) Right: One trajectory each for process  $n_t$ , i.e. a direct numerical simulation of  $A + A \rightarrow A$  (red, with jumps), and  $\hat{n}_t$ , Eq. (8.15) (blue-grey, continuous, rough). The rate is  $\nu = 1$ . We have chosen two trajectories which look “similar”. Note that  $\hat{n}_t$  is not monotonically decreasing.

Consider now the reaction-diffusion process with diffusion constant  $D$  and reaction rate  $A + A \xrightarrow{\nu} A$ . The action constructed in appendix C.20 reads

$$\mathcal{S}'[\phi^*, \phi] = \int_{x,t} \phi^*(x,t) \left[ \partial_t \phi(x,t) - D \nabla^2 \phi(x,t) \right] + \frac{\nu}{2} \left[ \phi^*(x,t) \phi(x,t)^2 + \phi^*(x,t)^2 \phi(x,t)^2 \right]. \quad (8.4)$$

The first two terms are similar to those appearing in the MSR formalism for diffusion (3.46), identifying the tilde fields there with star fields here. The next term  $\phi^*(x,t) \phi(x,t)^2$  is also intuitive: Two particles are destroyed, and one is created. The only surprising term is the last one. It appears in the formalism to ensure that the probability is conserved, and can be interpreted as a first-passage time problem, see appendix C.17. If the last term were not there, then we could interpret the action as an equation of motion for  $\phi(x,t)$ . To achieve the latter, let us decouple as in Eq. (1.6) the quartic term by introducing an auxiliary field  $\xi(x,t)$ , to be integrated over in the path integral,

$$\mathcal{S}'[\phi^*, \phi, \xi] = \int_{x,t} \phi^*(x,t) \left[ \partial_t \phi(x,t) - D \nabla^2 \phi(x,t) + \frac{\nu}{2} \phi(x,t)^2 - i\sqrt{\nu} \xi(x,t) \phi(x,t) \right] + \frac{1}{2} \xi(x,t)^2. \quad (8.5)$$

The corresponding equation of motion and noise correlations are

$$\partial_t \phi(x,t) = -\frac{\nu}{2} \phi(x,t)^2 + D \nabla^2 \phi(x,t) + i\sqrt{\nu} \phi(x,t) \xi(x,t), \quad (8.6)$$

$$\langle \xi(x,t) \xi(x',t') \rangle = \delta(t-t') \delta(x-x'). \quad (8.7)$$

This noise is imaginary. It has puzzled many researchers whether this is unavoidable [86, 87, 88, 89], or could even be beneficial [90].

For the moment, let us restrict our considerations to a single site, starting at time  $t = t_i$  with the initial state,  $\phi_{t_i} = \phi_i$ ,

$$\partial(t) \phi(t) = -\frac{\nu}{2} \phi(t)^2 + i\sqrt{\nu} \phi(t) \xi(t), \quad \langle \xi(t) \xi(t') \rangle = \delta(t-t'). \quad (8.8)$$



This equation is integrated from  $t = t_i$  to  $t_f$ . On the left of figure 8.1 we show the result for  $\phi_{t_f}$  for different realizations of the noise  $\xi(t)$ . Since  $\phi_{t_f}$  is complex, the question is how to interpret these states. The answer is that the probability distribution is given, in generalization of (8.3), by [6]

$$p_t^{\text{SEM}}(n) := \left\langle e^{-\phi_t \frac{\phi_t^n}{n!}} \right\rangle_{\xi} . \quad (8.9)_{\text{magicBIS}}$$

A complex  $\phi(t)$  is necessary, since the final distribution is *narrower* than a Poissonian<sup>2</sup>. The problem with the stochastic average (8.9) is that when  $\arg(\phi_t)$  grows in time, it is *dominated* by those  $\phi_t$  with the smallest real part, and the estimate (8.9) breaks down. A stochastic equation of motion for the coherent-state path integral is thus not a valid simulation tool.

In the next sections, we will follow a different strategy: We give up on the fact that the number  $n(t)$  of particles is discrete, and replace it by a continuous variable  $\hat{n}(t)$ . We then find

$$\frac{d\hat{n}(t)}{dt} = -\frac{\nu}{2}\hat{n}(t)(\hat{n}(t) - 1) + \sqrt{\frac{\nu}{2}\hat{n}(t)(\hat{n}(t) - 1)}\xi(t) , \quad \langle \xi(t)\xi(t') \rangle = \delta(t - t') . \quad (8.10)_{\text{a-process-B}}$$

Note that  $\hat{n}(t)$  is the particle number, and not the expectation of the particle number as in the coherent state, thus  $\langle n \rangle = \hat{n}(t)$ , and  $\langle n^2 \rangle^c = 0$ . Eq. (8.10) is rather similar to Eq. (8.8), especially at large  $\hat{n}(t)$ . The most notable difference is the appearance of a real noise. This has a straightforward statistical interpretation as the fluctuations appearing when starting from  $\hat{n}(0) = n_i$ . We show one realization of the discrete reaction-annihilation process on Fig. 8.1, along with one realization of (8.10), chosen to have roughly the same overall shape as the discrete process.

### 8.3 Stochastic noise as a consequence of the discreteness of the states

We now want to derive Eq. (8.10). To this aim let us simulate directly the random process  $A + A \xrightarrow{\nu} A$ . Each simulation run gives one possible realization of the process, in the form of an integer-valued monotonically decreasing function  $n(t)$ . Averaging over these runs, one samples the final distribution  $P_f(n)$ , or, equivalently, moments of  $n_f$ . We want to ask the question: Is there a continuous random process  $\hat{n}(t)$  which has the same statistics as  $n(t)$ ?

Let us consider a little more general problem: Be  $n(t)$  the number of particles at time  $t$ . With rate  $r_+$  the number of particles increases by one, and with rate  $r_-$  it decreases by one. This implies that after one time step, as long as  $r_{\pm}\delta t$  are small,

$$\langle n(t + \delta t) - n(t) \rangle = (r_+ - r_-)\delta t , \quad (8.11)$$

$$\langle [n(t + \delta t) - n(t)]^2 \rangle = (r_+ + r_-)\delta t . \quad (8.12)$$

The following *continuous random process*  $\hat{n}(t)$  has the same first two moments as  $n(t)$ ,

$$d\hat{n}(t) = (r_+ - r_-)dt + \sqrt{r_+ + r_-}\xi(t)dt , \quad (8.13)$$

$$\langle \xi(t)\xi(t') \rangle = \delta(t - t') . \quad (8.14)$$

This procedure can be modified to include higher cumulants of  $n(t + \delta t) - n(t)$ , leading to more complicated noise correlations. Results along these lines were obtained in Ref. [91] by considering cumulants generated in the effective field theory.

---

<sup>2</sup>It is impossible to construct a probability distribution which is narrower than a Poissonian by the sole superposition of Poissonians with positive coefficients.



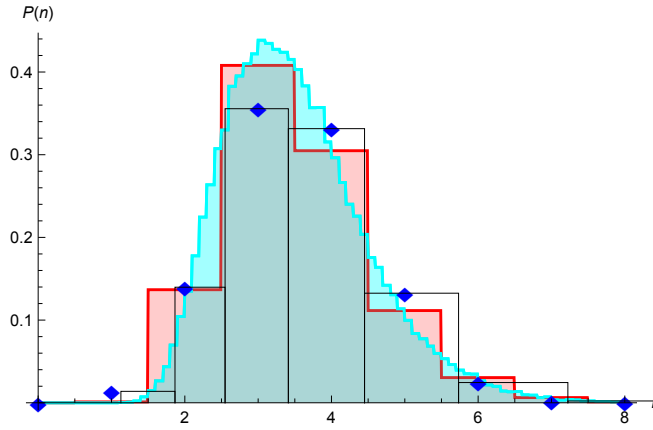


Figure 8.2: Result of a numerical simulation, starting with  $n_i = 15$  particles, and evolving for  $t_f - t_i = 0.025$ . Blue diamonds: Direct numerical simulation of the process  $A + A \rightarrow A$  with rate  $\nu = 1$ . Cyan: Distribution of the continuous random walk (8.15). Red: The latter distribution, when rounding  $n_f$  to the nearest integer. Black boxes: The size of the boxes in  $n$ -direction to obtain the result of the direct numerical simulation of the process  $A + A \rightarrow A$ . Both processes have first moment  $3.511 \pm 0.001$ , and second connected moment  $1 \pm 0.05$ ; the third connected moments already differ quite substantially, 0.75 versus 0.2.

## 8.4 Example: The reaction-annihilation process

In the case of the reaction-annihilation process, the rate  $r_+ = 0$ , and  $r_- = \frac{\nu}{2}\hat{n}(t)(\hat{n}(t) - 1)$ ; the latter, in principle, is only defined on integer  $\hat{n}(t)$ , but we will use it for all  $\hat{n}(t)$ . Thus the best we can do to replace the discrete stochastic process with a continuous one is to write

$$\frac{d\hat{n}(t)}{dt} = -\frac{\nu}{2}\hat{n}(t)(\hat{n}(t) - 1) + \sqrt{\frac{\nu}{2}\hat{n}(t)(\hat{n}(t) - 1)}\xi(t), \quad \langle \xi(t)\xi(t') \rangle = \delta(t - t'). \quad (8.15)_{\text{a-process}}$$

This is equation (8.15) given above. Using  $n_i = 15$ , and  $\nu = 1$ , we have shown two typical trajectories on figure 8.1 (right), one for the process  $n(t)$  (red, with jumps), and one for the process  $\hat{n}_t$  (blue-grey, rough). While by construction both processes have (almost) the same first two moments, clearly  $\hat{n}(t)$  looks different: It is continuous, which  $n(t)$  is not, and it can increase in time, which  $n(t)$  can not. One can also compare the distribution for  $t_f - t_i = 0.5$ , see figure 8.2. While the distribution of  $n_f$  is discrete (blue diamonds), that for  $\hat{n}_f$  is continuous (cyan). Rounding  $n_f$  to the nearest integer gives a different distribution (red). We have also drawn (black lines) the size of the boxes which would produce  $p(n)$  from  $p(\hat{n})$ . Clearly, there are differences. On the other hand, it is also evident that these differences diminish when increasing  $n_i$ .

## 8.5 Diffusion

We now derive the effective stochastic equation of motion for diffusion, i.e. hopping of grains from site  $i$  to site  $i \pm 1$  with rate  $D$ . This is represented on on Fig. 8.3. We can not directly write an equation of the form (8.13) for the particle number  $\hat{n}_i$  on site  $i$ , since it does not respect the conservation of the number of particles. The latter is realised by introducing the current  $J(i + \frac{1}{2}, t)$ : A positive current  $J(i + \frac{1}{2}, t) = 1$  represents a particle hopping from site  $i$  to  $i + 1$ . A negative current  $J(i + \frac{1}{2}, t) = -1$  corresponds to a particle hopping from site  $i + 1$  to site  $i$ . Each hopping has a rate  $D$ ; the rate for a given particle to leave a site is the coordination number  $2d$  times  $D$ . We thus arrive at the rate equations (with the hat again denoting

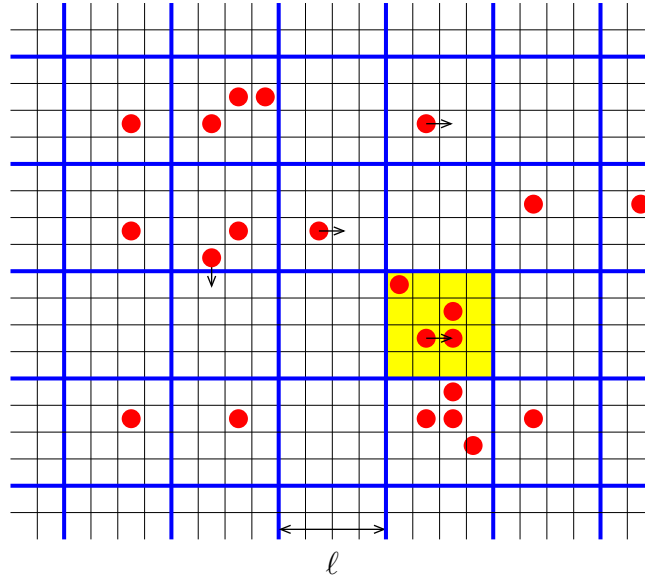


Figure 8.3: A coarse-grained lattice with box-size  $\ell = 4$ . The yellow box contains  $n = 4$  particles.

the variables of the continuous process)

$$d\hat{n}(i, t) = \left[ \hat{J}(i - \frac{1}{2}, t) - \hat{J}(i + \frac{1}{2}, t) \right] dt \quad (8.16)$$

$$\hat{J}(i + \frac{1}{2}, t) = D [\hat{n}(i, t) - \hat{n}(i + 1, t)] + \sqrt{D[\hat{n}(i, t) + \hat{n}(i + 1, t)]} \eta(i + \frac{1}{2}, t) \quad (8.17)$$

The white noise has correlations

$$\langle \eta(i + \frac{1}{2}, t) \rangle = 0, \quad \langle \eta(i + \frac{1}{2}, t) \eta(j + \frac{1}{2}, t') \rangle = \delta_{i,j} \delta(t - t'). \quad (8.18)$$

To perform the continuum limit, let us introduce the density of particles inside a box  $B_\ell(x)$  centered at  $x$  and of linear size  $\ell$ , as well as the ( $d$ -dimensional) current,

$$\rho(x, t) := \sum_{i \in B_\ell(x)} \frac{\hat{n}(i, t)}{\ell^d}, \quad J(x, t) := \sum_{i \in B_\ell(x)} \frac{\hat{J}(i + \frac{1}{2}, t)}{\ell^d} \quad (8.19)$$

which (in first approximation) is independent of the size of the box. (We dropped the hat for convenience of notation.) In terms of  $\rho$ , the stochastic equations become<sup>3</sup> (generalized to  $d$  dimensions)

$$\partial_t \rho(x, t) = -\nabla \cdot \vec{J}(x, t), \quad (8.20)$$

$$\vec{J}(x, t) = -D \nabla \rho(x, t) + \sqrt{2D \rho(x, t)} \vec{\eta}(x, t), \quad (8.21)$$

$$\langle \eta^i(x, t) \eta^j(x', t') \rangle = \delta^{ij} \delta^d(x - x') \delta(t - t'). \quad (8.22)$$

Note that there is no  $\ell$ -dependent factor, neither for the current, nor the noise term. Combining the first two equations yields

$$\partial_t \rho(x, t) = D \nabla^2 \rho(x, t) + \nabla \cdot [\sqrt{2D \rho(x, t)} \vec{\eta}(x, t)]. \quad (8.23)$$

<sup>3</sup>These equations are standard, undisputed, and appear frequently in the literature, see e.g. [92]. They are a special case of Eq. (17) of [93], itself equivalent to Eq. (4) of [87].

Let us step back and analyse the above findings; for simplicity of notation we again set  $d = 1$ . First of all, the diffusion process is constructed such that particles do not interact. A given particle will be on a chosen site with probability  $1/L$ , where  $L$  is the system size. If  $N = \bar{n}L$  is the total number of particles, and  $\bar{n}$  the mean particle number per site, then the probability to find  $n$  particles on a given site is

$$p(n) = \binom{N}{n} \left(\frac{1}{L}\right)^n \left(1 - \frac{1}{L}\right)^{N-n} \simeq e^{-\bar{n}} \frac{(\bar{n})^n}{n!}. \quad (8.24)$$

The last relation is valid in the limit of  $L$  large. We recuperate our old friend, the normalized coherent state  $e^{-\phi} |\phi\rangle$ , with  $\phi = \bar{n}$ . Note that in the CSPI, the analog of Eq. (8.23) is given by Eq. (C.103), namely

$$\partial_t \phi(x, t) = D \nabla^2 \phi(x, t). \quad (8.25)$$

Since the CSPI works with coherent states, it does not need the noise of Eq. (8.23). What diffuses is the “weight”  $\phi(x, t)$  of the coherent state, which is the mean particle number per site, termed  $\bar{n}$  above. Thus in the CSPI, both mean and variance of the number of particles on a site tends to  $\bar{n}$ . We checked with a numerical simulation that Eq. (8.23) indeed leads to a distribution of particles per site with mean and variance  $\bar{n}$ .

## 8.6 An effective stochastic field theory of the reaction process

Let us now construct an effective field theory of the reaction-diffusion process. Consider a lattice of size  $L^d$ , with particles on it, which can hop from one site to a neighbouring one with rate  $D$ . To simplify our considerations, let us suppose that we take the limit of  $\nu \rightarrow \infty$ : if a particle jumps on an occupied site, only one of them survives. To construct an effective field theory, we introduce boxes of size  $\ell$ . Each of these boxes contains  $n(x, t)$  particles at time  $t$ .

With rate  $D$ , a particle hops. Thus the probability with which a particle in a given box will hop is  $D n(x, t) \delta t$ ; that it will land on an occupied site and thus annihilate is

$$\delta_{\text{an}} n(x, t) \simeq D n(x, t) \delta t \times \frac{n(x, t) - 1}{\ell^d}. \quad (8.26)$$

The second factor is an approximation which neglects the correlations inside the box. If the particle had hopped out of its box, then the second factor should involve the density in the neighbouring box; writing the density in the same box is another approximation. Last not least, if the box is sufficiently large, then one can replace  $n(x, t) - 1 \rightarrow n(x, t)$ .

To perform the continuum limit, we use the density  $\rho(x, t)$  defined in Eq. (8.19). The equation of motion of this density then becomes

$$\partial_t \rho(x, t) = -D \rho(x, t)^2 + \sqrt{D} \rho(x, t) \xi(x, t) + D \nabla^2 \rho(x, t) + \nabla \left[ \sqrt{2D \rho(x, t)} \vec{\eta}(x, t) \right], \quad (8.27)$$

$$\langle \xi(x, t) \xi(x', t') \rangle = \delta(t - t') \delta^d(x - x'), \quad (8.28)$$

$$\langle \eta^i(x, t) \eta^j(x', t') \rangle = \delta^{ij} \delta(t - t') \delta^d(x - x'), \quad (8.29)$$

$$\langle \xi(x, t) \rangle = \langle \eta^i(x, t) \rangle = \langle \xi(x, t) \eta^i(x', t') \rangle = 0. \quad (8.30)$$

All factors of  $\delta t$  and  $\ell$  have disappeared, absorbed into a non-trivial dimension of  $\xi(x, t)$ , and  $\vec{\eta}(x, t)$ . Note that the diffusive noise is rarely written. The reason is that the coarse-grained density  $\rho(x, t)$  varies smoothly, thus

$$\nabla \left[ \sqrt{2D \rho(x, t)} \vec{\eta}(x, t) \right] \simeq \sqrt{2D \rho(x, t)} \nabla \vec{\eta}(x, t). \quad (8.31)$$

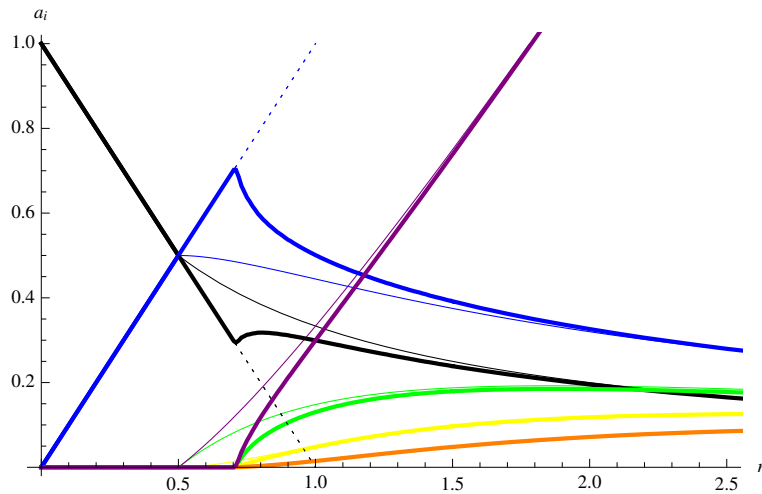


Figure 9.1: Thick lines: The order parameters of the Manna model, as a function of  $n$ , the average number of grains per site, obtained from a numerical simulation of the stochastic Manna model on a grid of size  $150 \times 150$  with periodic boundary conditions. We randomly update a site for  $10^7$  iterations, and then update the histogram 500 times every  $10^5$  iterations. Plotted are the fraction of sites that are: unoccupied (black), singly occupied (blue), double occupied (green), triple occupied (yellow), quadruple occupied (orange). The activity  $\rho = \sum_{i>1} a_i(i-1)$  is plotted in purple. No data were calculated for  $n < 0.5$ , where  $a_0 = e = 1 - n$ ,  $a_1 = n$ , and  $a_{i>2} = 0$  (inactive phase). Note that before the transition,  $a_0 = 1 - n$  and  $a_1 = n$ . The transition is at  $n = n_c = 0.702$ . Thin lines: The MF phase diagram, as given by Eqs. (9.10) ff. for  $n \leq \frac{1}{2}$ , and by Eqs. (9.11) ff. for  $n \geq \frac{1}{2}$ . We checked the latter with a direct numerical simulation.

Integrating the letter over a box of size  $\ell$  yields  $\eta(x, t)$  on the boundary, making it less relevant by a factor of  $1/\ell$ . It is customarily dropped as subdominant. Thus the effective stochastic description of the annihilation-diffusion process is

$$\partial_t \rho(x, t) = -D\rho(x, t)^2 + \sqrt{D}\rho(x, t)\xi(x, t) + D\nabla^2 \rho(x, t). \quad (8.32)$$

## 9 A phenomenological derivation of the stochastic field theory for the Manna model

In this section, we apply our considerations to a non-trivial example, the stochastic Manna model. We will see that our formalism permits a systematic derivation of the effective stochastic equations of motion. While the result is known in the literature [94, 95, 96, 97], it was there derived by symmetry principles, which are not always convincing. Furthermore, they leave undetermined all coefficients. While many of them can be eliminated by rescaling, our derivation will “land” on a particular line of parameter space, characterised by the absence of additional memory terms, see section 9.4.

### 9.1 Basic Definitions

The Manna sandpile was introduced in 1991 by S.S. Manna [98], as a stochastic version of the Bak-Tang-Wiesenfeld (BTW) sandpile [99]. It is defined as follows.

**Manna Model (MM).** Randomly throw grains on a lattice. If the height at one point is greater or equal to two, then with rate 1 move two grains from this site to randomly chosen neighbouring sites. Both grains may end up on the same site.

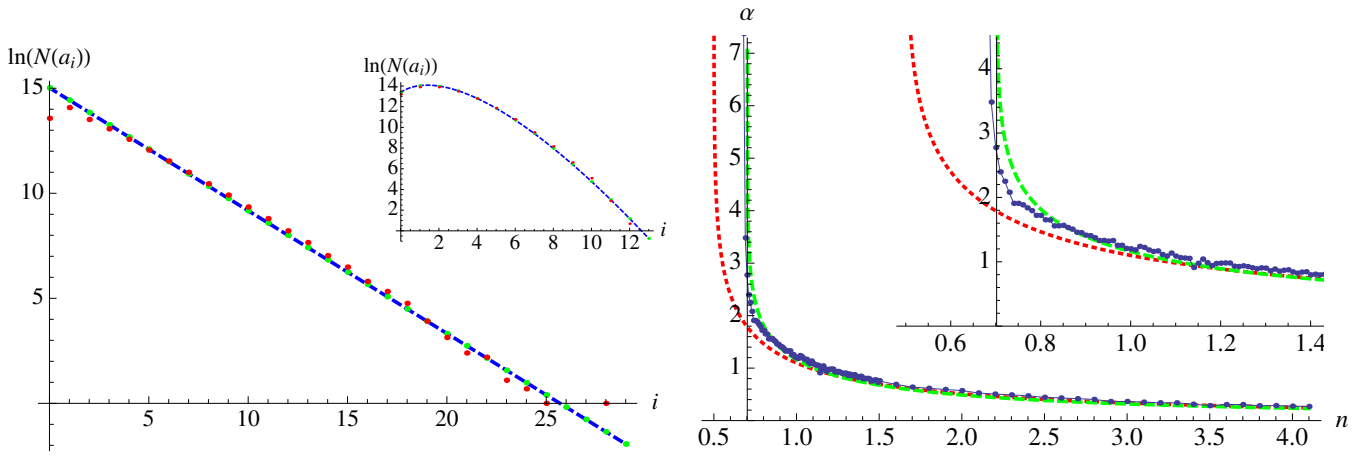


Figure 9.2: Left: (Unnormalized) histogram after many topplings for  $n = 2$ ; the probability that a site has  $i$  grains decays as  $e^{-0.585i}$ , for all  $i \geq 1$ . Inset: The initial distribution, a Poissonian. Right: The exponential decay coefficient  $\alpha$  as a function of  $n$ . The dots are from a numerical simulation. The dashed red line is the MF result (9.12). The green dashed line is a fit corresponding to  $\alpha \approx \frac{2}{3} \ln \left( \frac{(n + n_c)}{(n - n_c)} \right)$ . Inset: blow-up of main plot.

We start by analysing the phase diagram. We denote by  $a_i$  the fraction of sites with  $i$  grains. It satisfies the sum rule<sup>4</sup>

$$\sum_i a_i = 1. \quad (9.1) \text{normalization}$$

In these variables, the number of grains  $n$  per site can be written as

$$n := \sum_i a_i i. \quad (9.2) \text{197a}$$

The empty sites are

$$e := a_0. \quad (9.3)$$

The fraction of active sites is

$$a := \sum_{i \geq 2} a_i. \quad (9.4)$$

We also define the (weighted) activity as

$$\rho := \sum_{i \geq 2} a_i (i - 1). \quad (9.5)$$

Note that  $\rho$  satisfies the sum rule

$$n - \rho + e = 1. \quad (9.6) \text{sum-rule}$$

In order to take full advantage of this definition, one may change the toppling rules of the Manna model to those of the

**Weighted Manna Model (wMM)** : If a site contains  $i \geq 2$  grains, randomly move these grains to neighbouring sites with rate  $(i - 1)$ .

<sup>4</sup>Note that  $a_i$  has nothing to do with the operator  $\hat{a}_i$  used earlier.

On figure 9.1 (thick lines), we show a numerical simulation of the Manna model in a 2-dimensional system of size  $L \times L$ , with  $L = 150$ . There is a phase transition at  $n = n_c = 0.702$ . Close to  $n_c$ , the fraction of doubly occupied sites  $a_2$  grows linearly with  $n - n_c$ , and higher occupancy is small. Indeed, we checked numerically that for  $n > n_c$  the probability  $p_i$  to find  $i$  grains on a site decays exponentially with  $i$ , i.e.  $p_i \sim \exp(-\alpha_n i)$ , where  $\alpha_n$  depends on  $n$ , see figure 9.2. This is to be contrasted with the initial condition, where we randomly distribute  $n \times L^2$  grains on the lattice of size  $L \times L$ , and which yields a Poisson distribution, the coherent state  $|n\rangle$ , for the number of grains on each site, see inset of figure 9.2 (left). This result suggests that coherent states may not be the best representation for this system. It further implies that close to the transition,  $\rho \approx a$ , and we expect that the wMM and the original MM have the same critical behaviour. We come back to this question below.

## 9.2 MF solution

In order to make analytical progress, we now study the *topple-away* or Mean Field solution of the stochastic Manna sandpile, which we can solve analytically. We define:

**Mean-Field Manna Model (MF-MM).** If a site contains two or more grains, move these grains to any randomly chosen other site of the system.

The rate equations are, setting for convenience  $a_{-1} := 0$ :

$$\partial_t a_i = -a_i \Theta(i \geq 2) + a_{i+2} + 2 \left[ \sum_{j \geq 2} a_j \right] (a_{i-1} - a_i) . \quad (9.7) \text{ate:Manna}$$

Using the sum rule (9.1), they can be rewritten as

$$\partial_t a_i = -a_i \Theta(i \geq 2) + a_{i+2} + 2(1 - a_0 - a_1)(a_{i-1} - a_i) . \quad (9.8) \text{96}$$

We are interested in the steady state  $\partial_t a_i = 0$ . One can solve these equations by introducing a generating function. An alternative solution consists in realising that for  $i \geq 2$ , Eq. (9.8) admits a steady-state solution of the form

$$a_i = a_2 \kappa^{i-2} , \quad i > 2 . \quad (9.9) \text{213}$$

This reduces the number of independent equations  $\partial_t a_i = 0$  in Eq. (9.8) from infinity to three. Furthermore, there are the equations  $\sum_{i=0}^{\infty} a_i = 1$ , and  $\sum_{i=0}^{\infty} i a_i = n$ . Thus there are 5 equations for the 4 variables  $a_0$ ,  $a_1$ ,  $a_2$ , and  $\kappa$ . The reason we apparently have one redundant equation is due to the fact that we already used the normalisation condition (9.1) to go from Eq. (9.7) to Eq. (9.8).

These equations have two solutions: For  $0 < n < 1$ , there is always the solution for the *inactive* or *absorbing state*,

$$a_0 = 1 - n , \quad a_1 = n , \quad a_{i \geq 2} = 0 . \quad (9.10) \text{riv-sol}$$

For  $n > 1/2$ , there is a second non-trivial solution,

$$a_0 = \frac{1}{1 + 2n} , \quad a_{i > 0} = \frac{4n \left( \frac{2n-1}{2n+1} \right)^i}{4n^2 - 1} . \quad (9.11) \text{210}$$

(Note that  $a_2/a_1$  has the same geometric progression as  $a_{i+1}/a_i$  for  $i > 2$ , which we did note suppose in our ansatz.) Thus the probability to find  $i > 0$  grains on a site is given by the exponential distribution

$$p(i) = \frac{4n}{4n^2 - 1} \exp(-i \alpha_n) , \quad \alpha_n = \log \left( \frac{2n+1}{2n-1} \right) . \quad (9.12) \text{212}$$

Using these two solutions, we get the MF phase diagram plotted on figure 9.1 (thin lines). This has to be compared with the simulation of the Manna model on the same figure (thick lines). One sees that for  $n \geq 2$ , MF solution and simulation are getting almost indistinguishable. We have also checked with simulations that the Manna model has a similar exponentially decaying distribution of grains per site, with a decay-constant  $\alpha$  plotted on the right of figure 9.2.

### 9.3 The complete effective equations of motion for the Manna model

In this section, we give the effective equations of motion for the Manna model. Let us start from the mean-field equations for  $\rho(t)$  and  $n(t)$ . For simplicity of expressions, we use the weighted Manna model. The physics close to the transition should not depend on it. Let us start from the hierarchy of MF equations for the weighted Manna model. These are similar to Eq. (9.8), and can be rewritten as

$$\partial_t a_i = (1 - i)a_i \Theta(i \geq 2) + (i + 1)a_{i+2} + 2\rho(a_{i-1} - a_i). \quad (9.13) \text{MF-w-Manna}$$

#### Exercise 18: Prove Eq. (9.13).

For convenience, let us write explicitly the rate equation for the fraction of empty sites  $e \equiv a_0$ ,

$$\partial_t e = a_2 - 2\rho e \quad (9.14)$$

The first term, the gain  $r_+ = a_2$  comes from the sites with two grains, toppling away, and leaving an empty site. The second term, the loss term, is the rate at which one of the toppling grains lands on an empty site,  $r_- = 2\rho e$ .

We now follow the formalism developed in section 8.3, Eqs. (8.11)–(8.14). This yields

$$\partial_t e = a_2 - 2\rho e + \sqrt{a_2 + 2\rho e} \bar{\xi}_t, \quad (9.15)$$

where  $\langle \bar{\xi}_t \bar{\xi}_{t'} \rangle = \delta(t - t')/\ell^d$ , and  $\ell$  is the size of the box which we consider. Now remark that close to the transition,  $a_2 \approx \rho$ . Inserting this into the above equation, we arrive at

$$\partial_t e \approx \rho(1 - 2e) + \sqrt{\rho}\sqrt{1 + 2e} \bar{\xi}_t, \quad (9.16) \text{97}$$

Due to Eq. (9.6), the combination  $n - \rho + e = 1$ , and since  $n$  is conserved this implies  $\partial_t e \equiv \partial_t \rho$ . It is customary to write equation (9.16) for  $\partial_t \rho$ , instead of  $\partial_t e$ . Next we approximate  $\sqrt{1 + 2e}$  by the value of  $e$  at the transition, i.e.  $e \rightarrow e_c^{\text{MF}} = \frac{1}{2}$ , see the mean-field phase diagram in Fig. 9.1. Eliminating  $e$  via Eq. (9.6), we arrive at

$$\partial_t \rho \approx (2n - 1)\rho - 2\rho^2 + \sqrt{2\rho} \bar{\xi}_t. \quad (9.17)$$

Note that this equation gives back  $n_c^{\text{MF}} = \frac{1}{2}$ , and as a consequence of the conservation law  $n - \rho + e = 1$  also  $e_c^{\text{MF}} = \frac{1}{2}$ , used above in the simplification of the noise term.

Finally, let us suppose we have not a single box of size  $\ell$ , but a lattice of boxes, labeled by a  $d$ -dimensional label  $x$ . Each toppling event moves two grains from a site to the neighbouring sites, equivalent to a current

$$J(x, t) = -D\nabla\rho(x, t) + \sqrt{2D\rho(x, t)}\xi(x, t) \quad (9.18)$$

with diffusion constant  $D = 2 \times \frac{1}{2d} = \frac{1}{d}$ . The first factor of 2 is due to the fact that two grains topple. The factor of  $\frac{1}{2d}$  is due to the fact that each grain can topple in any of the  $2d$  directions, thus the rate  $D$  per direction is  $\frac{1}{2d}$ , resulting into  $D = 1/d$ . As discussed above, we will drop the noise term as subdominant.

This current changes both the activity  $\rho(x, t)$ , as the number of grains  $n(x, t)$ , resulting into a contribution for both  $\partial_t \rho(x, t)$ , and  $\partial_t n(x, t)$ . It does not couple to the density of empty sites. Using the sum-rule

(9.6)  $n - \rho + e = 1$ , implies the consistency relation  $\partial_t \rho(x, t) \equiv \partial_t n(x, t) + \partial_t e(x, t)$  for the current; this confirms that both  $\rho(x, t)$  and  $n(x, t)$  must couple to the same current.

Thus, we finally arrive at the following set of equations:

$$\partial_t \rho(x, t) = \frac{1}{d} \nabla^2 \rho(x, t) + [2n(x, t) - 1] \rho(x, t) - 2\rho(x, t)^2 + \sqrt{2\rho(x, t)} \xi(x, t), \quad (9.19)_{\text{eff:1}}$$

$$\partial_t n(x, t) = \frac{1}{d} \nabla^2 \rho(x, t), \quad \langle \xi(x, t) \xi(x', t') \rangle = \delta^d(x - x') \delta(t - t'). \quad (9.20)$$

This is known as the conserved directed percolation (C-DP) class. Instead of writing coupled equations for  $\rho(x, t)$  and  $n(x, t)$ , we can also write coupled equations for  $e(x, t)$  and  $\rho(x, t)$ :

$$\partial_t e(x, t) = [1 - 2e(x, t)] \rho(x, t) + \sqrt{2\rho(x, t)} \xi(x, t) \quad (9.21)_{\text{233}}$$

$$\partial_t \rho(x, t) = \frac{1}{d} \nabla^2 \rho(x, t) + \partial_t e(x, t) \quad (9.22)_{\text{234}}$$

The above equations for  $\rho$  and  $n$  were obtained in the literature [94, 95, 96, 97] by means of symmetry principles, but never properly derived. Evoking symmetry principles also leaves all coefficients undefined, and does not ensure that Eq. (9.21) is valid on a single site, i.e. is free of spatial derivatives. This locality will prove essential in the next section.

## 9.4 Excursion: Mapping to disordered elastic manifolds

In [100] it had been proposed to use these equations as a basis for mapping the effective field theory of the Manna model derived above onto driven disordered elastic systems. The identifications are

$$\rho(x, t) = \partial_t u(x, t) \quad \text{the velocity of the interface} \quad (9.23)$$

$$e(x, t) = \mathcal{F}(x, t) \quad \text{the force acting on the interface} \quad (9.24)$$

The second equation (9.22) is the time derivative of the equation of motion of an interface, subject to a random force  $\mathcal{F}(x, t)$ ,

$$\partial_t u(x, t) = \frac{1}{d} \nabla^2 u(x, t) + \mathcal{F}(x, t). \quad (9.25)_{\text{230}}$$

Since  $\rho(x, t)$  is positive,  $u(x, t)$  is for each  $x$  monotonously increasing. Instead of parameterizing  $\mathcal{F}(x, t)$  by space  $x$  and time  $t$ , it can be written as a function of space  $x$  and *interface position*  $u(x, t)$ . Setting  $\mathcal{F}(x, t) \rightarrow F(x, u(x, t))$ , the first equation (9.21) becomes

$$\begin{aligned} \partial_t \mathcal{F}(x, t) &\rightarrow \partial_t F(x, u(x, t)) \\ &= \partial_u F(x, u(x, t)) \partial_t u(x, t) \\ &= [1 - 2F(x, u(x, t))] \partial_t u(x, t) + \sqrt{2\partial_t u(x, t)} \xi(x, t). \end{aligned} \quad (9.26)$$

For each  $x$ , this equation is equivalent to the Ornstein-Uhlenbeck [101] process  $F(x, u)$ , defined by

$$\partial_u F(x, u) = 1 - 2F(x, u) + \sqrt{2} \xi(x, u), \quad (9.27)$$

$$\langle \xi(x, u) \xi(x', u') \rangle = \delta^d(x - x') \delta(u - u'). \quad (9.28)$$

It is a Gaussian Markovian process with mean  $\langle F(x, u) \rangle = 1/2$ , and variance in the steady state of

$$\langle [F(x, u) - \frac{1}{2}] [F(x', u') - \frac{1}{2}] \rangle = \frac{1}{2} \delta^d(x' - x) e^{-2|u - u'|}. \quad (9.29)_{\text{cor:FF}}$$



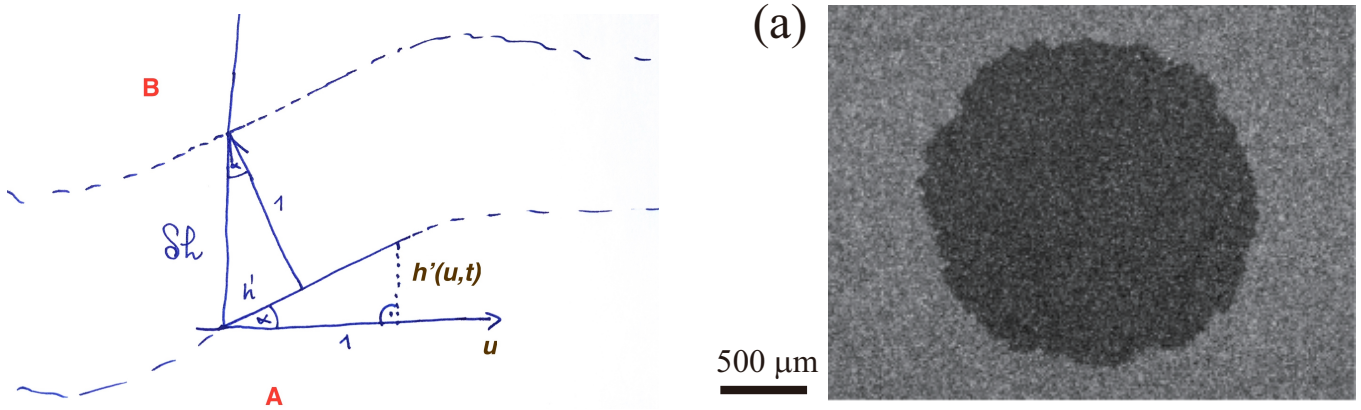


Figure 11.1: Left: An interface growing in its normal direction, with a phase A invading B. Right: An experimental realization using two phases of a nematic liquid crystal [103].

Writing the equation of motion (9.25) as

$$\partial_t u(x, t) = \frac{1}{d} \nabla^2 u(x, t) + F(x, u(x, t)) , \quad (9.30)$$

it can be interpreted as the motion of an interface with *position*  $u(x, t)$ , subject to a disorder force  $F(x, u(x, t))$ . The latter is  $\delta$ -correlated in  $x$  direction, and short-ranged correlated in  $u$ -direction. In other words, this is a disordered elastic manifold subject to Random-Field disorder. It can be treated via field theory. The latter relies on functional RG (see [102] for an introduction) for the *renormalized* version of the force-force correlator (9.29). Functional RG is nowadays well developed, and predicts not only a plethora of critical exponents [39], but also size, velocity and duration distributions [68], as well as the shape of avalanches [69].

Also note that Eq. (9.19) has a quite peculiar symmetry, namely the factor of 2 in front of both  $n(x, t)\rho(x, t)$  and  $-\rho(x, t)^2$ . As a consequence, Eq. (9.21) does not contain a term  $\sim \rho^2(x, t)$ , which would spoil the simple mapping presented above. The absence of this term *can not* be induced on symmetry arguments only. How this additional term, if present, can be treated is discussed in Ref. [100].

## 10 A good example to connect to elementary particle physics?

## 11 Burgers, KPZ, and Cole-Hopf

### 11.1 Non-linear surface growth: KPZ equation

Consider figure 11.1. What is seen is an interface between two phases, A and B. Phase A is stable, while phase B is unstable. The interface grows with a velocity  $\lambda(u, t)$  in its normal direction, increasing domain A, while diminishing B. Using the Monge representation  $\{u, h(u, t)\}$ ,  $u \in \mathbb{R}^N$  the growth in  $h$  direction is given by (see figure)

$$\delta h = \sqrt{1 + \nabla h(u, t)^2} \lambda(u, t) \delta t . \quad (11.1)$$

Assume that the growth is due to a discrete process. Following the prescription in section 8.3, the growth velocity  $\lambda(u, t)$  has a mean  $\lambda$  plus fluctuations  $\eta(u, t)$ ,

$$\lambda(u, t) = \lambda + \eta(u, t) , \quad \langle \eta(u, t) \eta(u', t') \rangle = 2D \delta(t - t') \delta^N(u - u') . \quad (11.2) \text{KPZ-noise}$$

This leads to

$$\partial_t h(u, t) = \lambda + \frac{\lambda}{2} [\nabla h(u, t)]^2 + \eta(u, t) + \dots, \quad (11.3)$$

where the dots indicate higher-order terms in  $(\nabla h)^2$ . This is (almost) the famous KPZ equation. To derive the latter, we first subtract the growth for a flat interface, setting  $h \rightarrow h - \lambda t$ , and finally add one more term to the equation

$$\partial_t h(u, t) = \nu \nabla^2 h(u, t) + \frac{\lambda}{2} [\nabla h(u, t)]^2 + \eta(u, t). \quad (11.4) \text{KPZ}$$

The additional term proportional to  $\nu$  describes diffusion along the interface, rendering it smoother.

## 11.2 Burgers equation

Taking one spatial derivative of Eq. (11.4) yields *Burgers'* equation. Defining

$$v(u, t) := \nabla h(u, t), \quad (11.5)$$

the latter reads

$$\partial_t v(u, t) = \nu \nabla^2 v(u, t) + \frac{\lambda}{2} \nabla v(u, t)^2 + \nabla \eta(u, t), \quad \langle \eta(u, t) \eta(u', t') \rangle = 2D \delta(t - t') \delta^N(u - u'). \quad (11.6) \text{Burgers}$$

Since

$$\frac{1}{2} \partial_j [v_i(u, t)^2] \equiv \frac{1}{2} \partial_j [\partial_i h(u, t)^2] = [\partial_i h(u, t)] [\partial_j \partial_i h(u, t)] \equiv [v_i(u, t) \nabla_i] v_j(u, t) \quad (11.7)$$

It can also be written as

$$\partial_t v(u, t) = \nu \nabla^2 v(u, t) + \lambda [v(u, t) \nabla] v(u, t) + \nabla \eta(u, t). \quad (11.8)$$

This is identical to Navier-Stokes' equation for incompressible fluids, with the crucial difference that Burgers' velocity is a total derivative,  $v(u, u) = \nabla h(u, t)$ , whereas for Navier-Stokes it is divergence free,  $\nabla v(u, t) = 0$ . For this reason, Burgers equation does not describe turbulence encountered e.g. in a fast-flowing river. It has, however, applications, e.g. to the large-scale structure of galaxies [104]. **\*\*\*cite more\*\*\***

## 11.3 Cole-Hopf transformation

Consider the  $N$ -dimensional KPZ equation (11.4) in Itô discretization, with noise as given in Eq. (11.2). We can eliminate the non-linear term by the so-called Cole-Hopf transformation

$$Z(u, t) := e^{\frac{\lambda}{2\nu} h(u, t) - D \frac{\lambda^2}{4\nu^2} t} \iff h(u, t) = \frac{2\nu}{\lambda} \ln Z(u, t) + \frac{D\lambda}{2\nu} t. \quad (11.9)$$

(Note that you might see this transformation without the factor of  $-D\lambda^2 t / (4\nu^2)$ ; this is then done in mid-point, i.e. Stratonovich discretization). Using Itô calculus, we obtain

$$\begin{aligned} dZ(u, t) &= \frac{\lambda}{2\nu} Z(u, t) dh(u, t) + \frac{\lambda^2}{8\nu^2} Z(u, t) dh(u, t)^2 - \frac{D\lambda^2}{4\nu^2} Z(u, t) dt \\ &= \frac{\lambda}{2\nu} Z(u, t) \left\{ \left( \nu \nabla^2 h(u, t) + \frac{\lambda}{2} [\nabla h(u, t)]^2 \right) dt + d\eta(u, t) \right\} \\ &= \nu \nabla^2 Z(u, t) dt + Z(u, t) \frac{\lambda}{2\nu} d\eta(u, t). \end{aligned} \quad (11.10)$$

\*\*\*check notation with  $d\eta$ \*\*\* Noting  $2\eta(u, t) \equiv V(u, t)$  this can be written as

$$\partial_t Z(u, t) = \nu \nabla^2 Z(u, t) + \frac{1}{2\nu} V(u, t) Z(u, t), \quad (11.11) \text{KPZ-CH}$$

$$\langle V(u, t) V(u', t') \rangle = \delta(t - t') R(u - u'), \quad (11.12)$$

$$R(u) = 2\lambda^2 D \delta^N(u). \quad (11.13)$$

We have already seen an analytical solution via a path integral, for given  $V$ ,

$$Z(u, t|V) = \int_{u(t_i)=u_i}^{u=u(t)} \mathcal{D}[u] e^{-\frac{1}{T} \int_{t_i}^t d\tau \frac{1}{2} u'(\tau)^2 - V(u(\tau), \tau)}, \quad T = 2\nu. \quad (11.14)$$

This is the path integral of a directed polymer in the quenched random potential  $V(u)$ . We can solve it in its  $n$ -times replicated form,

$$\begin{aligned} Z(u_1, \dots, u_n, t) &= \int_{u_\alpha(t_i)=u_{\alpha,i}}^{u_\alpha=u_\alpha(t)} \mathcal{D}[u_\alpha] \int \mathcal{D}[V] e^{-\frac{1}{T} \int_{t_i}^t d\tau \sum_{\alpha=1}^n [\frac{1}{2} u'_\alpha(\tau)^2 + V(u_\alpha(\tau))]} e^{-\frac{1}{4\lambda^2 D} \int_{u,\tau} V(u,\tau)^2} \\ &= \int_{u_\alpha(t_i)=u_{\alpha,i}}^{u_\alpha=u_\alpha(t)} \mathcal{D}[u_\alpha] e^{-\int_{t_i}^t d\tau \sum_\alpha \frac{1}{2T} u'_\alpha(\tau)^2 - \frac{1}{2T^2} \sum_{\alpha,\beta} R(u_\alpha(\tau) - u_\beta(\tau))}. \end{aligned} \quad (11.15)$$

We had discussed its solution in the  $T \rightarrow 0$ -limit in section 4.4, see Eq. (4.22).

Another possibility is to write a field theory for the  $n$ -times replicated field  $Z$ , i.e.  $Z \in \mathbb{R}^n$ , with

$$\mathcal{Z} = \int \mathcal{D}[Z] \mathcal{D}[\tilde{Z}] \mathcal{D}[V] e^{-\mathcal{S}_{\text{CH}}[Z, \tilde{Z}, V]}, \quad (11.16)$$

$$\mathcal{S}_{\text{CH}}[Z, \tilde{Z}, V] = \int_{u,t} \tilde{Z}(u, t) \left[ \partial_t Z(u, t) - \nu \nabla^2 Z(u, t) - \frac{1}{2\nu} V(u, t) Z(u, t) \right] + \frac{1}{4\lambda^2 D} \int_{u,t} V(u, t)^2. \quad (11.17)$$

Performing the average over  $V$  we obtain

$$\mathcal{Z} = \int \mathcal{D}[Z] \mathcal{D}[\tilde{Z}] e^{-\mathcal{S}_{\text{CH}}[Z, \tilde{Z}]}, \quad (11.18)$$

$$\mathcal{S}_{\text{CH}}[Z, \tilde{Z}] = \int_{u,t} \tilde{Z}(u, t) [\partial_t Z(u, t) - \nu \nabla^2 Z(u, t)] - \frac{\lambda^2 D}{\nu^2} [\tilde{Z}(u, t) Z(u, t)]^2. \quad (11.19)$$

Replacing  $t \rightarrow t\nu$ , we arrive at

$$\mathcal{S}_{\text{CH}}[Z, \tilde{Z}] = \int_{u,t} \tilde{Z}(u, t) [\partial_t Z(u, t) - \nabla^2 Z(u, t)] - \frac{g}{2} [\tilde{Z}(u, t) Z(u, t)]^2, \quad (11.20)$$

$$g = \frac{\lambda^2 D}{2\nu^3}. \quad (11.21)$$

Note that we did not explicitly write replicas, to perform the limit of  $n \rightarrow 0$  at the end. This is allowed as in Itô calculus the partition function  $\mathcal{Z} = 1$ . However to study the flow of the effective coupling constant  $g$ , we need at least two “replicas”, which can be thought of as “worldlines” of two particles, starting at different initial positions.

For later convenience, we note that Eq. (11.19) can also be written as

$$\mathcal{S}_{\text{CH}}[Z, \tilde{Z}] = \int_{u,t} \tilde{Z}(u, t) [\partial_t Z(u, t) - \nu \nabla^2 Z(u, t)] - \frac{1}{2T^2} \int_{u,u',t} \tilde{Z}(u, t) Z(u, t) R(u - u') \tilde{Z}(u', t) Z(u', t), \quad (11.22)$$

with \*\*\*check scaling with  $T$ , we expected a  $1/T$  for the first term\*\*\*

$$R(u) = T^2 g \delta^N(u). \quad (11.23)$$

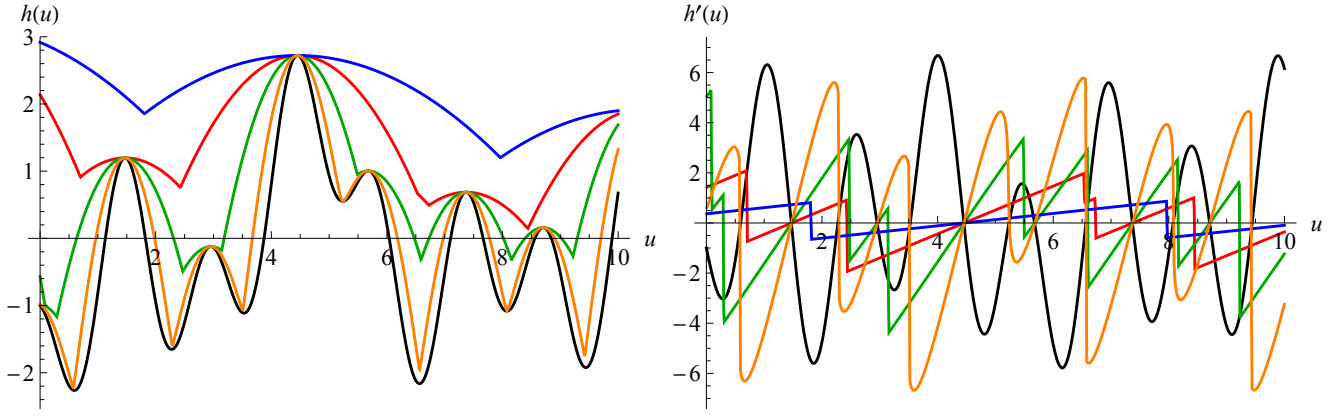


Figure 11.2: Left: Evolution of a random initial condition (black) at times  $\lambda t = 0$  (black, bottom),  $1/16$  (orange),  $1/4$  (green),  $1$  (red), and  $4$  (blue). Right: *ibid.* for the Burgers velocity  $v(u) := h'(u)$ .

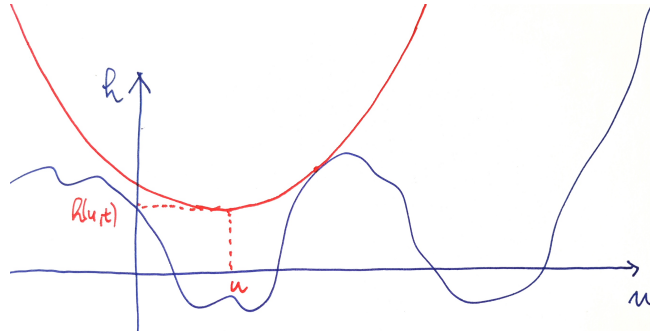


Figure 11.3: A geometrical solution to Eq. (11.26) is obtained by moving a parabola of curvature  $1/(2\lambda t)$  and centered at  $u$  (in red) down until it hits  $h'(u')$  in blue. Its minimum is then at  $h(u, t)$ .

## 11.4 Decaying KPZ, and shocks

To better understand the behavior of the KPZ equation (11.4), let us consider Eq. (11.4) for given initial condition  $h_0(u) := h(u, t = 0)$ , in absence of the noise  $\eta(u, t)$ . The Cole-Hopf transformed KPZ equation (11.11) then reduces to a diffusion equation, solved as

$$Z(u, t) = \int_{u'} \frac{e^{-\frac{(u-u')^2}{4\nu t}}}{(4\pi\nu t)^{d/2}} Z(u', 0) \quad (11.24)$$

Putting back the definition of  $Z$  in terms of  $h$ , we obtain (note that  $D = 0$ )

$$e^{\frac{\lambda}{2\nu} h(u, t)} = \int_{u'} \frac{e^{\frac{\lambda}{2\nu} \left[ h_0(u') - \frac{(u-u')^2}{2\lambda t} \right]}}{(4\pi\nu t)^{d/2}}. \quad (11.25)$$

It is interesting to consider the limit of  $\nu \rightarrow 0$ , equivalent to  $T \rightarrow 0$  for the directed polymer. Then

$$h(u, t) = \max_{u'} \left[ h_0(u') - \frac{(u-u')^2}{2\lambda t} \right]. \quad (11.26) \quad 1.26$$

This solution is formally equivalent to the solution (5.37) of the toy model introduced in section 5.4, replacing

$$-h_0(u) \rightarrow V(u) \quad (\text{the microscopic disorder}) \quad (11.27)$$

$$\frac{1}{\lambda t} \rightarrow m^2 \quad (11.28)$$

$$-h(u, t) \rightarrow \hat{V}(u) \quad (\text{the effective disorder at scale } m^2 = \frac{1}{\lambda t}). \quad (11.29)$$

As observed there, the function  $h(u, t)$  is composed of almost parabolic pieces. Geometrically, this can be obtained by approaching a parabola of curvature  $1/(\lambda t)$  from the top, and reporting as a function of its center  $u$  the position  $h(u, t)$  at which it first touches the initial condition  $h_0(u)$ .

## 11.5 All-order $\beta$ -function for KPZ

Let us now calculate the  $\beta$ -function associated to the model (11.20)-(11.21), following [105].

The only possible diagrams are chains of  $\curvearrowright$ , of the form  $\curvearrowright\curvearrowright$ ,  $\curvearrowright\curvearrowright\curvearrowright$  and so on or higher order vertices. The latter are irrelevant in perturbation theory. We therefore write

$$e^g \curvearrowright = 1 + g \curvearrowright + g^2 \curvearrowright\curvearrowright + g^3 \curvearrowright\curvearrowright\curvearrowright + g^4 \curvearrowright\curvearrowright\curvearrowright\curvearrowright + \dots + \text{higher order vertices} , \quad (11.30)$$

where the time-argument of the vertices grows from left to right, and each fat point is integrated over. Note that the combinatorial factor of  $\frac{1}{n!}$  which comes from the expansion of the exponential function at order  $g^n$  has canceled against the  $n!$  possibilities to order the vertices in time. In addition, any bubble appears with a combinatorial factor of 2, which cancels against factors of  $1/2$  from the vertex (11.20). So any of the chain diagrams in (11.30) still contains a factor of  $1/2$ .

To proceed further, we first suppress the “higher order vertices” in Eq. (11.30), as the only divergencies they may contain are sub-chains as those depicted in Eq. (11.30), that will be treated here.

Second, we can switch to Fourier-representation, thus regard the diagrams in Eq. (11.30) as a function of the external momentum  $p$  and frequency  $\omega$  instead of the coordinates  $x$  and  $t$ , and finally integrate over  $p$  and  $\omega$  instead of  $x$  and  $t$ . Then, each chain in Eq. (11.30) factorizes, i.e. can be written as product of the vertex  $\curvearrowright$  times a power of the elementary loop diagram (which is a function of  $p$  and  $\omega$ )

$$\xrightarrow{p, \omega} \underbrace{\curvearrowright\curvearrowright\curvearrowright\curvearrowright}_{n \text{ loops}} = (\text{loop}_{p, \omega})^n \curvearrowright . \quad (11.31) \text{fac-prop}$$

Eq. (11.30) is a geometric sum, equivalent to

$$1 + g \frac{1}{1 - g \text{loop}_{p, \omega}} \curvearrowright , \quad (11.32)$$

and one reads off the effective 4-point function

$$\Gamma_{ZZ\bar{Z}\bar{Z}}|_{p, \omega} = g \frac{1}{1 - g \text{loop}_{p, \omega}} . \quad (11.33) \text{eff Gamma 4}$$

As we shall show below, the loop integral in Eq. (11.33) is divergent for any  $p$  and  $\omega$  when  $d \rightarrow 2$ . Renormalisation means to absorb this divergence into a reparametrization of the coupling constant  $g$ : We claim that there is a function  $a = a(d)$ , such that the 4-point function is finite (renormalized) as a function of  $g_R$  instead of  $g$ , when setting

$$g = Z_g g_R \mu^{-\epsilon} \quad (11.34) \text{ren-bare}$$

with

$$Z_g = \frac{1}{1 + a g_R} , \quad \epsilon = d - 2 . \quad (11.35) \text{Zg}$$

$\mu$  is an arbitrary scale, the so-called renormalization scale. As a function of  $g_R$ , the 4-point function reads

$$\Gamma_{ZZ\bar{Z}\bar{Z}}|_{p, \omega} = \frac{g_R \mu^{-\epsilon}}{1 + (a - \mu^{-\epsilon} \text{loop}_{p, \omega}) g_R} . \quad (11.36) \text{Gamma4R}$$

To complete the proof, we have to calculate the elementary diagram,

$$\begin{array}{c} \xrightarrow{p,\omega} \quad \begin{array}{c} \frac{\omega}{2} + \nu, \frac{p}{2} + k \\ \text{---} \text{---} \text{---} \text{---} \text{---} \text{---} \\ \text{---} \text{---} \text{---} \text{---} \text{---} \text{---} \\ \frac{\omega}{2} - \nu, \frac{p}{2} - k \end{array} \quad \xrightarrow{p,\omega} \quad . \end{array} \quad (11.37)$$

This is

$$\int \frac{d^d k}{(2\pi)^d} \int \frac{d\nu}{2\pi} \frac{1}{\left(\frac{p}{2} + k\right)^2 + i\left(\frac{\omega}{2} + \nu\right)} \frac{1}{\left(\frac{p}{2} - k\right)^2 + i\left(\frac{\omega}{2} - \nu\right)}. \quad (11.38)$$

To perform the integration over  $\nu$ , the integration path can be closed either in the upper or lower half-plane. Closing it in the upper half-plane, we obtain:

$$\begin{aligned} \int \frac{d^d k}{(2\pi)^d} \frac{1}{\left(k + \frac{p}{2}\right)^2 + \left(k - \frac{p}{2}\right)^2 + i\omega} &= \int_0^\infty ds \int \frac{d^d k}{(2\pi)^d} e^{-s(2k^2 + \frac{1}{2}p^2 + i\omega)} \\ &= \frac{1}{(8\pi)^{d/2}} \int_0^\infty ds s^{-d/2} e^{-s(\frac{1}{2}p^2 + i\omega)} \\ &= \frac{1}{(8\pi)^{d/2}} \left(\frac{1}{2}p^2 + i\omega\right)^{d/2-1} \Gamma\left(1 - \frac{d}{2}\right). \end{aligned} \quad (11.39)$$

The 4-point function in Eq. (11.36) therefore depends on  $p$  and  $\omega$ , and more specifically on the combination  $\frac{1}{2}p^2 + i\omega$ . We now chose a subtraction scale, i.e. we demand that  $\Gamma_{ZZ\bar{Z}\bar{Z}}$  evaluated at  $\mu^2 = \frac{1}{2}p^2 + i\omega$  be

$$\Gamma_{ZZ\bar{Z}\bar{Z}} \Big|_{\frac{1}{2}p^2 + i\omega = \mu^2} = g_R. \quad (11.40)$$

This is achieved by setting

$$a = \frac{1}{(8\pi)^{d/2}} \Gamma\left(1 - \frac{d}{2}\right) \equiv \frac{2}{(8\pi)^{d/2}} \Gamma\left(2 - \frac{d}{2}\right) \frac{1}{\epsilon}. \quad (11.41)$$

Moreover, since

$$\frac{1}{\epsilon} \left(\frac{1}{2}p^2 + i\omega\right)^{d/2-1} \mu^{-\epsilon} \quad (11.42)$$

is finite in the limit  $\epsilon \rightarrow 0$  as long as the combination  $\frac{1}{2}p^2 + i\omega$  is finite, it can be read off from Eq. (11.36) that also  $\Gamma_{ZZ\bar{Z}\bar{Z}} \Big|_{p,\omega}$  is finite. (If useful, either  $p = 0$  or  $\omega = 0$  may safely be taken.) This completes the proof. Note that this ensures that the model is renormalizable to all orders in perturbation-theory, what is normally a formidable task to show [106].

The  $\beta$ -function that we shall calculate now is exact to all orders in perturbation theory. As usual, it is defined as the variation of the renormalized coupling constant, keeping the bare one fixed

$$\beta(g_R) = \mu \frac{\partial}{\partial \mu} \Big|_g g_R. \quad (11.43)$$

From Eq. (11.40) we see that it gives the dependence of the 4-point function on  $p$  and  $\omega$  for fixed bare coupling. Solving

$$g = \frac{g_R \mu^{-\epsilon}}{1 + a g_R} \quad (11.44)$$

for  $g_R$ , we obtain

$$g_R = \frac{g}{\mu^{-\epsilon} - a g}, \quad (11.45)$$

and hence

$$\beta(g_R) = \epsilon g_R(1 + a g_R). \quad (11.46)$$

Using  $a$  from Eq. (11.41), our final result is

$$\beta(g_R) = (d - 2)g_R - \frac{2}{(8\pi)^{d/2}}\Gamma\left(2 - \frac{d}{2}\right)g_R^2. \quad (11.47)\text{final result}$$

## 11.6 Failure of the all-order $\beta$ -function for KPZ, and relation to FRG

### 11.7 Quenched KPZ

### 11.8 The Carroro-Duchon equations

[74]

## 12 Passive advection and multiscaling

## 13 Non-equilibrium

# Appendices

## A Higher-loop calculations

### A.1 Basics

If one wants to go to order  $\epsilon^n$ , one needs (in general) to calculate all diagrams up to  $n$ -loop order. For this you need the leading  $n$  terms in the  $\epsilon$ -expansion of each diagram. To 1-loop order, this will be

$$\frac{1}{\epsilon}, \quad \epsilon^0, \quad \dots, \epsilon^{n-2}$$

up to an  $n$ -loop integral,

$$\frac{1}{\epsilon^n}, \quad \frac{1}{\epsilon^{n-1}}, \quad \dots, \frac{1}{\epsilon}$$

It is a basic error to retain from 1-loop diagrams only the leading  $1\epsilon$ -contribution, arguing that this is enough in the so-called minimal-subtraction scheme. This does not take into account that in minimal subtraction 2-loop diagrams are given with the pole-part of the 1-loop diagrams subtracted. Thus modifying e.g. normalizations in an  $\epsilon$ -dependent way will change the pole part of the 2-loop terms, and in particular those of the repeated 1-loop terms.

### A.2 1 loop in momentum space

The integral  $I_1$  is defined as

$$I_1 \equiv \text{---} \text{---} \text{---} := \int_k \frac{1}{(k^2 + m^2)^2} \quad (\text{A.1})_{1\text{-bis}}$$

It is calculated as follows:

$$I_1 = \int_k \int_0^\infty d\alpha \alpha e^{-\alpha(k^2+m^2)} = \left( \int_k e^{-k^2} \right) \int_0^\infty d\alpha \alpha^{1-\frac{d}{2}} e^{-\alpha m^2} = \left( \int_k e^{-k^2} \right) m^{-\epsilon} \Gamma\left(\frac{\epsilon}{2}\right). \quad (\text{A.2})_{f14}$$

The key trick employed here is to express the denominator by an integral over a parameter  $\alpha$ , known as  $\alpha$ -parametrization, or Schwinger representation. Its strong point is that the  $k$ -integrals can easily be done in any non-integer dimension  $d$ . For later convenience, define

$$\mathcal{N}_d := \int_k e^{-k^2} \equiv \int \frac{d^d k}{(2\pi)^d} e^{-k^2} = \frac{1}{(4\pi)^{d/2}}. \quad (\text{A.3})$$

This factor cancels in loop calculations which only depend on the ratio of diagrams, with an equal number of integrations. As we are free to choose our normalization, we can decide to absorb the non-singular factor

$$\epsilon I_1 = \mathcal{N}_d \epsilon \Gamma\left(\frac{\epsilon}{2}\right) m^{-\epsilon} = 2 \mathcal{N}_d \Gamma\left(1 + \frac{\epsilon}{2}\right) m^{-\epsilon} \quad (\text{A.4})_{1\text{-cis}}$$

into a redefinition of the integration measure (in  $k$ ) or the coupling constant. We can further evaluate all diagrams at  $m = 1$ , restoring if necessary the  $m$ -dependence at the end from power counting.

### A.3 1 loop in position space

We repeat the formulas given in Eq. (1.11) for a massless propagator.

$$C(x-y) := \langle \phi(x)\phi(y) \rangle_0 = \mathcal{C}_1 |x-y|^{2-d}, \quad \mathcal{C}_1 = \frac{1}{S_d(d-2)}, \quad S_d = \frac{2\pi^{d/2}}{\Gamma(d/2)}. \quad (\text{A.5})_{m:\text{cor2-bis}}$$



Then

$$I_1 \equiv \text{---} \simeq \mathcal{C}_1^2 S_d \int_a^L \frac{dx}{x} x^{4-d} = \mathcal{C}_1^2 S_d \frac{1}{\epsilon} (L^\epsilon - a^\epsilon) \quad (\text{A.6})_{1\text{-ps}}$$

One checks that

$$\frac{\mathcal{C}_1^2 S_d \frac{1}{\epsilon}}{\mathcal{N}_d \Gamma(\frac{\epsilon}{2})} = 1 + \epsilon \left( \log(2) - \frac{1}{2} - \gamma_E \right) + \mathcal{O}(\epsilon^2). \quad (\text{A.7})$$

## A.4 2 loops

Among the many techniques to evaluate higher-loop diagrams, let us introduce a very innocently looking, but useful one, namely

$$\frac{1}{k^2 + 1} = \frac{1}{k^2} - \frac{1}{k^2(k^2 + 1)}. \quad (\text{A.8})$$

The idea is that integrals over the massless propagator can be performed analytically, whereas the remaining integral is convergent, and can therefore be evaluated in the critical dimension. This decomposition is an art. Applied to our integral, it gives

$$\text{---} = \int_{k_1, k_2} \frac{1}{(1 + k_1^2)(1 + k_2^2)[1 + (k_1 + k_2)^2]^2} = J_1 - J_2 - J'_2 + J_3 \quad (\text{A.9})$$

$$J_1 = \int_{k_1, k_2} \frac{1}{k_1^2 k_2^2 [1 + (k_1 + k_2)^2]^2} \quad (\text{A.10})$$

$$J_2 = \int_{k_1, k_2} \frac{1}{k_1^2 (1 + k_1^2) k_2^2 [1 + (k_1 + k_2)^2]^2} \quad (\text{A.11})$$

$$J'_2 = \int_{k_1, k_2} \frac{1}{k_1^2 (1 + k_2^2) k_2^2 [1 + (k_1 + k_2)^2]^2} \quad (\text{A.12})$$

$$J_3 = \int_{k_1, k_2} \frac{1}{k_1^2 (1 + k_1^2) k_2^2 (1 + k_2^2) [1 + (k_1 + k_2)^2]^2}. \quad (\text{A.13})$$

We now calculate term by term,

$$\begin{aligned} J_1 &= \int_{k_1, k_2} \frac{1}{k_1^2 k_2^2 [1 + (k_1 + k_2)^2]^2} \\ &= \int_{k_1, k_2} \int_{\alpha_1, \alpha_2, \alpha_3 > 0} \alpha_1 e^{-\alpha_1[(k_1 + k_2)^2 + 1] - \alpha_2 k_1^2 - \alpha_3 k_2^2} \\ &= \mathcal{N}_d^2 \int_{\alpha_1, \alpha_2, \alpha_3 > 0} \alpha_1 \left[ \det \begin{pmatrix} \alpha_1 + \alpha_2 & \alpha_1 \\ \alpha_1 & \alpha_1 + \alpha_3 \end{pmatrix} \right]^{-d/2} \end{aligned} \quad (\text{A.14})$$

The integrals over  $\alpha_2$  and  $\alpha_3$  can be performed, and one obtains

$$J_1 = \mathcal{N}_d^2 \int_{\alpha_1 > 0} e^{-\alpha_1} \alpha_1^{3-d} \frac{2\pi}{(2-d)\sin(\frac{\pi d}{2})} = \mathcal{N}_d^2 \frac{2\pi \Gamma(\epsilon)}{(2-\epsilon)\sin(\frac{\pi \epsilon}{2})} \quad (\text{A.15})$$

This yields

$$\frac{J_1}{(\epsilon I_1)^2} = \frac{\Gamma(1 - \frac{\epsilon}{2}) \Gamma(\epsilon + 1)}{(2-\epsilon)\epsilon^2 \Gamma(\frac{\epsilon}{2} + 1)} = \frac{1}{2\epsilon^2} + \frac{1}{4\epsilon} + \frac{3 + \pi^2}{24} + \mathcal{O}(\epsilon) \quad (\text{A.16})$$

We used

$$\Gamma(x)\Gamma(1-x) = \frac{\pi}{\sin(\pi x)}. \quad (\text{A.17})_{\text{gamma-rule}}$$

Integrals  $J_2 = J'_2$  and  $J_3$  are convergent. If we only want to go to 2-loop order, we can neglect them. If we want to go further, we have to evaluate them: Using the same parametrization, and integrating first over those  $\alpha$ -parameters associated to massless propagators, we obtain after some sweating and simplifications

$$\begin{aligned}
J_2 = J'_2 &= \mathcal{N}_d^2 \int_{\alpha_1, \alpha_2, \alpha_3, \alpha_4 > 0} \frac{e^{-\alpha_1 - \alpha_4} \alpha_1}{[\alpha_3(\alpha_2 + \alpha_4) + \alpha_1(\alpha_2 + \alpha_3 + \alpha_4)]^{d/2}} \\
&= \left[ \frac{\pi^2}{24} + \mathcal{O}(\epsilon) \right] (\epsilon I_1)^2, \tag{A.18}
\end{aligned}$$

$$\begin{aligned}
J_3 &= \mathcal{N}_d^2 \int_{\alpha_1, \alpha_2, \alpha_3, \alpha_4, \alpha_5 > 0} \frac{e^{-\alpha_1 - \alpha_4 - \alpha_5} \alpha_1}{[(\alpha_2 + \alpha_4)(\alpha_3 + \alpha_5) + \alpha_1(\alpha_2 + \alpha_3 + \alpha_4 + \alpha_5)]^{d/2}} \\
&= \left[ \frac{5\pi^2 - 3\psi'(\frac{1}{3}) + 3\psi'(\frac{5}{6})}{216} + \mathcal{O}(\epsilon) \right] (\epsilon I_1)^2. \tag{A.19}
\end{aligned}$$

Here  $\psi(x) := \Gamma'(x)/\Gamma(x)$ , and we used that there are relations for  $\psi(x)$  and  $\psi(1-x)$ , obtained by taking a derivative of Eq. (A.17). Combining all terms we obtain

$$\frac{\text{triangle diagram}}{[\text{bubble diagram}]^2} = \frac{J_1 - J_2 - J'_2 + J_3}{(\epsilon I_1)^2} = \frac{1}{2\epsilon^2} + \frac{1}{4\epsilon} + \frac{-4\pi^2 + 27 - 3\psi'(\frac{1}{3}) + 3\psi'(\frac{5}{6})}{216} + \mathcal{O}(\epsilon). \tag{A.20}$$

## A.5 Nested divergences, and geometrical factors

In the last section, we showed that

$$\text{triangle diagram} = \frac{1}{2} [\text{bubble diagram}]^2 + \mathcal{O}(\frac{1}{\epsilon}) \tag{A.21}$$

The factor of  $\frac{1}{2}$  is not an accident, but of geometric origin. Without this precise factor, the theory would not be renormalizable. Let us give two motivations of this term. We first do this in momentum space: For this, we realize that if there is a momentum  $p$  running through, then at large momenta ( $\epsilon = 4 - d > 0$ )

$$\begin{aligned}
\frac{p \rightarrow \text{triangle diagram} \rightarrow p}{[\text{bubble diagram}]^2} &= S_d \int \frac{d^d k}{(2\pi)^d} \frac{1}{[(k + p/2)^2 + m^2][(k - p/2)^2 + m^2]} \\
&\simeq \frac{S_d}{(2\pi)^d} \int_0^\infty \frac{dk}{k} \frac{k^d}{(k^2 + m^2)^2} \times \left(\frac{m}{p}\right)^\epsilon \\
&\simeq \frac{S_d}{(2\pi)^d} \int_m^\infty \frac{dk}{k} \frac{k^d}{k^4} \times \left(\frac{m}{p}\right)^\epsilon \\
&= \frac{S_d}{(2\pi)^d} \frac{m^{-\epsilon}}{\epsilon} \times \left(\frac{m}{p}\right)^\epsilon \simeq \text{bubble diagram} \times \left(\frac{m}{p}\right)^\epsilon \tag{A.22}
\end{aligned}$$

Inserting this into the already calculated diagram, and using the same chain of approximations yields

$$\begin{aligned}
\text{triangle diagram} &\simeq \frac{S_d}{(2\pi)^d} \frac{m^{-\epsilon}}{\epsilon} \times \frac{S_d}{(2\pi)^d} \int_m^\infty \frac{dp}{p} \frac{p^d}{p^4} \times \left(\frac{m}{p}\right)^\epsilon \\
&= \frac{S_d}{(2\pi)^d} \frac{m^{-\epsilon}}{\epsilon} \times \frac{S_d}{(2\pi)^d} \frac{m^{-\epsilon}}{2\epsilon} \\
&\simeq \frac{1}{2} [\text{bubble diagram}]^2 \tag{A.23}
\end{aligned}$$

This factor of  $\frac{1}{2}$  can be understood geometrically: The sub-divergence appears only when the momentum running inside the lower loop is larger than the remaining momentum. A similar argument can be done in position space.

### Exercise 19: Geometrical factors for subdivergences

Show that the geometrical factor of  $1/2$  can also be understood in position space. Use a cutoff  $L$  for all distances appearing in the diagram.

## A.6 The diagram correcting friction in model A

Setting  $m = 1$ , the diagram (3.65) is

$$x,t \text{ --- } \text{---} y,t' = \int_{k_1, k_2} \frac{1}{k_1^2 + 1} \frac{1}{k_2^2 + 1} \frac{1}{(k_1 + k_2)^2 + 1} \frac{1}{k_1^2 + k_2^2 + (k_1 + k_2)^2 + 3} \quad (\text{A.24})$$

Going to the Schwinger representation yields

$$x,t \text{ --- } \text{---} y,t' = \mathcal{N}_d^2 \int_{s_1, s_2, s_3, s_4 > 0} e^{-s_1 - s_2 - s_3 - s_4} [(s_1 + s_3 + 2s_4)(s_2 + s_3 + 2s_4) - (s_3 + s_4)^2]^{-d/2}. \quad (\text{A.25})$$

Replacing  $s_i \rightarrow s_i s_1$  for all  $i > 1$  allows to isolate the pole in the  $s_1$  integration. The remaining integrals are finite, and can be evaluated to leading order in  $d = 4$ , resulting in

$$\begin{aligned} \frac{x,t \text{ --- } \text{---} y,t'}{[\epsilon \text{ --- } \text{---}]^2} &= \frac{1}{4\epsilon} \int_{s_1, s_2, s_3, s_4 > 0} \frac{1}{(3s_4^2 + 2(s_2 + s_3 + 1)s_4 + s_2 + s_2s_3 + s_3)^2} + \mathcal{O}(\epsilon^0) \\ &= \frac{3}{4\epsilon} \log\left(\frac{4}{3}\right) + \mathcal{O}(\epsilon^0) \end{aligned} \quad (\text{A.26})$$

## A.7 3 loops: an example

Calculate Mercedes-star diagram at 3-loop order. This integral has no subdivergences, thus should be order  $1/\epsilon$ .

$$\begin{aligned} \text{---} \text{---} \text{---} &= \int_{k,p,q} \frac{1}{k^2 + 1} \frac{1}{p^2 + 1} \frac{1}{q^2 + 1} \frac{1}{(k-p)^2 + 1} \frac{1}{(p-q)^2 + 1} \frac{1}{(q-k)^2 + 1} \\ &= \int_{k,p,q} \int_{\alpha_1, \alpha_2, \dots, \alpha_6 > 0} e^{-\alpha_1(k^2+1) - \alpha_2(p^2+1) - \alpha_3(q^2+1) - \alpha_4((k-p)^2+1) - \alpha_5((p-q)^2+1) - \alpha_6((q-k)^2+1)} \\ &= \left[ \int_k e^{-k^2} \right]^3 \int_{\alpha_1, \alpha_2, \dots, \alpha_6 > 0} e^{-\sum_{i=1}^6 \alpha_i} \det \begin{pmatrix} \alpha_1 + \alpha_4 + \alpha_6 & -\alpha_4 & -\alpha_6 \\ -\alpha_4 & \alpha_2 + \alpha_4 + \alpha_5 & -\alpha_5 \\ -\alpha_6 & -\alpha_5 & \alpha_3 + \alpha_5 + \alpha_6 \end{pmatrix}^{-d/2} \end{aligned} \quad (\text{A.27})$$

Replacing for  $i > 1$ ,  $\alpha_i \rightarrow \alpha_i \alpha_1$  yields

$$\begin{aligned} &\int_{\alpha_1, \alpha_2, \dots, \alpha_6 > 0} e^{-\sum_{i=1}^6 \alpha_i} \det \begin{pmatrix} \alpha_1 + \alpha_4 + \alpha_6 & -\alpha_4 & -\alpha_6 \\ -\alpha_4 & \alpha_2 + \alpha_4 + \alpha_5 & -\alpha_5 \\ -\alpha_6 & -\alpha_5 & \alpha_3 + \alpha_5 + \alpha_6 \end{pmatrix}^{-d/2} \\ &= \int_{\alpha_1, \alpha_2, \dots, \alpha_6 > 0} e^{-\alpha_1(1 + \sum_{i=2}^6 \alpha_i)} \alpha_1^{5-3d/2} \det \begin{pmatrix} 1 + \alpha_4 + \alpha_6 & -\alpha_4 & -\alpha_6 \\ -\alpha_4 & \alpha_2 + \alpha_4 + \alpha_5 & -\alpha_5 \\ -\alpha_6 & -\alpha_5 & \alpha_3 + \alpha_5 + \alpha_6 \end{pmatrix}^{-d/2} \end{aligned} \quad (\text{A.28})$$

Now we can extract the divergence in  $1/\epsilon$ ,

$$\begin{aligned} \int_0^\infty d\alpha_1 e^{-\alpha_1(1+\sum_{i=2}^6 \alpha_i)} \alpha_1^{5-\frac{3d}{2}} &= \Gamma\left(6 - \frac{3d}{2}\right) \left(1 + \sum_{i=2}^6 \alpha_i\right)^{\frac{3d}{2}-6} \\ &= \Gamma\left(\frac{3\epsilon}{2}\right) \left(1 + \sum_{i=2}^6 \alpha_i\right)^{-\frac{3\epsilon}{2}} = \frac{2}{3\epsilon} [1 + \mathcal{O}(\epsilon)] \end{aligned} \quad (\text{A.29})$$

So if the remaining integrals are finite, we can calculate them in  $d = 4$ . This proceeds as follows:

$$\begin{aligned} &\int_{\alpha_2, \dots, \alpha_6 > 0} \det \begin{pmatrix} 1 + \alpha_4 + \alpha_6 & -\alpha_4 & -\alpha_6 \\ -\alpha_4 & \alpha_2 + \alpha_4 + \alpha_5 & -\alpha_5 \\ -\alpha_6 & -\alpha_5 & \alpha_3 + \alpha_5 + \alpha_6 \end{pmatrix}^{-2} \\ &= \int_{\alpha_2, \dots, \alpha_6 > 0} \left[ \alpha_2 \alpha_3 + \alpha_2 \alpha_4 \alpha_3 + \alpha_4 \alpha_3 + \alpha_4 \alpha_5 \alpha_3 + \alpha_5 \alpha_3 + \alpha_2 \alpha_6 \alpha_3 + \alpha_4 \alpha_6 \alpha_3 + \alpha_5 \alpha_6 \alpha_3 \right. \\ &\quad \left. + \alpha_2 \alpha_5 + \alpha_2 \alpha_4 \alpha_5 + \alpha_4 \alpha_5 + \alpha_2 \alpha_6 + \alpha_2 \alpha_4 \alpha_6 + \alpha_4 \alpha_6 + \alpha_2 \alpha_5 \alpha_6 + \alpha_5 \alpha_6 \right]^{-2} \\ &= \int_{\alpha_2, \alpha_3, \alpha_4, \alpha_6 > 0} \left[ \alpha_4 \alpha_2 + \alpha_6 \alpha_2 + \alpha_2 + \alpha_3 + \alpha_3 \alpha_4 + \alpha_4 + \alpha_3 \alpha_6 + \alpha_6 \right]^{-1} \\ &\quad \times \left[ \alpha_2 \alpha_3 + \alpha_2 \alpha_4 \alpha_3 + \alpha_4 \alpha_3 + \alpha_2 \alpha_6 \alpha_3 + \alpha_4 \alpha_6 \alpha_3 + \alpha_2 \alpha_6 + \alpha_2 \alpha_4 \alpha_6 + \alpha_4 \alpha_6 \right]^{-1} \\ &= \int_{\alpha_3, \alpha_4, \alpha_6 > 0} \frac{1}{(\alpha_4 \alpha_3 + \alpha_6 \alpha_3 + \alpha_3 + \alpha_6)^2} \times \left[ \ln(\alpha_4 \alpha_3 + \alpha_6 \alpha_3 + \alpha_3 + \alpha_4 + \alpha_6) - \ln(\alpha_4 + \alpha_6 + 1) \right. \\ &\quad \left. + \ln(\alpha_4 \alpha_3 + \alpha_6 \alpha_3 + \alpha_3 + \alpha_4 \alpha_6 + \alpha_6) - \ln(\alpha_4) - \ln(\alpha_6 \alpha_3 + \alpha_3 + \alpha_6) \right] \\ &= \int_{\alpha_4, \alpha_6 > 0} \frac{\ln\left(\frac{(\alpha_4+1)(\alpha_6+1)}{\alpha_4 + \alpha_6 + 1}\right)}{\alpha_4 \alpha_6 (\alpha_4 + \alpha_6 + 1)} + \frac{\ln\left(\frac{(\alpha_6+1)(\alpha_4 + \alpha_6)}{\alpha_6(\alpha_4 + \alpha_6 + 1)}\right)}{\alpha_4 (\alpha_4 + \alpha_6 + 1)} + \frac{\ln\left(\frac{(\alpha_4+1)(\alpha_4 + \alpha_6)}{\alpha_4(\alpha_4 + \alpha_6 + 1)}\right)}{\alpha_6 (\alpha_4 + \alpha_6 + 1)} \\ &= \int_{\alpha_4 > 0} \frac{\text{Li}_2(-\alpha_4) - \text{Li}_2(-\frac{1}{\alpha_4})}{\alpha_4 + 1} + \frac{3 \ln^2(\alpha_4) + 6 \ln(\frac{1}{\alpha_4} + 1) \ln(\alpha_4 + 1) + 6 \text{Li}_2(-\frac{1}{\alpha_4}) + \pi^2}{6\alpha_4} \\ &= 6\zeta(3) \end{aligned} \quad (\text{A.30})$$

In units of the 1-loop diagram, this reads

$$\frac{\text{Diagram}}{[\epsilon \text{Diagram}]^3} = \frac{\zeta(3)}{2\epsilon} + \mathcal{O}(\epsilon). \quad (\text{A.31})$$


## B Supersymmetry techniques

### B.1 Basic rules for manipulating Grassmann variables

Grassmann variables are anticommuting variables which allow one to write a path-integral for bosons, in the same way as one does for bosons. There are only few rules to remember. If  $\chi$  and  $\psi$  are Grassmann variables, then

$$\chi \psi = -\psi \chi. \quad (\text{B.1})$$

This immediately implies that

$$\chi^2 = 0 . \quad (\text{B.2})$$

One introduces derivatives, and integrals through the same formula,

$$\int d\chi \chi \equiv \frac{d}{d\chi} \chi = 1 . \quad (\text{B.3})$$

One checks that they satisfy the usual properties associated to “normal” derivatives, and integrals.

### Exercise 20: Check for Jacobians in multidimensional integrals.

An important property is

$$\int d\bar{\chi} d\chi e^{-a\bar{\chi}\chi} = a . \quad (\text{B.4})$$

This is easily proven upon Taylor expansion. The minus sign in the exponential cancels with the minus sign obtained when exchanging  $\bar{\chi}$  with  $\chi$ , which is necessary since an integral or derivative is defined to act directly on the variable following it. This can be generalized to integrals over an  $n$ -component pair of vectors  $\vec{\bar{\chi}}$ , and  $\vec{\chi}$ :

$$\int d\vec{\bar{\chi}} d\vec{\chi} e^{-\vec{\bar{\chi}}\mathbb{A}\vec{\chi}} := \prod_{a=1}^n \int d\bar{\chi}^a d\chi^a e^{-\bar{\chi}^a \mathbb{A} \chi^a} = \det(\mathbb{A}) . \quad (\text{B.5})$$

It is proven by changing coordinates s.t.  $\mathbb{A}$  becomes diagonal. For comparison we give the corresponding formula for normal (bosonic) fields, noting  $\phi^a := \phi_x^a + i\phi_y^a$ ,  $\tilde{\phi}^a := \phi_x^a - i\phi_y^a$ ,

$$\int d\vec{\tilde{\phi}} d\vec{\phi} e^{-\vec{\tilde{\phi}}\mathbb{A}\vec{\phi}} := \prod_{a=1}^n \int \frac{d\phi_x^a d\phi_y^a}{\pi} e^{-\tilde{\phi}^a \mathbb{A} \phi^a} = \frac{1}{\det(\mathbb{A})} . \quad (\text{B.6})$$

Interestingly, when combining normal and Grassmanian integrals over the same number of variables into a product, the results of (B.5) and (B.6) cancel. This will be used below.

## B.2 Disorder averages with bosons and fermions

Another way to average over disorder is to use additional fermionic degrees of freedom. It is more commonly referred to as the supersymmetric method.

For concreteness, define

$$\mathcal{H}[u, V] = \int_x \frac{1}{2} [\nabla u(x)]^2 + \frac{m^2}{2} u(x)^2 + \mathcal{U}(u(x)) + V(x, u(x)) . \quad (\text{B.7})$$

Then the disorder-average of an observable is defined as

$$\overline{\mathcal{O}[u]} := \frac{\int \prod_{a=1}^r \mathcal{D}[u_a] \mathcal{O}[u_1] e^{-\frac{1}{T} \mathcal{H}[u_a, j_a, V]}}{\int \prod_{a=1}^r \mathcal{D}[u_a] e^{-\frac{1}{T} \mathcal{H}[u_a, 0, V]}} . \quad (\text{B.8})$$

The function  $\mathcal{U}(u)$  is an arbitrary potential, e.g. the non-linearity in Eq. (1.1),  $V(u) = g u^4$ . The random potential  $V(x, u)$  is as in section 4.2 given by Eq. (4.7). Its average is indicated by the overline. Remind

that the difficulty in evaluating (B.8) comes from the denominator. The replica trick used in section 4.4 allowed us to set  $r = 0$ , thus discarding the denominator. Here we follow a different strategy.

In the limit of  $T \rightarrow 0$  only configurations which minimize the energy survive; these configurations satisfy  $\frac{\delta \mathcal{H}[u_a, V]}{\delta u_a(x)} = 0$ , of which we want to insert a  $\delta$ -distribution into the path-integral. This has to be accompanied by a factor of  $\det \left[ \frac{\delta^2 \mathcal{H}[u_a, V]}{\delta u_a(x) \delta u_a(y)} \right]$ , such that the integral over this configuration is normalized to 1. This can be achieved by an additional integral over Grassmann variables, i.e. fermionic degrees of freedom, using that

$$\det \left[ \frac{\delta^2 \mathcal{H}[u, V]}{\delta u(x) \delta u(y)} \right] = \int \mathcal{D}[\bar{\psi}_a] \mathcal{D}[\psi_a] \exp \left( - \int_x \bar{\psi}(x) \frac{\delta^2 \mathcal{H}[u, V]}{\delta u(x) \delta u(y)} \psi(x) \right) \quad (\text{B.9})$$

This allows one to write the disorder average of any observable  $\mathcal{O}[u]$  as

$$\overline{\mathcal{O}[u]} = \int \prod_{a=1}^r \mathcal{D}[\tilde{u}_a] \mathcal{D}[u_a] \mathcal{D}[\bar{\psi}_a] \mathcal{D}[\psi_a] \mathcal{O}[u] \exp \left[ - \int_x \tilde{u}_a(x) \frac{\delta \mathcal{H}[u_a]}{\delta u_a(x)} + \bar{\psi}_a(x) \frac{\delta^2 \mathcal{H}[u_a]}{\delta u_a(x) \delta u_a(y)} \psi_a(y) \right]. \quad (\text{B.10})$$

This method was first introduced in [107, 108]. **\*\*\*talk about problems, failures, caveats.\*\*\***

Averaging over disorder yields with the force-force correlator  $\Delta(u) := -R''(u)$

$$\begin{aligned} \overline{\mathcal{O}[u]} &= \int \prod_a \mathcal{D}[u_a] \mathcal{D}[\tilde{u}_a] \mathcal{D}[\bar{\psi}_a] \mathcal{D}[\psi_a] \exp(-\mathcal{S}[u_a, \tilde{u}_a, \bar{\psi}_a, \psi_a]) \\ \mathcal{S}[\tilde{u}_a, u_a, \bar{\psi}_a, \psi_a] &= \int_x \sum_{a=1}^r \tilde{u}_a(x) \left[ (-\nabla^2 + m^2) u_a(x) + \mathcal{U}'(u_a(x)) \right] + \bar{\psi}_a(x) \left[ -\nabla^2 + m^2 + \mathcal{U}''(u_a(x)) \right] \psi_a(x) \\ &\quad - \sum_{a,b=1}^r \left[ \frac{1}{2} \tilde{u}_a(x) \Delta(u_a(x) - u_b(x)) \tilde{u}_b(x) - \tilde{u}_a(x) \Delta'(u_a(x) - u_b(x)) \bar{\psi}_b(x) \psi_b(x) \right. \\ &\quad \left. - \frac{1}{2} \bar{\psi}_a(x) \psi_a(x) \Delta''(u_a(x) - u_b(x)) \bar{\psi}_b(x) \psi_b(x) \right]. \end{aligned} \quad (\text{B.11})$$

We first analyze  $n = 1$ . Suppose that  $\Delta(u)$  is even and analytic to start with, then only the following terms survive from (B.11)

$$\begin{aligned} \mathcal{S}_{\text{Susy}}[u, \tilde{u}, \bar{\psi}, \psi] &= \int_x \tilde{u}(x) \left[ (-\nabla^2 + m^2) u(x) + \mathcal{U}'(u(x)) \right] + \bar{\psi}(x) \left[ -\nabla^2 + m^2 + \mathcal{U}''(u(x)) \right] \psi(x) \\ &\quad - \frac{1}{2} \tilde{u}(x) \Delta(0) \tilde{u}(x). \end{aligned} \quad (\text{B.12})$$

(We have used that  $\bar{\psi}_a^2 = \psi_a^2 = 0$  to eliminate the 4-fermion-term.) A particularly simple case are random manifolds, for which  $\mathcal{U}(u) = 0$ . Then “bosons”  $\tilde{u}$  and  $u$ , and “fermions”  $\bar{\psi}$  and  $\psi$  live apart from each other, all expectation values are trivially Gaussian, and dimensional reduction holds. When  $\mathcal{U}(u) \neq 0$ , things are more complicated, but as we will see in the next section, dimensional reduction still holds, at least formally.

The reason behind is that the action (B.12) possesses an apparent supersymmetry, which is most manifest when grouping terms together into a superfield

$$\Phi(x, \bar{\Theta}, \Theta) = u(x) + \bar{\Theta} \psi(x) + \bar{\psi}(x) \Theta - \bar{\Theta} \Theta \tilde{u}(x). \quad (\text{B.13})$$

The action (B.12) can then be written with the super Laplacian  $\Delta_s$  as

$$\mathcal{S}_{\text{Susy}} = \int d\bar{\Theta}d\Theta \int_x \frac{1}{2} \Phi(x, \bar{\Theta}, \Theta) (-\Delta_s + m^2) \Phi(x, \bar{\Theta}, \Theta) + \mathcal{U}(\Phi(x, \bar{\Theta}, \Theta)), \quad (\text{B.14})$$

$$\Delta_s := \nabla^2 + \Delta(0) \frac{\partial}{\partial \Theta} \frac{\partial}{\partial \bar{\Theta}}. \quad (\text{B.15})$$

As we will see in section B.4, the action is invariant under the action of two supergenerators

$$Q := x \frac{\partial}{\partial \Theta} - \frac{2}{\Delta(0)} \bar{\Theta} \nabla, \quad \bar{Q} := x \frac{\partial}{\partial \bar{\Theta}} + \frac{2}{\Delta(0)} \Theta \nabla, \quad \{Q, \bar{Q}\} = 0. \quad (\text{B.16})$$

This is sufficient to “prove” dimensional reduction.

### B.3 Recovering the renormalization of the disorder

For more than  $r = 1$  replicas, the theory is richer, and we can recover the renormalization of  $\Delta(u)$  itself. To this purpose set  $\mathcal{U}(u) = 0$ , and write

$$\begin{aligned} \mathcal{S}[\tilde{u}_a, u_a, \bar{\psi}_a, \psi_a] &= \sum_a \int_x \tilde{u}_a(x) (-\nabla^2 + m^2) u_a(x) + \bar{\psi}_a(x) (-\nabla^2 + m^2) \psi_a(x) - \frac{1}{2} \tilde{u}_a(x) \Delta(0) \tilde{u}_a(x) \\ &\quad - \sum_{a \neq b} \int_x \left[ \frac{1}{2} \tilde{u}_a(x) \Delta(u_a(x) - u_b(x)) \tilde{u}_b(x) - \tilde{u}_a(x) \Delta'(u_a(x) - u_b(x)) \bar{\psi}_b(x) \psi_b(x) \right. \\ &\quad \left. - \frac{1}{2} \bar{\psi}_a(x) \psi_a(x) \Delta''(u_a(x) - u_b(x)) \bar{\psi}_b(x) \psi_b(x) \right]. \end{aligned} \quad (\text{B.17})$$

Corrections to  $\Delta(u)$  are easily constructed by remarking that the interaction term quadratic in  $\tilde{u}$  is almost identical to the treatment of the dynamics in the static limit (i.e. after integration over times). The diagrams in question are

$$\text{Diagram 1} + \text{Diagram 2} + \text{Diagram 3} + \text{Diagram 4}, \quad (\text{B.18})$$

where an arrow indicates the correlation-function,  $x \rightarrow y = \langle \tilde{u}(x) u(y) \rangle = C(x - y)$ . This leads to (in the order given above)

$$\delta\Delta(u) = [-\Delta(u)\Delta''(u) - \Delta'(u)^2 + \Delta''(u)\Delta(0)] \int_{x-y} C(x - y)^2. \quad (\text{B.19})$$

where the last term (being odd) vanishes. This should be compared to the results of Eqs. (6.16)–(6.24).

A non-trivial ingredient is the cancellation of the acausal loop (6.25) in the dynamics, equivalent to the 3-replica term in the statics. This is provided by taking two terms proportional to  $\tilde{u}_a \Delta'(u_a - u_b) \bar{\psi}_b \psi_b$ , and contracting all fermions:

$$\text{Diagram 1} + \text{Diagram 2} = 0, \quad (\text{B.20})$$

since the fermionic loop (oriented wiggly line in the second diagram) contributes a factor of  $-1$ .

One can treat the interacting theory completely in a superspace formulation. The action is

$$\begin{aligned} \mathcal{S}[\Phi] &= \sum_a \int_{\bar{\Theta}, \Theta} \int_x \frac{1}{2} \Phi_a(x, \bar{\Theta}, \Theta) (-\Delta_s + m^2) \Phi_a(x, \bar{\Theta}, \Theta) \\ &\quad - \frac{1}{2} \sum_{a \neq b} \int_x \int_{\bar{\Theta}, \Theta} \int_{\bar{\Theta}', \Theta'} R(\Phi_a(x, \bar{\Theta}, \Theta) - \Phi_b(x, \bar{\Theta}', \Theta')). \end{aligned} \quad (\text{B.21})$$

Thus non-locality in replica-space or in time is replaced by non-locality in superspace, or more precisely in its anticommuting component. Corrections to  $R(u)$  all stem from “superdiagrams”, which result into bilocal interactions in superspace, not trilocal, or higher. The latter find their equivalent in 3-local terms in replica-space in the replica-formulation, and 3-local terms in time, in the dynamic formulation.

Supersymmetry is broken, once  $\Delta(0)$  changes, i.e. at the Larkin length. A seemingly “effective supersymmetry”, or “scale-dependent supersymmetry” appears, in which the parameter  $\Delta(0)$ , which appears in the Susy-transformation, changes with scale, according to the FRG flow equations for  $\Delta(u)$ , continued to  $u = 0$ .

## B.4 Supersymmetry and dimensional reduction

Let us study invariants of the action. Since  $\int_x \partial_x \mathcal{U}(\Phi) = \int_{\bar{\Theta}\Theta} \mathcal{U}(\Phi) = 0$ , the crucial term to focus on is the super-Laplacian. To simplify notations, we set

$$\rho := \Delta(0). \quad (\text{B.22})$$

By explicit inspection, we find that the two generators of super-translations

$$Q := x \frac{\partial}{\partial \Theta} + \frac{2}{\rho} \bar{\Theta} \nabla, \quad \bar{Q} := x \frac{\partial}{\partial \bar{\Theta}} - \frac{2}{\rho} \Theta \nabla \quad (\text{B.23})_{\text{su13}}$$

both commute with the Super-Laplacian, and anti-commute with each other,

$$[\Delta_s, Q] = [\Delta_s, \bar{Q}] = 0, \quad \{Q, \bar{Q}\} = 0. \quad (\text{B.24})_{\text{su14}}$$

The following combination is invariant under the action of  $Q$  and  $\bar{Q}$ ,

$$\bar{Q} \left( x^2 + \frac{4}{\rho} \bar{\Theta} \Theta \right) = Q \left( x^2 + \frac{4}{\rho} \bar{\Theta} \Theta \right) = 0. \quad (\text{B.25})_{\text{su15}}$$

Applying the Super-Laplacian gives<sup>5</sup>

$$\Delta_s \left( x^2 + \frac{4}{\rho} \bar{\Theta} \Theta \right) = 2(d-2). \quad (\text{B.26})_{\text{su16}}$$

We now calculate the super-propagator, which is the inverse of the super-Laplacian plus mass term in (B.14). To do so remark that

$$\left( m^2 - \nabla^2 - \rho \frac{\partial}{\partial \bar{\Theta}} \frac{\partial}{\partial \Theta} \right) \left( m^2 - \nabla^2 + \rho \frac{\partial}{\partial \bar{\Theta}} \frac{\partial}{\partial \Theta} \right) = (m^2 - \nabla^2)^2. \quad (\text{B.27})_{\text{su16b}}$$

This implies that

$$(m^2 - \Delta_s)^{-1} = \frac{m^2 - \nabla^2 + \rho \frac{\partial}{\partial \bar{\Theta}} \frac{\partial}{\partial \Theta}}{(m^2 - \nabla^2)^2}. \quad (\text{B.28})_{\text{su17}}$$

Therefore

$$C(x - x', \Theta - \Theta', \bar{\Theta} - \bar{\Theta}') = \frac{m^2 - \nabla^2 + \rho \frac{\partial}{\partial \bar{\Theta}} \frac{\partial}{\partial \Theta}}{(m^2 - \nabla^2)^2} \delta(x - x') \delta(\Theta - \Theta') \delta(\bar{\Theta} - \bar{\Theta}'). \quad (\text{B.29})_{\text{su18}}$$

---

<sup>5</sup>This relation comes out incorrectly in [107].



The  $\delta$ -functions are defined as

$$\int d\Theta \delta(\Theta - \Theta') f(\Theta) = f(\Theta'). \quad (\text{B.30})_{\text{su19}}$$

By direct calculation one finds

$$\delta(\Theta - \Theta') = \Theta' - \Theta = \int d\bar{\chi} e^{\bar{\chi}(\Theta' - \Theta)}. \quad (\text{B.31})_{\text{su20}}$$

One can therefore transform (B.29) completely into a representation in dual spaces of momentum ( $k$ -space) and super-coordinates ( $\chi$ -space) as

$$C(k, \bar{\chi}, \chi) = \frac{m^2 + k^2 + \rho \bar{\chi} \chi}{(m^2 + k^2)^2} \equiv \frac{1}{m^2 + k^2 + \rho \chi \bar{\chi}} \equiv \int_0^\infty ds e^{-s(m^2 + k^2 + \rho \chi \bar{\chi})}. \quad (\text{B.32})_{\text{su22}}$$

The final proof of dimensional reduction is performed with this representation of the super-correlator<sup>6</sup>. Any diagram can be written as

$$\int_{k_1} \int_{\bar{\chi}_1 \chi_1} \cdots \int_{k_n} \int_{\bar{\chi}_n \chi_n} \prod_{i=1}^n \left[ \int_0^\infty ds_i e^{-s_i(m^2 + k_i^2 + \rho \chi_i \bar{\chi}_i)} \right], \quad (\text{B.33})_{\text{su23}}$$

where some  $\delta$ -distributions have already been used to eliminate integrations over  $k$ 's, i.e. some of the  $k_i$ 's appearing in the exponential are not independent variables, but linear combinations of other  $k_j$ 's, and the same for the corresponding  $\chi_i$  and  $\bar{\chi}_i$ . The product of the exponential factors can be written as

$$\prod_{i=1}^n \left[ e^{-s_i(m^2 + k_i^2 + \rho \chi_i \bar{\chi}_i)} \right] = \exp \left( - \begin{pmatrix} k_1 \\ k_2 \\ \dots \\ k_n \end{pmatrix} \mathbb{W} \begin{pmatrix} k_1 \\ k_2 \\ \dots \\ k_n \end{pmatrix} \right) \exp \left( - \begin{pmatrix} \chi_1 \\ \chi_2 \\ \dots \\ \chi_n \end{pmatrix} \mathbb{W} \begin{pmatrix} \bar{\chi}_1 \\ \bar{\chi}_2 \\ \dots \\ \bar{\chi}_n \end{pmatrix} \right). \quad (\text{B.34})_{\text{su24}}$$

Integration over the  $k$ 's gives

$$\int_{k_1} \cdots \int_{k_n} e^{-\vec{k} \cdot \mathbb{W} \cdot \vec{k}} = \left( \frac{1}{4\pi} \right)^{ld/2} \det(\mathbb{W})^{-d/2}, \quad (\text{B.35})_{\text{su25}}$$

where  $l$  is the number of loops. Integration over  $\bar{\chi}$  and  $\chi$  gives

$$\int_{\bar{\chi}_1 \chi_1} \cdots \int_{\bar{\chi}_n \chi_n} e^{-\rho \bar{\chi} \cdot \mathbb{W} \cdot \bar{\chi}} = (\rho)^l \det(\mathbb{W}). \quad (\text{B.36})_{\text{su26}}$$

The product of the two factors (B.35) and (B.36) is the same as for a standard bosonic diagram in dimension  $d - 2$ . Remarking that there the expansion is in fact in temperature  $T$ , and combining these relations, we obtain after integration over the  $s_i$ :

$$l\text{-loop super-diagram in dimension } d = \left( \frac{\rho}{4\pi T} \right)^l \times l\text{-loop standard-diagram in dimension } d - 2. \quad (\text{B.37})_{\text{su27}}$$

---

<sup>6</sup>Note that one can also work in position-space[107]. Then the super-correlator is explicitly  $d$ -dependent, and one should check that this  $d$ -dependence comes out correctly.

This implies that for any observable  $\mathcal{O}(T)$

$$\mathcal{O}_{\text{disordered}}^d(\rho) = \mathcal{O}_{\text{thermal}}^{d-2}\left(T = \frac{\rho}{4\pi}\right). \quad (\text{B.38})$$

The above proof can be extended to theories with derivative couplings. The rules are as follows: Consider  $\mathcal{H}_s[\Phi]$  given in (B.14). To this, we can add an interaction in derivatives for a total of

$$\begin{aligned} \mathcal{H}_s[\Phi] = & \int d\bar{\Theta}d\Theta \int_x \frac{1}{2} \Phi(x, \bar{\Theta}, \Theta) (-\Delta_s + m^2) \Phi(x, \bar{\Theta}, \Theta) + \mathcal{U}(\Phi(x, \bar{\Theta}, \Theta)) \\ & + \mathcal{A}_1(\Phi(x, \bar{\Theta}, \Theta)) (-\Delta_s + m^2) \mathcal{A}_2(\Phi(x, \bar{\Theta}, \Theta)). \end{aligned} \quad (\text{B.39})$$

This theory is supersymmetric: Calculating diagrams in perturbation theory, we get additional vertices. These diagrams can be calculated from the same type of generating function (B.34). The trick is to use instead of an integral w.r.t.  $s$  a derivative w.r.t.  $s$ , taken at  $s = 0$ ,

$$(m^2 + k^2 + \rho\chi\bar{\chi}) = -\frac{d}{ds} \Big|_{s=0} e^{-s(m^2+k^2+\rho\chi\bar{\chi})}. \quad (\text{B.40})$$

## B.5 CDWs and their mapping onto $\phi^4$ -theory

Consider the fixed point (5.35) for CDWs. It has the form

$$\Delta(u) = \frac{g}{12} - \frac{g}{2}u(1-u) = \frac{g}{2}u^2 + \text{lower-order terms in } u. \quad (\text{B.41})$$

The renormalization can be gotten by retaining only terms of order  $u^2$ , and dropping lower-order terms which do not feed back into terms of order  $u^2$ . To this aim, consider the action (B.17), replacing  $\Delta(u) \rightarrow \frac{g}{2}u^2$ . We further go to center-of-mass coordinates, by introducing

$$u_1(x) = u(x) + \frac{1}{2}\phi(x), \quad u_2(x) = u(x) - \frac{1}{2}\phi(x), \quad (\text{B.42})$$

$$\tilde{u}_1(x) = \frac{1}{2}\tilde{u}(x) + \tilde{\phi}(x), \quad \tilde{u}_2(x) = \frac{1}{2}\tilde{u}(x) - \tilde{\phi}(x). \quad (\text{B.43})$$

The action (B.11) can then be rewritten as

$$\begin{aligned} \mathcal{S} = & \int_x \tilde{\phi}(x)(-\nabla^2 + m^2)\phi(x) + \tilde{u}(x)(-\nabla^2 + m^2)u(x) + \sum_{a=1}^2 \bar{\psi}_a(x)(-\nabla^2 + m^2)\psi_a(x) \\ & + \frac{g}{2}\tilde{u}(x)\phi(x) [\bar{\psi}_2(x)\psi_2(x) - \bar{\psi}_1(x)\psi_1(x)] - \frac{g}{8}\tilde{u}(x)^2\phi(x)^2 \\ & + \frac{g}{2} \left[ \tilde{\phi}(x)\phi(x) + \bar{\psi}_1(x)\psi_1(x) + \bar{\psi}_2(x)\psi_2(x) \right]^2. \end{aligned} \quad (\text{B.44})$$

Note that only  $\tilde{u}(x)$ , but not the center-of-mass  $u(x)$  appears in the interaction. While  $u(x)$  may have non-trivial expectations, it does not contribute to the renormalization of  $g$ , and the latter can be obtained by considering solely the first and last line of Eq. (B.44): This is a  $\phi^4$ -type theory, with one complex bosonic, and two complex fermionic fields. It can equivalently be viewed as complex  $\phi^4$ -theory at  $N = -1$ , or real  $\phi^4$ -theory with  $n = -2$ .

## C The coherent-state path integral (CSPI)

The coherent-state path integral (CSPI) is a formalism which evaluates *exactly* the *evolution of probabilities* for a stochastic process. To this aim, the different configurations of the system are represented as in quantum mechanics by  $n$ -particle states  $|n\rangle$ . This allows one to write probabilities  $p(n)$  as states, i.e. superpositions  $|\psi\rangle := \sum_{n=0}^{\infty} p(n) |n\rangle$ . The evolution operator is then encoded into a *Hamiltonian*, acting on these states. Finally, a path integral is constructed. Its eigenstates are coherent states, i.e. eigenfunctions of the annihilation operator to be defined below.

Having constructed an exact representation of the stochastic process as a coherent-state path integral, the latter can be studied with different methods: Either using perturbation theory, possibly coupled with renormalization group methods (section C.12), or by rewriting it as a *stochastic equation of motion* for the states  $|\psi\rangle$  (section C.18). We will study these techniques in turn.

In order not to overburden our notations in this section, we put space and time as an index, instead of as an argument.

### C.1 Quantization rules

Consider a single site which can be occupied by  $n$  particles (bosons),  $n = 0, 1, \dots$ . Denote this  $n$ -particle state by

$$|n\rangle := (\hat{a}^\dagger)^n |0\rangle, \quad (\text{C.1})$$

where  $|0\rangle$  is the normalized vacuum state  $\langle 0|0\rangle = 1$ . While  $\hat{a}^\dagger$  is the *creation* operator, its conjugate  $\hat{a}$  is the *annihilation* operator,  $\hat{a}|0\rangle = 0$ . They have canonical commutation rules

$$[\hat{a}, \hat{a}^\dagger] = 1. \quad (\text{C.2}) \text{commutator}$$

The scalar product between two states is

$$\langle n|m\rangle = \langle 0| \hat{a}^n (\hat{a}^\dagger)^m |0\rangle = n! \delta_{nm}. \quad (\text{C.3}) \text{norm}$$

This is proven by commuting all  $\hat{a}$  to the right, using Eq. (C.2). Thus  $|n\rangle$  is not normalized to 1, but to  $\langle n|n\rangle = n!$ . The number operator is  $\hat{n} := \hat{a}^\dagger \hat{a}$ , i.e.

$$\hat{n} |n\rangle \equiv \hat{a}^\dagger \hat{a} |n\rangle = n |n\rangle. \quad (\text{C.4})$$

We note for convenience that

$$\hat{a} \hat{a}^\dagger |n\rangle = (n+1) |n\rangle, \quad (\text{C.5})$$

$$\hat{a}^2 (\hat{a}^\dagger)^2 |n\rangle = (n+1)(n+2) |n\rangle, \quad (\text{C.6})$$

$$(\hat{a}^\dagger)^2 \hat{a}^2 |n\rangle = n(n-1) |n\rangle. \quad (\text{C.7})$$

### C.2 Master equation and Hamiltonian formalism

We now want to code a master equation for the occupation probability in this formalism. Suppose the probability for having  $n$  particles at time  $t$  is  $p_t(n)$ , with  $\sum_{n=0}^{\infty} p_t(n) = 1$ . We associate with this probability a state

$$|\psi_t\rangle := \sum_{n=0}^{\infty} p_t(n) |n\rangle \equiv \sum_{n=0}^{\infty} p_t(n) (\hat{a}^\dagger)^n |0\rangle. \quad (\text{C.8}) \text{psi-def}$$

Consider the master-equation for the probability  $p_t(n)$ ,

$$\partial_t p_t(n) = \frac{\nu}{2} \left[ (n+1)n p_t(n+1) - n(n-1)p_t(n) \right] + \mu \left[ (n+1)p_t(n+1) - np_t(n) \right] + \kappa \left[ (n-1)p_t(n-1) - np_t(n) \right].$$

In the first process two particles meet and annihilate with rate  $\nu$ :  $A + A \xrightarrow{\nu} A$ . In the second process, a particle decays with rate  $\mu$ :  $A \xrightarrow{\mu} \emptyset$ . In the third process a particle “gives birth” to two particles with rate  $\kappa$ :  $A \xrightarrow{\kappa} A + A$ . Note that probability is conserved,  $\sum_{n=0}^{\infty} \partial_t p_t(n) = 0$ .

We now want to derive the “Hamiltonian” associated to this master equation, in the form

$$\partial_t |\psi_t\rangle = \mathcal{H} |\psi_t\rangle. \quad (\text{C.9})_{\text{H-def}}$$

To this aim we multiply both sides of Eq. (C.9) with  $(\hat{a}^\dagger)^n |0\rangle$ , and then sum over  $n$ . The factors of  $n$  are expressed using the number operator  $\hat{n} = \hat{a}^\dagger \hat{a}$ ,

$$\begin{aligned} \partial_t \sum_{n=0}^{\infty} p_t(n) (\hat{a}^\dagger)^n |0\rangle &= \frac{\nu}{2} \sum_{n=0}^{\infty} \left[ p_t(n+1) \hat{a}^\dagger \hat{a}^2 \hat{a}^\dagger - p_t(n) (\hat{a}^\dagger)^2 \hat{a}^2 \right] (\hat{a}^\dagger)^n |0\rangle \\ &+ \mu \sum_{n=0}^{\infty} \left[ p_t(n+1) \hat{a} \hat{a}^\dagger - p_t(n) \hat{a}^\dagger \hat{a} \right] (\hat{a}^\dagger)^n |0\rangle \\ &+ \kappa \sum_{n=0}^{\infty} \left[ p_t(n-1) (\hat{a}^\dagger \hat{a} - 1) - p_t(n) \hat{a}^\dagger \hat{a} \right] (\hat{a}^\dagger)^n |0\rangle. \end{aligned} \quad (\text{C.10})$$

Note that we have taken advantage of relations (C.5) to (C.7) to simplify the expression. Next we use definition (C.8) to rewrite this expression in terms of  $|\psi_t\rangle$ . As an example consider the first term on the r.h.s.,  $\sum_{n=0}^{\infty} \hat{a}^\dagger \hat{a}^2 p_t(n+1) (\hat{a}^\dagger)^{n+1} |0\rangle \equiv \sum_{n=0}^{\infty} \hat{a}^\dagger \hat{a}^2 p_t(n) (\hat{a}^\dagger)^n |0\rangle = \hat{a}^\dagger \hat{a}^2 |\psi_t\rangle$ . We extended the sum to  $n=0$ , which is possible since the first term on the l.h.s. does not contribute, due to the preceding operators  $\hat{a}^2$ .

We thus arrive at

$$\partial_t |\psi_t\rangle = \frac{\nu}{2} \left[ \hat{a}^\dagger \hat{a}^2 - (\hat{a}^\dagger)^2 \hat{a}^2 \right] |\psi_t\rangle + \mu \left[ \hat{a} - \hat{a}^\dagger \hat{a} \right] |\psi_t\rangle + \kappa \left[ (\hat{a}^\dagger)^2 \hat{a} - \hat{a}^\dagger \hat{a} \right] |\psi_t\rangle. \quad (\text{C.11})_{\text{master3}}$$

Using Eq. (C.9), this identifies the Hamiltonian

$$\mathcal{H} = \frac{\nu}{2} \left[ \hat{a}^\dagger \hat{a}^2 - (\hat{a}^\dagger)^2 \hat{a}^2 \right] + \mu \left[ \hat{a} - \hat{a}^\dagger \hat{a} \right] + \kappa \left[ (\hat{a}^\dagger)^2 \hat{a} - \hat{a}^\dagger \hat{a} \right]. \quad (\text{C.12})_{\text{H1}}$$

This Hamiltonian is *normal-ordered*, i.e. all  $\hat{a}^\dagger$  stand left of all  $\hat{a}$ . It has all the terms expected from quantum mechanics, except that for each *expected* term there is a second term which does not change the particle number, and which ensures the *conservation of probability*. Indeed, conservation of probability can be written as

$$0 = \partial_t \sum_{n=0}^{\infty} p_t(n) \equiv \partial_t \langle 0 | e^{\hat{a}} |\psi_t\rangle = \langle 0 | e^{\hat{a}} \mathcal{H}(\hat{a}^\dagger, \hat{a}) |\psi_t\rangle = \langle 0 | \mathcal{H}(\hat{a}^\dagger + 1, \hat{a}) e^{\hat{a}} |\psi_t\rangle. \quad (\text{C.13})$$

For the first line we used that the  $1/n!$  in the definition of the exponential function cancels the normalization (C.3). For the second line we used that

$$e^{\lambda \hat{a}} f(\hat{a}^\dagger) = f(\hat{a}^\dagger + \lambda) e^{\lambda \hat{a}}, \quad (\text{C.14})$$

$$e^{\lambda \hat{a}^\dagger} f(\hat{a}) = f(\hat{a} - \lambda) e^{\lambda \hat{a}^\dagger}. \quad (\text{C.15})$$

Noting that an  $\hat{a}^\dagger$  inside  $\mathcal{H}$ , when acting to the left on  $\langle 0|$ , gives no contribution, we arrive at the *constraint of conservation of probability* for the *normal-ordered* Hamiltonian  $\mathcal{H}$

$$\mathcal{H}(\hat{a}^\dagger, \hat{a}) \Big|_{\hat{a}^\dagger \rightarrow 1} = 0 . \quad (\text{C.16})$$

Eq. (C.16) is a *necessary* condition to ensure that (C.13) holds; it is also *sufficient* since using (C.14) the state  $e^{\hat{a}} |\psi_t\rangle \equiv \sum_n p_t(n) (\hat{a}^\dagger + 1)^n |0\rangle$  can be chosen arbitrarily. Looking back at Eq. (C.12), we see that the second term inside each square bracket is such that at  $\hat{a}^\dagger = 1$  the sum of the two terms vanishes, thus as stated it ensures the *conservation of probability*.

### C.3 Combinatorics

Let us remark that the combinatorics used in the above processes is the basic combinatorics of choosing  $k$  out of  $n$  particles,  $\binom{n}{k}$ , relevant e.g. for the meeting probability of two particles. While this choice is canonic, situations may arise where the combinatorics is different. If the stochastic process was to contain factors non-polynomial in  $n$ , then the Hamiltonian (C.12) would not be as simple, and might e.g. become non-analytic in  $\hat{a}$  and  $\hat{a}^\dagger$ ; much of the technology developed here would no longer work. This holds especially true for the stochastic equation of motion to be introduced below, which relies on the fact that, via a suitable decoupling, the Hamiltonian can be rendered linear in  $\hat{a}^\dagger$ .

### C.4 Observables

Now consider an observable  $\mathcal{O}(n)$ , which depends only on the occupation number  $n$ . Using the same tricks as in Eq. (C.13), its expectation value can be written as

$$\begin{aligned} \langle \mathcal{O} \rangle_{\psi_t} &:= \sum_{n=0}^{\infty} \mathcal{O}(n) p_t(n) = \langle 0| e^{\hat{a}} \mathcal{O}(\hat{a}^\dagger \hat{a}) |\psi_t\rangle \equiv \langle 0| \mathcal{O}(\hat{a}^\dagger \hat{a} + \hat{a}) e^{\hat{a}} |\psi_t\rangle \\ &= \langle 0| \mathcal{O}_N(\hat{a}^\dagger + 1, \hat{a}) e^{\hat{a}} |\psi_t\rangle = \langle 0| \mathcal{O}_N(1, \hat{a}) e^{\hat{a}} |\psi_t\rangle . \end{aligned} \quad (\text{C.17})$$

In the last identity of the first line we used Eq. (C.14). Passing to the second line, we introduced the *normal-ordered* version of the operator  $\mathcal{O}$ , obtained by commuting all  $\hat{a}$  to the right and all  $\hat{a}^\dagger$  to the left. It is generically a function of  $a$  and  $\hat{a}^\dagger$ , not  $\hat{n} = \hat{a}^\dagger \hat{a}$ . The last line uses that  $\hat{a}^\dagger$  acting to the left vanishes.

### C.5 Coherent states

Coherent states play a key role in the path-integral formalism to be developed below. We define them here, and study some of its properties. Coherent states are constructed s.t.

$$|\phi\rangle := e^{\phi \hat{a}^\dagger} |0\rangle \quad \Rightarrow \quad \hat{a} |\phi\rangle = \phi |\phi\rangle . \quad (\text{C.18})$$

Let us start with  $\phi$  real and positive. Then *by definition* a coherent state has a Poisson probability distribution for  $n$ -fold occupation,

$$p(n) = e^{-\phi} \frac{\phi^n}{n!} . \quad (\text{C.19})$$

Note that the definition (C.18) does not contain the factor of  $e^{-\phi}$ , thus it is not normalized. This is for convenience reasons; one may think of it as a *histogram*.

States  $|\phi\rangle$  with a complex  $\phi$  are possible too. Since  $\phi$  is continuous, but the number  $n$  an integer, coherent states form an over-complete basis, even for  $\phi \geq 0$ . However, not all probability distributions can be written as a superposition of coherent states with positive weights, i.e. as

$$|\psi\rangle = \int_0^\infty d\phi \rho(\phi) e^{-\phi} |\phi\rangle \quad (\text{C.20})$$

with  $\rho(\phi) \geq 0$ . There are several ways out of this dilemma: One can use negative (or complex) weights  $\rho(\phi)$ , states with complex  $\phi$ , or a combination of both. The formalism to be developed below will exploit this freedom.

By definition, the adjoint state is

$$\langle\phi^*| = \langle 0| e^{\phi^* \hat{a}}. \quad (\text{C.21})$$

Eq. (C.14) implies that the scalar product is

$$\langle\phi^*|\phi\rangle = e^{\phi^* \phi}. \quad (\text{C.22})$$

Let us give an interpretation of the adjoint state: Apply  $\langle\phi^*|$  to the state  $|\psi_t\rangle$  defined in Eq. (C.8),

$$\rho_t(\phi^*) := \langle\phi^*|\psi_t\rangle = \sum_{n=0}^{\infty} p_t(n) (\phi^*)^n. \quad (\text{C.23})$$

This is nothing but the *generating function* of the probabilities  $p_t(n)$ ,  $n = 0, 1, 2, \dots$

Now consider the expectation value of a *normal-ordered* observable  $\mathcal{O}(\hat{n}) = \mathcal{O}_N(\hat{a}^\dagger, a)$  in a coherent state  $|\phi\rangle$ ,

$$\langle\mathcal{O}\rangle_\phi := \frac{\langle 0| e^{\hat{a}} \mathcal{O}_N(\hat{a}^\dagger, \hat{a}) e^{\phi \hat{a}^\dagger} |0\rangle}{\langle 0| e^{\hat{a}} \mathbb{1} e^{\phi \hat{a}^\dagger} |0\rangle} = \langle 0| e^{\phi \hat{a}^\dagger} \mathcal{O}_N((\hat{a}^\dagger + 1), (\hat{a} + \phi)) e^{\hat{a}} |0\rangle = \mathcal{O}_N(1, \phi). \quad (\text{C.24})$$

We used Eqs. (C.14) and (C.15), as well as the vanishing of  $\hat{a}$  acting on the vacuum to the right, and  $\hat{a}^\dagger$  to the left. To write the last line  $\mathcal{O}_N$  needs to be normal-ordered. Also note that a factor of  $e^\phi$  has canceled between numerator and denominator of the first line; it is necessary, since the coherent states (C.18) are not normalized to unity.

In coherent states, the number of particles is not fixed. We claim that

$$e^{\lambda \hat{n}} \equiv e^{\lambda \hat{a}^\dagger \hat{a}} = :e^{(\lambda-1)\hat{a}^\dagger \hat{a}}: . \quad (\text{C.25})$$

Its r.h.s. is called *normal-ordered* and denoted by “:” around the operators in question; it is defined by its Taylor expansion in  $\hat{a}^\dagger$  and  $\hat{a}$ , arranging all  $\hat{a}^\dagger$  to the left and all  $\hat{a}$  to the right, as if they were numbers. E.g. is  $:(\hat{a}^\dagger \hat{a})^2:$  defined to be  $(\hat{a}^\dagger)^2 \hat{a}^2$ .

The proof of Eq. (C.25) consists of two steps: Applying its l.h.s. to a coherent state yields

$$e^{\lambda \hat{a}^\dagger \hat{a}} |\phi\rangle := e^{\lambda \hat{a}^\dagger \hat{a}} e^{\phi \hat{a}^\dagger} |0\rangle = \sum_{n=0}^{\infty} e^{\lambda \hat{a}^\dagger \hat{a}} \frac{\phi^n (\hat{a}^\dagger)^n}{n!} |0\rangle = \sum_{n=0}^{\infty} e^{\lambda n} \frac{\phi^n (\hat{a}^\dagger)^n}{n!} |0\rangle = e^{e^\lambda \phi \hat{a}^\dagger} |0\rangle. \quad (\text{C.26})$$

Thus

$$\langle\phi^*| e^{\lambda \hat{a}^\dagger \hat{a}} |\phi\rangle = \langle 0| e^{\phi^* \hat{a}} e^{e^\lambda \phi \hat{a}^\dagger} |0\rangle = e^{e^\lambda \phi^* \phi}. \quad (\text{C.27})$$

On the other hand,

$$\begin{aligned} \langle\phi^*| :e^{(\lambda-1)\hat{a}^\dagger \hat{a}}: |\phi\rangle &= \sum_{n=0}^{\infty} \langle 0| e^{\phi^* \hat{a}} (e^\lambda - 1)^n \frac{(\hat{a}^\dagger)^n \hat{a}^n}{n!} e^{\phi \hat{a}^\dagger} |0\rangle \\ &= \sum_{n=0}^{\infty} \langle 0| e^{\phi^* \hat{a}} (e^\lambda - 1)^n \frac{(\phi^* \phi)^n}{n!} e^{\phi \hat{a}^\dagger} |0\rangle = e^{e^\lambda \phi^* \phi}. \end{aligned} \quad (\text{C.28})$$

This proves relation (C.25).

Using this relation, or directly the intermediate result Eq. (C.27) at  $\phi^* = 1$ , and the definition of an observable given in Eq. (C.24) yields

$$\langle e^{\lambda \hat{n}} \rangle_\phi = e^{(e^\lambda - 1)\phi}. \quad (\text{C.29})$$

The generating function of connected moments is the logarithm of this function,

$$\langle e^{\lambda \hat{n}} \rangle_\phi^c = (e^\lambda - 1)\phi. \quad (\text{C.30})$$

This means that the  $p$ -th connected moment of the number operator  $n$  is

$$\langle \hat{n}^p \rangle_\phi^c = \phi. \quad (\text{C.31})$$

Let us give some explicit examples

$$\langle \hat{n} \rangle_\phi = \phi, \quad \langle \hat{n}^2 \rangle_\phi = \phi(1 + \phi), \quad \langle \hat{n}^3 \rangle_\phi = \phi(1 + 3\phi + \phi^2), \quad \dots \quad (\text{C.32})$$

$$\phi = \langle \hat{n} \rangle_\phi, \quad \phi^2 = \langle \hat{n}(\hat{n} - 1) \rangle_\phi, \quad \phi^3 = \langle \hat{n}(\hat{n} - 1)(\hat{n} - 2) \rangle_\phi, \quad \dots \quad (\text{C.33})$$

The last set of relations can also be derived directly, see appendix B2 of [6].

## C.6 Many sites

We now generalize to  $L$  sites, denoted  $i = 1, \dots, L$ , with *creation* and *annihilation* operators  $\hat{a}_i^\dagger$  and  $\hat{a}_i$  for site  $i$ . The canonical commutation relations are in generalization of Eq. (C.2)

$$[\hat{a}_i, \hat{a}_j^\dagger] = \delta_{ij}. \quad (\text{C.34})$$

A state is then encoded as

$$|\psi\rangle = \sum_{n_1, \dots, n_L=0}^{\infty} p_t(n_1, \dots, n_L) (\hat{a}_1^\dagger)^{n_1} \dots (\hat{a}_L^\dagger)^{n_L} |0\rangle. \quad (\text{C.35})$$

We can also construct a coherent state out of single-particle coherent states,

$$|\psi\rangle := \bigotimes_{i=1}^L |\phi_i\rangle. \quad (\text{C.36})_{45}$$

## C.7 Coarse-graining

When constructing effective field theories, one often coarse grains, replacing the state variables of several sites by a common effective variable. For coherent states, this is particularly straight-forward: Suppose we have two sites with coherent states  $|\phi_1\rangle$  and  $|\phi_2\rangle$ , and we want to know what the probability to have  $n$ -fold occupation of the combined two sites is. We evaluate

$$p_{\text{comb}}(n) = \sum_{n_1=0}^n \left[ e^{-\phi_1} \frac{(\phi_1)^{n_1}}{n_1!} \right] \times \left[ e^{-\phi_2} \frac{(\phi_2)^{n-n_1}}{(n-n_1)!} \right] = e^{-(\phi_1+\phi_2)} \frac{(\phi_1 + \phi_2)^n}{n!}. \quad (\text{C.37})$$

Thus, combining two coherent states leads to a coherent state with the added weights,

$$|\phi_1\rangle \oplus |\phi_2\rangle \longrightarrow |\phi_1 + \phi_2\rangle. \quad (\text{C.38})$$

Finally, if we are interested in the probability for  $n$ -particle occupation of our system of size  $L$  given in Eq. (C.36), we get a state

$$|\Phi\rangle = \left| \sum_{i=1}^L \phi_i \right\rangle \quad (\text{C.39})_{\text{total-state}}$$

## C.8 Diffusion

Consider now the hopping of a particle from site  $i$  to site  $j$ , with *diffusion constant* (rate)  $D$ . The corresponding Hamiltonian is (as expected)

$$\mathcal{H} = D(\hat{a}_j^\dagger - \hat{a}_i^\dagger)\hat{a}_i. \quad (\text{C.40})$$

Having hopping both from  $i$  to  $j$  and from  $j$  to  $i$  with the same rate  $D$  leads to

$$\mathcal{H} = -D(\hat{a}_j^\dagger - \hat{a}_i^\dagger)(\hat{a}_j - \hat{a}_i). \quad (\text{C.41})$$

Note that by this definition the rate to leave a site in dimension  $d$  is  $2d \times D$ , and not  $D$ . In the continuum limit, and summing over all nearest-neighbour sites, this becomes the Hamiltonian of diffusion

$$\mathcal{H}_{\text{diffusion}} = -D \int_x \nabla \hat{a}_x^\dagger \nabla \hat{a}_x. \quad (\text{C.42})$$

To avoid overly cumbersome notations, we have set to 1 the lattice-cutoff  $a$ , which multiplies the lattice diffusion constant  $D$  by a factor of  $a^{2-d}$ .

## C.9 Resolution of unity

The path-integral representation we wish to establish is based on the coherent states defined in Eq. (C.18). The key relation which we are going to prove is the *resolution of unity*

$$\mathbb{1} = \frac{i}{2\pi} \int d\phi d\phi^* e^{-\phi\phi^*} |\phi\rangle \langle\phi^*|. \quad (\text{C.43})$$

The complex-conjugate pair is  $\phi = \phi_x + i\phi_y$ ,  $\phi^* = \phi_x - i\phi_y$ ; the integration measure is  $d\phi d\phi^* = \frac{2}{i} d\phi_x d\phi_y$ . Inserting these definitions, the r.h.s. of Eq. (C.43) can be rewritten as

$$\int \frac{d\phi_x d\phi_y}{\pi} e^{-\phi\phi^*} e^{\phi\hat{a}^\dagger} |0\rangle \langle 0| e^{\phi^*\hat{a}} = \sum_{n=0}^{\infty} \sum_{m=0}^{\infty} \int_0^{2\pi} \frac{d\theta}{\pi} \int_0^{\infty} dr r e^{-r^2} r^{n+m} e^{i\theta(n-m)} \frac{(\hat{a}^\dagger)^n}{n!} |0\rangle \langle 0| \frac{\hat{a}^m}{m!}, \quad (\text{C.44})$$

where in the last line we set  $\phi := r e^{i\theta}$ . The angular integral is vanishing for  $n \neq m$ , resulting in

$$\sum_{n=0}^{\infty} \int_0^{\infty} d(r^2) e^{-r^2} r^{2n} \frac{(\hat{a}^\dagger)^n}{n!} |0\rangle \langle 0| \frac{\hat{a}^n}{n!} = \sum_{n=0}^{\infty} \frac{1}{n!} (\hat{a}^\dagger)^n |0\rangle \langle 0| \hat{a}^n. \quad (\text{C.45})$$

Applying this expression to the state  $|m\rangle = (\hat{a}^\dagger)^m |0\rangle$ , only the term  $n = m$  in the sum contributes, and reproduces this state. This completes the proof.

Let us mention another commonly employed trick, namely of analytic continuation. This is most prominently employed in conformal field theory, see e.g. Ref. [109], to which we refer the reader for the subtleties. The essence is that  $\phi$  and  $\phi^*$  do *not have to be complex conjugates*, but that one may think of them as two independent variables, which together span  $\mathbb{C} \equiv \mathbb{R}^2$ . A *conceptionally* convenient choice is  $\phi$  real and  $\phi^*$  imaginary<sup>7</sup>.

<sup>7</sup>Consider the scalar product  $\langle n | \mathbb{1} | m \rangle \sim \int d\phi d\phi^* \phi^n (\phi^*)^m e^{-\phi\phi^*} = \int d\phi d\phi^* \phi^n (-\partial_\phi)^m e^{-\phi\phi^*} = m! \int d\phi d\phi^* \phi^{n-m} e^{-\phi\phi^*} \Theta(n > m)$ . For  $\phi$  real and  $\phi^*$  purely imaginary the integral  $\int d\phi^* e^{-\phi\phi^*}$  yields  $\delta(\phi)$ , and the former expression vanishes except for  $n = m$ .



## C.10 Evolution operator in the coherent-state formalism, and action

We are now in a position to construct the time evolution in the coherent-state formalism. To this aim write the evolution operator  $e^{\delta t \mathcal{H}} \simeq 1 + \delta t \mathcal{H}$  for a small time, and evaluate it in the coherent basis, by applying the resolution of unity (C.43) to both sides of  $e^{\delta t \mathcal{H}}$ . To avoid problems with not normal-ordered terms appearing in  $(\mathcal{H})^2$ , and higher, we choose  $\delta t$  infinitesimally small:

$$e^{\delta t \mathcal{H}(\hat{a}^\dagger, \hat{a})} = \frac{i}{2\pi} \int d\phi_{t+\delta t} d\phi_{t+\delta t}^* \frac{i}{2\pi} \int d\phi_t d\phi_t^* e^{-\phi_{t+\delta t} \phi_{t+\delta t}^* - \phi_t \phi_t^*} |\phi_{t+\delta t}\rangle \langle \phi_t^*| \langle \phi_{t+\delta t}^*| e^{\delta t \mathcal{H}(\hat{a}^\dagger, \hat{a})} |\phi_t\rangle . \quad (\text{C.46})_{27}$$

We need to evaluate the matrix element in question

$$\begin{aligned} \langle \phi_{t+\delta t}^* | e^{\delta t \mathcal{H}(\hat{a}^\dagger, \hat{a})} | \phi_t \rangle &\simeq \langle 0 | e^{\phi_{t+\delta t}^* \hat{a}} [1 + \delta t \mathcal{H}(\hat{a}^\dagger, \hat{a})] e^{\phi_t \hat{a}^\dagger} | 0 \rangle \\ &= e^{\phi_{t+\delta t}^* \phi_t} \langle 0 | e^{\phi_t \hat{a}^\dagger} [1 + \delta t \mathcal{H}(\hat{a}^\dagger + \phi_{t+\delta t}^*, \hat{a} + \phi_t)] e^{\phi_{t+\delta t}^* \hat{a}} | 0 \rangle . \end{aligned} \quad (\text{C.47})$$

We have used Eqs. (C.14) and (C.15) to commute the exponential operators. All operators  $\hat{a}$  are now acting on the vacuum to the right, thus do not give a contribution. The same holds true for  $\hat{a}^\dagger$  acting to the left. Further using the normalization of the vacuum state  $\langle 0 | 0 \rangle = 1$ , we finally arrive at

$$\langle \phi_{t+\delta t}^* | e^{\delta t \mathcal{H}(\hat{a}^\dagger, \hat{a})} | \phi_t \rangle = e^{\phi_{t+\delta t}^* \phi_t} e^{\delta t \mathcal{H}(\phi_{t+\delta t}^*, \phi_t)} + O(\delta t^2). \quad (\text{C.48})$$

Together with Eq. (C.46), we identify all terms for a time step from  $t$  to  $t + \delta t$  as  $e^{-\mathcal{S}_{t,t+\delta t} \delta t}$ , with

$$-\mathcal{S}_{t,t+\delta t} \delta t = [\phi_{t+\delta t}^* - \phi_t^*] \phi_t + \mathcal{H}(\phi_{t+\delta t}^*, \phi_t) \delta t = \phi_{t+\delta t}^* [\phi_t - \phi_{t+\delta t}] + \mathcal{H}(\phi_{t+\delta t}^*, \phi_t) \delta t . \quad (\text{C.49})_{30}$$

The expression  $\mathcal{S}_{t,t+\delta t}$  is termed the *action* for the time step from  $t$  to  $t + \delta t$ . The two possible forms were obtained by grouping with either of the factors of  $e^{-\phi_{t+\delta t} \phi_{t+\delta t}^* - \phi_t \phi_t^*}$  appearing in Eq. (C.46). Suppose for the following that we evolve from *small* to *large* times: Then the second line will be relevant; the unused factor of  $e^{-\phi_t \phi_t^*}$  at  $t=t_i$  will appear together with the initial state  $\phi_i$  as

$$e^{-\phi_t \phi_t^*} \langle 0 | e^{\phi_t^* \hat{a}} e^{\phi_i \hat{a}^\dagger} | 0 \rangle = e^{-(\phi_t - \phi_i) \phi_t^*} , \quad (\text{C.50})_{39}$$

where we used Eq. (C.14); when integrated over  $\phi_t^*$ , this identifies  $\phi_t$  as the initial state  $\phi_i$ . Note that when integrating from larger to smaller times, we would use the first line of Eq. (C.49), evolving from the final state  $\langle \phi_f |$  to smaller times; the factor  $e^{-\phi_{t+\delta t} \phi_{t+\delta t}^*}$  at  $t+\delta t=t_f$  would then fix  $\langle \phi_f | = \langle \phi_{t+\delta t} |$ . The formalism can thus be used both forward and backward in time, exchanging the role of  $\phi$  and  $\phi^*$ .

We now consider the forward version, evolving from an initial state  $|\phi_i\rangle$  at  $t = t_i$ . In the continuous limit, the *action* from time  $t = t_i$  to time  $t = t_f$  becomes

$$\mathcal{S}[\phi^*, \phi] := \int_{t_i}^{t_f} dt \phi_t^* \partial_t \phi_t - \mathcal{H}[\phi_t^*, \phi_t] . \quad (\text{C.51})_{\text{action}}$$

(Note that we replaced  $\phi_{t+\delta t}^* \rightarrow \phi_t^*$  in the Hamiltonian  $\mathcal{H}[\phi_{t+\delta t}^*, \phi_t]$ , which is valid in the small- $\delta t$  limit.)

The path-integral can then be written as

$$|\psi_f\rangle = \mathbf{T} e^{\int_{t_i}^{t_f} dt \mathcal{H}[\hat{a}_t^\dagger, \hat{a}_t]} |\phi_i\rangle = \int \mathcal{D}[\phi] \mathcal{D}[\phi^*] e^{-\mathcal{S}[\phi^*, \phi]} \Big|_{\phi_{t_i} = \phi_i} |\phi_{t_f}\rangle . \quad (\text{C.52})_{48b\text{-first}}$$

Note that (in the simplifying case of one time slice) the state  $|\phi_{t_f}\rangle$  corresponds to the state  $|\phi_{t+\delta t}\rangle$  in Eq. (C.46), thus is part of the path integral (i.e. integrated over). On the other hand, the state  $\langle \phi_t^* |$  in Eq. (C.46) corresponds to  $\langle \phi_{t_i}^* |$ . When applied to  $|\phi_i\rangle$ , and integrated over it yields the boundary condition  $\phi_{t_i} = \phi_i$ .

The time-index  $t$  at the operators  $\hat{a}$  and  $\hat{a}^\dagger$  is introduced for book-keeping purposes, to define the time-ordering operator  $\mathbf{T}$  as  $\mathbf{T}e^{\int_{t_i}^{t_f} dt \mathcal{H}[\hat{a}_t^\dagger, \hat{a}_t]} := \prod_{t=t_i}^{t_f, \delta t = \tau} e^{\tau \mathcal{H}[\hat{a}_t^\dagger, \hat{a}_t]}$ , putting smaller times to the right. (This is the same ordering as in the definition of the path integral.)

The final state  $|\psi_f\rangle$  is not a coherent state, but the superposition of coherent states  $|\phi_f\rangle$ . To formalize this better, suppose that the initial state is also a superposition of coherent states, each with weight  $\rho(\phi_i)$ , and normalized s.t.  $\int_{\phi_i} \rho(\phi_i) := \frac{i}{2\pi} \int d\phi_i d\phi_i^* \rho(\phi_i) = 1$ ,

$$|\psi_i\rangle = \int_{\phi_i} \rho(\phi_i) e^{-\phi_i} |\phi_i\rangle. \quad (\text{C.53})_{\text{initial-state-}}$$

Restricting support of  $\rho(\phi_i)$  to  $\phi_i > 0$  is included as a special case, with intuitive physical interpretation. The states  $e^{-\phi_i} |\phi_i\rangle$  are normalized, so that together with the normalization of the weight the state  $|\psi_i\rangle$  is normalized. Define

$$\mathcal{A}(\phi_f|\phi_i) := \int \mathcal{D}[\phi] \mathcal{D}[\phi^*] e^{-\mathcal{S}[\phi^*, \phi]} \Big|_{\phi_{t_i}=\phi_i}^{\phi_{t_f}=\phi_f}. \quad (\text{C.54})_{\text{48b-second}}$$

Then

$$|\psi_f\rangle = \int_{\phi_f} |\phi_f\rangle \int_{\phi_i} \mathcal{A}(\phi_f|\phi_i) \rho(\phi_i) e^{-\phi_i}. \quad (\text{C.55})_{\text{48b-third}}$$

By construction,  $|\psi_f\rangle$  is normalized, thus  $\mathcal{A}(\phi_f|\phi_i)$  defines the *transition amplitude*.

### C.11 The shift $\phi_t^* \rightarrow \phi_t^* + 1$

In Eq. (C.17) we had considered expectation values of an observable  $\mathcal{O}$ . Suppose we want to measure it at time  $t_f$ , evolved from  $|\phi_i\rangle$  at time  $t_i$  until time  $t_f$ ,

$$\langle \mathcal{O}_{t_f} \rangle = e^{-\phi_i} \langle 0 | e^{\hat{a}} \mathcal{O}_N(\hat{a}^\dagger, \hat{a}) \mathbf{T}e^{\int_{t_i}^{t_f} dt \mathcal{H}[\hat{a}_t^\dagger, \hat{a}_t]} | \phi_i \rangle. \quad (\text{C.56})_{\text{48-3}}$$

The factor of  $e^{-\phi_i}$  ensures that the initial state is normalized.

Remark now that  $\langle 0 | e^a = \langle 1 |$ . Going to the path-integral, this can be written as

$$\begin{aligned} \langle \mathcal{O}_{t_f} \rangle &= e^{-\phi_i} \langle 1 | \mathcal{O}_N(\hat{a}^\dagger, \hat{a}) \mathbf{T}e^{\int_{t_i}^{t_f} dt \mathcal{H}[\hat{a}_t^\dagger, \hat{a}_t]} | \phi_i \rangle \\ &= \int_{\phi_f} \int \mathcal{D}[\phi] \mathcal{D}[\phi^*] \mathcal{O}_N(1, \phi_f) e^{\phi_f - \phi_i} e^{-\mathcal{S}[\phi^*, \phi]} \Big|_{\phi_{t_i}=\phi_i}^{\phi_{t_f}=\phi_f}. \end{aligned} \quad (\text{C.57})_{\text{formulation-}}$$

The final scalar product yields  $\langle 1 | \mathcal{O}_N(\hat{a}^\dagger, \hat{a}) | \phi_f \rangle = \mathcal{O}_N(1, \phi_f) e^{\phi_f}$ . Note that it *does not fix*  $\phi_{t_f}^* = 1$ , as it would in absence of the operator  $\mathcal{O}_N(\hat{a}^\dagger, \hat{a})$ .

We now shift all variables  $\phi^* \rightarrow \phi^* + 1$ , to obtain

$$\langle \mathcal{O}_{t_f} \rangle = \int \mathcal{D}[\phi] \mathcal{D}[\phi^*] \mathcal{O}_N(1, \phi_f) e^{-\mathcal{S}'[\phi^*, \phi]} \Big|_{\phi_{t_i}=\phi_i}^{\phi_{t_f}^*=0} \quad (\text{C.58})_{\text{formulation-}}$$

$$\mathcal{S}'[\phi^*, \phi] := \int_{t_i}^{t_f} dt \phi_t^* \partial_t \phi_t - \mathcal{H}'[\phi_t^*, \phi_t] \quad (\text{C.59})_{\text{S'}}$$

$$\mathcal{H}'[\phi_t^*, \phi_t] := \mathcal{H}[\phi_t^* + 1, \phi_t] \quad (\text{C.60})_{\text{H'}}$$

Note that under this shift

$$\int_{t_i}^{t_f} dt \phi_t^* \partial_t \phi_t \longrightarrow \int_{t_i}^{t_f} dt (\phi_t^* + 1) \partial_t \phi_t = \phi_{t_f} - \phi_{t_i} + \int_{t_i}^{t_f} dt \phi_t^* \partial_t \phi_t \quad (\text{C.61})$$

Apart from the obvious change in the argument of  $\mathcal{H}$  this accounts for the cancelation of the factor of  $e^{\phi_f - \phi_i}$  in Eq. (C.57). John Cardy in his excellent lecture notes [110] calls this shift the Doi-shift. Its main advantage is that the field  $\phi^*$  has expectation zero (at least in the final state). This is particularly useful when interpreting the CSPI graphically, as we will see in the next section. In addition, the formulae are simpler, and more intuitive. Finally, it is advantages when evaluating the CSPI via a stochastic equation of motion, see section C.18. To distinguish between shifted, and unshifted action, we *put a prime on the shifted one*. In the shifted variables, Eqs. (C.54) and (C.55) take the form

$$\mathcal{A}'(\phi_f|\phi_i) := \int \mathcal{D}[\phi] \mathcal{D}[\phi^*] e^{-S'[\phi^*, \phi]} \Big|_{\phi_{t_i}=\phi_i}^{\phi_{t_f}=\phi_f}, \quad (\text{C.62})$$

$$|\psi_f\rangle = \int_{\phi_f} e^{-\phi_f} |\phi_f\rangle \int_{\phi_i} \mathcal{A}'(\phi_f|\phi_i) \rho(\phi_i). \quad (\text{C.63})$$

The initial state is still given by Eq. (C.53). If one starts from a coherent state  $|\phi_i\rangle$ , then Eq. (C.63) simplifies to

$$|\psi_f\rangle = \int_{\phi_f} e^{-\phi_f} |\phi_f\rangle \mathcal{A}'(\phi_f|\phi_i). \quad (\text{C.64})$$

## C.12 Graphical interpretation of the coherent-state path-integral, first-passage probabilities, and renormalization

Field theories of the type introduced above are often evaluated in perturbation theory, and interpreted graphically. To this aim, the part of the action linear in both  $\phi$  and  $\phi^*$  is solved explicitly, yielding a *single-particle propagator* or *response function*. One then starts with  $n$  particles, draws their trajectories, and studies how they interact via the terms non-linear in  $\phi$  and  $\phi^*$ . In this process, particles may be destroyed and created. In the following, we show how to derive this picture from the coherent-state path-integral, based on the shifted formulation in Eqs. (C.58)-(C.64).

## C.13 The initial condition

Start with a general initial state  $|\phi_{i,x}\rangle := e^{\int_x \phi_{i,x} \hat{a}_x^\dagger} |0\rangle$ . Let us create  $p$  particles, at positions  $x_1$  to  $x_p$ . In the operator picture, this is encoded by

$$\hat{a}_{x_1}^\dagger \dots \hat{a}_{x_p}^\dagger |0\rangle = \frac{\delta}{\delta \phi_{i,x_1}} \dots \frac{\delta}{\delta \phi_{i,x_p}} |\phi_{i,x}\rangle \Big|_{\phi_{i,x}=0}. \quad (\text{C.65})$$

Applying the path-integral formalism developed in sections C.10 and C.11, we obtain a field theory with action  $\mathcal{S}'$ , depending on the two fields  $\phi$  and  $\phi^*$ . In Eq. (C.50) we had derived the factor for the first time slice, on which we still have to shift  $\phi^* \rightarrow \phi^* + 1$ ; this has further to be multiplied by the factor of  $e^{-\int_x \phi_{i,x}}$  from the normalisation; writing both factors explicitly, this results into

$$e^{-\int_x (\phi_{x,t_i} - \phi_{i,x})(\phi_{x,t_i}^* + 1)} \times e^{\int_x -\phi_{i,x}}.$$

Note the cancelation for the terms proportional to  $\phi_{i,x}$ ; using Eq. (C.65), an initial condition with  $p$  particles at positions specified above is thus transferred to the path-integral as

$$\hat{a}_{x_1}^\dagger \dots \hat{a}_{x_p}^\dagger |0\rangle \longrightarrow \phi_{x_1,t_i}^* \dots \phi_{x_p,t_i}^*, \quad (\text{C.66})$$

and

$$\phi_{i,x} = 0. \quad (\text{C.67})$$

Graphically, we draw a particle emanating from position  $x$  at time  $t$  as a dot at that position in space-time, from which an arrow starts,

$$\uparrow_{x,t} \cdot \quad (\text{C.68})$$

## C.14 The propagator

Consider diffusion as given by the Hamiltonian in Eq. (C.42). According to Eq. (C.51) the action is

$$S'_0[\phi, \phi^*] = \int_{x,t} \phi_{x,t}^* \partial_t \phi_{x,t} + D \nabla \phi_{x,t}^* \nabla \phi_{x,t}. \quad (\text{C.69})_{S0}$$

This yields the propagator, alias Green, or response function (in Fourier space)

$$\uparrow = \langle \phi_{k,t'} \phi_{-k,t}^* \rangle = \Theta(t' - t) e^{-D(t'-t)k^2}. \quad (\text{C.70})$$

Transforming back to real space, this is

$$\uparrow = G_{x'-x}^{t'-t} := \langle \phi_{x',t'} \phi_{x,t}^* \rangle = \Theta(t' - t) \frac{e^{-\frac{(x-x')^2}{4D(t'-t)}}}{\sqrt{4\pi D(t'-t)}}. \quad (\text{C.71})_{\text{prop}}$$

It is solution of the partial differential equation

$$(\partial_{t'} - D \nabla_{x'}^2) G_{x'-x}^{t'-t} = \delta(x - x') \delta(t - t'). \quad (\text{C.72})$$

Probability is conserved, i.e.  $\int_{x'} G_{x'-x}^{t'-t} = 1$ .

## C.15 The interactions

To be specific, consider the annihilation process with rate  $\nu$



The Hamiltonian of this process was derived in Eq. (C.12),

$$\mathcal{H}_\nu[\hat{a}^\dagger, a] = \frac{\nu}{2} [\hat{a}^\dagger \hat{a}^2 - (\hat{a}^\dagger)^2 \hat{a}^2]. \quad (\text{C.74})_{71-2}$$

The corresponding term in the shifted action is

$$\begin{aligned} S'_\nu[\phi^*, \phi] &= - \sum_x \int_t \mathcal{H}_\nu[\phi_{x,t}^* + 1, \phi_{x,t}] = \frac{\nu}{2} \sum_x \int_t (\phi_{x,t}^* + 1) \phi_{x,t}^* \phi_{x,t}^2 \\ &= \frac{\nu}{2} \sum_x \int_t \begin{array}{c} \nearrow \\ \times \\ \searrow \end{array} + \begin{array}{c} \uparrow \\ \wedge \end{array} \end{aligned} \quad (\text{C.75})$$

Note that both terms have the same sign. Passing to the continuum yields

$$S'_\nu[\phi^*, \phi] = \frac{\nu \delta^d}{2} \int_{x,t} (\phi_{x,t}^* + 1) \phi_{x,t}^* \phi_{x,t}^2 \quad (\text{C.76})$$

Since we wish the total number of particles to be  $\sum_x \phi_{x,t} \rightarrow \int_x \phi_{x,t}$ , in the discrete version  $\phi_{x,t}$  is the number of particles on site  $x$ , whereas in the continuum version it is the density of particles, resulting in the additional factor of  $\delta^d$  in the action. Alternatively, we could keep  $\phi_{x,t}$  the number of particles in a box of size  $\delta$ . To avoid these problems, which are not essential for our discussion, we set  $\delta \rightarrow 1$ , except when specified otherwise.





One can try to resum explicitly the perturbation series. As we set up the framework, it is well defined for small  $\nu$ , and finite  $\tau$ . Under these circumstances, resummation is rather tedious, and the author of the present notes has decided to eliminate the corresponding calculations in order to keep the material readable.

We can, however, deduce the result in the limit of  $\tau \rightarrow 0$ , and  $\nu \rightarrow \infty$ : One first realizes that the distance between the two particles is again a random walk with a diffusion constant  $2D$  instead of  $D$ . It can thus be described by an action

$$\mathcal{S}_{\text{rel}}[\phi, \phi^*] = \int_{x,t} \phi_{x,t}^* \partial_t \phi_{x,t} + 2D \nabla \phi_{x,t}^* \cdot \nabla \phi_{x,t}. \quad (\text{C.90})_{\text{S0b}}$$

Second, the field  $\phi(x, t)$  is only defined for  $x \geq 0$ , and zero for  $x = 0$ : when the two particles meet, a single particle will propagate from that point on, and their relative position will be zero. This is known as Dirichlet boundary conditions, and can be solved with the *method of images* [111]. In dimension  $d = 1$ , this leads to

$$G_{x',x}^{t'-t} := \langle \phi_{x',t'} \phi_{x,t}^* \rangle = \Theta(t' - t) \frac{e^{-\frac{(x-x')^2}{8D(t'-t)}} - e^{-\frac{(x+x')^2}{8D(t'-t)}}}{\sqrt{8\pi D(t'-t)}}. \quad (\text{C.91})$$

Here  $x$  is the difference in position at the start, and  $x'$  the distance in position at the end. Note the difference to Eq. (C.71). Integrating over  $x'$  from zero to infinity, we obtain the probability that the two particles did not meet up to time  $t$ , knowing that they started at distance  $x$  at time 0,

$$p_{\text{survive}}(x, t) = \text{erf}\left(\frac{x}{\sqrt{8Dt}}\right). \quad (\text{C.92})$$

The probability  $p_1(t)$  given in Eq. (C.77) then is

$$p_1(t_f) = 1 - p_{\text{survive}}(x, t_f). \quad (\text{C.93})$$

This can be generalized to higher dimensions.

## C.18 Stochastic equation of motion for the coherent-state path integral

We established in Eq. (C.62) that the transition amplitude between the coherent states  $|\phi_i\rangle$  and  $|\phi_f\rangle$  is given by

$$\mathcal{A}'(\phi_f|\phi_i) = \int \mathcal{D}[\phi] \mathcal{D}[\phi^*] e^{-S'[\phi^*, \phi]} \Big|_{\phi_{t_i}=\phi_i}^{\phi_{t_f}=\phi_f}. \quad (\text{C.94})_{\text{48b}}$$

Note that we use the shifted action, thus shifted fields  $\phi^*$ , since then both  $\phi$  and  $\phi^*$  have zero expectation values, rendering all following considerations simpler.

Suppose now that the shifted Hamiltonian, and thus the shifted action have only *linear* and *quadratic* terms in  $\phi_t^*$ ; a term independent of  $\phi^*$  is absent due to the conservation of probability, Eq. (C.16),

$$\mathcal{H}'[\phi_t^*, \phi_t] = \phi_t^* \mathcal{L}[\phi_t] + \frac{1}{2} (\phi_t^*)^2 \mathcal{B}[\phi_t]. \quad (\text{C.95})_{\text{37}}$$

First consider  $\mathcal{B}[\phi_t] = 0$ , i.e. only a term linear in  $\phi_t^*$ . Then the saddle point obtained by variation w.r.t.  $\phi^*$  gives the exact solution to the path integral, encoded in the equation of motion, of  $\phi_t$

$$\partial_t \phi_t = \mathcal{L}[\phi_t], \quad \phi_{t_i} = \phi_i, \quad \mathcal{A}'(\phi_f|\phi_i) = \delta(\phi_f - \phi_{t_f}). \quad (\text{C.96})_{\text{EOM}}$$

Quite amazingly, an explicit solution for a non-linear path-integral has been given!

This simple solution is no longer possible if  $\mathcal{B}[\phi_t] \neq 0$ . To nevertheless use an equation of motion, we introduce a Gaussian random variable, i.e. white noise,  $\xi_t$ , to write  $e^{\frac{1}{2}\mathcal{B}[\phi_t](\phi_t^*)^2}$  as an expectation value over the noise,

$$e^{\frac{1}{2}\int_t \mathcal{B}[\phi_t](\phi_t^*)^2} = \left\langle e^{\int_t \phi_t^* \sqrt{\mathcal{B}[\phi_t]}\xi_t} \right\rangle_{\xi}, \quad \langle \xi_t \xi_{t'} \rangle_{\xi} = \delta(t - t'). \quad (\text{C.97})_{\text{BP-noise}}$$

Note that if  $\mathcal{B}[\phi_t]$  is *negative*, then the noise is *imaginary*. The sign of the root is irrelevant, since  $\xi_t$  is statistically invariant under  $\xi_t \rightarrow -\xi_t$ . With the noise, the equation of motion (C.96) changes to

$$\partial_t \phi_t = \mathcal{L}[\phi_t] + \sqrt{\mathcal{B}[\phi_t]}\xi_t, \quad \phi_{t_i} = \phi_i. \quad (\text{C.98})_{\text{RP}}$$

The interpretation is as follows: The transition amplitude  $\mathcal{A}'(\phi_f|\phi_i)$  can be sampled by simulating the Langevin equation (C.98), with initial condition and noise given by Eq. (C.97),

$$\mathcal{A}'(\phi_f|\phi_i) = \left\langle \delta(\phi_f - \phi_{t_f}) \right\rangle_{\xi}. \quad (\text{C.99})_{\text{O2}}$$

According to Eq. (C.58) an observable  $\mathcal{O}$  has then expectation at time  $t_f$

$$\langle \mathcal{O}_{t_f} \rangle = \langle \mathcal{O}_{\text{N}}(1, \phi_{t_f}) \rangle_{\xi}. \quad (\text{C.100})_{\text{EV}}$$

This is an intuitive result, with some caveats: First, we remind the replacement of  $\hat{a}^\dagger \rightarrow 1$ . Second,  $\mathcal{O}_{\text{N}}(\hat{a}^\dagger, \hat{a})$  is the normal-ordered version of the operator. E.g. is  $\hat{n}^2 = (\hat{a}^\dagger \hat{a})^2 = (\hat{a}^\dagger)^2 \hat{a}^2 + \hat{a}^\dagger \hat{a}$ , so that  $\langle \hat{n}_{t_f}^2 \rangle = \langle \phi_t^2 + \phi_t \rangle_{\xi}$ , see Eq. (C.32).

In appendix C.23 we give a formal proof of this relation, based uniquely on the CSPI. The formalism produces two terms, a linear term proportional to  $\frac{\delta}{\delta \hat{a}_x} \mathcal{O}(1, \hat{a})$ , and a quadratic term proportional to  $\frac{\delta}{\delta \hat{a}_x} \frac{\delta}{\delta \hat{a}_y} \mathcal{O}(1, \hat{a})$ . These two terms can then be interpreted as drift and diffusion terms in the Itô formalism. This gives an independent derivation of the process (C.98), and the relation (C.100).

If  $\sqrt{\mathcal{B}[\phi_t]}$  is real, one may think of equation (C.98) as describing what is “going on” in the system. This is not the case if  $\mathcal{B}[\phi_t]$  is negative, thus  $\sqrt{\mathcal{B}[\phi_t]}$  purely imaginary: Then generically, states sampled by the path integral are “non-physical” in the sense that they do not correspond to a probability density, even though the transition amplitude is given by Eq. (C.99). We will come back to this question in section C.22: There we will show that in the case of imaginary noise, the formalism works for short times, but breaks down for longer times.

In section 8.3 we propose a different physically motivated treatment, leading to a coarse-grained effective stochastic equation of motion with a real noise.

## C.19 Equation of motion for diffusion in the CSPI

Let us start with simple diffusion, with Hamiltonian

$$\mathcal{H}'[\hat{a}^\dagger, \hat{a}] := \mathcal{H}[\hat{a}^\dagger + 1, \hat{a}] = -D \int_x \nabla \hat{a}_x^\dagger \nabla \hat{a}_x. \quad (\text{C.101})$$

Note that the shift has no effect since only  $\nabla \hat{a}_x^\dagger$  appears. This implies the action, already given in Eq. (C.69)

$$\mathcal{S}'[\phi^*, \phi] = \int_{x,t} \phi_{x,t}^* \partial_t \phi_{x,t} + D \nabla \phi_{x,t}^* \nabla \phi_{x,t}. \quad (\text{C.102})$$

Variation w.r.t.  $\phi^*$  leads to the equation of motion

$$\partial_t \phi_{x,t} = D \nabla^2 \phi_{x,t}. \quad (\text{C.103})_{\text{diff}}$$



This is a very *simple* and actually *quite remarkable* equation: While diffusion is a noisy process, leading to fluctuations of the number of particles on a given site, Eq. (C.103) is an exact, *noiseless* equation. It tells us how the distribution of the number of particles on a given site evolves with time.

As a test, let us check that it keeps the *total particle-number* distribution fixed. Eq. (C.39) implies that at, say  $t = t_i$ , the total particle-number distribution is given by the coherent state

$$|\Phi\rangle = \left| \int_x \phi_{x,t_i} \right\rangle . \quad (\text{C.104})$$

Since for periodic boundary conditions  $\int_x \partial_t \phi_{x,t} = D \int_x \nabla^2 \phi_{x,t} = 0$ , the state  $|\Phi\rangle$  does not change over time. In particular, this implies particle-number conservation.

## C.20 Equation of motion for reaction diffusion in the CSPI

Consider the reaction-diffusion process  $A + A \xrightarrow{\nu} A$  with (shifted) action defined by Eqs. (C.69) and (C.75):

$$\mathcal{S}'[\phi^*, \phi] = \int_{x,t} \left\{ \phi_{x,t}^* \partial_t \phi_{x,t} + D \nabla \phi_{x,t}^* \nabla \phi_{x,t} + \frac{\nu}{2} [\phi_{x,t}^* \phi_{x,t}^2 + (\phi_{x,t}^*)^2 \phi_{x,t}^2] \right\} . \quad (\text{C.105})_{92a}$$

The corresponding equation of motion and noise are

$$\partial_t \phi_{x,t} = -\frac{\nu}{2} \phi_{x,t}^2 + D \nabla^2 \phi_{x,t} + i\sqrt{\nu} \phi_{x,t} \xi_{x,t} , \quad (\text{C.106})_{\text{SEOMApAg}}$$

$$\langle \xi_{x,t} \xi_{x',t'} \rangle = \delta(t - t') \delta(x - x') . \quad (\text{C.107})$$

This noise is imaginary. It has puzzled many researchers whether this is unavoidable [86, 87, 88, 89], or could even be beneficial [90]. We will come back to this question later.

## C.21 Dual formulation: Equation of motion for $\phi_t^*$

Note that one can define the dual process of Eq. (C.98), by exchanging in the dynamical action the roles of  $\phi$  and  $\phi^*$ : Suppose the Hamiltonian can be written in the form

$$\mathcal{H}[\phi_t^*, \phi_t] = \mathcal{L}^*[\phi_t^*] \phi_t + \frac{1}{2} \mathcal{B}^*[\phi_t^*] (\phi_t)^2 . \quad (\text{C.108})$$

The path integral for the generating function at time  $t_f$  then becomes

$$\rho_f(\phi^*) := \langle e^{\phi^* \phi_{t_f}} \rangle = \int \mathcal{D}[\phi] \mathcal{D}[\phi^*] e^{\phi^* \phi_{t_f} - \int_t \phi_t^* \partial_t \phi_t - \mathcal{H}[\phi_t^*, \phi_t]} \Big|_{\phi_{t_i} = \phi_i}^{\phi^* = \phi_{t_f}^*}$$

Note that this equation is written in terms of the unshifted Hamiltonian. Contrary to Eq. (C.57) it is normalized, since the left-most state is not  $\langle 0 | e^a = \langle 1 |$ . Integrating  $\int_t \phi_t^* \partial_t \phi_t$  by part, and noting that the boundary term changes in the exponential  $\phi^* \phi_{t_f} \rightarrow \phi_{t_i}^* \phi_i$ , yields

$$\rho_f(\phi^*) = \int \mathcal{D}[\phi] \mathcal{D}[\phi^*] e^{\phi_{t_i}^* \phi_i + \int_t \phi_t \partial_t \phi_t^* + \mathcal{H}[\phi_t^*, \phi_t]} \Big|_{\phi_{t_i} = \phi_i}^{\phi^* = \phi_{t_f}^*} \quad (\text{C.109})_{111}$$

This path integral is sampled by the stochastic process

$$-\partial_t \phi_t^* = \mathcal{L}^*[\phi_t^*] + \sqrt{\mathcal{B}^*[\phi_t^*]} \xi_t , \quad \phi_{t_f}^* = \phi^* . \quad (\text{C.110})_{\text{nv-EOM}}$$

It evolves the (dual) state  $\phi_t^*$  from  $t_f$  to  $t_i$ , backward in time, as is suggested by the sign of Eq. (C.110).

Consider now  $\mathcal{B}^* \equiv 0$ , such that the evolution becomes deterministic,  $-\partial_t \phi_t^* = \mathcal{L}^*[\phi_t^*]$ . Denote by  $\Psi_{t,t_f} : \phi^* = \phi_{t_f}^* \rightarrow \phi_t^*$ , this time evolution, i.e.

$$\phi_t^* = \Psi_{t,t_f}(\phi_{t_f}^*) . \quad (\text{C.111})$$

Note that  $\Psi_{t,t_f}(0) = 0$ , and  $\Psi_{t,t_f}(1) = 1$ .

As a concrete example, consider the branching process, including a possible annihilation  $A \rightarrow 0$

$$A \xrightarrow{\lambda_n} nA . \quad (\text{C.112})$$

Then

$$\mathcal{H}[\hat{a}^\dagger, \hat{a}] = \sum_n \lambda_n \left[ (\hat{a}^\dagger)^n \hat{a} - \hat{a}^\dagger \hat{a} \right] \equiv f(\hat{a}^\dagger) \hat{a} - f(1) \hat{a}^\dagger \hat{a} , \quad (\text{C.113})$$

where we defined  $f(x) := \sum_n \lambda_n x^n$ . The equation of motion (C.110) then becomes (there is no Doi-Shift)

$$-\partial_t \phi_t^* = f(\phi_t^*) - f(1) \phi_t^* , \quad \phi_{t_f}^* = \phi^* . \quad (\text{C.114})$$

To be explicit, choose  $\lambda_2 = 1$ , and all other  $\lambda_i = 0$ . We have to solve (backward in time) the equation  $\partial_t \phi_t^* = \phi_t^* - (\phi_t^*)^2$ . It has solution  $\phi_t^* = 1/[1 - e^{t_f-t}(1 - 1/\phi^*)]$ . The function  $\Psi$  then reads

$$\Psi_{t_f,t}(x) = \frac{x}{x + e^{t_f-t}(1-x)} . \quad (\text{C.115})$$

Using Eq. (C.109), this yields the generating function, evaluated at  $t = t_i$ ,

$$\rho_f(\phi^*) = \rho_i(\Psi_{t_f,t_i}(\phi^*)) . \quad (\text{C.116})$$

This is a classical result, see e.g. [112, 113]. Suppose one starts with a single particle at time  $t = 0$ ; then  $\rho_i(\phi^*) = \phi^*$ , and the above becomes

$$\rho_f(\phi^*) = \frac{\phi^*}{\phi^* + e^{t_f-t_i}(1-\phi^*)} . \quad (\text{C.117})_{\text{in-res-}\phi^*}$$

The probability to have  $n$  particles at time  $t_f$  is given by the  $n$ -th series coefficient, namely

$$p_n(t_f) = e^{t_i-t_f} (1 - e^{t_i-t_f})^{n-1} , \quad n \geq 1 . \quad (\text{C.118})$$

This is a rather simple expression.

We could also try to solve the problem by varying w.r.t.  $\phi^*$ , inducing the stochastic equation of motion

$$\partial_t \phi_t = \phi_t + i\sqrt{2\phi_t} \xi_t . \quad (\text{C.119})$$

This equation talks about the evolution of the state  $|\phi_t\rangle$ , who will become complex. We will discuss in the next section how this can be interpreted. Compared to the latter approach, the solution (C.117) is much more elegant, and explicit.

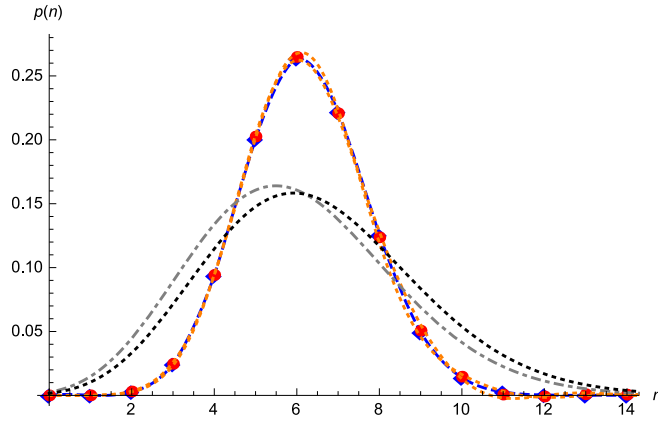


Figure C.1: Results for the process  $A + A \xrightarrow{\nu} A$ , using  $a_i = 15$ ,  $t_f - t_i = 0.2$ , and  $\nu = 1$ . Blue diamonds: direct numerical simulation with  $5 \times 10^5$  samples (partially hidden behind red dots). The blue dashed line is a guide for the eye. The statistical error bars are smaller than this line width. Red dots: Integration of the stochastic equation of motion, using  $\Re(\mathcal{P}_f^{\text{CS}}(n))$  from Eq. (C.120), for  $5 \times 10^4$  samples,  $\delta t = 10^{-3}$ . The orange dotted lines are  $|\Re(\mathcal{P}_f^{\text{CS}}(n)) \pm |\Im(\mathcal{P}_f^{\text{CS}}(n))|$ , defined for all real  $n$ , which is an estimate of the error. Both simulations ran about 100s. Within these errors, the agreement is excellent. The dot-dashed gray line is a Poisson-distribution with  $a_f = 6$ , which would be the result of Eq. (8.8) in the *absence* of noise. Taking into account the drift term  $\nu a_t/2$  induced by the noise in Eq. (8.8) leads to  $a = 6.43$ , (black, dotted). The real distribution is centered around this value, but is much narrower than a Poisson distribution.

## C.22 Testing stochastic equations of motion derived from the CSPI

To test the formalism, consider the reaction process  $A + A \xrightarrow{\nu} A$ , and integrate the stochastic equation of motion (8.8) for different noise realizations  $\xi_t$ , and with initial condition  $\phi_{t_i} = \phi_i$ , one obtains a (complex) result for  $\phi_f = \phi_{t_f}$ . One then measures the final distribution, as an average over all noise realizations,

$$p_f^{\text{SEM}}(n) := \left\langle e^{-\phi_f} \frac{\phi_f^n}{n!} \right\rangle_{\xi}. \quad (\text{C.120})_{\text{magic}}$$

The result is again shown on figure C.1 (red circles). One sees several things: First, the agreement between the direct numerical simulation of the decay process (blue diamonds, and blue dashed line as guide for the eye) and the stochastic equation of motion (red dots, and orange dashed lines, with error estimate) is quite good. This confirms that Eq. (C.120) is indeed applicable, *even though the final states  $\phi_f$  are complex*.

Second, the final distribution is much narrower than a Poisson distribution: both the Poissonian obtained for  $\phi = 6$  (gray dashed line, result of integrating Eq. (8.8), dropping the noise term), plotted on Fig. C.1, or the one including a drift term  $\nu \phi_t/2$  in Eq. (7.74) (black dashed line). Having a distribution narrower than a Poissonian is possible only with imaginary noise, which leads to a diffusion of the phase of  $\phi_t$ , see figure 8.1 (left). In contrast, real noise would to a *widening* of the distribution.

Third, using the stochastic equation of motion has its limits: Indeed, already for  $t_f - t_i = 0.5$ , the stochastic equation of motion gets appreciable error-bars, even with a large number  $s$  of samples, and for  $t_f - t_i = 1$  convergence is no longer assured. We tried an improved algorithm as follows: Instead of starting  $s$  “particles” at  $\phi(t_i) = \phi_i$ , and evolving them until time  $t_f$ , whenever one of these particles gets too large a phase (which promises to give a large value in  $e^{-\phi_f}$ ), we “split” the particle in two, each of which carries half of the weight (the original weight is  $w = 1/s$ ) of its “father”. If the phase is still too large, we split it again, propagating two particles with half the weight each. This procedure is repeated recursively. We have not been able to find parameters to improve the precision at constant execution time. We suspect that when splitting points, it becomes more probable that “bad regions” are reached, and while the weight of the corresponding points is reduced, the probability that they appear is increased. This is illustrated on figure

8.1 (left). This indicates that the convergence problem is severe, and no algorithm to overcome it has been found yet. We refer the reader to [90, 88, 114] for a more detailed discussion of the problems and partially successful attempts at their solution.

### C.23 Formal derivation of the evolution of expectation values in the coherent-state path-integral

Consider the expectation value (C.56) at time  $t_f$

$$\langle \mathcal{O}_{t_f} \rangle = e^{-\phi_i} \langle 0 | e^{\hat{a}} \mathcal{O}(\hat{a}^\dagger, \hat{a}) \mathbf{T} e^{\int_{t_i}^{t_f} dt \mathcal{H}[\hat{a}_t^\dagger, \hat{a}_t]} | \phi_i \rangle . \quad (\text{C.121})_{48\text{bb}}$$

We are interested in its temporal evolution. At a slightly smaller time, the observable  $\mathcal{O}$  had expectation

$$\begin{aligned} \langle \mathcal{O}_{t_f - \delta t} \rangle & \\ &= e^{-\phi_i} \langle 0 | e^{\hat{a}} e^{\delta t \mathcal{H}[\hat{a}^\dagger, \hat{a}]} \mathcal{O}(\hat{a}^\dagger, \hat{a}) \mathbf{T} e^{\int_{t_i}^{t_f - \delta t} dt \mathcal{H}[\hat{a}_t^\dagger, \hat{a}_t]} | \phi_i \rangle . \end{aligned} \quad (\text{C.122})_{48\text{c}}$$

Note that we have been able to add the factor  $e^{\delta t \mathcal{H}[\hat{a}^\dagger, \hat{a}]} \stackrel{\wedge}{=} e^{\delta t \mathcal{H}[\hat{a}_{t_f}^\dagger, \hat{a}_{t_f}]}$  since  $\mathcal{H}[\hat{a}^\dagger, \hat{a}]$ , when applied to the left to  $\langle 0 | e^{\hat{a}}$  vanishes, see section C.2. Thus the time derivative of the expectation value of an operator is given by its commutator with  $\mathcal{H}[\hat{a}^\dagger, \hat{a}]$ ,

$$\frac{d}{dt_f} \langle \mathcal{O}_{t_f} \rangle = \left\langle \left[ \mathcal{O}(\hat{a}^\dagger, \hat{a}), \mathcal{H}[\hat{a}^\dagger, \hat{a}] \right] \right\rangle , \quad (\text{C.123})_{57-2}$$

where the expectation is as in Eq. (C.121). To simplify the calculations, we show that if  $\mathcal{O}[\hat{a}^\dagger, \hat{a}]$  is normal-ordered,  $\mathcal{O}[\hat{a}^\dagger, \hat{a}] \equiv \mathcal{O}_N[\hat{a}^\dagger, \hat{a}]$ , then  $\mathcal{O}[\hat{a}^\dagger, \hat{a}]$  can be replaced by  $\mathcal{O}[1, \hat{a}]$ : indeed, Eq. (C.123) is proportional to

$$\begin{aligned} \langle 0 | e^{\hat{a}} \left( \mathcal{O}(\hat{a}^\dagger, \hat{a}) \mathcal{H}[\hat{a}^\dagger, \hat{a}] - \mathcal{H}[\hat{a}^\dagger, \hat{a}] \mathcal{O}(\hat{a}^\dagger, \hat{a}) \right) \dots \\ = \langle 0 | e^{\hat{a}} \left( \mathcal{O}(1, \hat{a}) \mathcal{H}[\hat{a}^\dagger, \hat{a}] - \mathcal{H}[\hat{a}^\dagger, \hat{a}] \mathcal{O}(1, \hat{a}) \right) \dots \end{aligned} \quad (\text{C.124})$$

since  $\langle 0 | e^{\hat{a}} \mathcal{O}(\hat{a}^\dagger, \hat{a}) = \langle 0 | e^{\hat{a}} \mathcal{O}(1, \hat{a})$ , and  $\langle 0 | e^{\hat{a}} \mathcal{H}[\hat{a}^\dagger, \hat{a}] = 0$ . Thus

$$\frac{d}{dt_f} \langle \mathcal{O}_{t_f} \rangle = \left\langle \left[ \mathcal{O}(1, \hat{a}), \mathcal{H}[\hat{a}^\dagger, \hat{a}] \right] \right\rangle . \quad (\text{C.125})_{57\text{b}}$$

Next, the commutator can be calculated by remarking that

$$\left[ \mathcal{O}(1, \hat{a}), \mathcal{H}[\hat{a}^\dagger, \hat{a}] \right] = \mathbf{W} \left( \mathcal{O}(1, \hat{a}), \mathcal{H}[\hat{a}^\dagger, \hat{a}] \right) . \quad (\text{C.126})$$

The operator  $\mathbf{W}$  denotes all possible Wick contractions between  $\mathcal{O}(1, \hat{a})$  and  $\mathcal{H}[\hat{a}^\dagger, \hat{a}]$ . To proceed we suppose that the Hamiltonian has only a linear and quadratic term in  $\hat{a}^\dagger$ , i.e.

$$\mathcal{H}[\hat{a}^\dagger, \hat{a}] = \int_x \hat{a}_x^\dagger \mathcal{L}_x[\hat{a}] + \frac{1}{2} \int_{x,y} \hat{a}_x^\dagger \hat{a}_y^\dagger \mathcal{B}_{x,y}[\hat{a}] , \quad (\text{C.127})_{100}$$

with  $\mathcal{B}_{xy}[\hat{a}] = \mathcal{B}_{yx}[\hat{a}]$ . Then the commutator will be

$$\left[ \mathcal{O}(1, \hat{a}), \mathcal{H}[\hat{a}^\dagger, \hat{a}] \right] = \int_x \frac{\delta}{\delta \hat{a}_x^\dagger} \mathcal{H}[\hat{a}^\dagger, \hat{a}] \frac{\delta}{\delta \hat{a}_x} \mathcal{O}(1, \hat{a}) + \frac{1}{2} \int_{x,y} \frac{\delta}{\delta \hat{a}_x^\dagger} \frac{\delta}{\delta \hat{a}_y^\dagger} \mathcal{H}[\hat{a}^\dagger, \hat{a}] \frac{\delta}{\delta \hat{a}_x} \frac{\delta}{\delta \hat{a}_y} \mathcal{O}(1, \hat{a}) \quad (\text{C.128})$$

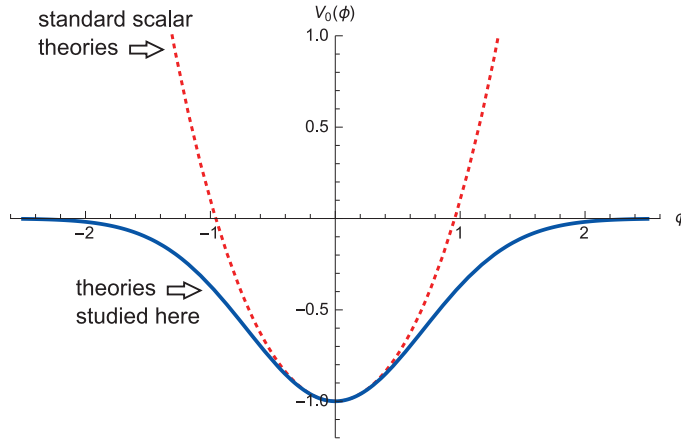


Figure D.1: The function  $\mathcal{V}_0(\phi)$ , for  $\phi^4$  theory (top, red, dashed), and a bounded potential (bottom, blue, solid).

As a consequence, the expectation (C.125) evaluates to

$$\frac{d}{dt_f} \langle \mathcal{O}_{t_f} \rangle = \left\langle \int_x \left( \mathcal{L}_x[\hat{a}] + \int_y \mathcal{B}_{x,y}[\hat{a}] \right) \frac{\delta}{\delta \hat{a}_x} \mathcal{O}(1, \hat{a}) \right\rangle + \frac{1}{2} \left\langle \int_{x,y} \mathcal{B}_{x,y}[\hat{a}] \frac{\delta}{\delta \hat{a}_x} \frac{\delta}{\delta \hat{a}_y} \mathcal{O}(1, \hat{a}) \right\rangle \quad (\text{C.129})_{\text{B9}}$$

We can give an interpretation in terms of a stochastic process  $\phi_t$  defined by

$$\partial_t \phi_{x,t} = \mathcal{L}_x[\phi] + \int_y \mathcal{B}_{x,y}[\phi] + \xi_{x,t}, \quad \langle \xi_{x,t} \xi_{x',t'} \rangle = \delta(t-t') \mathcal{B}_{x,x'}[\phi], \quad \mathcal{O}_{t_f} = \mathcal{O}(1, \phi_{t_f}). \quad (\text{C.130})_{\text{pbs-key}}$$

Indeed, applying the Itô formalism (see e.g. [115]) to the expectation  $\langle \mathcal{O}_{t_f} \rangle_\xi$  yields Eq. (C.129). Comparing Eq. (C.130) to Eq. (C.98), we note that the drift term also contains a term *linear* in  $\mathcal{B}$ . The reason is that to arrive at Eq. (C.98) the *shifted* Hamiltonian had been used. Indeed, this is accounted for by shifting in Eq. (C.127)  $\hat{a}^\dagger \rightarrow \hat{a}^\dagger + 1$ ,  $\mathcal{L}_x \rightarrow \mathcal{L}_x + \int_y \mathcal{B}_{x,y}$ , while  $\mathcal{B}_{x,y}$  remains unchanged. Thus Eqs. (C.98) and (C.130) are equivalent.

## D Non-trivial fixed points of the Renormalization Group

Evaluating the partition function of a field theory in presence of a potential  $\mathcal{V}_0(u)$  at constant background field  $u$  to 1-loop order, and normalizing with its counterpart at  $\mathcal{V}_0 = 0$ , one typically gets a flow equation of the form

$$\ln \left( \frac{\mathcal{Z}[u]}{\mathcal{Z}_0[u]} \right) = - \int^\Lambda \frac{d^d k}{(2\pi)^d} \ln \left( 1 + \frac{\mathcal{V}_0''(u)}{k^2 + m^2} \right). \quad (\text{D.1})_{\text{B}}$$

We have explicitly written an UV cutoff  $\Lambda$ . This equation is at the origin of *non-perturbative* renormalization group (NPRG) schemes [116, 117, 118, 119], (confusingly) also referred to as *exact RG*. To leading order, the effective action is  $\Gamma(u) = -\ln(\mathcal{Z}[u]/\mathcal{Z}_0[u])$ , and denoting its local part by  $\mathcal{V}(u)$ , we arrive at the following *functional* flow equation for the *renormalized* potential  $\mathcal{V}(u)$

$$-m \partial_m \mathcal{V}(u) = -m \partial_m \int^\Lambda \frac{d^d k}{(2\pi)^d} \ln \left( 1 + \frac{\mathcal{V}_0''(u)}{k^2 + m^2} \right). \quad (\text{D.2})_{\text{A}}$$

Keeping only the leading non-linear term [12] leads to the simple flow equation

$$-m \partial_m \mathcal{V}(u) = -m^{d-4} \frac{1}{2} \mathcal{V}''(u)^2 + \dots \quad (\text{D.3})$$

Note that this equation is very similar to the FRG flow equation (??) for disordered elastic manifolds. It reproduces the standard RG-equation for  $\phi^4$  theory; indeed, setting

$$\mathcal{V}(u) = m^{4-d} \frac{u^4}{72} g, \quad (\text{D.4})_{\text{phi4-potential}}$$

we arrive with  $\epsilon := 4 - d$  at

$$-m\partial_m g = \epsilon g - g^2 + \dots \quad (\text{D.5})_{\text{projection}}$$

This is the standard flow equation of  $\phi^4$  theory, with fixed point  $g_* = \epsilon$ . One knows that the potential (D.4) at  $g = g_*$  is attractive, i.e. perturbing it with a perturbation  $\phi^{2n}$ ,  $n > 2$ , the flow will bring it back to its fixed-point form.

This fixed point, and its treatment with the projected simplified flow equation (D.5) is relevant in many situations, the most famous being the Ising model. The form of its microscopic potential, which is plotted in figure D.1 (red dashed curve), grows unboundedly for large  $\phi$ . This is indeed expected for the Ising model, for which the spin, of which  $\phi$  is the coarse-grained version, is bounded.

There are, however, situations, where this is not the case. An example is the attraction of a domain wall by a defect. In this situation, one expects that the potential at large  $\phi$  vanishes, as plotted on figure D.1 (solid blue line). The question to be asked is then: Where does the RG flow lead? This is the question I asked myself.

As one sees from figure D.1, the *bounded* potential  $\mathcal{V}_0$  is negative. In order to deal only with positive quantities, we set  $\mathcal{V}(u) \equiv -\mathcal{R}(u)$ . The flow equation to be studied is

$$-m\partial_m \mathcal{R}(u) = m^{-\epsilon} \frac{1}{2} \mathcal{R}''(u)^2 + \dots \quad (\text{D.6})_{\text{flow-bare}}$$

As I show in my article [12], for generic smooth initial conditions as plotted on figure D.1:

- (i) The flow equation (D.6) develops a cusp at  $u = 0$ , and a cubic singularity at  $u = u_c > 0$ .
- (ii) The rescaled flow equation for the dimensionless function  $R(u)$

$$-m\partial_m R(u) = (\epsilon - 4\zeta)R(u) + \zeta u R'(u) + \frac{1}{2} R''(u)^2 + \dots \quad (\text{D.7})_{\text{flow-rescaled}}$$

has an infinity of fixed points  $-m\partial_m R(u) = 0$ , indexed by  $\zeta \in [\frac{\epsilon}{4}, \infty]$ .

- (iii) The solution chosen dynamically when starting from smooth initial conditions is  $\zeta = \frac{\epsilon}{3}$ . Its analytic expression for  $0 \leq u \leq 1$  reads

$$R_{\zeta=\frac{\epsilon}{3}}(u) = \epsilon \left[ \frac{1}{18} (1-u)^3 - \frac{1}{72} (1-u)^4 \right]. \quad (\text{D.8})_{\text{R-zeta=1/3}}$$

It vanishes for  $u > 1$ , and is continued symmetrically to  $u < 0$ .

This scenario is quite unusual: Normally, the perturbatively accessible fixed points of the RG flow have only one fixed point. In the few cases where there is more than one fixed point, the spectrum of fixed points is at least *discrete*. In contrast, here is a spectrum of fixed points. On the other hand, only one of them seems to be chosen. Thus experiments would only see this one fixed point.

It is yet not clear to which physical system it applies. As thoroughly discussed in the literature [120, 121, 122, 123, 124, 125], experiments describing wetting are usually described by a flow equation *linear* in  $\mathcal{R}(u)$ .

But to cite my colleague Thierry Giamarchi, “whenever there is a simple equation like this, it will be realized somewhere.”

# E Quantum Mechanics: Feynman path-integral and Keldysh formalism

## E.1 Real-time path-integral

Schrödinger says that

$$\langle q', t' | q, t \rangle = \langle q' | e^{-\frac{i}{\hbar} \hat{H}(t'-t)} | q \rangle . \quad (\text{E.1})_{1.1}$$

For small times, one can work with the linearized version, for which one needs:

$$\langle q' | \hat{H} | q \rangle . \quad (\text{E.2})_{1.2}$$

We specify

$$\hat{H} = \frac{\hat{p}^2}{2m} + V(\hat{q}) \quad (\text{E.3})$$

$$[\hat{p}, \hat{q}] = \frac{\hbar}{i} . \quad (\text{E.4})$$

Let us calculate (E.2)

$$\langle q' | \hat{H} | q \rangle = \int \frac{dp}{2\pi\hbar} \langle q' | p \rangle \langle p | \hat{H} | q \rangle = \int \frac{dp}{2\pi\hbar} e^{\frac{i}{\hbar} p(q'-q)} H(p, q) , \quad (\text{E.5})_{1.4}$$

where  $H(p, q)$  is the classical Hamilton-function

$$H(p, q) = \frac{p^2}{2m} + V(q) , \quad (\text{E.6})_{1.5}$$

and

$$\langle q | p \rangle = e^{ipq/\hbar} , \quad \int \frac{dp}{2\pi\hbar} |p\rangle \langle p| = 1 . \quad (\text{E.7})_{1.5b}$$

Writing  $\langle q', t' | q, t \rangle$  as the product of transition amplitudes for small time-slices and integrating over the intermediate steps, we have with the usual notation

$$\langle q', t' | q, t \rangle = \int \mathcal{D}[q] \mathcal{D}[p] e^{\frac{i}{\hbar} \int_t^{t'} p(t)\dot{q}(t) - H(p(t), q(t))} . \quad (\text{E.8})_{1.6}$$

Performing the integral over the  $p$ 's, which can always be done as long as the action is not more than quadratic in  $p$ , the result is (up to some normalization  $N$ )

$$\langle q', t' | q, t \rangle = \frac{1}{N} \int \mathcal{D}[q] e^{\frac{i}{\hbar} \int_t^{t'} L(q(t), \dot{q}(t))} , \quad (\text{E.9})_{1.7}$$

where  $L(q, \dot{q})$  is defined by (saddle-points for quadratic actions are exact!)

$$L(q, \dot{q}) = p\dot{q} - H(p, q) \Big|_{\dot{q} = \partial H(p, q) / \partial p} . \quad (\text{E.10})_{1.8}$$

We recognize this as the usual Legendre transform, relating the Hamilton-function  $H(p, q)$  to the Lagrange-function  $L(q, \dot{q})$ . Equation (E.9) is the famous Feynman path-integral, introduced in [126].

A direct derivation without introducing the field  $p$  can also be given. See section about the Laplace-DeGennes-transform where this is done in details for the Wick-rotated version.

**Question:** Which formulation is the fundamental one when  $H(p, q)$  is not quadratic in  $q$ ?

**Answer:** The formulation with  $H(p, q)$ . Our considerations with  $H(p, q)$  are completely general, whereas when working with  $L(q, \dot{q})$ , one has to make assumptions on the form of the kinetic term.

## E.2 Imaginary time path-integral: The partition function

We now use the normalizations as in section E.1, to calculate a path-integral representation for the partition function. This might not seem the most natural normalization to calculate  $\text{tr}(e^{-\beta\hat{H}})$ , since the latter does not contain  $\hbar$ ; however these are the appropriate normalizations in order to establish the connection between dynamics and thermodynamics.

We calculate the partition-function, thus

$$\mathcal{Z} = \text{tr}(e^{-\beta\hat{H}}) . \quad (\text{E.11})\text{mp6}$$

Using the Trotta formula to decompose  $\beta\hat{H}$  as  $\beta\hat{H} = \frac{1}{\hbar} \int_0^{\beta\hbar} d\tau \hat{H}$ , and using (E.5) we get

$$\mathcal{Z} = \int \mathcal{D}[q] \mathcal{D}[p] e^{\frac{1}{\hbar} \int_0^{\beta\hbar} d\tau (ip(\tau)\dot{q}(\tau) - H(p(\tau), q(\tau)))} . \quad (\text{E.12})\text{mp7}$$

In difference to (E.10), the weight-function is now the Euclidean action  $S_E[q, \dot{q}]$ , given by the saddle-point

$$0 = \frac{\partial}{\partial p} (ip\dot{q} - H(p, q)) \quad (\text{E.13})\text{mp8}$$

as

$$L_E(q, \dot{q}) = -L(q, i\dot{q}) , \quad S_E = \int_0^{\beta\hbar} d\tau L_E(q(\tau), \dot{q}(\tau)) . \quad (\text{E.14})\text{mp9}$$

The sign-convention in the definition of  $S_E$  is such that

$$\mathcal{Z} = \int \mathcal{D}[q] e^{-\frac{1}{\hbar} S_E} . \quad (\text{E.15})\text{mp10}$$

Also note that observables can be calculated, by inserting them into the path-integral. The path-integral naturally orders observables by their time (earlier to the right).

## E.3 The action for more general Hamiltonians and commutation-relations

We now want to construct the path-integral for more general Hamilton-operators and more general commutation-relations. Suppose that we have a quantum field theory given by ( $K_{xy}$  is supposed to be real):

$$\mathcal{H}(\hat{\phi}_x, \hat{\Pi}_x) , \quad [\hat{\Pi}_x, \hat{\phi}_y] = \frac{\hbar}{i} K_{xy} , \quad [\hat{\phi}_x, \hat{\phi}_y] = 0 , \quad [\hat{\Pi}_x, \hat{\Pi}_y] = 0 \quad (\text{E.16})\text{mg1}$$

This is sufficient to construct the path-integral, as one can see from the following: First, we construct the  $\phi$ -representation of the operator  $\hat{\Pi}_x$ :

$$\hat{\Pi}_x = \frac{\hbar}{i} \int_y K_{xy} \frac{\delta}{\delta\phi_y} , \quad (\text{E.17})\text{mg2}$$

which is checked by remarking that it reproduces the commutation-relation (E.16). To construct the path-integral, we need the basis-change from  $\phi$  to  $\Pi$ , which from  $(\Pi_x - \frac{\hbar}{i} \int_y K_{xy} \frac{\delta}{\delta\phi_y}) \langle\phi|\Pi\rangle = 0$  is inferred to be

$$\langle\phi|\Pi\rangle = \det [K_{xy}]^{-\frac{1}{2}} e^{\frac{i}{\hbar} \int_x \int_y \Pi_x K_{xy}^{-1} \phi_y} . \quad (\text{E.18})\text{mg3}$$

The normalization (often dropped) is checked from

$$\int \mathcal{D}[\Pi] \langle\phi|\Pi\rangle \langle\Pi|\phi'\rangle = \det [K_{xy}]^{-1} \int \mathcal{D}[\Pi] e^{\frac{i}{\hbar} \int_x \int_y (\phi_x - \phi'_x) K_{xy}^{-1} \Pi_y} = \int \mathcal{D}[\Pi'] e^{\frac{i}{\hbar} \int_x \int_y (\phi_x - \phi'_x) \Pi'_x} , \quad (\text{E.19})\text{mg4}$$



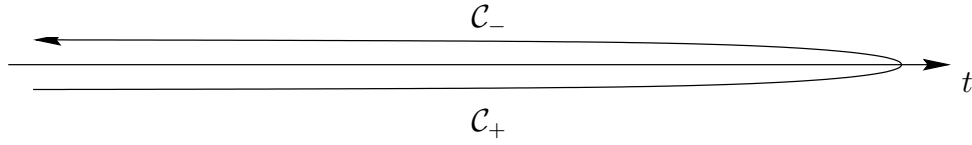


Figure E.1: The Keldysh contour

which is the  $\delta$ -distribution for  $\phi$ .

This gives the generalized path-integral

$$\langle \phi_{x,t} | \phi_{0,0} \rangle = \int \mathcal{D}[\phi] \mathcal{D}[\Pi] e^{\frac{i}{\hbar} \mathcal{S}} \quad (\text{E.20})$$

$$\mathcal{S} = \int_0^t dt \int_x \Pi_x K_{xy}^{-1} \dot{\phi}_y - \mathcal{H}(\phi, \Pi) \quad (\text{E.21})$$

Since from the action, we can calculate *all* observables, this also leads to the following

**Theorem:** A Quantum theory is given by its classical Hamilton-function, e.g. as a function of coordinates (or fields) and conjugate momenta, and their commutation relations.

## E.4 The Keldysh-formalism

Here, I construct some formulas as what is known as the “Keldysh-formalism”.

Denote for any contour  $\mathcal{C}$

$$S_{\mathcal{C}} := \int_{\mathcal{C}} dt L(q(t), \dot{q}(t)) . \quad (\text{E.22}) \times 1$$

We also use

$$S_+ := S_{\mathcal{C}_+} , \quad S_- := S_{\mathcal{C}_-} \quad (\text{E.23})$$

$$U_+ = e^{i/\hbar S_+} , \quad U_- = e^{i/\hbar S_-} . \quad (\text{E.24})$$

Let us call the time-variable on the lower path  $t_+$  (since it goes into positive direction) and that on the upper path  $t_-$ . Also  $q_+ = q(t_+)$  a.s.o. Thus

$$S_+ = \int dt m \frac{\dot{q}_+^2}{2} - V(q_+) \quad (\text{E.25})$$

$$S_- = \int dt m \frac{\dot{q}_-^2}{2} - V(q_-) . \quad (\text{E.26})$$

Now introduce coordinates in the center-of-mass system.

$$q_{\pm} := q \pm \check{q} \quad (\text{E.27})$$

$$q = \frac{1}{2} (q_+ + q_-) \quad (\text{E.28})$$

$$\check{q} = \frac{1}{2} (q_+ - q_-) . \quad (\text{E.29})$$

Then

$$S_{\mathcal{C}} := S_+ - S_- = \int dt (L_+ - L_-) , \quad (\text{E.30}) \times 5$$

since path  $\mathcal{C}_-$  has the opposite direction as path  $\mathcal{C}_+$ .

$$\begin{aligned}
S_{\mathcal{C}} &= \int_{t_i}^{t_f} dt m \left( \frac{\dot{q}_+^2}{2} - \frac{\dot{q}_-^2}{2} \right) - V(q_+) + V(q_-) \\
&= \int_{t_i}^{t_f} dt 2m \dot{q} \ddot{q} - V(q + \check{q}) + V(q - \check{q}) \\
&= - \int_{t_i}^{t_f} dt 2m \check{q} \frac{d^2}{dt^2} q + V(q + \check{q}) - V(q - \check{q}) ,
\end{aligned} \tag{E.31}$$

where in the last partial integration boundary terms are neglected.

One should be able to calculate correlation-functions by inserting fields into the contour-integral, say all in  $\mathcal{C}_+$ . This would give ( $q_1 := q(t_1)$ )

$$\begin{aligned}
\langle \mathcal{O}_1 \mathcal{O}_2 \rangle &= \int \mathcal{D}[q] \mathcal{D}[\check{q}] \mathcal{O}_1(q_1 + \check{q}_1) \mathcal{O}_2(q_2 + \check{q}_2) e^{\frac{i}{\hbar} S} \\
&= \int \mathcal{D}[q] \mathcal{D}[\check{q}] \mathcal{O}_1(q_1 + \check{q}_1) \mathcal{O}_2(q_2 + \check{q}_2) \\
&\quad \times \exp \left[ -\frac{i}{\hbar} \int_{t_i}^{t_f} dt 2m \check{q} \frac{d^2}{dt^2} q + V(q + \check{q}) - V(q - \check{q}) \right] .
\end{aligned} \tag{E.32}$$

Response-functions should be constructed by looking at an observable  $\mathcal{O}_2$  reacting to a change in the potential (a force)  $\delta\mathcal{L}(q, \dot{q}) = \delta(t - t_1) \mathcal{O}_1(q)$  at time  $t_1$ . (Note that making a change in  $\mathcal{L}$  is equivalent to making a change in  $-\mathcal{H}$ . Since the force is  $-\nabla V$ , this will for  $\mathcal{O}_1 = q$  be the response to a uniform force, with the correct sign.) Also note that this perturbation appears in both parts of the Keldysh-integral. Its linear response is

$$\begin{aligned}
&\frac{i}{\hbar} \int \mathcal{D}[q] \mathcal{D}[\check{q}] [\mathcal{O}_1(q_1 + \check{q}_1) - \mathcal{O}_1(q_1 - \check{q}_1)] \mathcal{O}_2(q_2 + \check{q}_2) \\
&\quad \times \exp \left[ -\frac{i}{\hbar} \int_{t_i}^{t_f} dt 2m \check{q} \frac{d^2}{dt^2} q + V(q + \check{q}) - V(q - \check{q}) \right] .
\end{aligned} \tag{E.33}$$

Choosing  $\mathcal{O}_1 = \mathcal{O}_2 = q$ , this gives

$$R_{qq} = \frac{2i}{\hbar} \langle \check{q}_1(q_2 + \check{q}_2) \rangle . \tag{E.34}$$

## E.5 A change in variables and the classical limit (MSR-action)

Starting at the path-integral

$$\begin{aligned}
&\int \mathcal{D}[q] \mathcal{D}[\check{q}] \mathcal{O}_1(q_1 + \check{q}_1) \mathcal{O}_2(q_2 + \check{q}_2) \\
&\quad \times \exp \left[ -\frac{i}{\hbar} \int_{t_i}^{t_f} dt 2m \check{q} \frac{d^2}{dt^2} q + V(q + \check{q}) - V(q - \check{q}) \right] ,
\end{aligned} \tag{E.35}$$

we define a new field  $\tilde{q}$

$$\tilde{q} := \frac{2i}{\hbar} \check{q} \equiv \frac{i}{\hbar} (q_+ - q_-) \tag{E.36}$$

In this new field, (E.35) becomes (the integration over  $\tilde{q}$  running from  $-i\infty$  to  $i\infty$ )

$$\begin{aligned}
&\int \mathcal{D}[q] \mathcal{D}[\tilde{q}] \mathcal{O}_1(q_1 + \frac{\hbar}{2i} \tilde{q}_1) \mathcal{O}_2(q_2 + \frac{\hbar}{2i} \tilde{q}_2) \\
&\quad \times \exp \left[ - \int_{t_i}^{t_f} dt m \tilde{q} \frac{d^2}{dt^2} q + \frac{i}{\hbar} V(q + \frac{\hbar}{2i} \tilde{q}) - \frac{i}{\hbar} V(q - \frac{\hbar}{2i} \tilde{q}) \right] ,
\end{aligned} \tag{E.37}$$

Using the convention of  $e^{-S}$ , we have

$$-S \equiv \frac{i}{\hbar} S \quad (\text{E.38})_{\text{m3.0}}$$

relating the new Keldysh-action to the real action.

$$S = \int_{t_i}^{t_f} dt m \tilde{q} \frac{d^2}{dt^2} q + \frac{i}{\hbar} V(q + \frac{\hbar}{2i} \tilde{q}) - \frac{i}{\hbar} V(q - \frac{\hbar}{2i} \tilde{q}) \quad (\text{E.39})_{\text{m3a}}$$

The classical limit is obtained upon taking  $\hbar \rightarrow 0$ . The action is then expanded as

$$S = \int_{t_i}^{t_f} dt \tilde{q} \left( m \frac{d^2}{dt^2} q + V'(q) - \frac{\tilde{q}^2 \hbar^2}{24} V'''(q) + \dots \right), \quad (\text{E.40})$$

which is just the MSR-action + higher order terms in  $\hbar$ .

## E.6 Boundary-conditions and the Feynman-Vernon-influence function

We want to study something like (note that  $E'_n$  need not be equivalent to  $\langle n | \mathcal{H} | n \rangle$ , but can be taken from an initial Hamiltonian  $\mathcal{H}'$ .)

$$\frac{1}{\mathcal{Z}} \sum_n \langle n | U_- \mathcal{O} U_+ | n \rangle e^{-\beta E'_n}. \quad (\text{E.41})_1$$

This can be written as the *Feynman-Vernon-influence-function* [127]

$$\int_{q_1} \int_{q_2} \frac{\langle q_1 | e^{-\beta \mathcal{H}'} | q_2 \rangle}{\mathcal{Z}} \langle q_2 | U_- \mathcal{O} U_+ | q_1 \rangle, \quad (\text{E.42})_2$$

where

$$\mathcal{Z} := \text{tr} \left( e^{-\beta \mathcal{H}'} \right). \quad (\text{E.43})$$

Let us now calculate some observables. For the moment, we prepare the system with a different Hamiltonian  $\mathcal{H}'$  than the time-evolving one  $\mathcal{H}$ . This condition will be dropped later.

$$\langle q_+(t) q_+(t') \rangle = \frac{1}{\mathcal{Z}} \text{tr} \left( e^{-\beta \mathcal{H}'} T^+ q(t) q(t') \right) \quad (\text{E.44})_1$$

On the l.h.s. stand expectation values in the path integral, whereas on the r.h.s. expectation values in the operator formalism.

$$q(t) := e^{i\mathcal{H}t} q e^{-i\mathcal{H}t} \quad (\text{E.45})_2$$

and  $T^+$  the time ordering operator, putting larger times to the left.  $T^-$  is the anti-time ordering operator, thus analogously

$$\langle q_-(t) q_-(t') \rangle = \frac{1}{\mathcal{Z}} \text{tr} \left( e^{-\beta \mathcal{H}'} T^- q(t) q(t') \right). \quad (\text{E.46})_3$$

Further, since  $q_+$  is always earlier on the contour,

$$\langle q_+(t) q_-(t') \rangle = \frac{1}{\mathcal{Z}} \text{tr} \left( e^{-\beta \mathcal{H}'} q(t) q(t') \right). \quad (\text{E.47})_4$$

Therefore, using our earlier definitions in (E.27) ff. we obtain with the time-ordering operator on the Keldysh-contour  $\mathcal{C}$

$$\langle q(t) q(t') \rangle = \frac{1}{4\mathcal{Z}} \text{tr} \left( e^{-\beta \mathcal{H}'} T_{\mathcal{C}} \{ (q_+(t) + q_-(t))(q_+(t') + q_-(t')) \} \right). \quad (\text{E.48})_5$$

Observing that e.g. for  $t < t'$ ,  $q_+(t)$  is always first in the trace, and  $q_-(t')$  always last, we get with (E.45)

$$\begin{aligned}\langle q(t)q(t') \rangle &= \frac{1}{2\mathcal{Z}} \text{tr} \left( e^{-\beta\mathcal{H}'} \{q(t)q(t') + q(t')q(t)\} \right) \\ &= \frac{1}{2\mathcal{Z}} \text{tr} \left( e^{-\beta\mathcal{H}'} \{q(t), q(t')\} \right) .\end{aligned}\tag{E.49}$$

Next is

$$\begin{aligned}\langle q(t)\check{q}(t') \rangle &= \frac{1}{4\mathcal{Z}} \text{tr} \left( e^{-\beta\mathcal{H}'} T_C [(q_+(t) + q_-(t))(q_+(t') - q_-(t'))] \right) \\ &= \frac{1}{4\mathcal{Z}} \text{tr} \left( e^{-\beta\mathcal{H}'} T_C [q_+(t)q_+(t') - q_+(t)q_-(t') + q_-(t)q_+(t') - q_-(t)q_-(t')] \right) \\ &= \Theta(t - t') \frac{1}{2\mathcal{Z}} \text{tr} \left( e^{-\beta\mathcal{H}'} [q(t), q(t')] \right) .\end{aligned}\tag{E.50}$$

Last:

$$\begin{aligned}\langle \check{q}(t)\check{q}(t') \rangle &= \frac{1}{4\mathcal{Z}} \text{tr} \left( e^{-\beta\mathcal{H}'} T_C [(q_+(t) - q_-(t))(q_+(t') - q_-(t'))] \right) \\ &= \frac{1}{4\mathcal{Z}} \text{tr} \left( e^{-\beta\mathcal{H}'} T_C [q_+(t)q_+(t') + q_-(t)q_-(t') - q_+(t)q_-(t') - q_-(t)q_+(t')] \right) \\ &= 0 .\end{aligned}\tag{E.51}$$

These formulas are similar to MSR. The Green-function (response-function) is causal, i.e. *retarded*. Note that from (E.50), and due to (E.51) the response-function is

$$R(t - t') := \frac{\delta \langle q(t) \rangle}{\delta L(t')} = \frac{2i}{\hbar} \langle \check{q}(t')q(t) \rangle\tag{E.52}9a$$

Using the above and the definition (E.36) of  $\tilde{q}$ , we arrive at the important formula

$$R(t, t') = \langle q(t)\tilde{q}(t') \rangle = \Theta(t - t') \frac{i}{\hbar} \text{tr} \left( e^{-\beta\mathcal{H}'} [q(t), q(t')] \right) .\tag{E.53}9$$

The correlation function is for comparison

$$C(t, t') = \langle q(t)q(t') \rangle = \frac{1}{2\mathcal{Z}} \text{tr} \left( e^{-\beta\mathcal{H}'} \{q(t), q(t')\} \right) .\tag{E.54}10$$

## E.7 FDT (quantum version)

Let us now derive the FDT. To do so, we need  $\mathcal{H}' = \mathcal{H}$ . (At least they have to commute. Otherwise  $e^{-\beta\mathcal{H}'}$  is not diagonal in the same basis as  $e^{it\mathcal{H}/\hbar}$ . Here we suppose, they are equal.) We use

$$\text{tr} \left( e^{-\beta\mathcal{H}} q(t)q(t') \right) = \sum_{n,m} \langle n | e^{\frac{i}{\hbar}\mathcal{H}t} q e^{-\frac{i}{\hbar}\mathcal{H}t} | m \rangle \langle m | e^{\frac{i}{\hbar}\mathcal{H}t'} q e^{-\frac{i}{\hbar}\mathcal{H}t'} | n \rangle e^{-\beta E_n}\tag{E.55}use$$

to insert a complete set of energy-eigenstates into both (E.49) and (E.50):

$$\langle q(t)q(t') \rangle = \frac{1}{2\mathcal{Z}} \sum_{n,m} |\langle n | q | m \rangle|^2 e^{-\beta E_n} \left( e^{i(t-t')(E_n - E_m)/\hbar} + e^{-i(t-t')(E_n - E_m)/\hbar} \right)\tag{E.56}$$

$$\langle q(t)\check{q}(t') \rangle = \Theta(t - t') \frac{1}{2\mathcal{Z}} \sum_{n,m} |\langle n | q | m \rangle|^2 e^{-\beta E_n} \left( e^{i(t-t')(E_n - E_m)/\hbar} - e^{-i(t-t')(E_n - E_m)/\hbar} \right) .\tag{E.57}$$

Both functions are (for  $t > t'$ ) real and imaginary part of  $\frac{1}{2\mathcal{Z}} \sum_{n,m} |\langle n|q|m\rangle|^2 e^{-\beta E_n} e^{i(t-t')(E_n-E_m)/\hbar}$ . We now go to frequency-space.

$$\begin{aligned}
\langle q(\omega)q(-\omega)\rangle &= \int_{-\infty}^{\infty} dt e^{-i\omega t} \langle q(t)q(0)\rangle \\
&= \int_{-\infty}^{\infty} dt e^{-i\omega t} \frac{1}{2\mathcal{Z}} \sum_{n,m} |\langle n|q|m\rangle|^2 e^{-\beta E_n} (e^{it(E_n-E_m)/\hbar} + e^{-it(E_n-E_m)/\hbar}) \\
&= \int_{-\infty}^{\infty} dt e^{-i\omega t} \frac{1}{2\mathcal{Z}} \sum_{n,m} |\langle n|q|m\rangle|^2 (e^{-\beta E_n} + e^{-\beta E_m}) e^{it(E_n-E_m)/\hbar} \\
&= \frac{1}{2\mathcal{Z}} \sum_{n,m} |\langle n|q|m\rangle|^2 (e^{-\beta E_n} + e^{-\beta E_m}) 2\pi\delta(\omega + (E_m - E_n)/\hbar) \\
&= (1 + e^{-\beta\omega\hbar}) \frac{1}{2\mathcal{Z}} \sum_{n,m} |\langle n|q|m\rangle|^2 e^{-\beta E_n} 2\pi\delta(\omega + (E_m - E_n)/\hbar). \tag{E.58}
\end{aligned}$$

The response function is (adding  $-i\delta$  to  $\omega$  to ensure convergence; also note the integral starts at  $t = 0$  due to the  $\Theta$ -function in (E.57).)

$$\begin{aligned}
&\langle q(\omega)\check{q}(\omega)\rangle \\
&= \int_0^{\infty} dt e^{-i\omega t - \delta t} \langle q(t)\check{q}(0)\rangle \\
&= \int_0^{\infty} dt e^{-i\omega t - \delta t} \frac{1}{2\mathcal{Z}} \sum_{n,m} |\langle n|q|m\rangle|^2 e^{-\beta E_n} (e^{it(E_n-E_m)/\hbar} - e^{-it(E_n-E_m)/\hbar}) \\
&= \int_0^{\infty} dt e^{-i\omega t - \delta t} \frac{1}{2\mathcal{Z}} \sum_{n,m} |\langle n|q|m\rangle|^2 (e^{-\beta E_n} - e^{-\beta E_m}) e^{it(E_n-E_m)/\hbar} \\
&= \frac{1}{2\mathcal{Z}} \sum_{n,m} |\langle n|q|m\rangle|^2 (e^{-\beta E_n} - e^{-\beta E_m}) \frac{1}{\delta + i\omega + i(E_m - E_n)/\hbar} \\
&= \frac{1}{2\mathcal{Z}} \sum_{n,m} |\langle n|q|m\rangle|^2 (e^{-\beta E_n} - e^{-\beta E_m}) \left[ \mathcal{P} \frac{-i}{\omega + (E_m - E_n)/\hbar} + \pi\delta(\omega + (E_m - E_n)/\hbar) \right]. \tag{E.59}
\end{aligned}$$

The real part of that is

$$(1 - e^{-\beta\hbar\omega}) \frac{1}{2\mathcal{Z}} \sum_{n,m} |\langle n|q|m\rangle|^2 e^{-\beta E_n} \pi\delta(\omega + (E_m - E_n)/\hbar). \tag{E.60}$$

The FDT is

$$\langle q(\omega)q(-\omega)\rangle = 2 \coth\left(\frac{\beta\hbar\omega}{2}\right) \Im \langle q(\omega)i\check{q}(-\omega)\rangle \tag{E.61}$$

In terms of the physical correlation  $C(\omega)$  and response-function  $R(\omega)$ , this is

$$C(\omega) = \hbar \coth\left(\frac{\beta\hbar\omega}{2}\right) \Im R(\omega). \tag{E.62}$$

In the limit of  $\hbar \rightarrow 0$ , this reduces to

$$C(\omega) \xrightarrow{\hbar \rightarrow 0} \frac{2}{\omega\beta} \Im R(\omega). \tag{E.63}$$

As a function of the time-difference, we state without proof the result

$$R(t) = \frac{\beta}{2} \Theta(t) \frac{d}{dt} C(t) . \quad (\text{E.64})_{\text{dt11}}$$

## E.8 The Matsubara-relation

Let us recall that (E.50) gives (if  $\mathcal{H} = \mathcal{H}'$ )

$$\langle q(t) \check{q}(0) \rangle = \Theta(t) \frac{1}{2\mathcal{Z}} \text{tr} \left( e^{-\beta\mathcal{H}} [q(t), q(0)] \right) , \quad (\text{E.65})_{\text{ma1}}$$

and from the second to last line of (E.59) its Fourier-transform is

$$\langle q(\omega) \check{q}(\omega) \rangle = \frac{1}{2\mathcal{Z}} \sum_{n,m} |\langle n|q|m \rangle|^2 (e^{-\beta E_n} - e^{-\beta E_m}) \frac{1}{\delta + i\omega + i(E_n - E_m)/\hbar} . \quad (\text{E.66})$$

We now define the imaginary time correlation-function (also called Matsubara-function) for  $0 \leq \tau \leq \beta\hbar$  (which can be continued analytically to  $\tau \in \mathbb{R}$  giving a  $\beta\hbar$ -periodic function.)

$$U(\tau) := \frac{1}{\mathcal{Z}} \text{tr} \left( e^{-(\beta-\tau/\hbar)\mathcal{H}} q e^{-(\tau/\hbar)\mathcal{H}} q \right) . \quad (\text{E.67})_{\text{ma3}}$$

Its Fourier-transform is defined for

$$\omega_n := \frac{2\pi n}{\beta\hbar} , \quad n \in \mathbb{Z} \quad (\text{E.68})_{\text{ma3.a}}$$

as

$$U(\omega_n) := \int_0^{\beta\hbar} d\tau e^{-i\omega_n \tau} U(\tau) . \quad (\text{E.69})_{\text{ma4}}$$

The inverse is

$$U(\tau) = \frac{1}{\beta\hbar} \sum_n e^{i\omega_n \tau} U(\omega_n) . \quad (\text{E.70})_{\text{ma4.a}}$$

Similar to what we have done to derive (E.66), see (E.59), we now insert two complete sets of eigenfunctions of  $\mathcal{H}$

$$\begin{aligned} U(\omega_n) &= \frac{1}{\mathcal{Z}} \int_0^{\beta\hbar} d\tau e^{-i\omega_n \tau} \text{tr} \left( e^{-(\beta-\tau/\hbar)\mathcal{H}} q e^{-\tau\mathcal{H}/\hbar} q \right) \\ &= \frac{1}{\mathcal{Z}} \int_0^{\beta\hbar} d\tau e^{-i\omega_n \tau} \sum_{n,m} |\langle n|q|m \rangle|^2 e^{-\beta E_m - \tau(E_n - E_m)/\hbar} \\ &= \frac{1}{\mathcal{Z}} \sum_{n,m} |\langle n|q|m \rangle|^2 (e^{-\beta E_n} - e^{-\beta E_m}) \frac{1}{-i\omega_n + (E_n - E_m)/\hbar} \\ &= \frac{i}{\mathcal{Z}} \sum_{n,m} |\langle n|q|m \rangle|^2 (e^{-\beta E_n} - e^{-\beta E_m}) \frac{1}{\omega_n + i(E_n - E_m)/\hbar} . \end{aligned} \quad (\text{E.71})$$

Note that by going from line 2 to 3, we have needed that  $\omega_n$  is quantised by (E.68); the factors of  $e^{-\beta E_n}$  and  $e^{-\beta E_m}$  are the boundary values of the integration. Comparing (E.66) and (E.71), we arrive at

$$\langle q(\omega) \check{q}(\omega) \rangle = \frac{1}{2i} U(\omega_n = i\omega + \delta) . \quad (\text{E.72})_{\text{ma6}}$$

The physical response-function is  $R(\omega) = \langle q(\omega)\tilde{q}(\omega) \rangle$  such that

$$R(\omega) = \frac{1}{\hbar} U(\omega_n = i\omega + \delta) . \quad (\text{E.73})_{\text{ma8}}$$

The correlation-function can then be obtained from the FDT (E.62) as

$$C(\omega) = \coth\left(\frac{\beta\hbar\omega}{2}\right) \Im U(\omega_n = i\omega + \delta) . \quad (\text{E.74})_{\text{ma10}}$$

One can also relate the response-function in the time-variable. Using (E.53) and the definition of  $U(\tau)$  in (E.67), we can write

$$R(t) = \Theta(t) \frac{i}{\hbar} [U(\tau \rightarrow it + \delta) - U(\tau \rightarrow it - \delta)] , \quad (\text{E.75})_{\text{ma12}}$$

where  $\delta$  serves to give the time-ordering. Equivalently, the correlation-function is from (E.54) obtained as

$$C(t) = \frac{1}{2} [U(\tau \rightarrow it + \delta) + U(\tau \rightarrow it - \delta)] , \quad (\text{E.76})_{\text{ma12bis}}$$

## E.9 Free theory

Study the quadratic action (note that the weight is  $e^{-\mathcal{S}}$ )

$$\mathcal{S} = \int_{x,t} \tilde{u} (m\partial_t^2 - \Delta) u + \frac{i}{\hbar} V(u + \frac{\hbar}{2i}\tilde{u}) - \frac{i}{\hbar} V(u(x,t) - \frac{\hbar}{2i}\tilde{u}) \quad (\text{E.77})$$

where  $V(u) = \kappa u^2$ . This gives

$$\mathcal{S} = \int_{x,t} \tilde{u} (m\partial_t^2 - \Delta + \kappa) u \quad (\text{E.78})$$

Two paths can be taken to calculate the response-function. First in analogy to MSR, we have directly

$$R(\omega, k) = \frac{1}{k^2 + \kappa - m\omega^2} , \quad (\text{E.79})_{\text{free3}}$$

where a priori it is not clear, which is the way to shift the poles from the axis. However, this could be obtained by demanding (E.79) to be causal (retarded). The other method is to use the Matsubara technique. The problem is, that one first has to construct the path-integral. Following the line of arguments that led from (E.25) to (E.39) and (E.40), we have for the Lagrange-function

$$L = \int_x \frac{m}{2} \left(\frac{d}{dt}u\right)^2 - \frac{1}{2}(\nabla u)^2 - \frac{\kappa}{2}u^2 \quad (\text{E.80})_{\text{free4}}$$

Continuing to Euclidean time, we have as Euclidean action the immediate generalization of (E.14):

$$S_E = \int_0^{\beta\hbar} d\tau \int_x \frac{m}{2} \left(\frac{d}{d\tau}u\right)^2 + \frac{1}{2}(\nabla u)^2 + \frac{\kappa}{2}u^2 \quad (\text{E.81})_{\text{free5}}$$

We know how to calculate the correlation-function of this model, which is the Matsubara-function ( $\omega_n \in \frac{2\pi}{\beta\hbar}\mathbb{N}$ ):

$$U(k, \omega_n) = \langle u(k, \omega_n)u(-k, -\omega_n) \rangle = \frac{\hbar}{k^2 + m\omega_n^2/\hbar^2 + \kappa} , \quad (\text{E.82})_{\text{free6}}$$

where the  $\hbar$  comes from  $e^{-S_E/\hbar}$ . Using relation (E.73), this gives for the response-function

$$R(k, \omega) = \frac{1}{\hbar} U(k, \hbar(i\omega + \delta)) = \frac{1}{k^2 - m(\omega - i\delta)^2 + \kappa} \quad (\text{E.83})_{\text{free7}}$$

We can check, that this is causal:

$$\int \frac{d\omega}{2\pi} e^{i\omega t} R(k, \omega) = \Theta(t) \frac{\sin\left(\frac{t\sqrt{k^2 + \kappa}}{\sqrt{m}}\right)}{\sqrt{m}\sqrt{k^2 + \kappa}} \quad (\text{E.84})_{\text{free8}}$$

## F Tools for self-avoiding membranes

### F.1 Equation of motion and redundant operators

The equation of motion reflects the invariance of the functional integral under a global rescaling of the field  $r$ . This has important consequences. Consider the expectation value of an observable  $\mathcal{O}$  in the free theory:

$$\langle \mathcal{O} \rangle_0 = \frac{\int \mathcal{D}[r] \mathcal{O} e^{-\frac{1}{2-D} \int_x \star}}{\int \mathcal{D}[r] e^{-\frac{1}{2-D} \int_x \star}}. \quad (\text{F.1})_{\text{EM1}}$$

We now perform a global rescaling of  $r(x)$ :

$$r(x) \longrightarrow (1 + \kappa)r(x). \quad (\text{F.2})$$

The expectation value of  $\mathcal{O}$ , Eq. (F.1) remains unchanged. Expanding up to first order in  $\kappa$  yields

$$\langle \mathcal{O} \rangle_0 = \frac{\int \mathcal{D}[r] \mathcal{O} (1 + \kappa [\mathcal{O}]_r) \left(1 - \frac{2\kappa}{2-D} \int_x \star\right) e^{-\frac{1}{2-D} \int_x \star}}{\int \mathcal{D}[r] \left(1 - \frac{2\kappa}{2-D} \int_x \star\right) e^{-\frac{1}{2-D} \int_x \star}}, \quad (\text{F.3})_{\text{EM2}}$$

where  $[\mathcal{O}]_r$  is the canonical dimension of the operator  $\mathcal{O}$ , measured in units of  $r$ , i.e. such that  $[r]_r = 1$ . Calculating the difference of Eqs. (F.1) and (F.3) gives:

$$\left\langle \mathcal{O} \int \star \right\rangle_0^{\text{conn}} = \nu [\mathcal{O}]_r \langle \mathcal{O} \rangle_0, \quad (\text{F.4})_{\text{Equation of}}$$

where  $^{\text{conn}}$  denotes the connected expectation value. For several operators we have

$$\left\langle \mathcal{O}_1 \mathcal{O}_2 \int \star \right\rangle_0^{\text{conn}} = \nu ([\mathcal{O}_1]_r + [\mathcal{O}_2]_r) \langle \mathcal{O}_1 \mathcal{O}_2 \rangle_0. \quad (\text{F.5})_{\text{Equation of}}$$

A specific example is

$$\left\langle \bullet \text{---} \bullet \int \star \right\rangle_0^{\text{conn}} = -\nu d \langle \bullet \text{---} \bullet \rangle_0. \quad (\text{F.6})$$

In the case of infinitely large membranes, these relations are equivalently valid for non-connected expectation values. (To prove this, remark that  $\langle \star \rangle_0 = 0$  by analytic continuation.)



Let us try to understand Eq. (F.4) perturbatively. For this purpose, it will turn out to be convenient to integrate by parts the free Hamiltonian as

$$\frac{1}{2} \int_x (\nabla r(x))^2 = \frac{1}{2} \int_x r(x)(-\Delta)r(x). \quad (\text{F.7})$$

For simplicity, we consider infinite membranes, such that connected expectation values can be replaced by standard ones. For computational convenience further suppose that  $\mathcal{O}[r]$  is a *function* of  $r(y)$ ,  $\mathcal{O}[r] = \mathcal{O}(r(y))$ . Then

$$\left\langle \mathcal{O}(r(y)) \int_x \text{---} \right\rangle_0 = \left\langle \mathcal{O}(r(y)) \frac{1}{2} \int_x r(x)(-\Delta)r(x) \right\rangle_0. \quad (\text{F.8})$$

We now proceed according to the following strategy: First contract the field  $r(x)$  which is preceded by  $(-\Delta)$  with any field in  $\mathcal{O}(r(y))$ . This yields (for normalizations and conventions see appendix ??)

$$\begin{aligned} \frac{1}{2} \int_x \left\langle r(x)(-\Delta_x)C(x-y) \frac{\partial \mathcal{O}(r(y))}{\partial r(y)} \right\rangle_0 &= \frac{2-D}{2} \int_x \left\langle r(x) \tilde{\delta}^D(x-y) \frac{\partial \mathcal{O}(r(y))}{\partial r(y)} \right\rangle_0 \\ &= \frac{2-D}{2} \left\langle r(y) \frac{\partial \mathcal{O}(r(y))}{\partial r(y)} \right\rangle_0. \end{aligned} \quad (\text{F.9})$$

Since  $\mathcal{O}$  is a homogeneous function in  $r$ , then

$$r(y) \frac{\partial \mathcal{O}(r(y))}{\partial r(y)} = [\mathcal{O}]_r \mathcal{O}(r(y)),$$

the operator is reproduced and we recover the equation of motion (F.4). Note that in this argumentation, it is irrelevant how the second field  $r$  of  $\text{---}$  is finally contracted.

In the case of several operators, the field  $r(x)$  which is preceded by  $(-\Delta)$  can be contracted with any of these operators, and one recovers Eq. (F.5).

Note also that without partially integrating the free action, no  $\tilde{\delta}^D$ -distribution is obtained and it is impossible to assign  $\text{---}$  to one of the points with which its fields are contracted: The integral is delocalized. This is a subtle point which was ingeniously avoided up to now. To understand this point remember that the renormalization of the coupling and by this means the  $\beta$ -function (2.118), not only contains the direct term  $\langle \text{---} \text{---} \text{---} \rangle$ , but also a term  $-\frac{2-D}{2} d \langle \text{---} \text{---} \text{---} \rangle$ . In exercise F.5 (page 164) the reader can show that the above arguments can be used to obtain this term directly.

We now turn to another concept, which is also a consequence of reparametrization invariance, namely redundant operators, as introduced by Wegner [128].

Consider the path-integral

$$\int \mathcal{D}[r] e^{-\mathcal{H}[r]} \quad (\text{F.10})$$

with the Hamiltonian of the interacting theory

$$\mathcal{H}[r] = \frac{Z}{2-D} \int_x \text{---} + bZ_b \mu^\epsilon \int_x \int_y \text{---} \text{---} \quad (\text{F.11})$$

and make a change of variables

$$r(x) \longrightarrow r(x) + \kappa(x) \mathcal{F}[r]. \quad (\text{F.12})$$

$\mathcal{F}[r]$  is an arbitrary function of  $r(x)$ , but may also involve fields  $r(y)$  at different points. (Explicitly, we think of  $\mathcal{F}[r] = f_1(r(x))$  or  $\mathcal{F}[r] = f_2(r(x), r(y))$  with  $x \neq y$ , where both  $f_1(r)$  and  $f_2(r, r')$  are functions of  $r$  and  $r, r'$  respectively. More general expressions for  $\mathcal{F}[r]$  including derivatives of  $r$  are possible, but

shall not be considered here.) Of course, since this is a simple variable-transformation, the path-integral itself remains unchanged, even-though formally new terms are generated<sup>8</sup>. These newly generated terms contain no physical information, and are thus called *redundant operators* [128]. They are useful in relating apparently different operators.

Let us extract the terms linear in  $\kappa(u) \sim \delta^D(u - x)$ . Two contributions have to be taken into account: First, from the expansion of the exponential, one obtains a term

$$- \mathcal{F}[r] \frac{\delta \mathcal{H}[r]}{\delta r(x)}. \quad (\text{F.13})$$

Second, the integration measure is changed, resulting in a term

$$\frac{\delta \mathcal{F}[r]}{\delta r(x)}. \quad (\text{F.14})$$

(Note that in the cases of  $\mathcal{F}[r] = f_1(r(x))$  or  $\mathcal{F}[r] = f_2(r(x), r(y))$  with *functions*  $f_1$  and  $f_2$ , this is equivalent to  $\frac{\partial \mathcal{F}[r]}{\partial r(x)} \tilde{\delta}^D(0)$ .) Combining both of them, we obtain the redundant operator

$$\mathcal{R} = \mathcal{F}[r] \frac{\delta \mathcal{H}[r]}{\delta r(x)} - \frac{\delta \mathcal{F}[r]}{\delta r(x)}. \quad (\text{F.15})$$

The second term just subtracts the contraction of  $\mathcal{F}[r]$  with the variation of the (free) quadratic part of the Hamiltonian  $\frac{\delta \mathcal{H}_0[r]}{\delta r(x)} = -(2-D)^{-1} \Delta r(x)$  at the same point. (This is the same structure as encountered within different discretization prescriptions in dynamic theories, see e.g. [25].) Since  $\frac{\delta \mathcal{F}[r]}{\delta r(x)} \sim \delta^D(0) \equiv \int d^D p$  is zero by analytic continuation, we will drop it in the following.

Let us now explore some of the consequences of the above construction. First set  $\mathcal{F}[r] := 1$ , yielding the redundant operator – or Dyson-Schwinger equation of motion [129] in the terminology of elementary particle physics:  $\mathcal{R} = 0$  with

$$\mathcal{R} = \frac{\delta \mathcal{H}[r]}{\delta r(x)} = \frac{Z}{2-D} (-\Delta) r(x) + b Z_b \mu^\epsilon \int_y \int_k (2ik) e^{ik[r(x)-r(y)]}. \quad (\text{F.16})$$

Another example is obtained by choosing  $\mathcal{F}[r] := r(x)$ , yielding the redundant operator

$$\mathcal{R} = \frac{Z}{2-D} r(x) (-\Delta) r(x) + b Z_b \mu^\epsilon \int_y \int_k [2ikr(x)] e^{ik[r(x)-r(y)]}. \quad (\text{F.17})$$

## F.2 Analytic continuation of the measure

We now define the explicit form for the integration measure in non-integer dimension  $D$  using the general formalism of distance geometry [130, 131].

The general problem is to integrate a function  $f(x_1, \dots, x_N)$ , which is invariant under Euclidean displacements (and therefore depends only on the  $N(N-1)/2$  relative distances  $|x_i - x_j|$  between these points) over the  $N-1$  first points (the last point is fixed, using translational invariance) in  $\mathbb{R}^D$  for non-integer  $D$ . In order to define the integration, let us take  $D \geq N-1$  and integer. For  $i < N$  we denote by  $y_i = x_i - x_N$  the  $i$ 'th distance-vector and by  $y_i^a$  its  $a$ 'th component ( $a = 1, \dots, D$ ).

---

<sup>8</sup>Also note that the inclusion of an observable  $\mathcal{O}[r(z)]$  is possible in the path-integral, but leads to additional contact-terms for  $z = x$ , and at other points on which  $\mathcal{F}[r]$  depends.

The integral over  $y_1$  is simple: Using rotation invariance, we fix  $y_1$  to have only the first ( $a = 1$ ) component non-zero. The measure becomes with the normalizations as listed in appendix ??

$$\int_{y_1} = \frac{1}{S_D} \int d^D y_1 = \int_0^\infty dy_1^1 (y_1^1)^{D-1}, \quad y_1 = (y_1^1, 0, \dots, 0). \quad (\text{F.18})$$

We now fix  $y_2$  to have only  $a = 1$  and  $a = 2$  as non-zero components. The integral over  $y_2$  consists of the integration along the direction fixed by  $y_1$  and the integration in the orthogonal space  $\mathbb{R}^{D-1}$ :

$$\int_{y_2} = \frac{1}{S_D} \int d^D y_2 = \frac{S_{D-1}}{S_D} \int_{-\infty}^\infty dy_2^1 \int_0^\infty dy_2^2 (y_2^2)^{D-2}, \quad y_2 = (y_2^1, y_2^2, 0, \dots, 0). \quad (\text{F.19})$$

For the  $j$ -th point, one proceeds recursively to integrate first over the hyper-plane defined by  $y_1, \dots, y_{j-1}$  and then the orthogonal complement:

$$\int_{y_j} = \frac{1}{S_D} \int d^D y_j = \frac{S_{D-j+1}}{S_D} \prod_{a < j} \int_{-\infty}^\infty dy_j^a \int_0^\infty dy_j^j (y_j^j)^{D-j}, \quad y_j = (y_j^1, \dots, y_j^j, 0, \dots, 0). \quad (\text{F.20})$$

The final result for an integral over all configurations of  $N$  points is

$$\prod_{j=1}^{N-1} \int_{y_j} = \frac{S_{D-1} \dots S_{D-N+2}}{S_D^{N-2}} \prod_{j=1}^{N-1} \left( \prod_{a=1}^{j-1} \int_{-\infty}^\infty dy_j^a \int_0^\infty dy_j^j (y_j^j)^{D-j} \right). \quad (\text{F.21})$$

This expression for the measure, now written in terms of the  $N(N-1)$  variables  $y_j^a$ , can be analytically continued to non-integer  $D$ . For  $D \leq N-2$  this measure is not integrable when some of the  $y_j^a \rightarrow 0$ . For  $D$  not integer, the integration is defined through the standard finite-part prescription. This means that the measure (F.21) becomes a distribution.

Let us make this explicit on the example of  $N = 3$  points. The measure is then

$$\frac{S_{D-1}}{S_D} \int_0^\infty dy_1^1 (y_1^1)^{D-1} \int_{-\infty}^{+\infty} dy_2^1 \int_0^\infty dy_2^2 (y_2^2)^{D-2}. \quad (\text{F.22})$$

It is well defined and integrable for  $D > 1$ . For  $D = 1$  the integral over  $y_2^2$  diverges logarithmically at  $y_2^2 \rightarrow 0$ , but this singularity is canceled by the zero of  $S_{D-1}$  and the measure becomes

$$\frac{1}{2} \int_0^\infty dy_1^1 \int_{-\infty}^{+\infty} dy_2^1 \int_0^\infty dy_2^2 \delta(y_2^2) = \frac{1}{4} \int_{-\infty}^\infty dy_1 \int_{-\infty}^\infty dy_2, \quad (\text{F.23})$$

thus it reduces to the measure for two points on a line. (The factor of  $\frac{1}{4} = \left(\frac{1}{2}\right)^2$  is due to our definition of the measure (??).) For  $0 < D < 1$  the integral over  $y_2^2$  diverges at  $y_2^2 \rightarrow 0$ , but this divergence is treated by a finite part prescription.

For integrals over  $N > 3$  points, a finite part prescription is already necessary for  $D < 2$ . This is the case of the 2-loop calculations, see section ??.

### F.3 IR-regulator, conformal mapping, extraction of the residue, and its universality

For the simple case of the MOPE-coefficients Eq. (2.106) and Eq. (2.112), the residues could easily be calculated directly. In more complicated situations however, it is useful to employ a more formal procedure

to extract the residue, which is presented now; first on the example of the 1-loop counter-terms, then in a more formal setting<sup>9</sup>.

Note from (2.106) that

$$\left\langle \left( \text{diagram} \right) \Big|_{\epsilon} \right\rangle_L = -\frac{1}{2D} \int_{x < L} x^{D-\nu d} = -\frac{1}{2D} \frac{1}{\epsilon} L^\epsilon. \quad (\text{F.24})_{\text{sss}}$$

(For the normalization of the measure, see appendix ??). The residue can most easily be extracted by applying  $L \frac{\partial}{\partial L}$  to (F.24). This yields

$$L \frac{\partial}{\partial L} \left\langle \left( \text{diagram} \right) \Big|_{\epsilon} \right\rangle_L = -\frac{1}{2D} L \int_x x^{D-\nu d} \delta(x-L) = -\frac{1}{2D} L^\epsilon. \quad (\text{F.25})$$

So the residue of Eq. (F.24) is

$$\left\langle \left( \text{diagram} \right) \Big|_{\epsilon} \right\rangle_\epsilon = \lim_{\epsilon \rightarrow 0} L \frac{\partial}{\partial L} \left\langle \left( \text{diagram} \right) \Big|_{\epsilon} \right\rangle_L = -\frac{1}{2D}. \quad (\text{F.26})$$

We can apply this recipe to the second 1-loop counter-term:

$$\left\langle \left( \text{diagram} \right) \Big|_{\epsilon} \right\rangle_L = \int_{x < L} \int_{y < L} \left( \text{diagram} \right), \quad (\text{F.27})$$

since it is also proportional to  $L^\epsilon$ . We thus have to calculate

$$L \frac{\partial}{\partial L} \left\langle \left( \text{diagram} \right) \Big|_{\epsilon} \right\rangle_L = L \left[ \int_{x < y=L} + \int_{y < x=L} \right] (x^{2\nu} + y^{2\nu})^{-d/2}. \quad (\text{F.28})_{\text{ssss}}$$

We now introduce a general method which is very useful to manipulate and simplify such integrals. It relies on (global) conformal transformations in position space and is called conformal mapping of sectors. It has first been introduced in [132], where a geometric interpretation can be found. We will explain the method on a concrete example and then state the general result.

Let us consider the second integral on the r.h.s. of (F.28)

$$L \int_{y < x=L} (x^{2\nu} + y^{2\nu})^{-d/2} = L \int_0^\infty \frac{dx}{x} x^D \int_0^\infty \frac{dy}{y} y^D (x^{2\nu} + y^{2\nu})^{-d/2} \delta(x-L) \Theta(y < x). \quad (\text{F.29})$$

Now two changes of variables are performed: The first one

$$x \longrightarrow \tilde{x}, \quad x = \tilde{x} y L^{-1} \quad (\text{F.30})$$

leads to

$$L^{1-D+\nu d} \int_0^\infty \frac{d\tilde{x}}{\tilde{x}} \tilde{x}^D \int_0^\infty \frac{dy}{y} y^{2D-\nu d} (\tilde{x}^{2\nu} + L^{2\nu})^{-d/2} \delta(\tilde{x} y L^{-1} - L) \Theta(L < \tilde{x}). \quad (\text{F.31})$$

The second one

$$y \longrightarrow \tilde{y}, \quad y = \tilde{y} \tilde{x}^{-1} L \quad (\text{F.32})$$

yields

$$L^{1+D} \int_0^\infty \frac{d\tilde{x}}{\tilde{x}} \tilde{x}^{D-\epsilon} \int_0^\infty \frac{d\tilde{y}}{\tilde{y}} \tilde{y}^\epsilon (\tilde{x}^{2\nu} + L^{2\nu})^{-d/2} \delta(\tilde{y} - L) \Theta(L < \tilde{x}), \quad (\text{F.33})$$

---

<sup>9</sup>This section may be skipped upon first reading.

which using  $\tilde{y} = L$  finally gives

$$L^{1+\epsilon} \int_0^\infty \frac{d\tilde{x}}{\tilde{x}} \tilde{x}^{D-\epsilon} \int_0^\infty \frac{d\tilde{y}}{\tilde{y}} \tilde{y}^D (\tilde{x}^{2\nu} + \tilde{y}^{2\nu})^{-d/2} \delta(\tilde{y} - L) \Theta(\tilde{y} < \tilde{x}) . \quad (\text{F.34})$$

Replacing the second integral on the r.h.s. of Eq. (F.28) by Eq. (F.34) gives

$$L \frac{\partial}{\partial L} \left\langle \begin{array}{c} \text{---} \text{---} \text{---} \\ \text{---} \text{---} \end{array} \right\rangle_L = L^{1+\epsilon} \int_0^\infty \frac{dx}{x} x^D \int_0^\infty \frac{dy}{y} y^D (x^{2\nu} + y^{2\nu})^{-d/2} \max(x, y)^{-\epsilon} \delta(y - L) . \quad (\text{F.35})$$

Now one distance (here  $y$ ) is fixed, whereas the integral over the other distance (here  $x$ ) runs from 0 to  $\infty$ . The former constraint  $\max(x, y) = L$  has been transformed into the factor  $\max(x, y)^{-\epsilon}$  times the constraint  $y = L$ .

Before generalizing this formula, we shall show how it can be used in practice. The residue in  $\frac{1}{\epsilon}$  (which determines the corresponding 1-loop counter-term) is given by the simple formula with  $d_c(D) = 4D/(2 - D)$ :

$$\left\langle \begin{array}{c} \text{---} \text{---} \text{---} \\ \text{---} \text{---} \end{array} \right\rangle_\epsilon = \int_0^\infty \frac{dx}{x} x^D (x^{2\nu} + 1)^{-d_c(D)/2} = \frac{1}{2 - D} \frac{\Gamma\left(\frac{D}{2-D}\right)^2}{\Gamma\left(\frac{2D}{2-D}\right)} . \quad (\text{F.36})$$

The subleading term can analogously be calculated by expanding  $(x^{2\nu} + 1)^{-(d-d_c(D))/2}$  and  $\max(x, y)^{-\epsilon}$  in  $\epsilon$ . We obtain the convergent integral representation

$$\left\langle \begin{array}{c} \text{---} \text{---} \text{---} \\ \text{---} \text{---} \end{array} \right\rangle_{\epsilon^0} = \int_0^\infty \frac{dx}{x} x^D (x^{2\nu} + 1)^{-d_c(D)/2} \left( \frac{1}{2 - D} \ln(x^{2\nu} + 1) - \ln(\max(x, 1)) \right) . \quad (\text{F.37})$$

This method extends to the integrals which appear in the counter-terms associated to the contraction of any number of points. In general, we have to compute integrals over  $N(N - 1)$  distances  $x, y, \dots$ , of the form

$$I(\epsilon) = \int_{\max(x, y, \dots) \leq L} f(x, y, \dots) \quad (\text{F.38})$$

with a homogeneous function  $f$  such that the integral has a conformal weight (dimension in  $L$ )  $\kappa$ :  $I(\epsilon) \sim L^\kappa$ . For the integrals which appear in  $n$ -loop diagrams, this weight is simply

$$\kappa = n \epsilon . \quad (\text{F.39})$$

The integral over the distances is defined by the  $D$ -dimensional measure (F.21). The residue is extracted from the dimensionless integral

$$J(\epsilon) = \kappa L^{-\kappa} I(\epsilon) = L^{-\kappa} L \frac{\partial}{\partial L} I(\epsilon) = L \int_{\max(x, y, \dots) = L} f(x, y, \dots) \max(x, y, \dots)^{-\kappa} . \quad (\text{F.40})$$

The domain of integration can be decomposed into ‘‘sectors’’, for instance

$$\{ \dots < y < x = L \} , \{ \dots < x < y = L \} , \quad (\text{F.41})$$

and we can map these different sectors onto each other by global conformal transformations. For instance we can rewrite the integral (F.40) as

$$J(\epsilon) \equiv L \int_{x=L; y, \dots} f(x, y, \dots) \max(x, y, \dots)^{-\kappa} \equiv L \int_{y=L; x, \dots} f(x, y, \dots) \max(x, y, \dots)^{-\kappa} . \quad (\text{F.42})$$

The constraint on the maximum of the distances is replaced by the constraint on an arbitrarily chosen distance.

This mapping of sectors is one of the basic tools used in calculating more complicated diagrams, e.g. at the 2-loop order or for the disorder-dynamics.

Also note that it implies the universality of the leading pole in  $1/\epsilon$ : Fixing the longest, the shortest or one of the intermediate distances always give the same leading pole. Finally, starting from these regularizations, any other one can be constructed.

## F.4 Factorization for $D = 1$

The methods described so far also apply to polymers. For polymers however, some simplifications are valid. Let us first give a simple (perturbative) example before stating the general result, namely the equivalence of polymers with the limit of zero components for a  $\phi^4$ -model.

In perturbation theory, we may consider expectation values with two dipoles inserted. The simplification for a polymer is, that its 1-dimensional nature enforces an ordering of the intervening points, resulting into topologically different diagrams, as exemplified by the equation below:

$$\text{Diagram} \xrightarrow{D \rightarrow 1} \text{Diagram 1} + \text{Diagram 2} + \text{Diagram 3} . \quad (\text{F.43})$$

It turns out that topologically different diagrams are also different analytically, whereas for membranes, a single diagram contains all these contributions. This is due to the additive nature of the polymer correlation-function, which reads for ordered points  $x_1 < x_2 < x_3$ :

$$C(x_1 - x_2) + C(x_3 - x_2) = C(x_3 - x_1) . \quad (\text{F.44})$$

This property is used to simplify the perturbation expansion.

## F.5 Exercises for Self-Avoiding Manifolds with solutions

### Exercise 21: Example of the MOPE

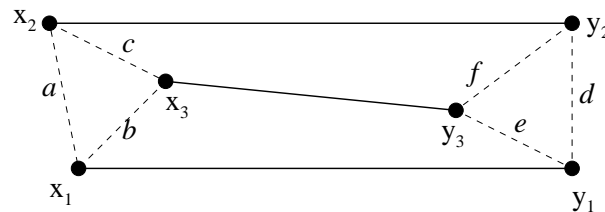


Figure F.1: The distances and the points in (F.45)

Calculate the MOPE-coefficient  $\left( \begin{array}{c} \text{Diagram} \\ \text{Diagram} \end{array} \right)$ .

## Solution

Start from

$$\begin{aligned}
 & \begin{array}{c} \bullet \text{---} \bullet \text{---} \bullet \text{---} \bullet \\ x_1 \quad y_1 \quad x_2 \quad y_2 \quad x_3 \quad y_3 \end{array} \\
 &= \int_k \int_p \int_q :e^{ikr(x_1)}::e^{ipr(x_2)}::e^{iqr(x_3)}::e^{-ikr(y_1)}::e^{-ipr(y_2)}::e^{-iqr(y_3)}: \quad . \quad (F.45)
 \end{aligned}$$

These dipoles shall be contracted like

$$\begin{array}{c} \bullet \text{---} \bullet \text{---} \bullet \text{---} \bullet \end{array} \longrightarrow \begin{array}{c} \bullet \bullet \\ \bullet \bullet \end{array} \quad . \quad (F.46)$$

We therefore use the OPE for the points  $x_1$ ,  $x_2$  and  $x_3$ , supposed the differences between these points become small:

$$:e^{ikr(x_1)}::e^{ipr(x_2)}::e^{iqr(x_3)}: = :e^{i(k+p+q)r((x_1+x_2+x_3)/3)}: e^{kp a^{2\nu} + kq b^{2\nu} + pq c^{2\nu}} \quad . \quad (F.47) \text{p:MOPE2}$$

The new variables for the distances between the points are given in figure F.1. An analogous relation is valid for  $y_1$ ,  $y_2$  and  $y_3$ . In order to retain only the most important contribution, we expand

$$:e^{i(k+p+q)r((x_1+x_2+x_3)/3)}: = :e^{i(k+p+q)r((x_1+x_2+x_3)/3)} (1 + O(\nabla r)) : \quad (F.48)$$

and neglect the contributions of order  $O(\nabla r)$  because they are proportional to irrelevant operators. After a shift in the integration-variable  $q$ ,

$$q \longrightarrow q - k - p ,$$

equation (F.45) becomes:

$$\begin{aligned}
 & \int_q :e^{iqr((x_1+x_2+x_3)/3)}::e^{-iqr((y_1+y_2+y_3)/3)}: \times \\
 & \times \int_k \int_p e^{kp(a^{2\nu} + d^{2\nu}) + k(q-k-p)(b^{2\nu} + e^{2\nu}) + p(q-k-p)(c^{2\nu} + f^{2\nu})} \quad . \quad (F.49)
 \end{aligned}$$

The integral over  $q$  yields the  $\delta$ -distribution plus higher derivatives of this distribution. The latter are irrelevant operators and can be neglected. As they come from the expansion of this exponential factor in  $q$ , we only have to retain the last factor, evaluated at  $q = 0$ . This gives:

$$\begin{aligned}
 & \int_k \int_p e^{kp(a^{2\nu} + d^{2\nu}) - k(k+p)(b^{2\nu} + e^{2\nu}) - p(k+p)(c^{2\nu} + f^{2\nu})} \\
 & = \left[ (b^{2\nu} + e^{2\nu})(c^{2\nu} + f^{2\nu}) - \frac{1}{4} (b^{2\nu} + e^{2\nu} + c^{2\nu} + f^{2\nu} - a^{2\nu} - d^{2\nu})^2 \right]^{-d/2} \quad . \quad (F.50)
 \end{aligned}$$

This can still be factorized as is known from ancient Heron:

$$\begin{aligned}
 & \left( \begin{array}{c} \bullet \bullet \\ \bullet \bullet \end{array} \middle| \bullet \text{---} \bullet \right) = \\
 & \left[ \frac{1}{4} \left( \sqrt{a^{2\nu} + d^{2\nu}} + \sqrt{b^{2\nu} + e^{2\nu}} + \sqrt{c^{2\nu} + f^{2\nu}} \right) \left( \sqrt{b^{2\nu} + e^{2\nu}} + \sqrt{c^{2\nu} + f^{2\nu}} - \sqrt{a^{2\nu} + d^{2\nu}} \right) \right. \\
 & \left. \left( \sqrt{a^{2\nu} + d^{2\nu}} + \sqrt{c^{2\nu} + f^{2\nu}} - \sqrt{b^{2\nu} + e^{2\nu}} \right) \left( \sqrt{a^{2\nu} + d^{2\nu}} + \sqrt{b^{2\nu} + e^{2\nu}} - \sqrt{c^{2\nu} + f^{2\nu}} \right) \right]^{-d/2} \quad (F.51)
 \end{aligned}$$

## Exercise 22: Impurity-like interactions

Show that there is no term proportional to  $\tilde{\delta}^d(r(0))$  in the MOPE of  $n$  dipoles with  $\tilde{\delta}^d(r(0))$ . Show also that this implies that the full dimension of  $\tilde{\delta}^d(r(0))$  is  $-\nu^*d$ .

### Solution

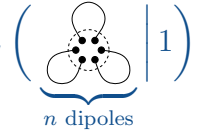
The MOPE of  $\tilde{\delta}^d(r(0)) = \int_k e^{ikr(0)}$  with  $n$   $\delta$ -interactions is

$$\begin{aligned} & \int_k e^{ikr(0)} \int_{p_1} e^{ip_1[r(y_1)-r(z_1)]} \dots \int_{p_n} e^{ip_n[r(y_n)-r(z_n)]} = \\ & = \int_k \int_{p_1} \dots \int_{p_n} :e^{ikr(0)} e^{ip_1[r(y_1)-r(z_1)]} \dots e^{ip_n[r(y_n)-r(z_n)]}: \times \\ & \quad \times e^{\sum_{j=1}^n kp_j[C(y_j)-C(z_j)]} e^{\frac{1}{2} \sum_{i=1}^n \sum_{j=1}^n p_i p_j [C(y_i-y_j)+C(z_i-z_j)-C(y_i-z_j)-C(y_j-z_i)]} . \end{aligned} \quad (\text{F.52})$$

The leading term proportional to  $\tilde{\delta}^d(r(0)) = \int_k e^{ikr(0)}$  is

$$\int_k e^{ikr(0)} \int_{p_1} \dots \int_{p_n} e^{\frac{1}{2} \sum_{i=1}^n \sum_{j=1}^n p_i p_j [C(y_i-y_j)+C(z_i-z_j)-C(y_i-z_j)-C(y_j-z_i)]} . \quad (\text{F.53})$$

Note that from  $e^{\sum_{j=1}^n kp_j[C(y_j)-C(z_j)]}$  only the leading term 1 has to be taken, since subleading terms generate derivatives of the  $\delta$ -distribution  $\tilde{\delta}^d(r(0))$ . However, Eq. (F.53) is nothing but the MOPE



times  $\tilde{\delta}^d(r(0))$ , and the divergence is subtracted by the counter-term proportional to the volume, or equivalently by normalizing expectation values by the full partition function. Therefore, the only renormalization to  $\tilde{\delta}^d(r(0))$  comes from the anomalous dimension of the field  $r$ , leading to the above stated dimension of  $-\nu^*d$ .

## Exercise 23: Equation of motion

Show that the factor of  $Z^{d/2}$  which intervenes in the renormalization of the coupling  $b_0 = b\mu^\epsilon Z_b Z^{d/2}$  and thus in the renormalization group  $\beta$ -function can also be understood with the help of the equation of motion or redundant operators.

### Solution

Two kinds of counter-terms are needed: Counter-terms proportional to  $\bullet \longleftarrow \bullet$  (taken care of in the renormalization factor  $Z_b$ ), and counter-terms proportional to  $\dagger$ , (taken care of in the renormalization factor  $Z$ ). The latter appear in the form

$$\frac{1}{2-D} \int_x \dagger_x e^{-b\mu^\epsilon Z_b \int_x \int_y x \longleftarrow y} , \quad (\text{F.54})$$

and using the equation of motion can be interpreted as

$$-\frac{d}{2} Z_b b \mu^\epsilon \int_x \int_y x \longleftarrow y e^{-b\mu^\epsilon Z_b \int_x \int_y x \longleftarrow y} . \quad (\text{F.55})$$

Exponentiation then leads to

$$e^{-\frac{Z}{2-D} \int_x \dagger_x - b\mu^\epsilon Z_b \int_x \int_y x \longleftarrow y} \xrightarrow{\text{Eqn. of motion}} e^{-\frac{1}{2-D} \int_x \dagger_x - b\mu^\epsilon Z_b Z^{d/2} \int_x \int_y x \longleftarrow y} , \quad (\text{F.56})$$

as stated above.

The same is achieved by using the concept of redundant operators.



### Exercise 24: Tricritical point with modified 2-point interaction

Study the tricritical point, which appears when one demands that the renormalized coupling proportional to self-avoidance,  $\bullet\text{---}\bullet$ , vanishes. Show that for  $D > 4/3$ , the next-to-leading operator dominating the tricritical point, is  $\bullet\text{---}\text{---}\bullet$ . Determine the MOPE-coefficients to leading order, following the lines of section ?? . Show that the  $\beta$ -function has an IR-stable fixed point and calculate the anomalous scaling exponent  $\nu^*$ . This problem was first discussed in [132, 18].

#### Solution

Let us start from the bare Hamiltonian

$$\mathcal{H}[r_0] = \frac{1}{2-D} \int_x \frac{1}{2} (\nabla r_0(x))^2 + b_0 \int_x \int_y (-\Delta_r) \tilde{\delta}^d(r_0(x) - r_0(y)) . \quad (\text{F.57})$$

The canonical dimension of the coupling constant  $b_0$  is

$$\epsilon' := [b_0]_\mu = 3D - 2 - \nu d \quad (\text{F.58})$$

and the model has UV-divergences, i.e. poles in  $\epsilon'$ , for  $\epsilon' = 0$ . As in section ?? two renormalizations are needed, namely

$$r(x) = Z^{-1/2} r_0(x) \quad (\text{F.59})$$

$$b = Z^{-d/2-1} Z_b^{-1} \mu^{-\epsilon'} b_0 . \quad (\text{F.60})$$

At 1-loop order, the counter-terms are in analogy to Eqs. (2.115) and (2.116)

$$Z = 1 - \frac{b}{\epsilon'} (2-D) \left\langle \begin{array}{c} \text{---} \\ \text{---} \\ \text{---} \end{array} \right\rangle_{\epsilon'} + O(b^2) , \quad (\text{F.61})$$

$$Z_b = 1 + \frac{b}{\epsilon'} \left\langle \begin{array}{c} \text{---} \\ \text{---} \\ \text{---} \end{array} \right\rangle_{\epsilon'} + O(b^2) . \quad (\text{F.62})$$

However note, that the leading term of the MOPE of  $\bullet\text{---}\bullet$  is proportional to  $\bullet\text{---}\text{---}\bullet$ , such that (scale-dependent) fine-tuning is necessary in order to stay at the tri-critical point.

The residues  $\left\langle \begin{array}{c} \text{---} \\ \text{---} \\ \text{---} \end{array} \right\rangle_{\epsilon'}$  and  $\left\langle \begin{array}{c} \text{---} \\ \text{---} \\ \text{---} \end{array} \right\rangle_{\epsilon'}$  are analytic functions of  $D$  for  $0 < D < 2$  [132]

$$\begin{aligned} \left\langle \begin{array}{c} \text{---} \\ \text{---} \\ \text{---} \end{array} \right\rangle_{\epsilon'} &= -\frac{1}{2-D} \\ \left\langle \begin{array}{c} \text{---} \\ \text{---} \\ \text{---} \end{array} \right\rangle_{\epsilon'} &= \frac{10D - D^2 - 8}{2(2-D)^3} \frac{\Gamma\left(\frac{D}{2-D}\right)^2}{\Gamma\left(\frac{2D}{2-D}\right)} . \end{aligned} \quad (\text{F.63})$$

The  $\beta$ -function and the scaling dimension  $\nu(b)$  of the field  $r$  are as in Eqs. (2.118) and (2.119) defined as

$$\beta(b) := \mu \frac{\partial}{\partial \mu} \Big|_{b_0} b , \quad \nu(b) := \frac{2-D}{2} - \frac{1}{2} \mu \frac{\partial}{\partial \mu} \Big|_{b_0} \ln Z . \quad (\text{F.64})$$

The new  $\beta$ -function has a non-trivial IR-fixed point  $b^* > 0$  for  $\epsilon' > 0$  and the scaling dimension of the

membrane at the  $\Theta$ -point becomes<sup>10</sup>

$$\begin{aligned} \nu^* &= \frac{2-D}{2} \left[ 1 - \epsilon' \frac{\langle \text{loop} | \dagger \rangle_{\epsilon'} }{\langle \text{loop} | \text{---} \rangle_{\epsilon'} - \nu(d+2) \langle \text{loop} | \dagger \rangle_{\epsilon'}} + O(\epsilon'^2) \right] \\ &= \frac{2-D}{2} \left[ 1 + \frac{\epsilon'}{\frac{10D - D^2 - 8}{2(2-D)^2} \frac{\Gamma(\frac{D}{2-D})^2}{\Gamma(\frac{2D}{2-D})} + 2D} + O(\epsilon'^2) \right]. \end{aligned} \quad (\text{F.65})$$

### Exercise 25: Consequences of the equation of motion

Show that [133]

$$\langle \text{loop} | \text{---} \rangle_{\epsilon^{-1}} = -\frac{\nu d}{2} \langle \text{loop} | \text{---} \rangle_{\epsilon^{-1}} + O(\epsilon^0) \quad (\text{F.66})$$

$$\langle \text{loop} | \dagger \rangle_{\epsilon^{-1}} = -\nu(d+2) \langle \text{loop} | \dagger \rangle_{\epsilon^{-1}} + \langle \text{loop} | \dagger \rangle_{\epsilon^{-1}} \langle \text{loop} | \dagger \rangle_{\epsilon^0} + O(\epsilon^0). \quad (\text{F.67})$$

### Solution

Details are given in appendix C of [133]. The idea is to use the equation of motion (F.4) to write

$$\langle \iiint \iiint \int \text{---} \rangle_0 = -2\nu d \langle \iiint \iiint \int \text{---} \rangle_0. \quad (\text{F.68})$$

Identifying divergences proportional to  $\text{---}$  on both sides and again using Eq. (F.4) then yields Eq. (F.66).

The second identity (F.67) is proven along the same lines by starting from

$$\langle \iiint \int \text{---} \dagger \rangle_0 = -\nu d \langle \iiint \int \text{---} \rangle_0. \quad (\text{F.69})$$

### Exercise 26: Finiteness of observables within the renormalized model

Show that within the renormalized model (2.97) and to first order in  $b$ , the expectation value of  $\mathcal{O} = e^{ik[r(s)-r(t)]}$  as given for the bare model in Eq. (2.64) is UV- and IR-finite.

<sup>10</sup>Note a misprint in Eq. (12.32) of [133]. Using the extrapolations for  $\nu^*(d+2)$  (expansion about the mean-field result  $\nu_{\text{MF}} = \frac{2D}{2+d}$ ) or  $\nu^*(d+4)$  (expansion about the Flory result  $\nu_{\text{Flory}} = \frac{2+D}{4+d}$ ) in three dimensions yields results very comparable to the Flory estimate of  $\nu^* = 0.57$ .

## Solution

Two counter-terms are relevant at first order in the renormalized coupling  $b$ , namely  $\Delta\mathcal{H}_1$ , Eq. (2.102) and  $\Delta\mathcal{H}_+$ , Eq. (2.104). The third 1-loop term,  $\Delta\mathcal{H}_-$ , Eq. (2.104), will only show up at order  $b^2$ . Also note, that the first one,  $\Delta\mathcal{H}_1$ , has already been taken into account in Eq. (2.64), due to the normalization introduced in Eq. (2.45).

At first order in the renormalized coupling  $b$ , we thus only have to take care of the counter-term (2.104), with the full tensorial structure, resulting in

$$\langle \mathcal{O} \rangle_b = e^{-k^2 C(s-t)} \times \left\{ 1 + b\mu^\epsilon \iint_{x,y} \left[ 1 - \exp\left(\frac{1}{4}k^2 \frac{[C(s-x) + C(t-y) - C(s-y) - C(t-x)]^2}{C(x-y)}\right) + \frac{1}{4}k^2 \frac{[(x-y)\nabla_z(C(s-z) - C(t-z))]^2}{C(x-y)} \Theta(|x-y| < L) \right] C(x-y)^{-d/2} + O(b^2) \right\}, \quad (\text{F.70})$$

where  $z$  may either be chosen as  $x$  or  $y$ , or the symmetrized version may be used. The terms in the big square brackets exactly cancel the divergence for small  $x-y$ . Note that there is a possible IR-divergence for  $|x-y| \rightarrow \infty$ . In the original term, this is regularized by the observable-positions  $s$  and  $t$ , which effectively cut off the integral at  $|x-y| \approx |s-t|$ . In the counter-term, the IR-cutoff is explicit.

## G Non-analytic expectation values

Suppose that

$$G := \begin{pmatrix} \langle xx \rangle & \langle xy \rangle \\ \langle yx \rangle & \langle yy \rangle \end{pmatrix} = \begin{pmatrix} 1 & t \\ t & 1 \end{pmatrix} \quad \Rightarrow \quad G^{-1} = \frac{1}{1-t^2} \begin{pmatrix} 1 & -t \\ -t & 1 \end{pmatrix} \quad (\text{G.1})$$

Then

$$\langle |x| \rangle = \sqrt{\frac{2}{\pi}} \quad (\text{G.2})$$

$$\langle \text{sgn}(x)\text{sgn}(y) \rangle = \frac{2}{\pi} \text{asin}(t) \quad (\text{G.3})$$

$$\langle |xy| \rangle = \frac{2}{\pi} (\sqrt{1-t^2} + t \text{asin}(t)) \quad (\text{G.4})$$

$$\langle xy^2 \text{sgn}(y) \rangle = 2\sqrt{\frac{2}{\pi}} t \quad (\text{G.5})$$

$$\langle x^2 \text{sgn}(x) y^2 \text{sgn}(y) \rangle = \frac{2}{\pi} (3t\sqrt{1-t^2} + \text{asin}(t) + 2t^2 \text{asin}(t)) \quad (\text{G.6})$$

$$\langle |xy^3| \rangle = \frac{2}{\pi} ((2+t^2)\sqrt{1-t^2} + 3t \text{asin}(t)) \quad (\text{G.7})$$

$$\langle f(x)\delta(y) \rangle = \sqrt{\frac{1-t^2}{2\pi}} \langle f(x\sqrt{1-t^2}) \rangle \quad (\text{G.8})$$

## H Notations

1. greek indices  $\alpha, \beta, \dots$  for replicas
2. latin indices for components
3. \*\*\*  $F(u, x)$  or  $F(x, u)$  ???\*\*\*

Diagrams globally defined in Tikz

$$\backslash LH = \begin{array}{c} \bullet \\ \diagdown \quad \diagup \\ \bullet \quad \bullet \\ \text{---} \end{array} \quad (\text{H.1})$$

$$\backslash Ione = \begin{array}{c} \bullet \quad \bullet \\ \text{---} \end{array} \quad (\text{H.2})$$

$$\backslash Ionexy = x \begin{array}{c} \bullet \quad \bullet \\ \text{---} \end{array} y \quad (\text{H.3})$$

$$\backslash IoneExy = x \begin{array}{c} \diagdown \quad \diagup \\ \bullet \quad \bullet \\ \text{---} \end{array} y \quad (\text{H.4})$$

$$\backslash Isunset = \begin{array}{c} \bullet \quad \bullet \\ \text{---} \end{array} \quad (\text{H.5})$$

$$\backslash Isunsetxy = x \begin{array}{c} \bullet \quad \bullet \\ \text{---} \end{array} y \quad (\text{H.6})$$

$$\backslash IsunsetE = \begin{array}{c} \bullet \quad \bullet \\ \text{---} \end{array} \quad (\text{H.7})$$

$$\backslash IsunsetExy = x \begin{array}{c} \bullet \quad \bullet \\ \text{---} \end{array} y \quad (\text{H.8})$$

$$\backslash Ii = \begin{array}{c} \bullet \\ \diagdown \quad \diagup \\ \bullet \quad \bullet \\ \text{---} \end{array} \quad (\text{H.9})$$

## References

- Amit [1] D.J. Amit and V. Martin-Mayor, *Field Theory, the Renormalization Group, and Critical Phenomena*, World Scientific, Singapore, 3rd edition, 1984.
- JustinBook2 [2] J. Zinn-Justin, *Phase Transitions and Renormalization Group*, Oxford University Press, Oxford, 2007.
- CardyBook [3] J. Cardy, *Scaling and Renormalization in Statistical Physics*, Cambridge University Press, 1996.
- KardarBook [4] Mehran Kardar, *Statistical Physics of Fields*, Cambridge University Press, 2007.
- BrézinBook [5] E. Brézin, *Introduction to Statistical Field Theory*, Cambridge University Press, 2010.
- Wiese2015 [6] K.J. Wiese, *Coherent-state path integral versus coarse-grained effective stochastic equation of motion: From reaction diffusion to stochastic sandpiles*, *Phys. Rev. E* **93** (2016) 042117, [arXiv:1501.06514](https://arxiv.org/abs/1501.06514).
- Lubensky [7] P.M. Chaikin and T.C. Lubensky, *Principles of condensed matter physics*, Cambridge University Press, Cambridge, 1995.
- Fedorenko2018 [8] K.J. Wiese and A.A. Fedorenko, *Field theories for loop-erased random walks*, *Nucl. Phys. B* **946** (2019) 114696, [arXiv:1802.08830](https://arxiv.org/abs/1802.08830).

- Middleton1994 [9] O. Narayan and A.A. Middleton, *Avalanches and the renormalization-group for pinned charge-density waves*, *Phys. Rev. B* **49** (1994) 244–256.
- Majumdar1992 [10] S.N. Majumdar, *Exact fractal dimension of the loop-erased self-avoiding walk in two dimensions*, *Phys. Rev. Lett.* **68** (1992) 2329–2331.
- Kogut1974 [11] K. Wilson and J. Kogut, *The renormalization group and the  $\varepsilon$ -expansion*, *Phys. Rep.* **12** (1974) 75–200.
- Wiese2016 [12] K.J. Wiese, *Dynamical selection of critical exponents*, *Phys. Rev. E* **93** (2016) 042105, [arXiv:1602.00601](https://arxiv.org/abs/1602.00601).
- Vicari2002 [13] M. Campostrini, A. Pelissetto, P. Rossi and E. Vicari, *25th-order high-temperature expansion results for three-dimensional ising-like systems on the simple-cubic lattice*, *Phys. Rev. E* **65** (2002) 066127.
- DeGennes1972 [14] P.-G. De Gennes, *Exponents for the excluded volume problem as derived by the Wilson method*, *Phys. Lett. A* **38** (1972) 339–340.
- Lubensky1987 [15] J.A. Aronovitz and T.C. Lubensky,  *$\varepsilon$ -expansion for self-avoiding tethered surfaces of fractional dimension*, *Europhys. Lett.* **4** (1987) 395–401.
- Nelson1987 [16] M. Kardar and D.R. Nelson,  *$\varepsilon$  expansions for crumpled manifolds*, *Phys. Rev. Lett.* **58** (1987) 1289 and 2280 E.
- Schoenberg1937 [17] I.J. Schoenberg, *On certain metric spaces arising from euclidean spaces by change of metric and their embedding in hilbert space*, *Annals of Mathematics* **38** (1937) 787–793.
- DDG4 [18] F. David, B. Duplantier and E. Guitter, *Renormalization theory for the self-avoiding polymerized membranes*, (1997), [cond-mat/9702136](https://arxiv.org/abs/cond-mat/9702136).
- DDG3 [19] F. David, B. Duplantier and E. Guitter, *Renormalization and hyperscaling for self-avoiding manifold models*, *Phys. Rev. Lett.* **72** (1994) 311.
- Diehl1986 [20] H.W. Diehl, *Field-theoretical approach to critical behaviour of surfaces*. Volume 10 of *Phase Transitions and Critical Phenomena*, pages 76–267, Academic Press London, 1986.
- DeWitt1984 [21] B. De Witt, *The spacetime approach to quantum field theory in relativity, groups and topology II*. Volume XL of *Les Houches, école d’été de physique théorique 1983*, North Holland, 1984.
- WieseHabil [22] K.J. Wiese, *Polymerized membranes, a review*, Volume 19 of *Phase Transitions and Critical Phenomena*, Academic Press, London, 1999.
- Boltzmann1868 [23] L. Boltzmann, *Studien über das Gleichgewicht der lebendigen Kraft zwischen bewegten materiellen Punkten*, *Wiener Berichte* **58** (1868) 517–560.
- MSR [24] P.C. Martin, E.D. Siggia and H.A. Rose, *Statistical dynamics of classical systems*, *Phys. Rev. A* **8** (1973) 423–437.
- Janssen1992 [25] H.K. Janssen, *On the renormalized field theory of nonlinear critical relaxation*, in *From Phase Transitions to Chaos*, Topics in Modern Statistical Physics, pages 68–117, World Scientific, Singapore, 1992.
- Janssen1985 [26] H.K. Janssen, *Feldtheoretische methoden in der statistischen mechanik*, Vorlesungsmanuskript Uni Düsseldorf (1985).

- Halperin1977 [27] P.C. Hohenberg and B.I. Halperin, *Theory of dynamical critical phenomena*, *Rev. Mod. Phys.* **49** (1977) 435.
- Yaglom1960 [28] I. M. Gel'fand and A. M. Yaglom, *Integration in functional spaces and its applications in quantum physics*, *J. Phys. A* **1** (1960) 48.
- Smilansky1977 [29] S. Levit and U. Smilansky, *A theorem on infinite products of eigenvalues of Sturm-Liouville type operators*, *Proceedings of the American Mathematical Society* **65** (1977) 299–302.
- ColemanBook [30] S. Coleman, *Aspects of Symmetry*, Cambridge University Press, 1985.
- Doussal1998 [31] S. Lemerle, J. Ferré, C. Chappert, V. Mathet, T. Giamarchi and P. Le Doussal, *Domain wall creep in an Ising ultrathin magnetic film*, *Phys. Rev. Lett.* **80** (1998) 849.
- Rolley2002 [32] S. Moulinet, C. Guthmann and E. Rolley, *Roughness and dynamics of a contact line of a viscous fluid on a disordered substrate*, *Eur. Phys. J. E* **8** (2002) 437–443.
- Larkin1977 [33] K.B. Efetov and A.I. Larkin, *Sov. Phys. JETP* **45** (1977) 1236.
- Larkin1970 [34] A.I. Larkin, *Sov. Phys. JETP* **31** (1970) 784.
- Narayan1992b [35] O. Narayan and D.S. Fisher, *Critical behavior of sliding charge-density waves in 4-epsilon dimensions*, *Phys. Rev. B* **46** (1992) 11520–49.
- Narayan1992a [36] O. Narayan and D.S. Fisher, *Dynamics of sliding charge-density waves in 4-epsilon dimensions*, *Phys. Rev. Lett.* **68** (1992) 3615–18.
- Chauve2003 [37] P. Le Doussal, K.J. Wiese and P. Chauve, *Functional renormalization group and the field theory of disordered elastic systems*, *Phys. Rev. E* **69** (2004) 026112, [cond-mat/0304614](#).
- Chauve2002 [38] P. Le Doussal, K.J. Wiese and P. Chauve, *2-loop functional renormalization group analysis of the depinning transition*, *Phys. Rev. B* **66** (2002) 174201, [cond-mat/0205108](#).
- Wiese2000a [39] P. Chauve, P. Le Doussal and K.J. Wiese, *Renormalization of pinned elastic systems: How does it work beyond one loop?*, *Phys. Rev. Lett.* **86** (2001) 1785–1788, [cond-mat/0006056](#).
- Mézard1996 [40] L. Balents, J.P. Bouchaud and M. Mézard, *The large scale energy landscape of randomly pinned objects*, *J. Phys. I (France)* **6** (1996) 1007–20, [cond-mat/9601137](#).
- Doussal2006b [41] P. Le Doussal, *Finite temperature Functional RG, droplets and decaying Burgers turbulence*, *Europhys. Lett.* **76** (2006) 457–463, [cond-mat/0605490](#).
- Wiese2006 [42] A.A. Middleton, P. Le Doussal and K.J. Wiese, *Measuring functional renormalization group fixed-point functions for pinned manifolds*, *Phys. Rev. Lett.* **98** (2007) 155701, [cond-mat/0606160](#).
- Wiese2006a [43] P. Le Doussal and K.J. Wiese, *How to measure Functional RG fixed-point functions for dynamics and at depinning*, *EPL* **77** (2007) 66001, [cond-mat/0610525](#).
- Wiese2006a [44] A. Rosso, P. Le Doussal and K.J. Wiese, *Numerical calculation of the functional renormalization group fixed-point functions at the depinning transition*, *Phys. Rev. B* **75** (2007) 220201, [cond-mat/0610821](#).
- Fisher1993 [45] L. Balents and D.S. Fisher, *Large- $N$  expansion of 4 -  $\epsilon$ -dimensional oriented manifolds in random media*, *Phys. Rev. B* **48** (1993) 5949–5963.

- oopPrivate [46] S. Scheidl, Private communication about 2-loop calculations for the random manifold problem. 2000-2004.
- icerDiplom [47] Yusuf Dincer, *Zur Universalität der Struktur elastischer Mannigfaltigkeiten in Unordnung*, Master's thesis, Universität Köln, 1999.
- oussal2001 [48] P. Chauve and P. Le Doussal, *Exact multilocal renormalization group and applications to disordered problems*, *Phys. Rev. E* **64** (2001) 051102/1–27, [cond-mat/0006057](#).
- Wiese2017 [49] C. Husemann and K.J. Wiese, *Field theory of disordered elastic interfaces to 3-loop order: Results*, *Nucl. Phys. B* **932** (2018) 589–618, [arXiv:1707.09802](#).
- oussal2018 [50] K.J. Wiese, C. Husemann and P. Le Doussal, *Field theory of disordered elastic interfaces at 3-loop order: The  $\beta$ -function*, *Nucl. Phys. B* **932** (2018) 540–588, [arXiv:1801.08483](#).
- leton1995 [51] A.A. Middleton, *Numerical results for the ground-state interface in a random medium*, *Phys. Rev. E* **52** (1995) R3337–40.
- Fisher1985 [52] M. Kardar, D.A. Huse, C.L. Henley and D.S. Fisher, *Roughening by impurities at finite temperatures (comment and reply)*, *Phys. Rev. Lett.* **55** (1985) 2923–4.
- horn1992 [53] T. Nattermann, S. Stepanow, L.-H. Tang and H. Leschhorn, *Dynamics of interface depinning in a disordered medium*, *J. Phys. II (France)* **2** (1992) 1483–8.
- leton1992 [54] AA. Middleton, *Asymptotic uniqueness of the sliding state for charge-density waves*, *Phys. Rev. Lett.* **68** (1992) 670–673.
- sher1993a [55] O. Narayan and D.S. Fisher, *Threshold critical dynamics of driven interfaces in random media*, *Phys. Rev. B* **48** (1993) 7030–42.
- auth2001b [56] A. Rosso and W. Krauth, *Origin of the roughness exponent in elastic strings at the depinning threshold*, *Phys. Rev. Lett.* **87** (2001) 187002, [cond-mat/0104198](#).
- Kolton2012 [57] Ezequiel E. Ferrero, Sebastián Bustingorry and Alejandro B. Kolton, *Non-steady relaxation and critical exponents at the depinning transition*, *Phys. Rev. E* **87** (2013) 032122, [arXiv:1211.7275](#).
- hanty2016 [58] P. Grassberger, D. Dhar and P. K. Mohanty, *Oslo model, hyperuniformity, and the quenched Edwards-Wilkinson model*, *Phys. Rev. E* **94** (2016) 042314.
- rauth2002 [59] A. Rosso, A.K. Hartmann and W. Krauth, *Depinning of elastic manifolds*, *Phys. Rev. E* **67** (2003) 021602, [cond-mat/0207288](#).
- Wiese2008a [60] P. Le Doussal and K.J. Wiese, *Driven particle in a random landscape: disorder correlator, avalanche distribution and extreme value statistics of records*, *Phys. Rev. E* **79** (2009) 051105, [arXiv:0808.3217](#).
- Wiese2016 [61] M. Delorme, P. Le Doussal and K.J. Wiese, *Distribution of joint local and total size and of extension for avalanches in the Brownian force model*, *Phys. Rev. E* **93** (2016) 052142, [arXiv:1601.04940](#).
- peri2006b [62] G. Durin and S. Zapperi, *The Barkhausen effect*, in G. Bertotti and I. Mayergoyz, editors, *The Science of Hysteresis*, page 51, Amsterdam, 2006, [cond-mat/0404512](#).
- ntorsi1990 [63] B. Alessandro, C. Beatrice, G. Bertotti and A. Montorsi, *Domain-wall dynamics and Barkhausen effect in metallic ferromagnetic materials. I. Theory*, *J. Appl. Phys.* **68** (1990) 2901.



- Montorsi1990b [64] B. Alessandro, C. Beatrice, G. Bertotti and A. Montorsi, *Domain-wall dynamics and Barkhausen effect in metallic ferromagnetic materials. II. Experiments*, *J. Appl. Phys.* **68** (1990) 2908.
- Colaioni2008 [65] F. Colaioni, *Exactly solvable model of avalanches dynamics for Barkhausen crackling noise*, *Advances in Physics* **57** (2008) 287, [arXiv:0902.3173](#).
- Wiese2011b [66] A. Dobrinevski, P. Le Doussal and K.J. Wiese, *Non-stationary dynamics of the Alessandro-Beatrice-Bertotti-Montorsi model*, *Phys. Rev. E* **85** (2012) 031105, [arXiv:1112.6307](#).
- Muñoz2005 [67] I. Dornic, H. Chaté and M.A. Muñoz, *Integration of Langevin equations with multiplicative noise and the viability of field theories for absorbing phase transitions*, *Phys. Rev. Lett.* **94** (2005) 100601.
- Wiese2012a [68] P. Le Doussal and K.J. Wiese, *Avalanche dynamics of elastic interfaces*, *Phys. Rev. E* **88** (2013) 022106, [arXiv:1302.4316](#).
- Wiese2014a [69] A. Dobrinevski, P. Le Doussal and K.J. Wiese, *Avalanche shape and exponents beyond mean-field theory*, *EPL* **108** (2014) 66002, [arXiv:1407.7353](#).
- DobrinevskiPhD [70] A. Dobrinevski, *Field theory of disordered systems – avalanches of an elastic interface in a random medium*, PhD Thesis, ENS Paris (2013), [arXiv:1312.7156](#).
- Wiese2016 [71] G. Durin, F. Bohn, M.A. Correa, R.L. Sommer, P. Le Doussal and K.J. Wiese, *Quantitative scaling of magnetic avalanches*, *Phys. Rev. Lett.* **117** (2016) 087201, [arXiv:1601.01331](#).
- Wiese2017 [72] Z. Zhu and K.J. Wiese, *The spatial shape of avalanches*, *Phys. Rev. E* **96** (2017) 062116, [arXiv:1708.01078](#).
- Wiese2008c [73] P. Le Doussal and K.J. Wiese, *Size distributions of shocks and static avalanches from the functional renormalization group*, *Phys. Rev. E* **79** (2009) 051106, [arXiv:0812.1893](#).
- Wiese2011b [74] P. Le Doussal and K.J. Wiese, *First-principle derivation of static avalanche-size distribution*, *Phys. Rev. E* **85** (2011) 061102, [arXiv:1111.3172](#).
- Wiese2008 [75] P. Le Doussal, A.A. Middleton and K.J. Wiese, *Statistics of static avalanches in a random pinning landscape*, *Phys. Rev. E* **79** (2009) 050101 (R), [arXiv:0803.1142](#).
- Wiese2009a [76] A. Rosso, P. Le Doussal and K.J. Wiese, *Avalanche-size distribution at the depinning transition: A numerical test of the theory*, *Phys. Rev. B* **80** (2009) 144204, [arXiv:0904.1123](#).
- LaursonPrivate [77] L. Laurson, private communication.
- Alava2013 [78] L. Laurson, X. Illa, S. Santucci, K.T. Tallakstad, K.J. Måløy and M.J. Alava, *Evolution of the average avalanche shape with the universality class*, *Nat. Commun.* **4** (2013) 2927.
- Wiese2013 [79] A. Dobrinevski, P. Le Doussal and K.J. Wiese, *Statistics of avalanches with relaxation and Barkhausen noise: A solvable model*, *Phys. Rev. E* **88** (2013) 032106, [arXiv:1304.7219](#).
- Jagla2016 [80] L.E. Aragon, A.B. Kolton, P. Le Doussal, K.J. Wiese and E. Jagla, *Avalanches in tip-driven interfaces in random media*, *EPL* **113** (2016) 10002, [arXiv:1510.06795](#).
- Wiese2015 [81] T. Thiery, P. Le Doussal and K.J. Wiese, *Spatial shape of avalanches in the Brownian force model*, *J. Stat. Mech.* **2015** (2015) P08019, [arXiv:1504.05342](#).



- oussal2016 [82] T. Thiery and P. Le Doussal, *Universality in the mean spatial shape of avalanches*, EPL **114** (2016) 36003, [arXiv:1601.00174](#).
- Durin2005 [83] S. Zapperi, C. Castellano, F. Colaiori and G. Durin, *Signature of effective mass in crackling-noise asymmetry*, Nat. Phys. **1** (2005) 46–49.
- Wiese2015 [84] M. Delorme and K.J. Wiese, *Maximum of a fractional Brownian motion: Analytic results from perturbation theory*, Phys. Rev. Lett. **115** (2015) 210601, [arXiv:1507.06238](#).
- Wiese2016b [85] M. Delorme and K.J. Wiese, *Extreme-value statistics of fractional Brownian motion bridges*, Phys. Rev. E **94** (2016) 052105, [arXiv:1605.04132](#).
- Munoz1998 [86] M.A. Muñoz, *Nature of different types of absorbing states*, Phys. Rev. E **57** (1998) 1377–1383.
- Lefevre2006 [87] A. Andreanov, G. Biroli, J.P. Bouchaud and A. Lefèvre, *Field theories and exact stochastic equations for interacting particle systems*, Phys. Rev. E **74** (2006) 030101.
- Luck2011 [88] D. Gredat, I. Dornic and J.M. Luck, *On an imaginary exponential functional of Brownian motion*, J. Phys. A **44** (2011) 175003.
- TauberBook [89] U.C. Täuber, *Critical Dynamics: A Field Theory Approach to Equilibrium and Non-Equilibrium Scaling Behavior*, Cambridge University Press, 2014.
- Kitahara2002 [90] O. Deloubrière, L. Frachebourg, H.J. Hilhorst and K. Kitahara, *Imaginary noise and parity conservation in the reaction  $A + A \rightleftharpoons 0$* , Physica A **308** (2002) 135–147.
- Tauber2005 [91] H.K. Janssen and U.C. Täuber, *The field theory approach to percolation processes*, Annals of Physics **315** (2005) 147 – 192.
- Koga1993 [92] K. Kawasaki and T. Koga, *Relaxation and growth of concentration fluctuations in binary fluids and polymer blends*, Physica A **201** (1993) 115 – 128.
- Dean1996 [93] D.S. Dean, *Langevin equation for the density of a system of interacting langevin processes*, J. Phys. A **29** (1996) L613–L617.
- Vespignani2000 [94] R. Pastor-Satorras and A. Vespignani, *Field theory of absorbing phase transitions with a nondiffusive conserved field*, Phys. Rev. E **62** (2000) R5875–R5878.
- Zapperi1998 [95] A. Vespignani, R. Dickman, M.A. Muñoz and S. Zapperi, *Driving, conservation, and absorbing states in sandpiles*, Phys. Rev. Lett. **81** (1998) 5676–5679.
- Munoz2008 [96] J.A. Bonachela, M. Alava and M.A. Munoz, *Cusps in systems with (many) absorbing states*, Phys. Rev. E **79** (2009) 050106(R), [arXiv:0810.4395](#).
- Alava2003 [97] M. Alava, *Self-organized criticality as a phase transition*, pages 69–102, Nova Science Publishers, New York, NY, USA, 2003, [cond-mat/0307688](#).
- Manna1991 [98] S.S. Manna, *Two-state model of self-organized critical phenomena*, J. Phys. A **24** (1991) L363–L369.
- Wiesenfeld1987 [99] P. Bak, C. Tang and K. Wiesenfeld, *Self-organized criticality - an explanation of  $1/f$  noise*, Phys. Rev. Lett. **59** (1987) 381–384.

- Wiese2014a [100] P. Le Doussal and K.J. Wiese, *An exact mapping of the stochastic field theory for Manna sandpiles to interfaces in random media*, [Phys. Rev. Lett. \*\*114\*\* \(2014\) 110601](#), [arXiv:1410.1930](#).
- Ornstein1930 [101] G. E. Uhlenbeck and L. S. Ornstein, *On the theory of the Brownian motion*, [Phys. Rev. \*\*36\*\* \(1930\) 823–841](#).
- Doussal2006 [102] K.J. Wiese and P. Le Doussal, *Functional renormalization for disordered systems: Basic recipes and gourmet dishes*, [Markov Processes Relat. Fields \*\*13\*\* \(2007\) 777–818](#), [cond-mat/0611346](#).
- Sano2012 [103] K.A. Takeuchi and M. Sano, *Evidence for geometry-dependent universal fluctuations of the Kardar-Parisi-Zhang interfaces in liquid-crystal turbulence*, [J. Stat. Phys. \*\*147\*\* \(2012\) 853–890](#).
- Shandarin1989 [104] S. N. Gurbatov, A. I. Saichev and S. F. Shandarin, *The large-scale structure of the universe in the frame of the model equation of non-linear diffusion*, [Monthly Notices of the Royal Astronomical Society \*\*236\*\* \(1989\) 385–402](#).
- Wiese1998a [105] K.J. Wiese, *On the perturbation expansion of the KPZ-equation*, [J. Stat. Phys. \*\*93\*\* \(1998\) 143–154](#), [cond-mat/9802068](#).
- Zinn [106] J. Zinn-Justin, *Quantum Field Theory and Critical Phenomena*, Oxford University Press, Oxford, 1989.
- Sourlas1979 [107] G. Parisi and N. Sourlas, *Random magnetic fields, supersymmetry, and negative dimensions*, [Phys. Rev. Lett. \*\*43\*\* \(1979\) 744–5](#).
- Sourlas1982 [108] G. Parisi and N. Sourlas, *Supersymmetric field theories and stochastic differential equations*, [Nucl. Phys. B \*\*B206\*\* \(1982\) 321–32](#).
- Dotsenko1988 [109] V.I. S. Dotsenko, *Lectures on conformal field theory*, [Advanced Studies in Pure Mathematics \*\*16\*\* \(1988\) 123–170](#).
- Cardy2006 [110] John Cardy, *Reaction-diffusion processes*, Lectures held at Warwick University, unpublished (2006).
- JacksonBook [111] J. D. Jackson, *Classical Electrodynamics*, John Wiley & Sons, 1998.
- Rozanov1975 [112] Y. Rozanov, *Processus Aléatoires*, Mir, Moscow, 1975.
- Peliti1985 [113] L. Peliti, *Path integral approach to birth-death processes on a lattice*, [J. Phys. \(France\) \*\*46\*\* \(1985\) 1469–1483](#).
- Wiese2011 [114] A. Dobrinevski, P. Le Doussal and K.J. Wiese, *Interference in disordered systems: A particle in a complex random landscape*, [Phys. Rev. E \*\*83\*\* \(2011\) 061116](#), [arXiv:1101.2411](#).
- KampenBook [115] N.G. Van Kampen, *Stochastic Processes in Physics and Chemistry*, Elsevier, 2011.
- Hasenfratz1968 [116] A. Hasenfratz and P. Hasenfratz, *Renormalization group study of scalar field theory*, [Nucl. Phys. B \*\*270\*\* \(1986\) 687–701](#).
- Houghton1973 [117] F.J. Wegner and A. Houghton, *Renormalization group equation for critical phenomena*, [Phys. Rev. A \*\*8\*\* \(1973\) 401–12](#).
- Polchinski1984 [118] J. Polchinski, *Renormalization and effective Lagrangians*, [Nucl. Phys. B \*\*231\*\* \(1984\) 269–95](#).
- Wetterich2002 [119] J. Berges, N. Tetradis and C. Wetterich, *Non-perturbative renormalization flow in quantum field theory and statistical physics*, [Phys. Rep. \*\*363\*\* \(2002\) 223–386](#).

- Leibler1983a [120] E. Brézin, B.I. Halperin and S. Leibler, *Critical wetting: the domain of validity of mean field theory*, *J. Phys. (France)* **44** (1983) 775–783.
- Leibler1983 [121] E. Brézin, B.I. Halperin and S. Leibler, *Critical wetting in three dimensions*, *Phys. Rev. Lett.* **50** (1983) 1387.
- Huse1985 [122] D.S. Fisher and D.A. Huse, *Wetting transitions: A functional renormalization-group approach*, *Phys. Rev. B* **32** (1985) 247–256.
- Healy1983 [123] E. Brézin and T. Halpin-Healy, *Scaling functions for 3d critical wetting*, *J. Phys. (France)* **48** (1987) 757–761.
- Fisher1987 [124] R. Lipowsky and M.E. Fisher, *Scaling regimes and functional renormalization for wetting transitions*, *Phys. Rev. B* **36** (1987) 2126–2241.
- DombGreen [125] G. Forgas, R. Lipowsky and T.M. Nieuwenhuizen, *The behaviour of interfaces in ordered and disordered systems*. Volume 14 of *Phase Transitions and Critical Phenomena*, pages 136–376, Academic Press London, 1991.
- Feynman1948 [126] R.P. Feynman, *Space-time approach to non-relativistic quantum mechanics*, *Rev. Mod. Phys.* **20** (1948) 367–387.
- Feynman2000 [127] R.P. Feynman and F.L. Vernon, *The theory of a general quantum system interacting with a linear dissipative system*, *Annals of Physics* **281** (2000) 547–607.
- DombGreen [128] F. Wegner, *The critical state, general aspects*, in C. Domb and M. Green, editors, *The Renormalization Group and its Applications*, Volume 6 of *Phase Transitions and Critical Phenomena*, page 7 ff., Academic Press London, 1986.
- ItzyksonZuber [129] C. Itzykson and J.-B. Zuber, *Quantum Field Theory*, Mac Graw-Hill, Singapore, 1985.
- Blumenthal1953 [130] L.M. Blumenthal, *Theory and applications of distance geometry*, Clarendon Press, Oxford, 1953.
- DDG2 [131] F. David, B. Duplantier and E. Guitter, *Renormalization theory for interacting crumpled manifolds*, *Nucl. Phys. B* **394** (1993) 555–664, [hep-th/9211038](#).
- David1995 [132] K.J. Wiese and F. David, *Self-avoiding tethered membranes at the tricritical point*, *Nucl. Phys. B* **450** (1995) 495–557, [cond-mat/9503126](#).
- David1997 [133] K.J. Wiese and F. David, *New renormalization group results for scaling of self-avoiding tethered membranes*, *Nucl. Phys. B* **487** (1997) 529–632, [cond-mat/9608022](#).